Technical Transactions

Czasopismo Techniczne

Volume 8

Year 2017 (114)

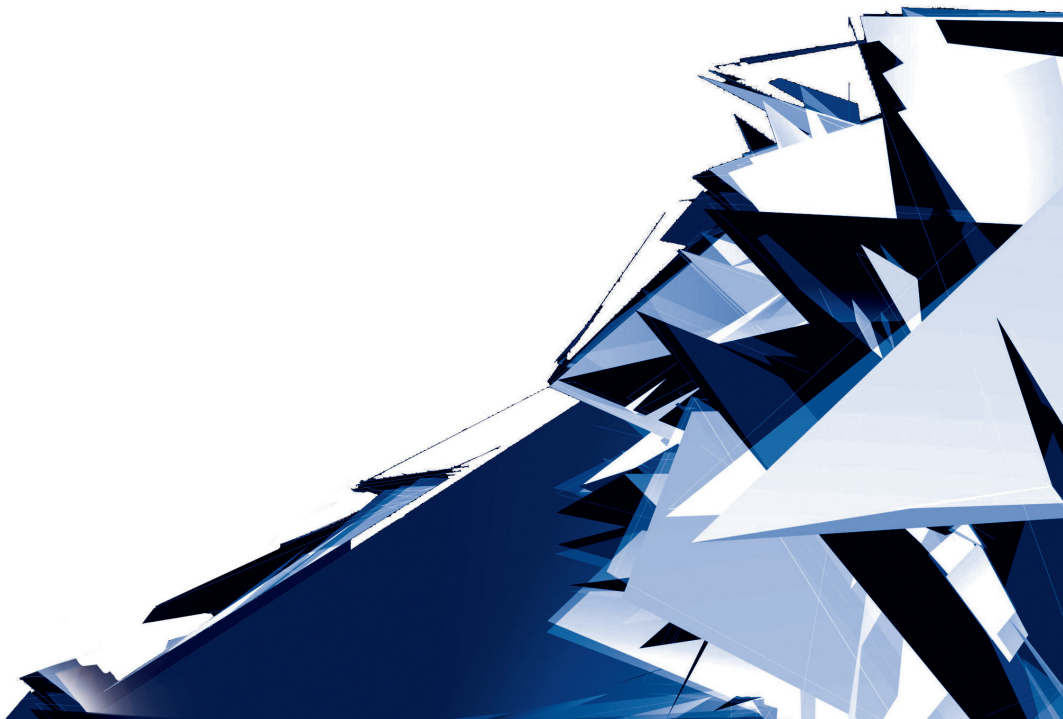

ISSN 0011-4561

Basic version of each Technical Transactions magazine is its online version
Pierwotną wersją każdego zeszytu Czasopisma Technicznego jest jego wersja online

Contents

TECHNICAL TRANSACTIONS 8/2017
CZASOPISMO TECHNICZNE 8/2017
ARCHITECTURE
DOI: 10.4467/2353737XCT.17.124.6875

Anita Pawlak-Jakubowska (anita.pawlak-jakubowska@polsl.pl)
Krystyna Romaniak
Geometry and Engineering Graphics Centre, Silesian University of Technology

Class II mechanisms in the construction of retractable roofs

Mechanizmy klasy II w budowie ruchomych przekryć dachowych

Abstract

This work presents retractable roofs of new designs based on class II mechanisms. Firstly, roofs that are currently in existence were analysed in terms of the mechanisms involved in their construction. Then, the possibility of constructing a roof based on the variety of quadruples in which all links are joined with roof panels was investigated. The boundary conditions that have to be fulfilled by such a construction were specified. Ultimately, research models were constructed with the use of construction solutions similar to those applied in buildings currently in existence.

Keywords: membrane roof, retractable roof, mechanisms class II

Streszczenie

W artykule przedstawiono propozycję nowych rozwiązań ruchomych dachów w oparciu o mechanizmy klasy II. W pierwszej kolejności przeanalizowano istniejące zadaszenia pod kątem występujących w ich budowie mechanizmów. W kolejnym etapie sprawdzono możliwość skonstruowania zadaszenia opartego na różnego rodzaju czworobokach, których wszystkie człony połączone są z panelami dachowymi. Określono warunki brzegowe, które musi spełniać tego typu konstrukcja. Ostatecznie zbudowano modele badawcze, stosując rozwiązania konstrukcyjne analogiczne do rozwiązań używanych w istniejących obiektach.

Słowa kluczowe: dachy membranowe, ruchome dachy, mechanizmy klasy II

1. Introduction

One of the biggest challenges that 21st century designers are faced with is mobile architecture, sometimes also described as the architecture in motion, kinetic or dynamic architecture. Moving walls and ceilings, roofs that can retract horizontally (in and out) and vertically (up and down), rotating facades and segments of a construction are examples of this type of architecture. The element of building construction that recently has undergone the most rapid development is the retractable roof. New possibilities in terms of materials and manufacturing technologies bring about the construction of retractable roofs that are increasingly larger in size and retract much faster. The changing shape of the retractable cover of a construction constitutes a key factor in its visual and esthetic perception. It is also expected to be in harmony with the surroundings and enhance the attractiveness of the entire building.

Retractable roofs with their construction based on class II mechanisms were singled out for the analysis. It included retractable roofs on constructions such as the Reliant Stadium in Houston (USA), Marlins Park Stadium in Florida (USA) and Wimbledon Centre Court (UK).

The analysis of building structures with retractable roofs inspired a quest for new solutions regarding the structure of mechanisms. With reference to already existing solutions, the class II mechanisms were subject to thorough examination. Preliminary analysis provided all possible solutions containing rotary and prismatic kinematic pairs for two assembly options. The research covered constructions with roof panels directly connected with the mechanism coupler or mounted on the coupler plane. This preliminary analysis resulted in determining the boundary conditions following a number of conditions restricting the area of research. The results obtained from the analysis constitute the main topic discussed in this paper.

2. Second class mechanisms in the construction of roofs for sports stadiums

At the first stage, the retractable roofs were analysed in terms of the movement that they performed. Two methods of movement were specified i.e. rotary and translation/forward movement (Fig. 1). In general, roof panels are directly attached to drives, of which movement is imposed by the shape of railings. If it is circular, the independent variable appearing in translation equations is an angle, whereas in the case of line-shaped railings, it is a line quality.

a) b)

Fig. 1. Retractable roofs with a four-bar linkage: a) Reliant Stadium in Houston, USA (source: http://www.uni-systems.com/en/projects/featured-projects/reliant-stadium, access: 29.12.2015), b) Marlins Park in Florida, USA (source: www.uni-systems.com, access: 29.12.2015)

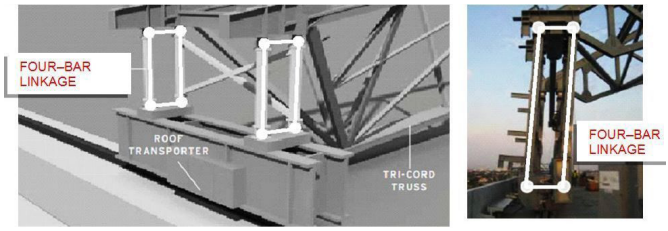

a) b)

Fig. 2. Roofs with movement: a) rotary along railings – Fukuoka Dome stadium, Japan (source: https://upload.wikimedia.org/wikipedia/commons/8/84/Fukuoka_Seaside_Momochi_Aerial_Shoot.jpg, access: 29.12.2015), b) translating along lines – PGE National Stadium in Warsaw (source: https://en.wikipedia.org/wiki/National_Stadium,_Warsaw#/media/File:POL_Stadion_Narodowy_Warszawa_09.jpg, access: 29.12.2015)

The roofs of the Reliant Stadium in Houston (USA) and Marlins Park in Florida (USA) are constructed with the use of two four-bar-linkages that can accommodate the impact of sudden gusts of wind (Fig. 2). Hence, each panel is able to perform movement that is transversal to the direction in which the roof is progressing. The range of movement of the Reliant Stadium roof panels is 21.5 inches with respect to the base.

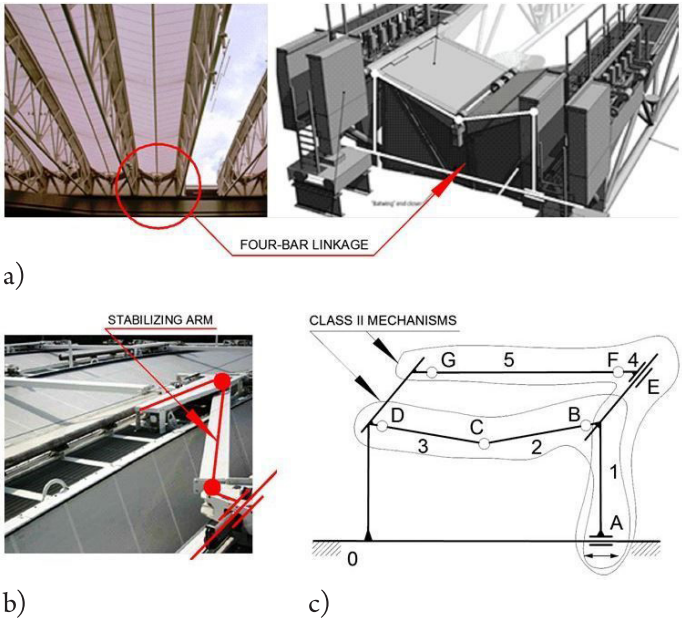

a) b) c)

Fig. 3. The roof of Wimbledon Centre Court (UK) with 2nd class mechanisms: a) four-bar linkage connected to the roof panels (source: https://commons.wikimedia.org/wiki/File:Flickr_-_Carine06_-_The_roof_is_closing.jpg, access: 29.12.2015), b) the mechanism determining the maximum distance between the panels (source: http://www.moog.com/literature/ICD/Moog-Wimbledon_Roof_Electromechanical_Actuators-article-en.pdf, access: 29.12.2015), c) diagram of the mechanisms (by A. Pawlak-Jakubowska)

Two class II mechanisms were specified in the roof of the Wimbledon Centre Court (UK). The roof panels covered with technical materials are attached to one of the mechanisms (Fig. 3). The other mechanism maintains constant distances between trusses with membranes. One link of this mechanism is called a stabilizing arm with its length defining the maximum distance between girders (Fig. 3b).

Located between two drives, the two roof panels (links 2 and 3 in Fig. 3c) are interconnected to each other and to the lattices in a rotary manner (kinematic pairs B, C, D). The movement of the roof panels is triggered by the motion of the first drive (link 1 in Fig. 3c) while the other drive is blocked. This first drive is a driving device for both the roof panels and the mechanism determining the maximum opening of the roof segment (links 4 and 5). The stabilising arm 5 is connected with the lattice girder and link 4 (kinematic pairs F and G) in a rotary manner. Link 4 performs a translation along the lattice girder (kinematic pair E). Fig. 4 presents the translatory movement of the roof links located between two drives. The movement of the driving device 1 causes links 2 and 3 to move the roof to the position, which ensures the minimum gradient required for water drainage.

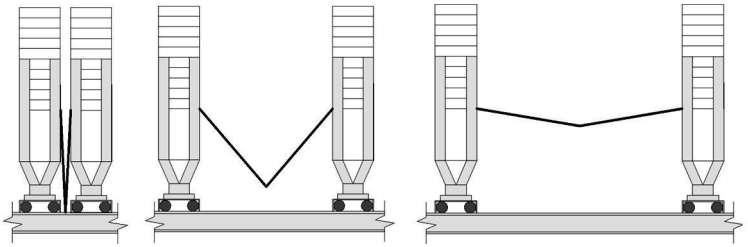

Fig. 4. Roof panels located between two driven trucks in Wimbledon Centre Court: a) open , b) movement, c) retracted roof (all by A. Pawlak-Jakubowska)

The analysis of construction solutions used in the retractable roofs such as Reliant Stadium in Houston (USA), Marlins Park in Florida (USA) and Wimbledon Centre Court (UK) inspired a search for new roof forms regarding the structure of mechanisms.

3. Construction of research roof models based on class II mechanisms

In order to specify the possible designs for retractable membrane roofs that are linked with class II mechanisms, a number of conditions have been considered, which have to be fulfilled by such mechanisms. Correct functioning of the mechanisms depends on the length of the moving links and the range of movement of the driving link. The ratio of the lengths of individual links decides on the category the mechanism belongs to. There are three categories, namely: double-crank, crank-rocker, drag-link and double-rocker mechanisms[1].

[1] This division is connected witch Grashof condition [4, p. 40-49], [5, p. 46-53].

In order to specify the movement performed by the roof joined with the mechanism, all its theoretical solutions that contained translation and rotary kinematic pairs have been considered [6, p. 95-101]. The extreme (turning) as well as idle positions were determined. In addition, the issue of the roof - coupler joining point was covered in the research, as in the following two cases:

- a roof panel directly joined with the coupler – then its movement defines the trajectory of the roof movement.
- The connecting point of the roof panel is located on the so-called coupler plane – then the roof trajectory depends on where the point is on the coupler plane.

Having done the analysis and considered that a vast area of research needs to be covered, the discussion on the issue of the roof connection with the use of a coupler plane was omitted.

Hence, very detailed research has been carried out on roof panels directly joined to the links of the mechanism. Exploiting a wide range of possibilities of parametric modelling in AutoCAD, the translation of the mechanism links was determined. The obtained data was used to define viable solutions that fulfil the following imposed boundary conditions:

1) The inclination angles of panels such as, for example, roof slopes should take values between 10° and 85°. This assumption brings about proper water drainage and simultaneously sorts out the issue of roofing over an enclosed area, such as a courtyard. Criteria adopted regarding the inclination of panels (links) enable a collision-free movement of the roof.
2) All panels connected to links of the mechanism must function as roof slopes. Hence, if, during a movement, one panel covers the other from the top (Fig. 5a), such a position is eliminated from the movement range. This ondition restricted the movement range of individual links.
3) The solutions requiring the installation of a circular gutter were eliminated. They are cases in which the adjacent links form a V-shaped basket while moving, thus making rainwater gather between the panels (links). The task of draining water while the panels move horizontally is relatively straightforward, whereas doing it while the panels move along an arch (Fig. 5b) becomes a bit of a challenge, among others, in terms of installing an arch-shaped gutter.
4) Translation kinematic pairs are located exclusively at the base. This condition results from the analysis of constructions with retractable roofs in which the prismatic kinematic pairs often connect the roof with the lower link of the construction.

The obtained results were analysed in terms of the adopted boundary conditions, whereby several mechanisms were selected for further analysis. A variety of possibilities for covering an area with the use of roofings that harnesses two mechanisms of class II were taken into consideration. Symmetrical and non-symmetrical mechanism connections were examined considering the same and different types of mechanisms. Consequently, the roofs constructed on the basis of a symmetrical connection of two identical mechanisms were selected for a detailed analysis due to their viable and technologically less challenging construction (two driving devices of the same type, the links in the joined mechanisms of identical lengths and

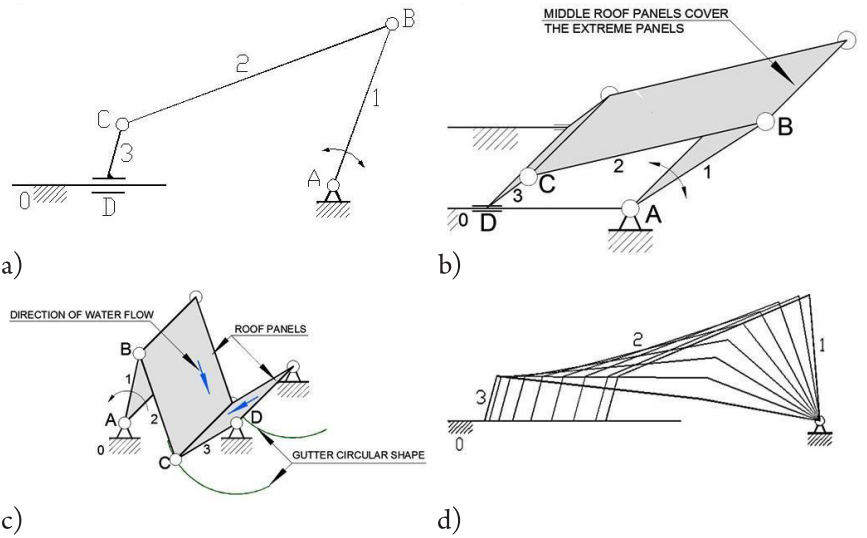

Fig. 5. Class II mechanisms with a rotary driving link: a) mechanism diagram (by K. Romaniak), b) roof panel 2 covers panel 1 from the top (by A. Pawlak-Jakubowska), c) an arch-shaped gutter (by A. Pawlak-Jakubowska), d) restricted movement range (by A. Pawlak-Jakubowska)

the gutters can be installed at the same level). A mixed combination of class II mechanisms imposes the use of different drives (rotary and translatory), panels of different dimensions and, in some cases, the gutters must be installed at different levels.

A detailed analysis has been carried out for four models constructed on the basis of two class II mechanisms that were joined together. The research method was illustrated on the example of the mechanisms with a rotary drives, three rotary kinematic pairs and one prismatic kinematic pair (Fig. 5a). In the two symmetrically joined mechanisms, the drives are located on the outer edges of the roof and the prismatic kinematic pairs can be found in the central link of the construction (Fig. 6a). Thus, the roof retracts starting from the outer edges towards the centre of the covered area. Symmetrically located roof panels can perform a synchronised movement or each link of the roof can move independently. The percentage rate of the covered area was assessed following a dimensionless analysis, which mainly aimed at establishing proportional relationships between the lengths of individual links. The following letter symbols have been adopted: a, b, c – lengths of the moving links, d – the length of the base (Fig. 6b).

A constant angle between the base and link 3 (a shape angle) has been noted as κ.

A detailed analysis exploited the possibilities of parametric modelling available through the AutoCAD software. For model number 1 the following assumptions were adopted:

- constant length of a driven link (coupler) b,
- the lengths of links 1 and 2 proportional to b:
- $a = (i + 0.1)b$, $c = (i + 0.1)b$, where $i = 0, 0.1, \ldots, 0.9$,
- different values of a shape angle κ (85°, 60°, 45°, 30°, 15°),
- movement range of link 1 (10° - 85°).

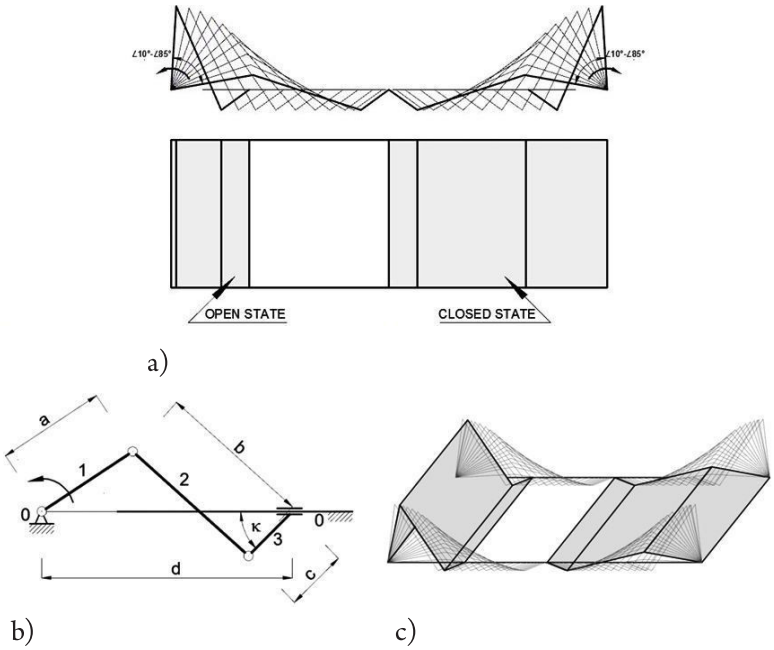

Fig. 6. Model with a rotary driving link: a) open and retracted roof respectively, b) notation of the lengths of individual links of mechanism, c) roof axonometry (all by A. Pawlak-Jakubowska)

As a result of the carried out research, the percentage values of the open area (noted as *O* in Table 1) and the d values were assessed. The adopted assumption was that the satisfying result would be the opening of 70% or more of the covered area. In addition, it was significant to obtain as large as possible span *d*, which defines the area of covered space. It was agreed that a satisfactory result would be a value greater than 1.8*b*. Table 1 presents a fragment of the results obtained; in bold the data fulfilling adopted criteria. Empty spaces mean that driving link 1 does not reach values within the full range of movement (10°-85°).

Table 1. Percentage values of the open roof space and *d* lengths in relation to selected lengths *a* and *c* proportional to a given *b* and adopted values of angle κ

		Angle κ = 85°		**Angle κ = 60°**		**Angle κ = 45°**		**Angle κ = 30°**		**Angle κ = 15°**	
		O [%]	*d*	*O* [%]	*d*	*O* [%]	*d*	*O* [%]	*d*	*O* [%]	*d*
a=0,7*b*	*c*=0	56	1,68*b*	56	1,68*b*	56	1,68*b*	56	1,68*b*	56	1,68*b*
	c=0,1*b*	60	1,67*b*	58	1,71*b*	56	1,74*b*	54	1,76*b*	53	1,77*b*
	c=0,2*b*	69	1,65*b*	63	1,74*b*	59	1,79*b*	55	1,83*b*	51	1,86*b*
	c=0,3*b*	90	1,63*b*	72	1,76*b*	63	1,84*b*	56	1,91*b*	50	1,95*b*
	c=0,4*b*	–	–	–	–	**72**	**1,88*b***	58	1,98*b*	50	2,05*b*
	c=0,5*b*	–	–	–	–	–	–	61	2,05*b*	49	2,14*b*

		Angle κ = 85°		Angle κ = 60°		Angle κ = 45°		Angle κ = 30°		Angle κ = 15°	
		O [%]	*d*	*O* [%]	*d*	*O* [%]	*d*	*O* [%]	*d*	*O* [%]	*d*
a=0,8*b*	*c*=0	63	1,78*b*	63	1,78*b*	63	1,78*b*	63	1,78*b*	63	1,78*b*
	c=0,1*b*	71	1,76*b*	68	1,8*b*	66	1,83*b*	63	1,85*b*	61	1,87*b*
	c=0,2*b*	90	1,74*b*	**78**	**1,83*b***	**71**	**1,88*b***	65	1,93*b*	60	1,96*b*
	c=0,3*b*	–	–	–	–	–	–	68	2*b*	59	2,05*b*
	c=0,4*b*	–	–	–	–	–	–	**77**	**2,07*b***	59	2,14*b*
	c=0,5*b*	–	–	–	–	–	–	–	–	59	2,23*b*
a=0,9*b*	*c*=0	73	1,87*b*	73	1,87*b*	73	1,87*b*	73	1,87*b*	73	1,87*b*
	c=0,1*b*	**91**	**1,86*b***	**84**	**1,9*b***	**80**	**1,93*b***	**75**	**1,95*b***	**72**	**1,96*b***
	c=0,2*b*	–	–	–	–	–	–	**84**	**2,02*b***	**72**	**2,05*b***
	c=0,3*b*	–	–	–	–	–	–	–	–	**73**	**2,14*b***

Table 2 presents selected examples of roofs constructed with the use of data highlighted in bold in Table 1. For consecutive values of angle κ, the diagrams of mechanisms constituting the base of a roof construction were presented with given lengths of individual links determined proportionally to the *b* length. Horizontal projection of the roof illustrates the open space percentage, whereas a vertical projection shows translations of individual roof panels.

Table 2. Examples of roofs fulfilling boundary conditions

No.	Angle κ	Values of *a*, *b*, *c* and *d* specified for one mechanism	Horizontal and vertical roof projections
1	85°	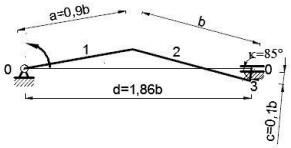	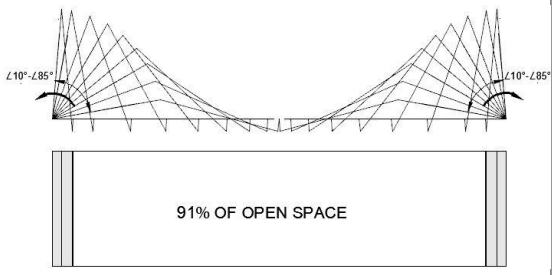
2	60°	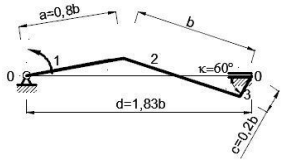	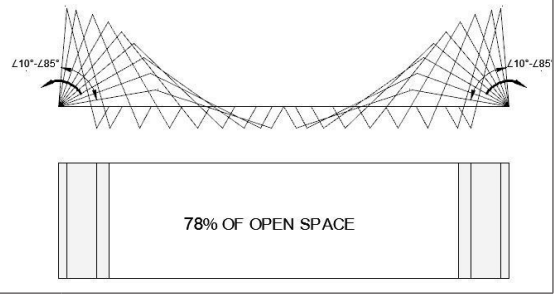

No.	Angle κ	Values of *a, b, c* and *d* specified for one mechanism	Horizontal and vertical roof projections
3	45°	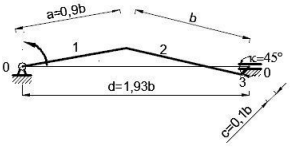	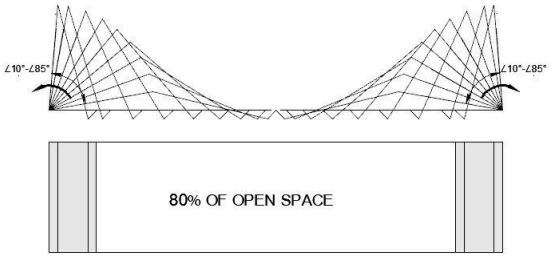
4	30°	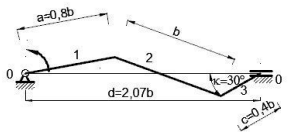	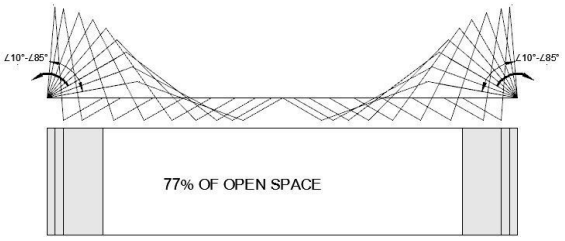

For the model where $a = 0{,}8b$, $c = 0{,}2b$ and angle $\kappa = 60°$, as much as 78% of the roof open space can be obtained (Fig. 7). When specified, the translations of individual panels determine a working space of the whole roof. By analogy, a similar analysis was carried out for the remaining solutions presented in Table 2.

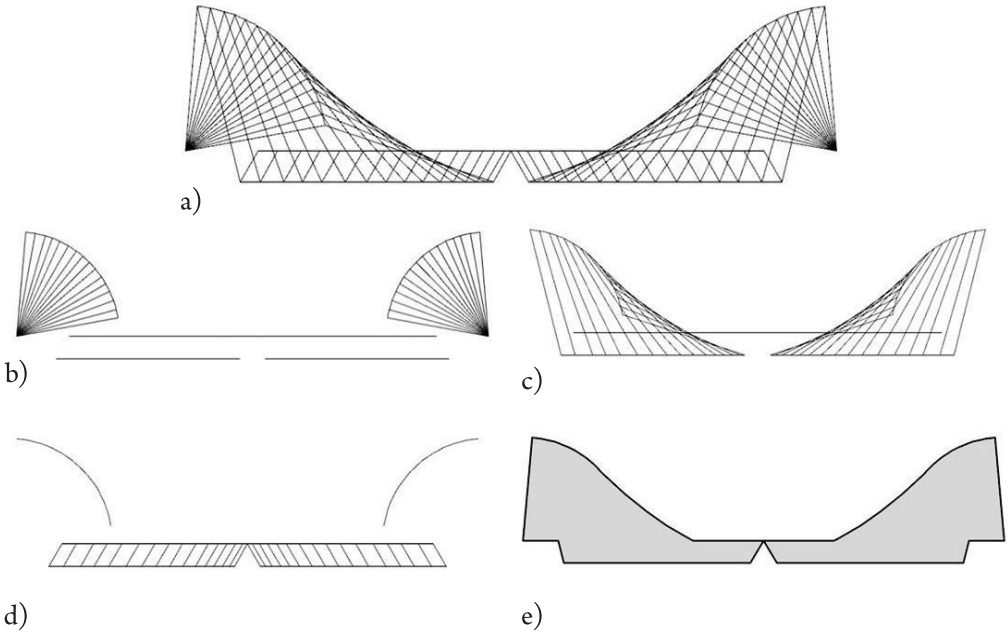

Fig. 7. Movements of: a) links 1,2 and 3, b) driving link 1, c) link 2, d) link 3, e) roof working space (all by A. Pawlak-Jakubowska)

To drain water from the panels of a model with a rotary driving link, the installation of gutters and downpipes is required. From the driving panels, the rainwater runs down to a gutter located at the base level and then into a downpipe (Fig. 8). As the angle between panels 2 and 3 is variable, a flexible gutter can be installed, which will take the water to a gutter that is linked to a downpipe. This type of gutter system makes it possible for water drainage to occur in every position of the roof, open or closed, and even when the roof stops at any moment of its movement.

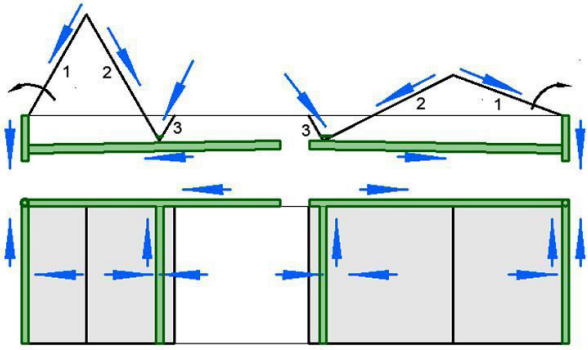

Fig. 8. Water drainage from the roof (by A. Pawlak-Jakubowska)

Finally, the last stage of the research focused on digital models made with the use of the Autodesk Inventor Professional 2016 software. This particular software provides tools for making a model and then performing kinematic simulation.

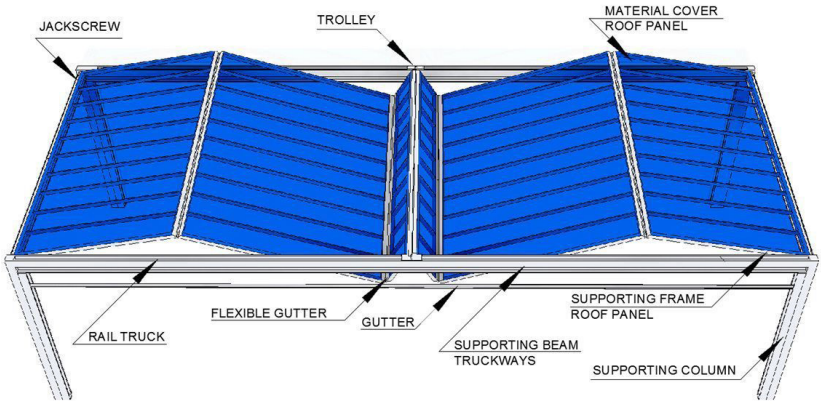

Fig. 9. Components of the research model (by A. Pawlak-Jakubowska)

Exploiting information regarding retractable roof construction technologies [2], the solutions for the construction of individual elements of research models were proposed (Fig. 9).

4. Conclusions

The quest for new designs of retractable roofs went through several stages. Firstly, all theoretically possible solutions for class II mechanisms with rotary and translation kinematic pairs were determined. The set of solutions was subject to numerous selections that considered a variety of conditions. Thus, boundary conditions were specified, which should be fulfilled by roofs joined with selected mechanisms. Finally, several solutions were selected and used to build research models. A research model is a set of roofs built on the basis of one mechanism of a specific structure. For each such a model, a detailed investigation was carried out in terms of its kinematics, for example, its movement range and working area, as well as the water drainage method. The solutions, which fulfilled adopted assumptions i.e. the percentage of the open space over 70%, were selected. Ultimately, construction solutions for individual elements of the models were proposed. The solutions were modelled on real roofs currently in existence.

The research carried out and the results obtained indicate the possibility of determining new designs of retractable roofs based on structural and kinematic research of mechanisms. In currently existing retractable roofs built on the basis of class II mechanisms, two panels are joined with the driving links of mechanism at most. In the solutions proposed in this work, a driving link is also joined with roof panels and functions as a roof segment.

References

[1] Gerfen K., *Wimbledon Centre Court Retractable roof,* The Journal of the American Institute of Architects ARCHITECKT, 2009, http://www.architectmagazine.com/technology/detail/wimbledon-centre-court-retractable-roof_o (access: 18.12.2015).

[2] Ishii K., *Structural Design of Retractable Roof Structures,* WIT Press, Southampton, Boston, 2000.

[3] MACHINE Design by Engiers for Engineers.

[4] http://www.moog.com/literature/ICD/Moog-Wimbledon_Roof_Electromechanical_Actuators-article-en.pdf (access: 18.12.2015).

[5] Młynarski T., Listwan A. i Pazderski E., T*eoria mechanizmów i maszyn. Cz. III Analiza kinematyczna mechanizmów,* Wydawnictwo Politechniki Krakowskiej, Kraków 1999, 40–49.

[6] Norton R.L., *Kinematics Design of Machinery: An Introduction to the Synthesis and Analysis of Mechanisms and Machine,* McGraw Hill, 1999, 46–53.

[7] Pawlak-Jakubowska A., Romaniak K., *Modelowanie geometrii przekryć ruchomych,* Modelling in Engineering, 25(56)/2015, 95–101.

[8] Uni–System, www.uni-systems.com (access: 18.12.2015).

TECHNICAL TRANSACTIONS 8/2017
CZASOPISMO TECHNICZNE 8/2017
ARCHITECTURE
DOI: 10.4467/2353737XCT.17.125.6876

Mariusz Twardowski (mt@twardowskiwokan.pl)
Institute of Urban Design, Faculty of Architecture, Cracow University of Technology

Oscar niemeyer's ibirapuera park in são paulo built with one line

Park ibirapuera w são paulo oscara niemeyera zbudowany jedną kreską

Abstract

Niemeyer's extraordinary ability to present his projects with one line comes from the inspiration of the landscape, the hills surrounding Copacabana Beach, and the female body. Sketching since he was younger, the architect has improved his line so much that one line was enough to explain the whole project. One of the realizations built with one line was the Ibirapuera Park in São Paulo, opened in 1954. The buildings created there, showed a glimpse of Sugarloaf Mountain, women and their curvilinear forms.

Keywords: Oscar Niemeyer, Parque Ibirapuera, women, São Paulo

Streszczenie

Niezwykła zdolność Oscara Niemeyera do przedstawiania jedną kreską swoich projektów wywodzi się z inspiracji krajobrazem, wzgórzami otaczającymi plażę Copacabana i kobiecym ciałem. Szkicujący od młodych lat architekt tak dopracował swoją kreskę tak, że wystarczyła jedna linia, która tłumaczyła cały projekt. Jedną z realizacji zbudowanych jedną kreską był Park Ibirapuera w São Paulo otwarty w 1954 roku. Kolejne budynki tam powstające uwidaczniały zauroczenie projektanta górą Głowa Cukru, kobietami i ich krzywoliniowymi formami.

Słowa kluczowe: Oscar Niemeyer, Parque Ibirapuera, kobiety, São Paulo

1. Fascinations

Oscar Niemeyer was one of the most esteemed architects in the world who has created his own style of communication over the years. However, to better understand and appreciate Niemeyer's thinking, his sketches and buildings based on these sketches, we should investigate his inspirations with women and female shapes, surroundings, mountains, the Copacabana beach, in more detail.

He has been drawing ever since he was young. Sketches of the ocean, the waves, the mountains appeared from the beginning of his works. As he was growing up, more and more women were appearing on sketches he made. He wrote in his 1988 memoirs *The Curves of Time*: "I am not attracted to straight angles or to the straight line, hard and not inflexible, created by man. I am attracted to free-flowing, sensual curves. The curves that I find in the mountains of my country, in the sinuousness of its rivers, in the waves of the ocean, and on the body of the beloved woman" [10, p. 3].

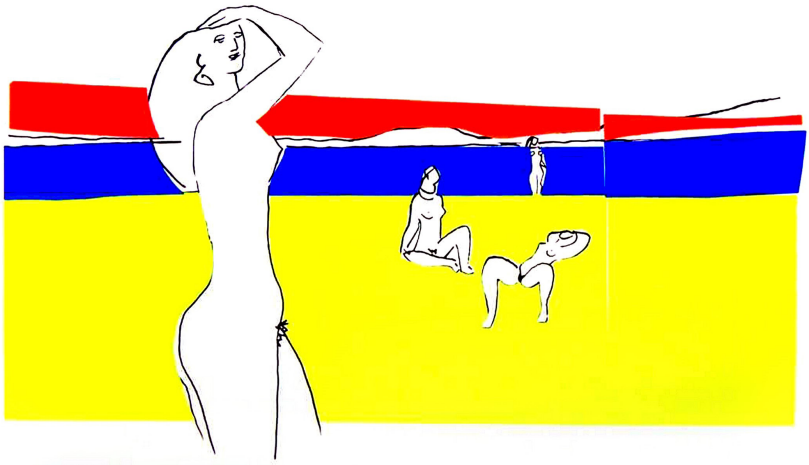

Fig. 1. One of Niemeyer's drawings presenting naked women on the Copacabana Beach In Rio de Janeiro (source: Fundação Oscar Niemeyer, www.niemeyer.org.br/desenho/gravuras, access: 22.03.2017)

The fascination of landscape and feminine shapes was expressed in the forms of concrete solids designed by him. Linear drawings of his projects are nothing but drawings of women in the landscape. Further buildings are arising from these shapes. The scale of the building does not matter for Niemeyer. The large, monumental buildings of Brasilia, or smaller ones like the Teatro Popolar in Niteroy, all relate in some way to the sketched organic forms. Brasilia - his great ideological and political fight for beautiful buildings - is a huge complex of buildings that, even being perpendicular forms resulting from its rigid function, contain the curves of female lines from his drawings. Thanks to this, his works surprise to this day, being masterpieces for tens of years. "I search for surprise in my architecture. A work of art should cause the emotion of newness" [11] he said. Buildings from concrete curves look futuristic even today. The Cathedral of Brasilia explodes like a volcano from the ground, taking congregation to the last road.

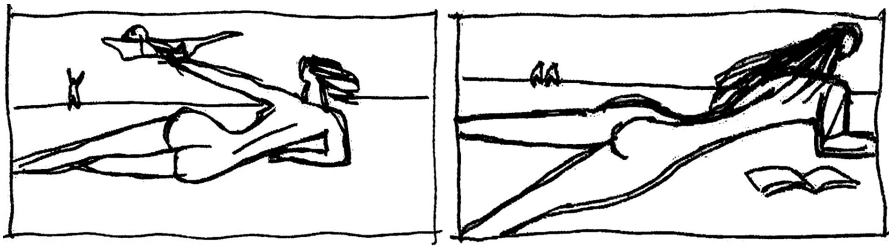

Fig. 2. View from Niemeyer's office window to his inspirations, photography of the drawing on the tracing-paper presenting on the exhibition of Oscar Niemeyer's works in Museum of Contemporary Art in Macau, 05.2011 (photo by M. Twardowski)

For Niemeyer, the curves of hips, sensually spread legs, or the perfect "baroque buttocks" are the germ of every project that combines Brazilian sensuality and tons of reinforced concrete. "I draw a woman with a single line and imagine how the building surrounds her" [12].

One of the most delightful projects, in which the fascination of Niemeyer with the woman and her body is very noticeable, is the Ibirapuera Park. The line started by the view of women on Copacabana and the landscape in São Paulo was transformed into reality. The park was designed in conjunction with his favorite landscape architect Roberto Burle Marx[1] and the agronomist Otávio Agusto de Teixeira Mendes.

Before the 400th anniversary of the founding of São Paulo, on the 21st of August 1954 when the park was opened, there were only wetlands and favelas [4]. Everything was turned into ponds, park, alleys and buildings. The constructed recreational space has often been compared to Central Park in New York or Tokyo's Ueno Park.

2. History

In the early 20th century, São Paulo was already a large city (250,000 inhabitants). When, at the end of the 1920s, more than half a million people were living in the city, the mayor came up with the idea of creating a magnificent recreational park like the Central Park in New York. Initially, the idea fell, but twenty years later, the area was drained and space for a new park was prepared. The organizing committee of the city's 400th anniversary celebration chose Oscar Niemeyer and Roberto Burle-Marx to design it (part of the Burle Marx's project was later replaced by design of Otávio Agusto de Teixeira Mendes). When it was decided that buildings would appear in the park, the citizens were very disappointed. Dozens of residents wishing only for greens and alleys were protesting. However, the city maintained its decision to create a park with varied functions and buildings. The park was opened on time, but construction continued for several years. It was completed in 2005[2].

[1] Roberto Burle Marx, lanscape architekt, painter, with Oscar Niemeyer they become tandem in tens of projects. First design in which they were co-working was Brasilian Pavilion for New York World's Fair in 1939. He was also a staunch follower of the protection of Brazilian Amazon forests.

[2] In 2016 Paulo Mendes da Rocha designed meeting and event square just behind main entrance and betweet Oca and Auditorium buildings.

3. Composition and function

„Mayor of São Paulo proposed me the design of the Ibirapuera Park. Together with the architects Hélio Uchôa and Lotufo and Kneese de Melo, we developed a preliminary concept" [8, p. 31].

Three large exhibition buildings, a monumental main entrance to the museum and an auditorium, were all designed. The complex was going to be connected by a single-storey pavilion. All in green, surrounded by a large artificial lake (Lago das Garças) and pond. Alleys surrounded the buildings and ran along the water. Buildings – longitudinal cubes – even if from a distance, seemed to be squat forms, which were lacking loftiness in the park's surroundings, in a close perspective, they began to fleet, almost hanging above the ground. Each of them stood on pillars and all ground floors were smaller than the remaining storeys. Retreating ground floors made the upper floors float in greenery. The one-story building was the complete opposite of the others. It flowed from building to building between greenery, becoming the most memorable structure in the park. It was the most similar to the forms drawn in Niemeyer's sketches and the most feminine in its form. An auditorium in the shape of a section of a sphere and a theatre were going to be built on both sides of the main axis of the entrance from the obelisk of Heroes of 1932. However, the theatre did not come into life

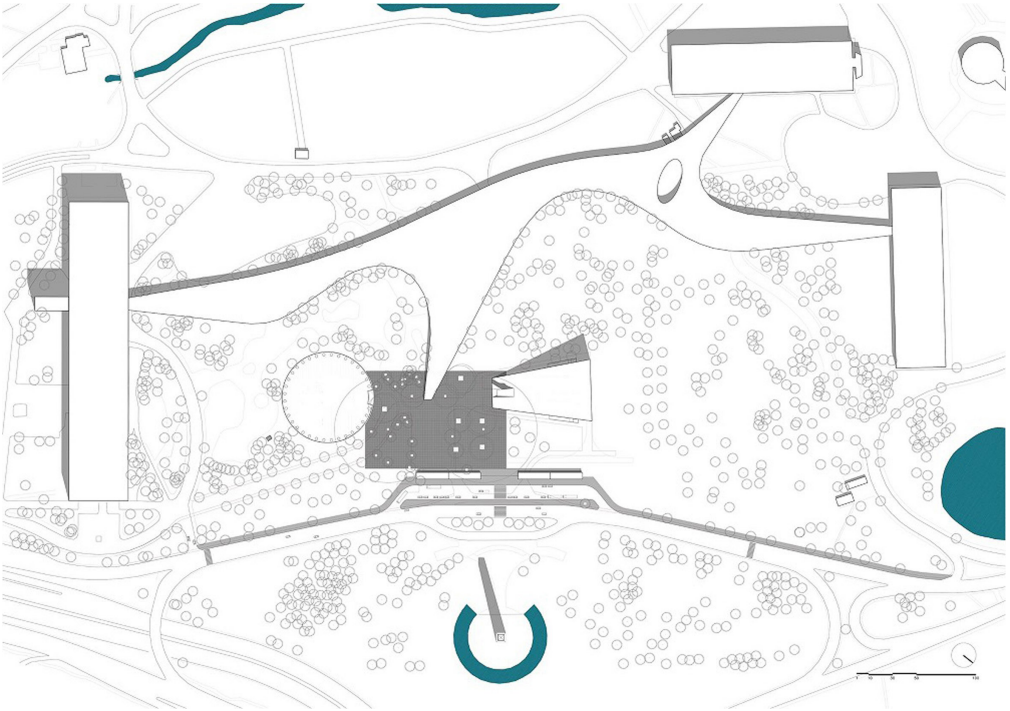

Fig. 3. Piece of art of Oscar Niemeyer. Ibirapuera Parque in São Paulo on the site plan (project of the square in parking place between Oca and Auditorium buildings, proj. Paulo Mendes de Rocha, 2016), (source: *Paulo Mendes da Rocha fala sobre projeto para o Parque Ibirapuera*, [in:] Patrimonio, 06.05.2016, http://patrimoniohistorico.prefeitura.sp.gov.br/paulo-mendes-da-rocha-fala-sobre-seu-projeto-para-o-parque-ibirapuera/ (access; 25.03.2017)

until the 21st century. An astronomical observatory and a Japanese Pavilion were built on the west side of the park. The park has a variety of recreational functions. Cycling, jogging and walking trails, football pitches, outdoor gyms, tennis courts. Parks for skateboards and bicycles, squares for yoga and combat sports, were all added a little later. The buildings included galleries and museums. The Biennale Foundation found its place in the largest building. In the subsequent cubes, there are more galleries and museums, also in the Oca building. On the opposite side, a triangular auditorium was built in 2005.

Niemeyer describes his composition[3]: "After entering the park, a square was planned. On both sides, there are two buildings – the exhibition dome and the geometric auditorium. Both buildings, made from reinforced concrete, were painted in white. On the axis of the square stood the "Great Marquee". The amorphous sculptural form is the entrance to the park. The "Marquise" did not divide the park in half, I advised to remove some of the walls so that the form became more fleeting and translucent" [9, p. 74]. "To finish the original plan, which I worked on 50 years ago, on the opposite side of the concrete dome, I designed an auditorium for 850 people with conference rooms" [8, p. 286].

4. Buildings in the park

The basic concept of the Ibirapuera Park was to design several major buildings, which were going to create the core of the project, along with minor buildings hidden in the greenery. Currently, many of the buildings have changed their functions. It seems that it was a good result because the previous functions of these buildings did not fit into the basic recreational function of the park.

4.1. Biennale Pavilion

Pavilhão Ciccillo Matarazzo (1957), the largest building in the park designed by Oscar Niemeyer and Hélio Uchôa, on its eastern side, is a pure cube, where the main body of the building was hung on columns above the smaller ground floor. In several places, staircases are poking out from the building and they lead viewers of Biennale to the greenery of the park. Inside the building, there are ramps leading to different levels. Sometimes, they run straight; another time, they turn and sometimes turn back. Just like sunbathing, sparingly dressed women on Copacabana beach captured by the Master's line. The complex (25,000 m^2) creates an amazingly three-dimensional space closed by glazing with Niemeyer's favourite brise soleil. Firstly, just after opening, it was the Palace of Industry. Since the fourth edition of the Biennale, it is the headquarters of this great art festival. Nowadays, every two years, there is the São Paulo Fashion Week, equally as famous as the Venetian Art Biennale, as well as other exhibitions, presentations made by famous artists from all over the world.

[3] Niemeyer described Grande Marquise in memories after complete of the last building in the park – auditorium. For 60 years space under the roof was slowly annexing for new rooms and storages losing its transparency.

Fig. 4. Biennale Pavilion (photo by M. Twardowski)

4.2. Nations Palace

Pavilhão Manoel da Nóbrega (1959) is located on the western side of the park, at the other end of the one-storey Grande Marquise pavilion. In a smaller scale than the Biennale Pavilion, however, on a similar compositional basis, the pavilion is dropped above the ground floor. Building facades are not completely glazed and there are no brise soleil. After the opening, there was a town hall and a city council. Currently, since 2004, Museu Afro Brasil is located there. The museum is dedicated to the history, ethnography and art of black residents of Brazil. In this small building, there are about 6000 paintings, sculptures, photographs, documents and other artefacts dating back to the 15th century. The redesigned interiors include spaces for temporary exhibitions, a theatre room and a library.

Fig. 5. Nations Palace (photo by M. Twardowski)

4.3. Old Palace

Pavilhão das Culturas Brasileiras (1959) is a twin building of the Nations Palace. The structure of the building, identical to the previous one, is connected to the other two pavilions by the one-storey Grande Marquise. Designed by Oscar Niemeyer, the pavilion (originally called Pavilhão Engenheiro Armando de Arruda Pereira) was designed as the headquarters of the Municipal Data Processing Company Prodam (Companhia de Processamento de Dados do Município). After quite a long renovation, in 2010, the pavilion became available for the Museum of Brazilian Culture. On the area of 6.780 m2, there are works of native art, design, crafts, graffiti and tattoos. Apart from the exhibition space, there is a library, an auditorium and a café.

4.4. Great Marquee

The "Grande Marquise" connecting the main buildings and directions in the park is a one-story building flowing through the park. It is the core of the park – almost as the span of a lying woman, which is 620 m long with a width between 10 and 80 m. Its amorphous shapes lead visitors to the following buildings: Pavilhão Bienal, Museu Afro Brasil, OCA and Pavilhão das Culturas. The area of the building is 28,800 m^2. The roof was based on 121 columns [5]. At the beginning (in 1952), the whole building was a closed pavilion. In closest distance from Biennale Pavilion, in 1982, the Museum of Modern Art (Museu de Arte Moderna) was built (proj. Lina Bo Bardi) [3]. After a long renovation and reopening in 2012, many glazing and walls were removed. While designing the auditorium at the beginning of the 21st century, Niemeyer noted that the Marquee with glazing and walls divide the park into two parts. Currently, besides the Museum of Contemporary Art, there are restaurants and covered open spaces, which are used by playing children, skateboarders, bicyclers, roller skaters and exercisers. You can get the impression that Niemeyer's buildings, shaped in a way most inspired by the landscape, nature and the shape of the woman's body, are also most favoured by the city residents. Since most of the area under the roof has been freed from the walls and become open, connected with surrounding greenery, the building has become extremely fleeting and not overwhelming and most people spend their time right here.

Fig. 6. Grand Marquee (photo by M. Twardowski)

4.5. Oca

The building was formerly known as "Palácio das Exposições" (Exhibitions Palace). For the last few years, there was Museu da Aeronáutica (Museum of Aviation) and Museu do Folclore (Museum of Folklore). It was designed by Niemeyer in 1951. The area of the building is about 10,000 m^2. Recently, the dome was renovated again, all museums were moved to other locations in São Paulo and the building returned to its original function. The other Brazilian Pritzker Prize winner Paulo Mendez da Rocha (with studio MMBB) was responsible for the project. The space of the building was renovated; the three-dimensional glow of the building was brought back. The small elements from the Grand Marquee were dismantled at one end to create more free space between around dome. Reinforced concrete was renewed and the dome painted in white. Mendes da Rocha recalls: "The Marquee (Marquise) must appear and open to the park and paths with some space from the building" [1]. The building is very recognizable. Its form, in the shape of a slightly flattened dome, perfectly fits into the greenery and other design elements of the park. This is another element, where, during the design process, the author took inspiration from the hills surrounding his office and the shape of the female body. It is almost like another master's line sketched on one of the tracing papers. Inside, there is a large number of beautiful curves

Fig. 7. Oca (photo by M. Twardowski)

that turn into ramps and planes, penetrating into the dome. By penetrating the columns, they create floors, ceilings and sometimes walls, which allow to present paintings and are the background for exhibited sculptures. The whole creates an unusual system for the most complex exhibitions that are hidden under the dome.

4.6. Auditorium

Auditório Ibirapuera, designed by Oscar Niemeyer from the 1950s, had different forms. However, in 2005, one of the simplest and the most minimalist visions of Niemeyer was realized. The trapezoidal form was raised from one side to the shape of a triangle in cross section. Functionally divided into 3 parts: the auditorium, the foyer and the space leading from the outside to the centre highlighted by a waving roof. An unusual metal roof painted in red emphasizes the entrance. This red tongue became the building's logo. It is officially called *Labareda* – a flame. It became so popular that when Niemeyer was asked to design trainers for Converse, he was inspired by his auditorium to such an extent that he created white shoes with a red tongue, reminding the *Labareda* of his building [2].

Inside, in the foyer, the space remains empty with the red low relief designed by Luis Antonio Vallandro Keating and flowing as sculpture steps leading to the higher levels of the auditorium. The area of the building is about 7.000 m^2. The main auditorium is designed for 806 seats [14]. Under the upper part of the auditorium, there were designed rehearsal rooms and lecture halls for the music school. An interesting solution was to locate the scene at the

Fig. 8. Auditorium (photo by M. Twardowski)

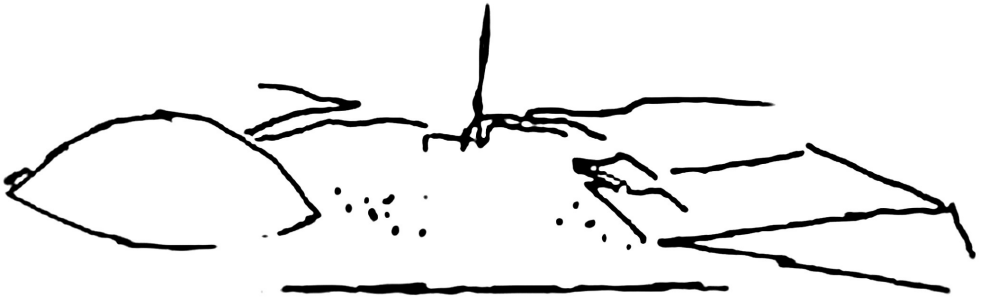

Fig. 9. Oca and Auditorium on a Niemeyer's sketch (source: Fundação Oscar Niemeyer, www.niemeyer.org.br/desenho/gravuras, access: 22.03.2017)

gable end wall of the designed triangle. Giant steel, red doors can be pulled apart and the scene becomes a place for outdoor concerts and audiences gathered across the building in open space of the park.

4.7. Japanese Pavilion

The building located on the most western site of the park is the Japanese Pavilion, which was donated by the Japanese government in 1954. This pavilion was designed in São Paulo not by accident. The city is home to the largest ethnic Japanese minority in the world. It was inspired by the Katsura Palace in Kyoto. The interior patio area is a place where people who are exercising or running can relax, contemplating at a pond with ornamental carps. The pond is surrounded by greenery imported from Japan. The building houses a small Japanese memory and culture museum with an exhibition of ceramics, warrior costumes and other Japan-specific items.

4.8. Planetarium

Planetário Professor Aristóteles Orsini (1957) is the only building besides the Japanese Pavilion, not designed by Niemeyer (proj. Antonio Carlos, Eduardo Corona and Roberto G. Tibau Pitombo). The Planetarium resembles a flying saucer. It is the first building in the southern hemisphere, whose dome exceeds a diameter of 20 meters. Residents come here to watch the projection of sky over São Paulo and listen to lectures on the most famous stars, constellations and earth movements.

4.9. Other buildings

Next to the park, there are several other monuments and buildings: the Department of Agriculture (currently the Museum of Contemporary Art of the University of São Paulo), the Sports Arena Velodrome, nursery, gardening school, the School of Astrophysics, the Open University of the Environment and Culture of Peace (UMAPAZ), Ginásio do Ibirapuera

(1957, proj. Ícaro de Castro Mello), The Monument to the Bandeiras, Ibirapuera obelisk 72 m heigh. They are surrounding or are adjacent to the park, creating functional endings for visitors staying in the park or passing through the park; however, they do not belong to the Ibirapuera Park directly.

5. Summary

The park became a part of the city's climate. It is adored by the locals. On non-working days, it is crowded. In 2015, in a summary of The Guardian magazine, the park was voted the most interesting park in the world (leaving behind The High Line in New York or Parque Güell in Barcelona) [7].

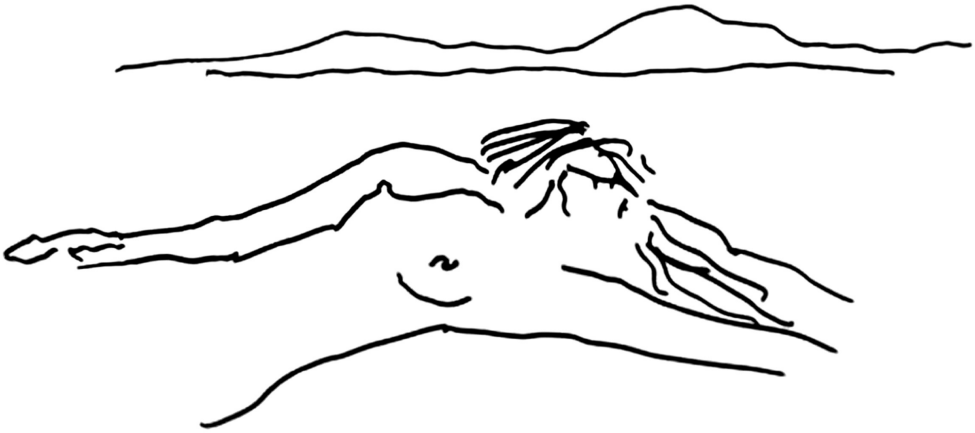

Fig. 10. „Curved and straight lines" – women and hills above Copacabana beach (source: Fundação Oscar Niemeyer, www.niemeyer.org.br/desenho/desenhos, access: 22.03.2017)

"My work is not about 'form follows function,' but 'form follows beauty' or, even better, 'form follows feminine.'"[6, p. 35]. "I deliberately disregarded the right angle and rationalist architecture designed with ruler and square to boldly enter the world of curves and straight lines offered by reinforced concrete. This deliberate protest arose from the environment in which I lived, with its white beaches, its huge mountains, its old baroque churches, and the beautiful suntanned women" [10, p. 62] wrote Niemeyer. And that is how, with the help of the world of curves and straight lines, he created one of the most beautiful and recognizable parks in the world. This sense of fun and joy, fascination by the feminine shapes and landscape around the beloved Copacabana beach transformed into the unique lines that last in Oscar Niemeyer since his youth years, will still be alive in its buildings. He made an extraordinary injection of passion and emotion into the monotonous world of modernism.

"I pick up my pen. It flows. A building appears. There it is. There is nothing more to say" [13].

Translations: Agnieszka Żabicka

References

[1] *A redescoberta de Niemeyer, Oscar Niemeyer, Paulo Mendes da Rocha e MMBB arquitetos: Oca do Ibirapuera*, [in:] Projeto Design, ARCO, São Paulo, 05.01.2010, arcoweb.com.br/projetodesign/arquitetura/oscar-niemeyer-paulo-mendes-da-rocha-mmbb-arquitetos-oca-do-01-05-2000 (access: 28.03.2017).

[2] Drumm, P., *Niemeyer Inspired By Curvaceous Brazilian Women For His Converse Collection*, The Architects Newspaper, 06.11.2012, https://archpaper.com/2012/11/product-niemeyer-inspired-by-curvaceous-brazilian-women-for-his-converse-collection (access: 25.03.2017).

[3] Entini, C.E., *Marquise do Ibirapuera foi projetada por Niemeyer*, Acervo, 13.12.2012, http://acervo.estadao.com.br/noticias/acervo,marquise-do-ibirapuera-foi-projetada-por-niemeyer,8775,0.htm (access: 25.03.2017).

[4] *História e Fotografias Históricas*, Parque Ibirapuera Conservação, São Paulo, http://parqueibirapuera.org/parque-ibirapuera/historia-mais-completa (access: 20.03.2017).

[5] *Marquise do Parque Ibirapuera*, Parque Ibirapuera Conservação, São Paulo, http://parqueibirapuera.org/areas-externas-do-parque-ibirapuera/marquise-do-parque-ibirapuera (access: 20.03.2017).

[6] Metz T., *Form Follows Feminine: Niemeyer, 90, Is Still Going Strong*, Architectural Record, December 1997.

[7] Moore R., *Green Space, The 10 Best Parks*, The Guardian, London 07.08.2015, www.theguardian.com/culture/2015/aug/07/10-best-parks-urban-green-spaces-high-line-new-york-hampstead-london-park-guell-barcelona (access: 18.03.2017).

[8] Niemeyer O., *Minha arquitetura1937–2004*, Revan, Rio de Janeiro 2000.

[9] Niemeyer O., *Oscar Niemeyer: 1999–2009*, 7 Letras, Rio de Janeiro 2009.

[10] Niemeyer O., *The Curves of Time: The Memoirs of Oscar Niemeyer*, 2000, Phaidon, New York 2007.

[11] Oscar Niemeyer Quote Citation, [in:] BrainyQuote.com. Xplore Inc, 2017, www.brainyquote.com/quotes/quotes/o/oscarnieme479739.html (access: 29.03.2017).

[12] Oscar Niemeyer Quote Citation, [in:] BrainyQuote.com. Xplore Inc, 2017, www.brainyquote.com/quotes/quotes/o/oscarnieme419624.html (access: 29.03.2017).

[13] Oscar Niemeyer Quote Citation, [in:] BrainyQuote.com, Xplore Inc, 2017, www.brainyquote.com/quotes/quotes/o/oscarnieme479751.html (access: 29.03.2017).

[14] *Quem somos*, [in:] „Auditorio Ibirapuera Oscar Niemeyer", São Paulo 2011, www.auditorioibirapuera.com.br/quem-somos (access: 12.03.2017).

TECHNICAL TRANSACTIONS 8/2017
CZASOPISMO TECHNICZNE 8/2017
CHEMISTRY
DOI: 10.4467/2353737XCT.17.126.6877

Joanna Kuc (e-mail)
Adam Grochowalski
Marianna Kostina
Department of Engineering and Chemical Technology, Faculty of Chemical Engineering and Technology, Cracow University of Technology

Determination of the diastase activity in honeys

Oznaczanie aktywności diastatycznej miodów

Abstract

The diastatic number in five samples of honey has been determined by two methods: according to guidelines included in Polish standard PN-88/A-77626 and the Phadebas method. Research shows that the storage of honeys did not have a significant impact on lowering of diastatic number. However, long-term storage of honey was characterized a reduction of the diastase number. The correlation between the two applied methods was very strong ($r = 0.921$).

Keywords: diastase number, honey

Streszczenie

Oznaczono liczbę diastazowa w pięciu miodach metodą rekomendowaną w normie PN-88/A-77626 i według metody Phadebas. Badania wskazują, że warunki przechowywania miodów nie miały większego wpływu na obniżenie liczy diastazowej. Jednak przechowywanie miodów przez dłuższy czas powoduje obniżenie wartości liczby diastazowej. Korelacja pomiędzy dwoma stosowanymi metodami była bardzo silna ($r = 0{,}921$).

Słowa kluczowe: liczba diastazowa, miód

1. Introduction

Honey is known as a traditional high-grade and health-promoting natural food product. The antibacterial and anti-inflammatory properties as well as antioxidant activities have led to the application of honey in medicine [1, 2].

Honey, like every food product intended for sale, should have a certain quality determined by the applicable legislation [3]. The appropriate organoleptic and chemical parameters are provided only with proper preparation, processing and storage of honey. Any strange tastes, odours or food ingredients cannot be present in honey marketed for human consumption. Honey also must not have begun to ferment or have been heated in the way that destroyed or significantly inactivated the natural enzymes. The main quality parameters of honey are: diastase activity, concentration of proline and electrical conductivity, as well as the content of free acid, hydroxymethylfurfural (HMF) and sucrose [3].

Diastase (α-amylase) is one of the predominant enzymes in honey, next to invertase and glucose oxidase, which is added to honey by the bee during the collection and ripening of flower nectar [4]. One unit of diastase activity is defined as that amount of α-amylase, which will convert 0.01 gram of starch to the prescribed end-point in one hour at 40 °C. The results are expressed in Schade units per gram of honey and termed Diastase Number (DN) [5].

By the end of 2002, in Poland, DN was determined based on the guidelines contained in Polish standard PN-88/A-77626 [6], which recommended the Schade procedure for the measurement of diastase activity [7]. Currently, Regulation of the Minister of Agriculture and Rural Development of January 14th, 2009 (Dz. U. No. 17, pos. 94) [8] is valid in Poland. This regulation is in accordance with the EU Honey Directive 2001/110/EC and the guidelines of the International Honey Commission (IHC) [9] formed in 1990 in order to establish a new standard for honey. IHC recommended Phadebas assays as the official analysis methods for the determination of diastase activity in honey.

In the PN-88/A-77626 method, the diastatic activity of the honey is determined based on a distribution of the starch solution by α-amylase. The Phadebas method uses a synthetic biochemical substrate known as the *Phadebas tablets,* which are a water-insoluble, cross-linked starch polymer dyed in blue. The tablets are hydrolyzed by α-amylase to water-soluble form and the absorbance of the blue solution is a function of the diastase activity. The method is based on measurement of the absorbance of the solution at 620 nm against distilled water [10].

The EU Honey Directive 2001/110/EC states that the honey marketed for consumption must meet the following criteria for DN: no less than 8 Schade units for most of honey and no less than 3 for honeys with low natural enzyme content e.g. citrus honeys [3].

The aim of the study was to control the diastatic activity of several varieties of honeys obtained from different sources: directly from beekeepers and purchased in a store. The honey samples were stored under various conditions to assess the effects of temperature and time of storage on the DN value. In the presented studies, the two methods were applied and compared. The diastase activity was measured according to the method recommended by Polish standard PN-88/A-77626 and according to the Phadebas test recommended by the valid Regulation of the Minister of Agriculture and Rural Development of January 14th, 2009 (Dz. U. No. 17, pos. 94).

2. Materials and methods

Samples of several varieties of honeys from different sources and stored under different conditions comprised the research materials. Characteristics of the samples are summarized in Table 1.

Table 1. Characteristic of analysed honey samples

Sample	Type of honey	Origin	Condition and time of storage
H1	Multiflorous	Non-commercial; from southern of Poland	Stored for 2 month at 4 °C
H2			Stored for 2 months at room temperature
H3	Multiflorous	Commercial; from EU countries and non-EU	Stored on a store shelf (lack of information about the time), and then in the cupboard for 4 years
H4	Buckwheat	Commercial; from EU countries and non-EU	Stored on a store shelf (lack of information about the time), and then in the cupboard for 2 years
H5	Honeydew	Commercial; lack of information about the origin	Stored on a store shelf (lack of information about the time), and then in the cupboard for 2 years

The diastase activity expressed by DN was measured according to Polish standard PN-88/A-77626 method (Method A) and the Phadebas method (Method B). DN determination was performed in three repetitions for each method.

Method A is based on the distribution of the starch by α-amylase. The first step of the research was to prepare the starch solution. Anhydrous starch was dissolved in water and the suspension was rapidly brought to the boil point. The flask was stirred constantly and boiled gently for approx. 3 minutes. The solution was immediately transferred to a 100 mL volumetric flask, cooled down rapidly to room temperature and made up to volume with water. The clear blue solution was made on the day of use.

Iodine solution was prepared by dissolving of 10.0 g of twice-sublimated iodine and 20.0 g of potassium iodide in 40 mL of water. The solution was diluted to 500 mL and kept in a closed dark bottle.

Ten grams of honey was dissolved in 25 mL of distilled water saturated with toluene and titrated with sodium hydroxide solution (0.05 mol/L). Phenolophtalein was used as an indicator in the titrations. After titration, the solution was transferred to a 100 mL volumetric flask and made up to volume with water.

In the next step, the following were added to 12 polypropylene tubes: the solution of honey, water, acetic acid, sodium chloride and 1% starch solution in the amounts indicated in Table 2 [6]. Test tubes were placed in a water bath at 45–50 °C and incubated for one hour. The tubes were then cooled and 1–2 drop of 0.05 mol/L of iodine solution was added to each one. The change of colours of the solutions was observed immediately.

Table 2. DN values in the prepared samples

Sample no.	Honey solution [mL]	Water [mL]	Acetic acid [mL]	Sodium chloride [mL]	Starch solution [mL]	DN
1	10.0	4.0	0.5	0.5	1.0	1.0
2	10.0	2.5	0.5	0.5	2.5	2.5
3	10.0	0.0	0.5	0.5	5.0	5.0
4	7.7	2.3	0.5	0.5	5.0	6.5
5	6.0	4.0	0.5	0.5	5.0	8.3
6	4.6	5.4	0.5	0.5	5.0	10.9
7	3.6	6.4	0.5	0.5	5.0	13.9
8	2.8	7.2	0.5	0.5	5.0	17.9
9	2.1	7.9	0.5	0.5	5.0	23.8
10	1.7	8.3	0.5	0.5	5.0	29.4
11	1.3	8.7	0.5	0.5	5.0	38.5
12	1.0	9.0	0.5	0.5	5.0	50.0

Diastase activity in the honeys was also determined using Phadebas tablets (Phadebas Amylase Test, Magle AB, Sweden) by a photometric method (Method B) using Shimadzu UV-160A spectrophotometer. Absorbance at 620 nm of the analysed solutions was directly proportional to the diastatic activity of the honey samples.

The first step of Method B was to prepare acetate buffer by dissolving 13.6 g of sodium acetate trihydrate in water. The pH of the solution was adjusted to 5.2 with glacial acetic acid. The solution was diluted to 1L with distilled water and stored in a glass bottle.

One gram of honey was weighed, quantitatively transferred to a 100 mL volumetric flask and made up to volume with acetate buffer. Five millilitres of the sample was transferred to the test tube and placed in a water bath at 40 °C. At the same time, under the same conditions, the blank (5 mL of acetate buffer) was heated in a water bath at 40 °C. After 15 minutes, 1 Phadebas tablet was added to the two solutions, stirred (approx. 10 sec.) and placed back into the water bath at 40 °C. After exactly 30 minutes, 1 mL of sodium hydroxide solution was added for interrupt the enzyme reaction.

In the next step, the solutions were centrifuged (5 minutes; 1500 rpm) and the absorbance was measured at 620 nm against distilled water as the reference sample.

The DN, repeatability and reproducibility were calculated based on the models specified in the instruction for Phadebas method [10]

3. Results and discussion

In Method A, a colour change were observed. The purple colour indicated a complete hydrolysis of starch. Based on the data contained in Table 2, the appropriate value of DN was chosen. Fig. 1 shows an example image illustrating the experiment by Method A for sample

H3. In tubes 5 and 6, incomplete hydrolysis of starch is observed. The reaction is complete only in tube 7. The DN for the solution in tube 7 is 13.9 Schade units.

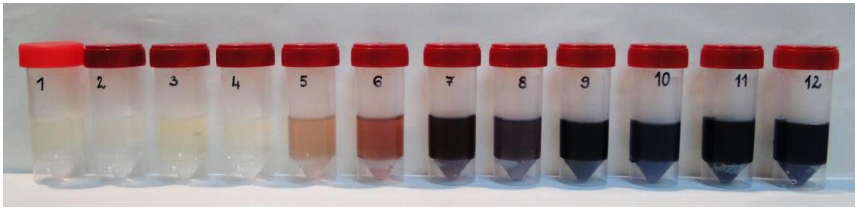

Fig. 1. The picture of honey sample 3 prepared by Method A

Diastase activity determined using Phadebas tablets is proportional to the absorbance at 620 nm.

The repeatability (r) and reproducibility (R) determined by Method B were calculated based on equations specified by the Phadebas producer [10]:

$$r = 0.02+0.03\cdot\Delta A_{620}$$
$$R = 0.04+0.32\cdot\Delta A_{620}$$

0.02, 0.03, 0.04 and 0.32 means constant to account for the relationship between the diastatic activities of honey, ΔA_{620} is the difference in absorption of the test solution of honey and the blank.

The results of repeatability and reproducibility are summarized in Table 3.

Table 3. Summary of repeatability (r) and reproducibility (R) for Method B

Sample	r	R
H1	0.04	0.24
H2	0.04	0.21
H3	0.03	0.11
H4	0.03	0.12
H5	0.03	0.13

For Method B, the DN of the samples were calculated from linear regression of diastase number against ΔA_{620} yielded the following relation [10]:

$$DN=28.2\cdot\Delta A_{620}+2.64$$

The results of DN calculated by Method A and Method B are summarized in Table 4. Correlation between DN obtained by the two methods is shown in Fig. 2.

Table 4. DN values obtained by the two used methods

Sample	DN by Method A	DN by Method B
H1	23.9	20.3
H2	17.9	17.6
H3	13.9	9.0
H4	10.9	9.4
H5	10.9	11.0

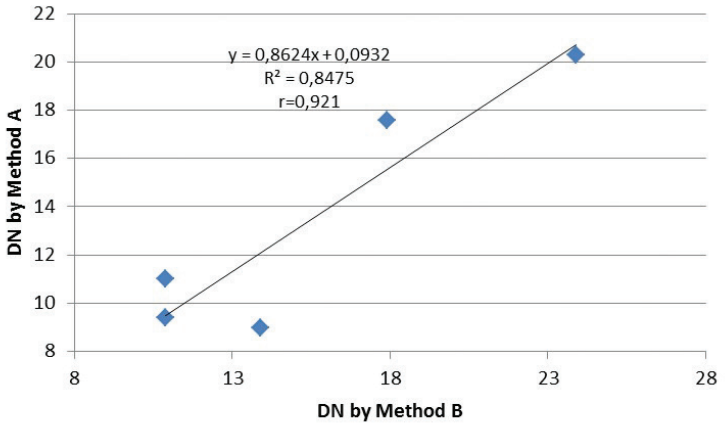

Fig. 2. Correlation between DN by Method A and Method B

The biggest difference between Method A and Method B occurred in the case of a sample of multiflorous honey H3. A possible explanation might be that the Phadebas test uses a defined substrate, whereas commercially available starch may vary considerably in quality. The differences in the two methods could also be explained by the lower precision of enzymatic methods. In the case of the other samples, the differences between the two methods were very small. Correlation between DN obtained by the two methods was very strong. The correlation coefficient (*r-Pearson*) for the methods is 0.921.

The DN values marked by Method B are very similar to the results of tests conducted in accordance with Method A. All tested samples were within regulatory requirements because the DN is greater than 8. The highest value activity of α-amylase has a non-commercial flower honey H1 derived directly from the beekeeper and stored at 4 °C. The same honey samples, but stored at room temperature, are characterized by slightly lower DN (17.6). This insignificant difference may indicate little effect of storage conditions on the value of DN in fresh honey. The lowest DN was marked for multiflorous honey H3. To determine the effect of storage conditions on diastatic activity of honeys, further studies are indicated.

4. Conclusions

Two different methods were used to determine the number of diastase in honeys: the method recommended in Polish standard PN-88/A-77626 and the Phadebas method. There is a strong correlation between the diastase activities determined by using those two methods.

References

[1] Al-Mamary M., Al-Meeri A., Al-Habori M., *Antioxidant activities and total phenolics of different types of honey,* Nutrition Research 22, 2002, 1041–1047.

[2] Mandal M.D., Mandal S., *Honey: Its medicinal property and antibacterial activity,* Asian Pacific Journal of Tropical Biomedicine 1, 2011, 154–160.

[3] Council Directive 2001/110/EC of 20 December 2001 relating to honey. Official Journal of the European Communities, http://www.ihc-platform.net/honeydirective2001.pdf (access: 23.05.2017).

[4] Persano Oddo L., Baldi E., Accorti M., *Diastatic Activity of Some Unifloral Honeys*, Apidologie, 21, 1990, 17–24.

[5] Diastase Activity (a-AMYLASE) in Honey Assay Procedure K-Amzhy 10/07. Megazyme International Ireland 2007, https://www.megazyme.com/docs/analytical-applications-downloads/amylase_in_honey_30602 (access: 23.05.2017).

[6] Polska norma PN-88/A-77626 Miód pszczeli, Wyd. Normal, Alfa, Warszawa 1988.

[7] Schade J. E., Marsh G.L., Eckert J. E., *Diastatic activity and hydroxymethylfurfural in honey and their usefulness in detecting heat adulteration,* Food Research 23, 1958, 446-463.

[8] Rozporządzenie Ministra Rolnictwa i Rozwoju Wsi z dnia 14 stycznia 2009 r. w sprawie metod analiz związanych z dokonywaniem oceny miodu (Dz. U. Nr 17 poz. 94).

[9] Harmonised methods of the International Honey Commission. Stefan Bogdanov, Bee Product Science, http://www.ihc-platform.net/ihcmethods2009.pdf (access: 23.05.2017).

[10] Honey Diastase Test. Instructions for use, Magle AB, Sweden 2010, www.phadebas.com (access: 23.05.2017).

TECHNICAL TRANSACTIONS 8/2017
CZASOPISMO TECHNICZNE 8/2017
CIVIL ENGINEERING
DOI: 10.4467/2353737XCT.17.127.6878

Krystyna Araszkiewicz (krystyna.araszkiewicz@zut.edu.pl)
Faculty of Civil Engineering and Architecture, West Pomeranian University of Technology Szczecin

Anna Tryfon - Bojarska
Aleksander Szerner
Skanska S.A.

Modern information management throughout a construction project life cycle – selected issues concerning digitization in construction and a case study

Nowoczesne zarządzanie informacją w cyklu życia obiektu budowlanego – wybrane zagadnienia cyfryzacji w budownictwie oraz studium przypadku

Abstract

The use of innovative technologies and digitisation tools may significantly improve the preparation and execution of a construction project. The article discusses the results of the latest research concerning digitisation in construction and an innovative model of communication between participants of a construction project in reference to the Building Information Modelling method, the concept of Integrated Project Delivery and Facility Management principles. Conclusions from the analysis of results of implementation of innovative, digital tools and information management techniques will be presented using case studies of three construction projects - the construction of the New Karolinska Solna University Hospital in the Stockholm region, an office building in Wrocław and the expansion of the national road No. 8 to meet the parameters of an express road at the Wyszków–Poręba hub.

Keywords: information management, digitisation, BIM, construction project life cycle, Facility Management

Streszczenie

Wykorzystanie nowoczesnych technik i narzędzi cyfryzacji może w istotny sposób usprawniać przygotowanie i realizację przedsięwzięcia budowlanego. W artykule omówiono wyniki najnowszych badań związanych z cyfryzacją w budownictwie i nowoczesnym modelem komunikacji pomiędzy uczestnikami przedsięwzięcia budowlanego, w nawiązaniu do metody Building Information Modelling (BIM), koncepcji Integrated Project Delivery oraz według założeń Facility Management. Przedstawiono wyniki analizy wdrożenia nowoczesnych, cyfrowych narzędzi i technik zarządzania informacją na przykładzie trzech przedsięwzięć budowlanych – budowy szpitala uniwersyteckiego w Sztokholmie New Karolinska Solna, biurowca we Wrocławiu oraz rozbudowy drogi krajowej nr 8 do parametrów drogi ekspresowej Wyszków–węzeł Poręba.

Słowa kluczowe: zarządzanie informacją, cyfryzacja, BIM, cykl życia obiektu budowlanego, Facility Management

1. Introduction

Information technology (IT) is of crucial importance for business development and efficiency. The latest trends in management are associated with the use of semantic technologies, the ontology of management and cyber-physical systems [1]. Digitization is increasingly used in the economy through the involvement of technology and digital tools in business development, the creation of jobs and the generation of gross domestic product. However, the construction industry in Europe is characterized by a low level of digitization. This is because this industry is represented by few medium-sized companies on the market. There are large and very large companies in this industry that regularly work with small subcontractors using IT tools. However, the sector consists primarily of small subcontractors that perform small jobs, such as renovation and retrofit, and often operate semi-legally. Most of these organizations use traditional solutions rather than sophisticated information and communication technologies (ICT) in business management. The industry is also stretched between large companies and small renovation and construction teams in Poland. This translates into low results of construction in the ranking of the digitization of the European and Polish economies [2].

The aim of this article is to present the latest research on the digitization of the construction sector and IT supporting information and communication management throughout the construction project life cycle. Furthermore, the article discusses the analysis of the implementation of modern digital tools and techniques for managing information through the example of three construction projects.

The research methods include a literature review involving publications from 2010 to 2016, selected on the basis of keywords related to digitization in the construction industry, using online databases of scientific papers (Science Direct, Google Scholar, BASE). The empirical part is based on the case study method. Both the literature review and the practical application of IT are presented with reference to the Building Information Modelling (BIM) method in a context of the concept of Integrated Project Delivery and information management in the operation phase of a building according to the principles of Facility Management.

2. Specific features of information management in the construction industry

Information management involves the acquisition, classification, collection, processing, presentation, dissemination and implementation of information. Construction and installation companies manage a wide range of data flow, including [3]:

- information required to develop an bid, cost estimation (price lists, price catalogues), the base estimation of the subject matter of the contract and its revaluation during the project implementation;
- the knowledge base developed during the project implementation;
- analytical elements and project optimization;
- project implementation;
- building maintenance.

According to Parsanezhad, effective management of so much data requires constant acquisition, analysis and flow of information in a multidisciplinary environment throughout the building life cycle. The association BuildingSMART defines this approach as a holistic business process involving the generation and use of data in order to design, construct and then use a building. To ensure the efficiency of the information flow, it is essential to identify three main phases in the building life cycle and to treat the use phase with the same significance as the first two phases, i.e. design and construction [4].

There is an important relationship between the organization's information system and its strategy and organizational structure. Understanding information systems is essential to understanding technological changes in enterprises. A huge and varied collection of information at a construction company can be organized into systems associated with one another [2]:

- supporting decisions including simulation systems;
- risk management;
- taking part in information exchange between systems of various manufacturers at the level of source data;
- managing knowledge at an organization Information databases on technology usefulness;
- analysis of competition based on offers and offer prices as well as the current involvement into projects;
- supporting analysis of contracts;
- supporting project management and project portfolio management;
- supporting quality management system and environmental protection system;
- supporting document flow;
- production settlement;
- supporting logistics and supply management;
- supporting technical documentation management;
- preparing cost estimates along with unit prices of equipment, materials and costs of labour for a given company;
- monitoring vehicles and machines with the use of GPS;
- databases relating to enforcement standards and average prices of materials, labour and equipment;
- supporting management with a completed/handed-over facility, device, e.g. building, motorway or expensive construction equipment;
- information about the history of expenditure incurred, the profit generated, work time and return on investment.

Hadaya and Pellerin believe that an important feature of the construction project life cycle, affecting the conditions of information management, is a large number of participants in the project, who are in different locations, use a variety of information techniques and tools and work with data at different levels of specificity and with information at different levels of abstraction [5]. Viljama and Peltomaa indicate that varying technologies and different levels of technological competence among subcontractors and other project participants lead to difficulties with effective integration of data and their use in construction projects.

Necessary information may be dispersed and included in different systems characterized by varying degrees of technological advancement [6]. According to Bankvall *et al.* it is essential to disseminate IT tools and techniques under these specific conditions in order to improve information flow and management throughout the construction project life cycle. Information standards should support the digitization process [7]. Lönngren *et al.* identify the standardization of information as potentially the most important factor in stimulating the productivity of the construction industry [8].

The benefits from the implementation of ICT solutions in the architecture, engineering and construction (AEC) sector can be enormous, especially considering the effects of management activities. Digital techniques and tools implemented in the construction industry include:

- the virtual network (Internet);
- wireless communication;
- virtual reality (VR), mixed reality (MR) and augmented reality (AR);
- the BIM method in a broad sense;
- data exchange and management.

The use of digital information in the construction industry is a developing trend, which strongly affects the ability to anticipate and solve engineering problems throughout the construction project life cycle. The increasing availability of advanced techniques generates new types of digital sets of information, electronic documents and models of buildings, as well as spatially oriented information that is archived using the global positioning system. Information is most often processed on a construction site using traditional methods, which are relatively slow, associated with a high risk of human error and thus inefficient. Furthermore, project participants do not know all important parameters of the processes covered by the construction project. This implies management challenges, especially in the area of construction control [8]. The supply chain phase in the building life cycle is an important area of research on information management in this life cycle.

2.1. Information in supply chain management in the construction industry

A construction supply chain is characterized by [9]:

– convergence at the site of construction materials;
– one-off projects facilitated by repeatable processes of project organizations;
– a make-to-order supply chain – delivery on request.

From the point of view of a construction company, a supply chain should raise the value delivered to customers and establish new performance standards which require optimization in many areas. Even if adapted to the needs, the flow of information about the scope of supply may not be sufficient and so information management skills become important. The dynamics of internationalization and globalization processes, as well as increased competition in the construction market make traditional models of information management insufficient to carry out construction projects in an efficient and successful manner [10].

In supply chain management, it is necessary to integrate a number of areas that are the source of diverse information. These include design, material requirements planning,

product delivery and subcontractor management. Digital techniques help integrate different sets of information, acting as a key facilitator. The main advantage is the ability to share strategic, tactical and operational information. One of the results is the reduction of costs associated with the precise planning of logistic processes and the possibility of their accurate monitoring [11]. Information management in modern supply chains should be organized in such a way as to implement the principle of 3V (visibility, velocity, versatility). Visibility focuses on resources, inventories in particular (inventory visibility), and indicates that they can be monitored throughout the supply chain. Velocity is the ability to meet the needs and perform a contract in a short time. Versatility means the ability to work with suppliers and customers under different conditions of delivery (coordination versatility). These elements constitute the three pillars of adaptive supply chains. IT tools and techniques greatly facilitate implementation of the 3V principle in construction supply chains [10].

2.2. IT technology and BIM

In the modern building life cycle, information management can be organized through the use of BIM technology and an interactive communication platform. A BIM model is a database that helps project managers use information through unlimited access to the digital documentation of projects, gathered in an IT communication system. Underwood and Isikdag claim that BIM, defined not only as building information modelling but also as a method for information management, acts like a shared information backbone through the life cycle of the project [12]. The BIM approach involves information management based on the exchange of information using the model and for example IFC format, even if most of the processes are based upon traditional means of communication, such as the exchange of paper documents in the form of printouts or face-to-face meetings of project participants [13]. In the construction project life cycle, BIM involves the integration of information flowing between the parties throughout the life cycle, in line with the IPD (Integrated Project Delivery). The essence of this method is to produce and process digital information about each phase of the construction project life cycle. BIM involves intensive collaboration between stakeholders, which is a basis for an effective exchange of information and data flow. This cooperation can contribute to a better integration of the previously dispersed construction sector and participants of construction projects, thus improving the economic efficiency [14]. Redmond *et al.* indicate that the letter "I" in the acronym "BIM" concerns synchronization of information across the construction project life cycle, the aim of which is to increase the speed and efficiency of work processes and facilitate management decision-making based on well-organized and adequate solutions [15]. Nicał and Wodyński indicate the following application areas of BIM [16]:

- the real-time resource location – productivity and safety can be optimized through integration of a BIM model with Radio Frequency Identification (RFID) technology or the barcode-based system;

- digital data management system that allows for real-time storing, finding and sharing these data;
- planning renovation or retrofit and developing a feasibility study for these works;
- activities related to the operation and maintenance of the building;
- energy analysis and simulation, control of electronic systems in the building management phase as part of Facility Management;
- health and safety management during construction and operation.

There is a growing interest among researchers and practitioners in the use of IT technology and BIM throughout the building life cycle, which means that construction managers will need to be added to the group of participants using the platform for data exchange and communication. The scope of information required for effective property management is extensive, and the main problems related to this issue are associated with access to information and the completeness and timeliness of data. Information contained in traditional two-dimensional as-built documentation is much dispersed. Its use for analysis, decisions and actions related to building operation can be time consuming and costly. Facility Management (FM) is a new concept in Poland aimed at lowering the cost of building operation, improving the quality of resources, investing in real estates to fit the current needs of both owners and users, as well as at identifying and using hidden reserves. The International Facility Management Association defines FM as the practical coordination of physical jobs with people and an organization that integrates the principles of business administration, architecture and the maintenance of technical objects. The scope of information required in FM activities depends on the specifics of the property management system, but it generally includes necessary data on space management, technical maintenance and work to ensure the comfort of users. The integration of hardware and software responsible for the proper operation of technical installations in a building may significantly reduce operating costs, improve the working conditions of people residing in the building, increase their sense of security and shorten the payback period of the investment. The integration of energy management, security, fire protection and other necessary installations may be particularly effective. Management software should allow insight into accurate data, thus enabling a quick reaction to events.

According to Nicał and Wodyński, the major challenges and barriers associated with the practical implementation of such a holistic approach are as follows [16]:

- unclear roles and responsibilities regarding the BIM model;
- vaguely defined roles and competences of the project participants;
- data requirements – level of development (LOD) needed;
- the role of FMs is underestimated in the construction project life cycle and the lack of FM input during the early stages of the project delivery process;
- interoperability concern – information exchange and transfer;
- the lack of BIM knowledge/experience among FM practitioners;
- change-resistant attitude, lack of cases proving the positive business value.

3. Case studies

3.1. New Karolinska Solna Hospital

The world-class university hospital New Karolinska Solna (NKS) belongs to the Karolinska Insittutet, one of Sweden's leading medical universities (Fig. 1). The hospital is located in Sweden, in the city of Solna in the Stockholm region. The construction of NKS is a PPP project realised by a public partner: Stockholm County Council (Stockholms läns landsting) and private partners: Skanska Sweden, Skanska Infrastructure Development, Skanska UK, and the British investment fund Innisfree. The partnership agreement between Stockholm County Council and Swedish Hospital Partners, a partnership established by Skanska and Innisfree provides for funding, construction as well as maintenance and management of the new hospital by 2040. After completing the tasks of design, construction and funding of the endeavour, the project company will be obliged to provide the service of hospital availability which means, maintaining the technical state of the hospital's buildings at the contractual level for a specified time. The maintenance and use of the building include a series of other services such as: cleaning, maintenance of the building or logistics necessary for the proper functioning of the contractual hospital infrastructure. Initial approval of the project by the investor took place in December 2008, then on 31 March 2009 an invitation to tender was published, while the submissions to the tender ended on 30 September 2009. The letter of intent was signed with the private partner in December 2009. The design work began in 2010, after the final agreement was concluded. The estimated project value was SEK 14.5 billion. According to the schedule, the investment is being implemented in stages and the first patients were served already in 2016, in buildings constructed during stage 1. The end of all construction work along with the transfer for use of all the buildings is planned for 2018.

The main goals the contractor had to complete included:

- creating a building of high architectural standards, both internal and external as well as in the close vicinity of the building,
- applying construction solutions which will support effective and optimal processes of resource utilisation,
- realisation of the rules of sustainable construction combined with smart building concept principles.

NKS is going to be one of the first hospitals in the world that follows the strict environmental guidelines of the international LEED Gold certification, which requires the environment-friendly material and technology solutions in the course of the construction of the building. One of the applied examples are the green roofs which serve as thermo-insulation and have a positive effect on the energy balance and internal climate of the building.

Creating the environment for sustainable transport related to the building's use is yet another solution. 10% of the parking spots are going to be fitted with charging stations for electric cars. The building's energy supply is planned to make use of geothermal energy, which will cover 65% of the energy needed for heating and cooling purposes. The environmental

Fig. 1. Visualisation of NKS Hospital building. Source: Skanska materials

guidelines were taken into account from the earliest stages of the project and decision-making processes in the following areas: energy-efficiency, minimisation of the environmental impact of the project, environmental certification by an independent entity, balanced materials and waste management, provision for high quality microclimate inside the buildings.

Parameters approved at the conceptual stage of the project should be considered along with the initial principles which illustrate the scale of the project. These include:

- 1800 people being present on the construction site during the most intensive construction period,
- the buildings will feature approx. 8000 rooms including patient rooms, 36 operating theatres, 8 radiation units, 168 doctor's surgeries as well as laboratories and lecture halls,
- the buildings will have 12 floors with a total area of 320 000 m^2, including a 2-level underground parking.

The concept of the NKS building life cycle assumed that the end users of the hospital complex such as doctors and medical staff will be included in the design process as soon as possible, in order to take their needs related to patient care such as privacy and safety of the patients, into account. One of the earliest principles was to provide one, dedicated room for each patient, where he will stay for the whole treatment time, in order to reduce the need to transport him within the hospital, between the wards.

Management of such a large and complex project is a challenge. One of the main principles aimed to facilitate it was to use the BIM method throughout the life cycle of the process as well as supportive techniques – Virtual Design & Construction. BIM tools were used to calculate life cycle risks over 28-year operation and maintenance PPP contract, including the regular upkeep

of components and the periodical replacement of larger equipment. The models were also used in energy simulations for the building, which will support the project in achieving its ambitious energy targets. An as-built BIM model was prepared, including comprehensive structure with regard to placement, function and product. The model comprises generic objects with relevant information only, linked to information, directly (in the model) or indirectly (through links or related databases). From the very beginning, it was assumed that the model would be updated throughout the use of the building, being a valuable source of information for the building's administration. After the contract is finished it will be handed over to the public partner.

The project included innovative solutions at the design stage, which were intended to facilitate the information flow between the users during subsequent stages of the life cycle of the project and provide the means for proper communication with end users of the hospital. The contractors decided to use Autodesk Revit combined with a newly developed and industry specific application. The team of designers together with their Autodesk Partner Cad-Q have developed cloud-based database solutions to handle room descriptions, fixtures and change management. This technology links the databases with the design tool Revit in order to process the information in a database environment instead of in the design mode. Everyone involved was working according to one and the same model of the project [17]. The designers together with the doctors and medical staff were discussing the placing the certain elements in certain rooms. This discussion was supported by usage of a virtual room, where common meetings were held. The BIM model was converted into Virtual Reality, so the doctors and nurses could feel the space that they could work in in the future. This solution caused the reduction of post construction failures thank to the engagement of the final product user at the design stage.

At the realisation stage, BIM was used to analyse the work stages in detail, support the project logistics, support the communication on the project and all analytical aspects. For the needs of the project the 4D schedule was created together with information about the cost analysis, and information about material delivery. The parametric model of the hospital was connected with the temporary schedule, which helped to see the daily situation of the project: which work will be completed, were H&S hazards will be located, how to plan the materials delivery, how many people should work on a certain day and in which part of the project. BIM integration scope during construction included:

- equipment data collection,
- document collection,
- issue tracking,
- commissioning scripts.

At the building's utilisation management stage, the BIM model was designed to support the hospital utilisation processes, helping the building's administrator in running installation check-ups and understanding their functioning. For example, information that the model provides on floor space facilitates planning of cleaning and other hospital upkeep. If a lamp breaks, the model will show not only what type of lamp it is, but also whether a ladder will be necessary to replace it. It is also possible to draw conclusion on the priority of measures, as it is more important that everything functions optimally in an operating theatre than in a break room.

Fig. 2. NKS Mobile Application Screen. Source: Skanska

Another example of an interesting FM-related solution is a system called JiT cabinets, designed to supply the hospital with medical materials and accessories. The system was designed together with the future users of the building and the supplier of FM software and hardware for new NKS buildings. The JiT cabinets for equipment and materials are located in niches at several places on every floor close to the main corridors. The cabinets are the final link in an automated chain that leads to the user, such as staff in an operating theatre. The contents are readily visible and easily accessible. Material supply to the cabinets takes place mainly using robots that control trucks loaded with textiles or sterile goods to and from the units. Virtually all transport takes place using these robot trucks, automated guided vehicles (AGV), which have their own lifts and will carry out around 1600 transports per day. Since the operation planning system can talk with the sterile unit's IT systems, everything will be in place when it is needed. The chain includes sterilisation, material supply and the so-called value-added process that consists of the AGVs and the JiT stores.

The information management system designed for the NKS Hospital includes solutions made to inform the external stakeholders, including the local community. A showroom available to anyone interested in the project was designed and built. With the help of film, images and an interactive model everyone will learn more about the NKS project and the future healthcare system. To strengthen the communication concerning the project information a special application was created (Fig. 2), which everybody could load on their mobile.

The NKS project's app allows navigation round the hospital area and inside the main building. Thanks to this application everyone can see what it will look like when it is fully open.

3.2. Green 2 Day office building

The construction of the Green 2 Day office building in Wrocław is yet another example of digital technologies being adopted for the purposes of construction process. The building will be located in the centre of the city, its office space will be 17 000 m^2. The building was designed in accordance with LEED Gold standards. The solutions used in its design include energy use reduction by 25% and water use reduction by 45% compared to local standards. The construction stage is planned for 25 months.

A cloud-based BIM 360 Docs app is used for project management in this case. This tool allows the contractor to store and manage project files online from any location, and to exchange comments and suggestions between various participants of the process, using technical documentation, which facilitates horizontal coordination. Documents are kept in order in an online repository; the members of the contractor's team can access all the up-to-date files the contractual documentation comprises. Thanks to additional apps, the tool monitors the weather and the conditions during the process of mounting specific elements. The data is then archived. This enables the software to store the data which may be relevant for the maintenance process of the building for future users. In the contemplated example, the BIM 360 Docs app is used on mobile devices and in smart kiosks, which are used for H&S (health and safety) briefings and short operational meetings, facilitating the communication on the contractor's team. In executing the analysed investment, also the BIM 360 Field application was used, whose application allowed components to be monitored during the entire process of development. Components from many groups (prefabricates, components of mechanical systems, switch gears, slings) are coded in the system using unique numbers. Some components also use links in the form of QR codes that allow to be read from the label placed on a component by means of a tool built into the BIM 360 Field and to immediately go to the website of a given component. Prefabricated components such as posts and beams receive labels with codes at the manufacturing plant while during acceptance of the delivery, the supervisor has access to entire workshop documentation of the component after reading the code. Mechanical system components (control units, fans, fire dampers), besides access to catalogue cards, drawings, selection cards and lists, feature additional properties that help in simplifying the process of planning start-ups. These properties are entered by contractors responsible for a given area. Thanks to the above, start-up meetings relate to planning and resolving problems and there is no need to spend time on information gathering.

The use of these tools has an impact primarily on savings of time which would normally be used for hosting technical meetings, gathering information and coordinating communication on the construction site. The construction manager, during inspection and prior to daily meetings, takes photos using a portable device (tablet), and then during the meeting, he prepares notes. Particular subcontractors are saved in the database and the system. The names of their employees and tasks planned for the upcoming day are recorded. In the project discussed, the use of BIM 360 Team, including the BIM360 Docs application, is pilot-like in character. For initial identification of results, a survey was completed among 20 participants of the investment process, representing the supervising inspector, the investor and the general contractor.

The respondents' answers show that the average weekly time savings achieved thanks to the use of digital tools covered by the BIM360 system is 5.5 hours. Other advantages listed by the respondents included improved arrangement of documentation flow in the process and a significant improvement of information flow relating to occupational health and safety [18].

3.3. The expansion of the national road 8 between Warsaw and Białystok

The subject of this project is the expansion of the national road 8, in order to adjust it to the express road parameters in the following section: Wyszków–'Poręba' interchange (with the interchange) from km 516+482.66 to km 529+470.00, 12.987 km altogether. The investment comprises roadworks, including the construction of the S8 express road, road interchanges (3 interchanges) along with the construction and expansion of transverse roads, expansion of existent roads within the area of the investment, reconstruction of existent traffic routes crossing with the planned investment, construction of crossings, vehicle inspection stations, pavements, exits, bus stops, access roads, surface and subterranean drainage systems, road passages (including animal passages) as well as land reclamation of the area where the existing roads are dismantled. The investment also includes bridge-building work, engineering construction such as viaducts on the transverse roads and sectoral work covering additional equipment [19]. The project is being implemented in accordance with a traditional contractual "build" model. In this model, the contractor receives technical documentation and design from the investor. In this case, the investor gave the contractor the documents in a traditional form since he did not have the construction project in a parametric version. The contractor decided to use project digitisation technology in order to use the parametrised project to build BIM models which will then be used to plan and schedule project work, and for the work with controlled construction equipment. Therefore, in order to apply the principles of the BIM method, the 2D documentation had to be transferred to the digital project and supplemented with spatial information. The models were built using modern tools such as unmanned aerial vehicles, laser technology and satellite measurement tools. These tools provided spatial information in the form of 3D images and helped verify the state of groundwork. Digital tools were also used to facilitate the communication during works. Smart kiosk stations were used to provide access to the up-to-date information about the project in the form of a digital model linked with satellite pictures. The kiosks were used by every party and person engaged in the construction process. Smart kiosks were also used to perform H&S training sessions (Health and Safety) using 3D models. Another example of the use of digital technologies by the contractor of the expansion of road S8 are the apps used to improve the onsite reporting system, which rely on the GPS service and allow live exchange of the information. Drones and laser scanning are also used to verify the state of work in the contemplated project (Fig. 3).

In this investment, the effects of using digital technologies were analysed in comparison with the results obtained with traditional methods used in the previous projects completed by the contractor. Hiring a subcontracting geodetic company to conduct the inventory of 13 kilometres of the road with cross-sections every 25 m, would require 7 days of measurements

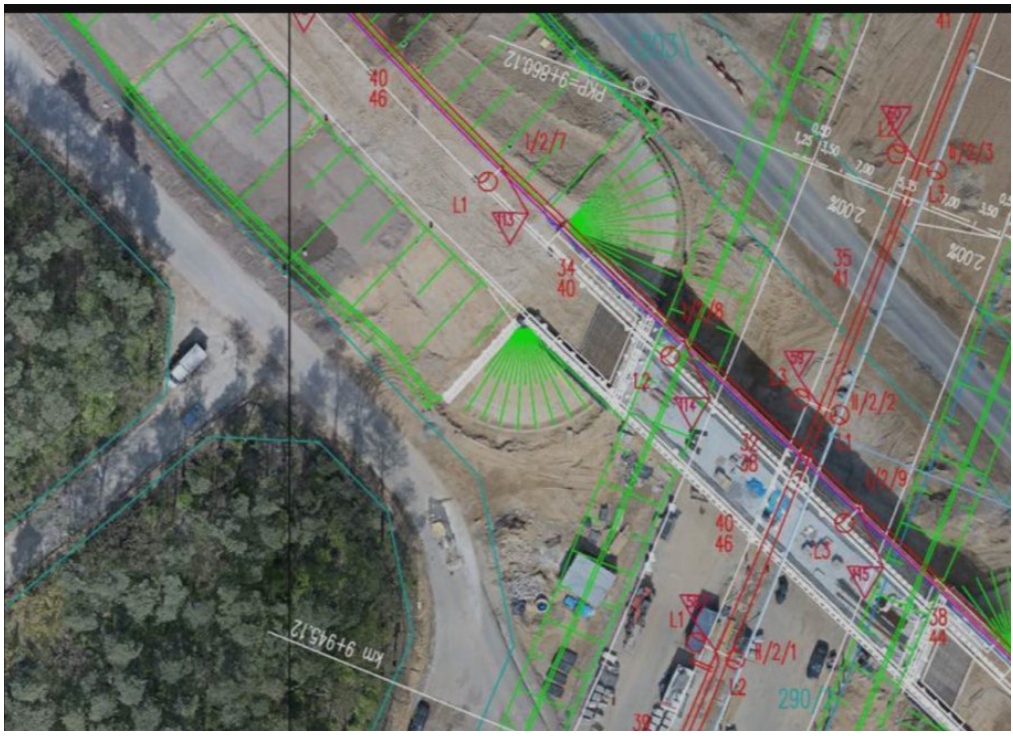

Fig. 3. Digital verification of the state of work. Source: Skanska

and 2 more days for data processing. The data acquired using traditional methods is relatively light (approx. 100 MB) which limits the detail level of the performed inventory. Inventory of the same piece of roadwork using digital technology, which produces ortophotogrametric images, requires 1 day for the flights and 3 days of data processing. The obtained spatial data set is large (12 GB) and provides a very detailed image of the work progress.

4. Conclusions

The article discusses the possibilities of information and communication management in construction projects, using modern technologies and digitization tools. Results of an analysis of three construction investments in the context of the digitization scope of the building project life cycle indicate that there are benefits resulting primarily from saving time and reducing the workload of the processes carried out at the stages of both preparation and execution of construction work. The accuracy of gathered and processed data and the possibility of inter-industry real-time coordination are other effects of the use of IT tools in the presented case studies. The construction of the NKS hospital is an example of an investment implemented from the very beginning with the participation of the users of the facility being designed and built, through the use of digitization and combining BIM with

the Facility Management concept. The FM concept is related to the necessity of managing an elaborate collection of data, including information generated at the stage of design and construction of a building. The BIM model, suitably updated and interpreted, may constitute a significant source of support for the administrators of the property, influencing the comfort, quality and safety of utilization of the building. However, developing a model of cooperation as well as digital communication and information exchange between all the participants in the life cycle of a construction project, taking into account the users and administrators of the buildings, requires further in-depth research.

References

[1] Arak P., Bobiński P., *Czas na przyspieszenie – Cyfryzacja gospodarki Polski* [online], www.research.politykainsight.pl (access: 02.11.2016).

[2] Chyba Z., *Struktura zarządzania nowatorskimi technologiami informacyjnymi, komunikacyjnymi i automatyką,* Zeszyty Naukowe. Organizacja i Zarządzanie, Vol. 83, 2015, 83–91.

[3] Szymański T., *Systemy informatyczne wspierające organizacje z sektora budownictwo*, Zarządzanie i Finanse, R. 11, nr 1, cz. 4, 2013, 543–557.

[4] Parsanezhad P., *An overview of information logistics for FM&O business processes*, [in:] *Conference Materials – European Conference on Product and Process Modelling*, eds. Mahdavi A., Martens B., Scherer R., 17–19 September 2014, Vienna, Austria.

[5] Hadaya P., Pellerin R., *Determinants of construction companies' use of web–based interorganizational information systems*, Supply Chain Management: An International Journal, Vol. 15 (5), 2010, 371–384.

[6] Viljamaa E., Peltomaa I., *Intensified construction process control using information integration*, Automation in Construction Vol. 39, 2014, 126–133.

[7] Bankvall L., Bygballe L.E., Dubois A., Jahre M., *Interdependence in supply chains and projects in construction*, Supply Chain Management: An International Journal, 15 (5), 2010, 385–393.

[8] Lönngren H., Rosenkranz C., Kolbe H., *Aggregated construction supply chains: success factors in implementation of strategic partnerships,* Supply Chain Management: An International Journal, 15 (5), 2010, 404–411.

[9] Vrijhoef R., Koskela L., *The four roles of supply chain management in construction*, European Journal of Purchasing & Supply Management, Vol.6, 2000, 169–178.

[10] Szymczak M., *Modele zarządzania informacją w łańcuchu dostaw*, Organizacja i Kierowanie, Vol. 4, 2013, 26–40.

[11] Fulford R., Standing C., *Construction industry productivity and the potential for collaborative practice,* International Journal of Project Management, Vol. 32, 2014, 315–326.

[12] Underwood J., Isikdag U., *Emerging technologies for BIM 2.0.*, Construction Innovation, Vol. 11 (3), 2011, 252–258.

[13] Yalcinkaya M., Arditi D., *Building Information Modeling (BIM) and the construction management body of knowledge,* The IFIP WG5.1 10th International Conference on Product Lifecycle Management – PLM13, Nantes, France, 6–10 July 2013.
[14] Arayici Y., Egbu Ch., Coates P., *Building Information Modelling (BIM) implementation and remote construction projects: issues, challenges, and critiques,* ITcon, Vol. 17, 2012, 75–92.
[15] Redmond A., Hore A., Alshawi M., West R., *Exploring how information exchanges can be enhanced through Cloud BIM*, Automation in Construction, Vol. 24, 2012, 175–183.
[16] Nicał A.K., Wodyński W., *Enhancing Facility Management through BIM 6D*, Procedia Engineering, Vol. 164, 2016, 299–306.
[17] https://www.bimeye.com/case/new-karolinska-solna/ (access: 03.01.2017).
[18] Smoliński M., Skanska Biuro Projektów Advanced BIM, materiały prezentujące wyniki badań ankietowych związanych z zastosowaniem BIM360 Team, 2016.
[19] Dokumentacja kontraktowa i materiały informacyjne, Skanska S.A.

TECHNICAL TRANSACTIONS 8/2017
CZASOPISMO TECHNICZNE 8/2017
CIVIL ENGINEERING
DOI: 10.4467/2353737XCT.17.128.6879

Katarzyna Biadała (kbiadala@izwbit.pk.edu.pl)
Institute of Construction and Transportation Engineering and Management, Faculty of Civil Engineering, Cracow University of Technology

Selection of a cooperation model in investments implemented in the system of public-private partnership in Poland

Wybór modelu współpracy w inwestycjach budowlanych realizowanych w systemie partnerstwa publiczno-prywatnego w Polsce

Abstract

Public-private partnership is a form of investment implementation based on the distribution of tasks, responsibilities and the form of risk among the public and private parties. This division enables the most economically efficient means of investment implementation to be achieved. The paper presents an analysis of the selection of a cooperation model concerning the parties in public-private partnership, depending on the sector and specificity of the task.

Keywords: public-private partnership, concession, cooperation model

Streszczenie

Partnerstwo publiczno-prywatne jest formą realizacji przedsięwzięcia opartą na podziale zadań, odpowiedzialności i postaci ryzyka pomiędzy stronę publiczną i prywatną. Przez tak wykonany podział osiąga się najbardziej efektywny ekonomicznie sposób realizacji inwestycji. W artykule przedstawiono analizę wyboru modelu współpracy między stronami partnerstwa publiczno-prywatnego w zależności od sektora oraz specyfiki zadania.

Słowa kluczowe: partnerstwo publiczno-prywatne, koncesja, model współpracy

1. Introduction

The European Commission in the published guidelines defines public-private partnership (PPP) as a partnership between the public and private sectors in order to implement an investment or to provide services traditionally provided by the public sector. It is assumed that both parties achieve benefits appropriate to the degree of the implementation of their tasks. By giving each sector an opportunity to do what they excel at, public services and the infrastructure are executed and provided in the most economically effective way. The main aim of PPP is, therefore, the development of such relations between the parties that the risk is borne by the party which can control it best [14]. Depending on the specificity of the investment project, the distribution of tasks or the advancement of an integrated approach to the investment, the partners can choose various models of cooperation. The models are described in section 2 of the paper.

The paper presents an analysis of the selection of the cooperation model between the parties in the public-private partnership, depending on the sector and task specificity.

2. Cooperation models within PPP

the general understanding of PPP relates to various models of organizational and legal performance of public duties. The present paper focuses on two categories of investment projects implemented within PPP. One category includes the legal basis on which the signing of the contract by the parties rests, namely:

- Law on Public-Private Partnership [11],
- the Act on Concession for Work or Services [12] / Act on Concessions for Construction Work or Services [13].

Between the PPP law and the act on concessions for construction work or services certain differences concerning the following issues can be found:

- remuneration for the private party for the execution of the subject of the order,
- the types of risk involved in the project implementation,
- the scope of tasks and obligations assumed by the individual contractor,
- ownership of assets involved in the project,
- the creation of a special purpose company with mixed capital,
- the need to obtain the consent of the third parties to conclude the contract.

The differences concerning private party remuneration relate to the fact that in the concession the remuneration is derived from the fees paid by the holders of the contract, while within PPP it can be derived solely from the public budget.

Concerning the types of risks involved in the investment, the difference between the acts lies in the issue of risk allocation. The act on concession imposes that the whole economic risk is carried by the concessionaire. On the other hand, the PPP law allows any distribution of the risk category between the contractual parties.

The scope of tasks and obligations in PPP is subject to great freedom, including co-financing the investment by the private partner, while concession defines the concessionaire's obligation involving the design, construction, financing and maintenance of the subject of the contract.

The difference concerning the ownership of assets involved in the project means that within concession the assets intended by the contracting authority for the implementation of the investment remain in his/her possession during the term of the contract and after its completion. In contrast, in PPP the asset used in the project (regardless of who was its original owner) is transferred to the public entity after the contract expires.

Only the PPP law includes records about the possibility of creating a special purpose company with mixed capital and the need to obtain the consent of the Ministry of Finance for the projects co-financed from the state budget in the amount of at least 100,000,000 PLN.

The second category includes the principles of cooperation between parties. In the case of execution of construction projects, the most frequently chosen models of cooperation are the so-called integrated models which include the following:

- BOT (Build-Operate-Transfer),
- DBFO (Design-Build-Finance-Operate),
- BOO (Build-Own-Operate),
- BTL(Build-Transfer-Lease).

Description of integrated models

BOT (Build-Operate-Transfer)

This model of investment execution involves a private investor constructing the project, operating it and then handing it over to the public partner who performs regulatory and supervisory functions. The investment is financed by the public party, who also owns the infrastructure constructed in the process. The essence of this variant is the transfer of the risks associated with the operation, construction and design work. BOT is appropriate for projects in which accurate and effective operation and maintenance of the infrastructure used to perform public tasks plays a significant role [1, 9].

DBFO (Design-Build-Finance-Operate)

In this model the private partner designs a relevant infrastructure, independently financing construction and design works. For the duration of the contract the investment is owned by a private investor, after which the infrastructure is transferred to the public entity. This model is the closest to concession. The essence of this type of cooperation is the commitment of the investment capital which is in the resources of the private sector to the needs of the public, as well as the transfer of the risk related to infrastructure design, construction, financing and operating to the private sector. All the variants of this form of PPP assume a maximum concentration of the responsibility for the implementation of the project on the private partner. DBFO means a suitable cooperation in projects in which proper and effective operation and maintenance of infrastructure used for public tasks plays a significant role [1, 9].

BOO (Build-Own-Operate)

A characteristic feature of this model of project implementation is the fact that after a predetermined time no takeover of the investment by the public partner takes place, but the private investor may charge users. Within the contract of this type, the private sector is responsible for the design of the investment. Additionally, the private partner is accountable for the technical implementation of the task and ensures financing.

BOO involves an initial private ownership in which, after cooperation expires, the breakdown of assets are transferred to the public sector. Directly, the private sector is the operator, who is the one to provide services. The burden of ongoing expenditures, maintenance and conservation belong to the private partner duties, who is also responsible for the ongoing marketing of services [1, 9].

BTL (Build-Transfer-Lease)

In this model of project implementation the private entity finances and executes the investment, taking the risk of cost overruns and delays in the project implementation. After the required technical parameters of the subject of the contract, obtained as a result of tests, the ownership is transferred to the public party, while the private entity operates the building on behalf of the public entity under lease. The private partner is responsible for designing the investment, its technical execution and ensures financing.

Contrary to the BOO model, the breakdown of assets are controlled by the public sector from the beginning to the end of the investment.

The operator, i.e. the provider of services is, depending on circumstances, a public or private partner.

In the case of maintenance and conservation the main role is played by circumstances, while bearing expenses belongs directly, or to a larger extent, on the private partner.

Marketing is believed to require considerable activity on the part of both private and public sector [1, 9].

3. Selection of the cooperation model

in accordance with the project database on http://www.ppp.gov.pl [15], out of 113 investments for which contracts had been signed, 38 involved a procedure of private partner selection based on the PPP law [11], and 75 were based on the law on concessions [13]. 26 investments took account of public works concession, while 49 – service concession. The distribution of this division with regard to the sectors is shown in Fig. 1.

As the database mentioned above and Fig. 1. reveal, public entities may use a PPP model in a variety of sectors, implementing investments of various specifications. Among the projects executed on the basis of PPP law [11], as in the case of the Act on Concessions, one may distinguish those that involve only construction works and those that encompass services.

Of all the projects that involved signing a contract, special attention was paid to those concerning the construction or alteration of a building and road infrastructure, parking sites

Fig. 1. The procedure of selecting the private partner including a division into sectors. Source: own study on the basis of a project database retrieved from http://www.ppp.gov.pl/baza/Strony/baza_projektow_ppp.aspx

included. Out of the projects for which contracts were concluded on the basis of the Act on Concessions [12] 7 concerning buildings and 5 concerning parking sites and road infrastructure were selected. On the other hand, of 38 projects for which contracts were concluded on the basis of the PPP law [11], 5 related to buildings and 4 to road infrastructure. Details are presented in Fig. 2. The projects were assigned to such sectors as health care, transport infrastructure, sport and tourism, public buildings, waste management, education and housing.

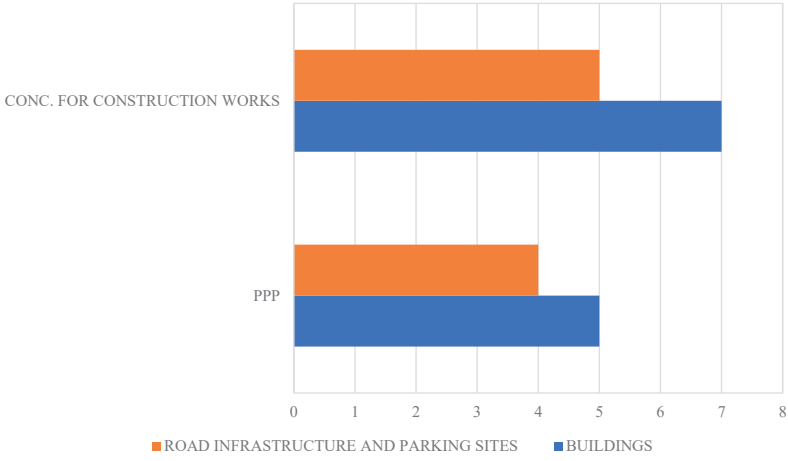

Fig. 2. The distribution of investment projects, including the construction/alteration of buildings and road infrastructure, parking sites including. Source: own study on the basis of a project database retrieved from http://www.ppp.gov.pl/baza/Strony/baza_projektow_ppp.aspx

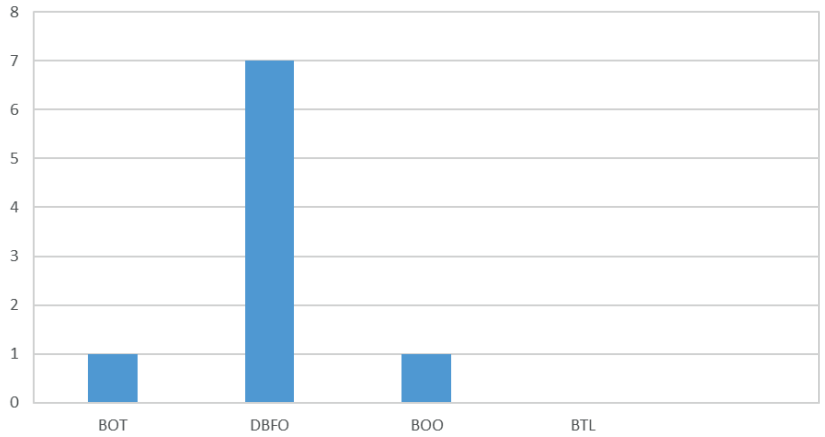

Fig. 3. A model of project implementation under the Law on Public-Private Partnership. Source: own study on the basis of data contained in, i. a., [2-8, 10]

To assess the selection of the integrated model for projects implemented on the basis of the Law on PPP, an analysis of documents for the 9 projects related to buildings and road infrastructure mentioned above was performed. The analysis concerned mainly the scope of the tasks entrusted to the private partner and the division of project financing between the parties.

As Fig. 3 reveals, of the 4 integrated models analysed here, the most frequently chosen one is DBFO (Design-Build-Finance-Operate) which was selected for 78% of investments. BOT (Build-Operate-Transfer) and BOO (Build-Own-Operate) models were chosen for 11% of cases, while BTL (Build-Transfer-Lease) model was not selected at all.

Of projects implemented within the DBFO model, two involved the DBOD (Design-Build-Operate-Deliver) form, which is a variation of DBFO.

The cases analysed reveal a tendency to select a concession for construction works and the DBFO model more frequently as the form of cooperation between the public party and the private partner. Both models allow the public entity to raise the capital of the private sector for investment purposes, which increases the chances to accelerate the construction program and development. They allow the greater part of risk to be transferred to the private sector. For the private partner the choice of one of these models allows the actual costs of the investment to be specified taking into account its entire life cycle.

Despite such widespread interest, both forms of cooperation have disadvantages that may be the source of risk for both parties. In the DBFO model and the concession on construction works there is a high probability of the private partner's underestimating the cost of the investment. Such underestimation had previously resulted in breaking the contract by the private party; therefore, the public entity should take into account the risk of early termination of the contract and the need for the emergence of a new private partner. Currently, the public entity, prior to such an event, secures themselves, for example, by determining the minimum

amount of insurance or creditworthiness which the contractor should possess at the time of the submitting the offer. An additional risk that the public entity needs to consider relates to failing to achieve the technical parameters contained in the provisions of the agreement at the moment of the hand-over of the object.

In contrast, the choice of the concession model, in which the remuneration for the private partner constitutes exclusively a right to the use of the object and enjoying the resulting profits, the possible risk involves the fall in an interest in the infrastructure made available and reducing the resulting profits. With the concession contracts concluded for a period of up to 30 years, consideration of such risks, estimating the cost of investment and the selection of a project implementation model can be evaluated not earlier than after the termination of the first signed contracts, that is in over 20 years.

4. Conclusions

The Law on Public-Private Partnership does not force a public entity to choose any particular model of cooperation. They make the choice themselves on the basis of, for instance, specificity of the project, initially approved distribution of risk or way of financing the planned investment. This procedure must be always preceded by a deep analysis of the factors affecting the project and the public entity should not be tempted to transfer all the risk to the private partner.

In the future the data presented in the article will be extended and compiled with data of PPP investments on the European market. At the same time, the distribution of tasks, responsibilities and the form of risk among the public and private parties, which affects the choice of cooperation model, will be analysed.

References

[1] Ćwik D., *Modele współpracy w ramach partnerstwa publiczno-prywatnego*, Gospodarka Materiałowa i Logistyka, No. 5/2014.

[2] Herbst I., Jadach-Sepioło A., *Raport ze studiów przypadku PPP*, Polska Agencja Rozwoju Przedsiębiorczości, Warszawa 2012.

[3] Informacja o planowanym partnerstwie publiczno-prywatnym http://bip.walcz.pl/content.php?cms_id=2857%7C%7Cm=13 (access: 15.02.2017).

[4] Ogłoszenie o zamówieniu http://www.dzp.cm-uj.krakow.pl/siwz/540/ogloszenie_PPP.pdf (access: 15.02.2017).

[5] Ogłoszenie o zamówieniu http://bip.um.olawa.pl/Article/get/id,22282.html (access: 15.02.2017).

[6] Ogłoszenie o udzieleniu zamówienia http://bip.ustka.ug.gov.pl/Article/get/id,18607.html (access: 15.02.2017).

[7] Ogłoszenie o zamówieniu http://www.biuletyn.net/nt-bin/_private/krobia/2419.pdf (access: 15.02.2017).
[8] Ogłoszenie o zamówieniu http://ugkarczmiska.bip.lubelskie.pl/upload/pliki/ogloszenie_o_zamowieniu_PPP_do_BIP.pdf (access: 15.02.2017).
[9] *Partnerstwo publiczno-prywatne. Poradnik*, Urząd Zamówień Publicznych, Warszawa 2010.
[10] *Podpisanie umowy PPP i zamknięcie finansowe w projekcie pn. „Budowa budynku sądu rejonowego w Nowym Sączu przy ul. Grunwaldzkiej"* – pierwszy projekt administracji rządowej realizowany w formule PPP. Platforma Partnerstwa Publiczno-Prywatnego, 12.2015.
[11] Ustawa z dn. 19 grudnia 2008 r. o partnerstwie publiczno-prywatnym (Dz. U. 2009 Nr 19 poz. 100 z późn. zm.).
[12] Ustawa z dn. 21 października 2016 r. o umowie koncesji na roboty budowlane lub usługi (Dz. U. 2016 poz. 1920).
[13] Ustawa z dn. 9 stycznia 2009 r. o koncesji na roboty budowlane lub usługi (Dz. U. 2009 Nr 19 poz. 101 z późn. zm.) – nieobowiązująca.
[14] *Wytyczne dotyczące udanego partnerstwa puliczno–prywatnego*, Komisja Europejska, styczeń 2013.
[15] http://www.ppp.gov.pl/baza/Strony/baza_projektow_ppp.aspx (30.11.2016).

TECHNICAL TRANSACTIONS 8/2017
CZASOPISMO TECHNICZNE 8/2017
CIVIL ENGINEERING
DOI: 10.4467/2353737XCT.17.129.6880

Karolina Jerzak
Agnieszka Dziadosz (agnieszka.dziadosz@put.poznan.pl)
Institute of Structural Engineering, Faculty of Civil and Environmental Engineering, Poznan University of Technology

Competitiveness of a building company within the organisational life cycle

Konkurencyjność przedsiębiorstwa budowlanego w kontekście cyklu życia organizacji

Abstract

The role and the meaning of a construction company on the market is variable depending on the phase of the life cycle of the company in a given moment. The processes and the services offered by a company are dependent on time and how the business activities of the company are developed as well as the barriers which the company encounters at specific stages of the business activities of the enterprise. In this specific context competitiveness can be understood not only as a comparison of the position of the company with other enterprises functioning within a given sector but as a resultant of possibilities and chances created by an organization in the context of its life cycle. The main aim of this article is to try and assess the influence of the life cycle of a construction company on its market behaviour taking into account the theoretical consideration of competitiveness.

Keywords: organizational life cycle, competitiveness, barriers of entry

Streszczenie

Rola i znaczenie przedsiębiorstwa budowlanego na rynku jest zmienna w zależności od fazy życia, w jakim się ono w danym momencie znajduje. Procesy i usługi oferowane przez przedsiębiorstwo uzależnione są bowiem od czasu i rozwoju działalności oraz barier jakie napotyka w poszczególnych etapach działalności. W tym kontekście konkurencyjność może być rozumiana nie tylko jako porównanie pozycji przedsiębiorstwa z innymi działającymi w danym sektorze, ale jako wypadkowa możliwości i szans stwarzanych przez organizację w kontekście cyklu jej życia. Celem niniejszego artykułu jest próba oceny wpływu fazy życia przedsiębiorstwa budowlanego na jej zachowania rynkowe przy uwzględnieniu teoretycznych rozważań konkurencyjności.

Słowa kluczowe: cykl życia organizacji, konkurencyjność, bariery wejścia

1. Introduction

Competitiveness in definition is the connection of the results achieved by a company in comparison to other enterprises functioning within a given sector. The key element in order to be able to achieve a considerable competitive advantage are the networks of the company and the measures taken within the organization itself, which indicate that the meaning and importance of human capital is a factor influencing the marking of barriers for competitiveness. The role and the influence of human capital on the development of an enterprise is difficult to measure, therefore enterprises more often undertake actions intended at trying to identify the influence of intangible factors.

P.F. Drucker posited a thesis that both tangible assets such as machinery and capital take constitute a background role and the basic value will be knowledge [1]. The key skills and competences included in the resources of an enterprise may constitute the basis for gaining a permanent competitive advantage for an organization. This is considered as the resource-based approach [2], where the source of knowledge is both the environment of an enterprise as its interior. The resource-based approach constitutes a further amplification of strategic management and refers to an analysis of the stakeholders as a source of knowledge which can be transformed and used within a company as a factor in its development. Competitiveness can be seen as the ability to learn, improve and implement new ideas and services or organizational structures.

The competitiveness of an enterprise differs with regard to the phase of the life cycle it is in. The connection of identifying the life cycle of an organization with patterns of how to manage an organization can become a powerful tool in gaining competitive advantage and ensuring sustainability [3]. Enterprises similarly to living organisms are born, develop and connect with others then die [4], and at each stage there are specific difficulties and conditions.

Every single enterprise functions within a strictly defined sector, which sets the conditions and sets the particular phases of development, as well as the unique manner of identifying key factors of success. The main aim of this article is to try and assess the influence of the phase of the life cycle of a construction organization on its market behaviour taking into account the theoretical consideration of competitiveness. Theoretical conceptions of the life cycle of an organization will be presented in this article together with the identification of the factors of competitiveness. The last part of the article presents the primary analysis on the basis of the research conducted on construction companies of medium size operating in the Polish market and there will be a presentation of conclusions on the basis of theoretical consideration.

2. The life cycle of an enterprise – literature review

The Organizational Life Cycle (OLC) is according to S. Hanks 'a unique configuration of variables connected the context of an organization, its strategy and structure' [5]. Enterprises use the Organizational Life Cycle as a means of assessment and identification of the changes

taking place in an organization. Taking into account the general assumptions each and every organization undergoes the process of birth, development and in the end death or rebirth.

Scientists have not been able to find a consensus with regard to the division of a life cycle within an organization into fixed stages This may be caused by the fact that they conducted their research in different sectors of business activities of various enterprises. However, life cycles are dependent on the compilation of internal possibilities of an enterprise as well as the external forces influencing it [6].

A three stage division of the cycle being the birth, youth and maturity have been proposed by G. H. Lippitt and W. H. Schmidt [7], who indicated that entering the next stage is connected to a crisis with regard to critical managerial concerns such as survival and stability in a simple birth, youth and maturity format [8].

A four stage model of power (Forming, Development, Maturity and Disappearance) is dependent on time and abrupt changes force a change in the concept of management which was proposed by H. Mintzberg. The struggle for power is related to a desire for personal rewards on the part of top management. While the decline stage of an organizational life cycle does not spell certain death, it does require a turnaround [9] or a revolutionary change in strategy, structure, decision-making style, and situation for a successful return to a more stable or growth stage [8]. R.E. Quinn and K.S. Cameron were the ones to introduce the four stage cycle starting with the Entrepreneurial stage, the Collectivity stage, the Formalization stage, finishing with the Elaboration of the Structure stage [10].

The various definitions are dependent on the sector which the enterprises function in as well as the management style, which in turn is reflected in the stages of development of an organization similar to those of a metamorphosis (where the company goes through typical cycles in time), crises (when after achieving the next stage a crisis is necessary in order to be able to move to the next stage), the development of the market (the key element being outward directing), the behavioural changes (where each and every stage requires a change in managerial approach) and the structural change (where the structure of the organization at a particular stage is not beneficial, be it the previous stage or the forthcoming one) [11].

The most popular model is that presented by L. Greiner, who portrays the transition from one stage to the next in the development of an organization through crises. Furthermore he indicates that the necessity of maintaining professionalism in management leads to an increase in bureaucracy [12].

Greiner indicated that crises are inevitable; however, they can be solved by evolution or revolution. The evolution process is less risky; however, it requires timing skills from management. All of the processes in an organization should be analysed on a regular basis leading to their improvement [4].

In the model presented above, it is necessary to solve conflicts at particular stages, otherwise the organization reaches a standstill and does not develop. The cycles force a constant analysis of the company by the management, be it with regard to external or internal factors.

Regardless of the phase the company is in, the most important factor is the analysis of the shareholders and the behavioural patterns of competition in a given sector. Departing from the market reality and concentrating strictly on internal assessment and analysis may lead

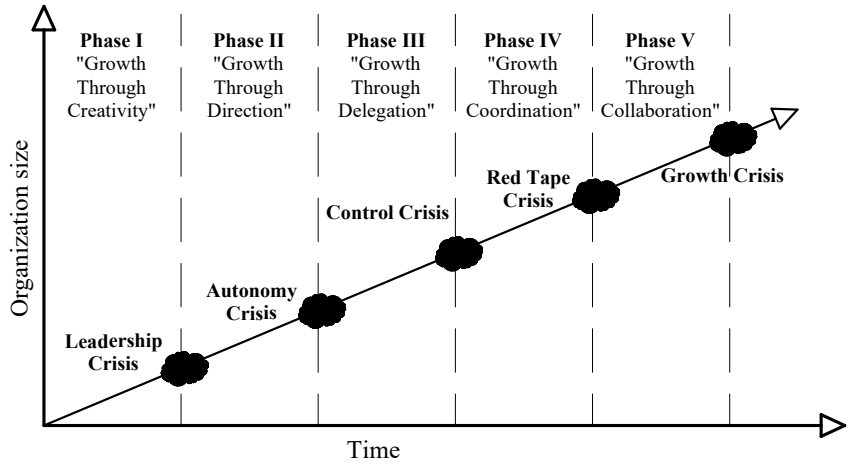

Fig. 1. Models of the organizational life cycle by L. Greiner [4]

to the fall of an organization due to supersession by competition. The development of an enterprise is also supported by the knowledge possessed by its members as well as that which is concluded from the previous crisis phase.

An organization which has undergone the birth stage regardless of the life cycle model, faces a challenge connected to involving employees in competition activities, in addition to which it becomes necessary to manage change and invest in solutions which will enable a competitive position to be obtained at the beginning and then be maintained.

3. The competitiveness of a construction company

The definition of competitiveness differs with regard to the sector analysed [14], time, and geographical horizon. Porter states that there is no universal definition of competitiveness and at the same time he indicated that productivity is the source of competitive advantage [15].

Regardless of the fact scientists are putting all their effort into normalizing both the definition of 'competitiveness' as well as the method of measuring its level. When it comes to the construction market this can be difficult due to the heterogeneous business activities of the market. According to J. Bossak, the most important factor with regard to competitiveness for the building company would be selling construction work and assembly services with a profit [16].

Table 1. Comparison of competitiveness definitions depending on the scale [17]

Level	Formed by	Key elements of the system	Assumptions
Competitiveness on a national level	B.R. Scott and G.C. Lodge [18]	"A country's ability to create, produce, distribute and/or service products in international trade while earning rising returns on its resources".	The theory assumes that all goods are accessible on the international market and they compete with other goods from markets with varied cost structures. Productivity is the key factor for ensuring a substantial return from their business activities together with minimizing costs. [17]
Competitiveness on a company level	Aldington Report [19]	"A company is competitive if it can produce products and services of superior quality and lower costs than its domestic and international competitors. Competitiveness is synonymous with a company's long-term profit performance and its ability to compensate its employees and provide superior returns to its owners."	In order to be competitive within a sector, knowledge of market needs, the ability to generate low costs of both business activities and services constitute a vital element.

The sources for competitive advantage can be divided with regard to their approach into:

- **the resource-based approach** where knowledge, human capital, technological advancement and experience with the appropriate connection have a huge impact on limiting the ability of competition to gain unique resources. The resource-based approach can be applied when the organization has passed its birth phase, due to the fact that before that stage it is not able to assess its possessed resources and skills in connection to the past and further the business experience is relatively small.
- **the position-based approach** where the sector which the organization is active in is analysed. Its competitiveness is dependent on M. E. Porter's five forces functioning in the sector, meaning that the organization is forced to alter its position with regard to environmental and market forces.

Within the construction sector competitiveness depends on three factors: the size of the business, the scope of activities and location [20]. Of equal importance in order to gain a competitive position is the strategy of the lowest price, which can be used as an effect of scale – the more contracts are signed the stronger the reaction of the sector upon appearance taking

advantage of the price of the competitor in a tender. The source of competitive advantage may come from intangible assets such as employee experience, know-how, managerial skills when it comes to strategic analysis, and gaining and maintaining loyal suppliers and sub-suppliers of goods and services. According to M. E. Porter the source of competitive advantage may be cost leadership, differentiation of services and the concentration strategy, this approach coincides with the hypothesis of the author of the article.

Competitiveness requires both an analysis of the company internally as well as the external factors and the business activities of the organizations functioning on the market in the same sector. The connection between competitive advantage and the final product is connected to the possessed competences of a given company.

The concept of competitiveness based on competences was devised by C.K. Prahalad and G. Hamel, for whom the most crucial issue is collective learning by the organization, most importantly being expressed in the coordination of productive skills and the streams of technology [21]. The key competences are communication, employee commitment and persistence. The constant need for developing the key competences may have its effects in gaining and maintaining competitive advantage [22].

4. The organizational life cycle and the competitive position on the basis of primary research

Construction organizations are forced to face various barriers and internal and external challenges when they go through the particular stages of their life cycle, which disturb their business activities and can become a threat for their further functioning. Intense concentration on the external problems by the management of the company without taking into account the internal situation of a company can cause conflicts and cleaving between the vision of the company owners for obtaining new contracts and the activities of employees who are not fully aware of it. The situation may also be reversed when the management of the company pays too much attention to which stage the company is in and overestimates the meaning of the role of human capital, while not reacting to the market activities of competition. Finding a comfortable position is of great importance and is a huge challenge, but is worth undergoing.

In the subsequent part of the thesis the results of a primary survey conducted in the months of March and April 2016 based on a full list of medium sized construction companies functioning on the market within the general construction sector are presented. A pilot survey conducted using the direct survey method (questionnaire) was used. During the research both the skill of identifying the barriers for a specific enterprise, the relations with the shareholder as well as the assessment of human capital in the company were verified. The measured collectivity is rather small – it is aimed to extend the research on small enterprises and those executing projects apart from the function of maintaining other services than general construction services, but in the scope of the research, companies providing transport services and delivery of goods will not be taken into account. The main aim of this research was to verify the research hypotheses connected to both the ability of the management to

identify the barriers to entry and to strengthening the position of the company in the market on the basis of the theory and the analysis of the environment of the company as well as the initial correlation of the existence between particular elements of intellectual capital of an enterprise to be able overcome the barriers to entry and strengthening the position of the company in the market.

In order to be able to assess the life cycle of an organization, the L. Greiner model has been applied, meaning that it comprises phases such as the creation phase, the formalization phase, and delegation, coordination, and cooperation phases. While conducting research one enterprise refused to take part in the survey which may indicate an ongoing crisis in one of the phases. It has been assumed that in the next survey the interviewer will try to obtain data connected to identifying risk and its strength as well as a means of overcoming it.

The issues connected to the influence of the organizational life cycle on the organizations' market behaviour constitute a challenge for the management of the company, mainly due to the necessity of getting to know and choosing the proper model of assessment. The methods of identification presented in the article create intrinsic barriers and limitations which have been defined by the author as:

- having no connection with methodology with the construction sector.

The building market is characterized by much variability, resulting mainly from macroeconomic factors as well as the intensity of rivalry in the sector. This has a significant influence on the market behaviour of the company with regard to the manner of running the business and the ability to set barriers for competition.

In general the companies go through a cycle of birth, development, and death; however, in a more detailed exploration these phases undergo growth. Adjusting one of the existing models or the creation of a new life cycle model dedicated strictly to the building sector can lead to improvements in decision making and forecasting for management;

- existing models do not define the barriers of transition between phases.

The enterprises which were taken into account when conducting the research have been functioning in the building sector for 10 years, concurrently the results indicate that there is a discrepancy between the time the organization has been in the market and the unambiguous identification of the phase which they are in. The assumed and presented research model in the article is based on available data which has been grouped and was subject to analysis. After having conducted the analysis, the author indicates that in order to be able to appropriately use the model it is necessary to conduct a deeper analysis of every enterprise, which would constitute in the further stages a basis for building a temporary working table and an unambiguous indication of crises as evidence of going through the particular phases. With regard to the sample tested there was no opportunity due to the managements' fear of providing too much information, which indicates another conclusion about the need to create an even more detailed analysis tool directed at only identifying the phase of the life cycle of particular enterprises;

- lack of retrospective analyses.

When conducting the research a key factor was the absence of retrospective analyses, which would allow a comparison of newly obtained data with those obtained in the past. Entering the building sector requires overcoming financial and legal barriers as well as those connected to enlisting new suppliers of goods and investors. This research was directed mainly at medium sized enterprises, which itself constitutes a barrier to preparing the management to create a model and delegating a person responsible for drawing up the matrix;

- fear of the researcher's objectivity.

The model board should have a person responsible for it, who will on a regular and daily basis analyse the market behaviour of the company and observe the organization from the inside, which would lead to the identification of going through the particular phases. The interviews conducted with the management indicate a high level of caution in providing answers to the questionnaire, although the aim of the questionnaire was known to those being questioned. This leads to a primary conclusion that the researcher should be a person within an organization; however, not dependent on the board in order to be able to maintain his or her impartiality.

By presenting the selected primary results of pilot studies in the context of a theoretical definition of the life cycle, its role and meaning for the competitiveness of a building enterprise, an identification of both the limitations of analysis as well as an indication of the key meaning of the connection of the organisational life cycle with the competitive behaviour of a company in the building sector is possible.

The analyses and identification of the Organisational Life Cycle by single primary research is rather complicated in order to be able to assess the life cycle according to the scheme proposed by L. Greiner, which has been extended by the identification elements included in the imprint of the primary research.

According to the abovementioned method of identifying the life cycle the diagram presents the following results.

On the basis of the research conducted, a difficulty was encountered in connection with the unambiguous definition of the phase of the organisational life cycle. This discrepancy

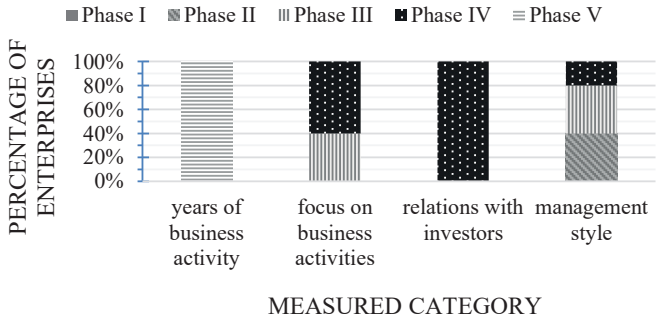

Fig. 2. Identifying the organisational life cycle on the basis of the criteria selected

may be the result of the methodology of the research assumed, i.e. the enterprises which were being researched for the first time gave no opportunity to refer to previous results. The results obtained may also indicate that the companies are not developing linearly, meaning that they are not going through the particular phases on every level of their business activities simultaneously, but rather they try to complete their competences depending on market needs, which moreover is also concurrent with Abraham Maslow's model.

When it comes to the life cycle of an organisation the most important issue is the assessment of the competitive position of a company functioning in a given sector. In this research an assumption has been made that the starting point for identifying the competitive position of a company may be the recognition of the components of the micro environment and assessment made by the management, if they play an important role in the choice of strategy of the development of the company. While conducting the research eleven factors in the micro environment were taken into account, indicated in the diagram below, rating the ability of assessment and indication by the company management of the areas which have an influence on the company's development strategy.

With the usage of a key for coding each obtained answer a score has been defined (the answers ranging from definitely not important to definitely important have received a score from 1 to 5) and next the average was calculated, the results are presented in the diagram below.

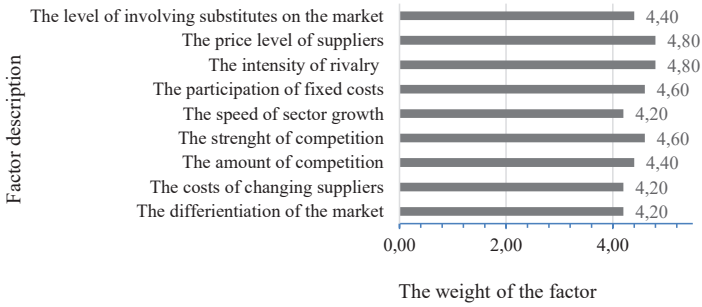

Fig. 3. The identification of the factors from the micro environment

5. Summary

The aim of the paper was to make an assessment of the influence of the phase of a medium sized building company's life as a general entity on its market behaviour, taking into account the theoretical assumptions connected to competition. In order to achieve, the aim in the first part of the article a critical review of literature was comprehended connected to the organizational life cycle as well as competitiveness which constitutes the basis for the analysis of the primary results from pilot studies.

During the research, a difficulty was encountered in connection to the unambiguous definition of the phase of the organisational life cycle. The author intends to continue observing

the aforementioned phenomenon in the main research studies as well as by expanding the number of companies tested to conclude the identification of the phase of a given company's life.

In the research it has been assumed that the starting point for identifying the competitive position of the company is the recognition of key components of the microenvironment and the assessment conducted by the management, as long as it is significant in terms of the choice of business development strategy.

The results indicate that enterprises identify the level of rivalry among the companies within a given sector as the most crucial barriers for conducting business. This factor together with the strength of the competition and a very high level of cost factors are rated by the enterprises tested as high and may lead to an intense price war in the sector and to building new barriers precluding the access of new companies onto the market.

The high fixed costs which are incurred by the company due to running the business when trying to achieve the best price for the investor may lead to the fall of an enterprise or in the best case to cost cutting be it the redundancy of highly qualified staff or the delegation of the employees to many projects at the same time. As a result there may be a significant drop in the quality of goods produced or services provided.

By presenting the primary results of the pilot studies in the context of a theoretical definition of the life cycle, the role and meaning of the phases of the life cycle for the competitiveness of a building company, an identification of both the limitations of the analysis and the key meaning of the connection of the phase of the life cycle with the competitive behaviour of a company in the building sector is possible.

Identifying which phase of the life cycle a company is in may be slightly complicated by the absence of an unambiguous assessment model.

Moreover such an analysis should constitute an element of a company's strategy and be subject to recurrent assessment – only then only then will it be possible to take steps aimed at verifying the competitive strategy in connection to the phases of the life cycle. This connection appears to be the key element in the functioning of an organisation with regard to the relationship between the internal crises and the behaviour of the competition in a given sector.

In order to verify the presented hypotheses the author plans to extend the test group and add more questions to the questionnaire connected to life cycle and competitive strategy.

References

[1] Drucker P.F., *Ten New Society of Organization*, Harvard Business Review, 9/10, 3–17, 1992.

[2] Leonard–Barton D., *Wellsprings of Knowledge. Building and Sustaining the Sources of Innovaion,* Harvard Business School Press, Boston, 1995.

[3] Shirokova G., *Organisational life–cycle: The characteristics of developmental stages in Russian companies created from scratch*, JEEMS 1/2009, 2009, 65–83.

[4] Brzeziński S., Stefańczyk P., *Use of enterprise growth theory in management of small and medium sized enterprises*, Polish Journal of Management Studies, 2013, 315–325.

[5] Hanks S., *An Empirical Examination of The Organizational Life Cycle in High Technology Firms*, Doctoral Dissertation, University of Utah, 1990.
[6] Ul Hassan F. S., Shah B., Khan N., Ikramullah M., Zaman T., *Exploring the relationships among organizational life cycle stages and different traits of organizational culture*, Business and Management Review, Vol. 1(7), September, 2011, 103–112.
[7] Lippitt G.L., Schmidt W.H., *Crises in a Developing Organization*, Havrard Business Review, no. 45, 6, 1967, 102–112.
[8] Lester D.L., *Organizational life cycle and innovation among entrepreneurial enterprises*, Journal of Small Business Strategy, Vol. 19, No. 2, Fall/Winter, 2008/2009, 38–40.
[9] Mintzberg H., *Mintzberg on management*, NY: The Free Press, New York 1989, 296.
[10] Quinn R.E., Cameron K.S., *Organization life cycles and shifting criteria of effectiveness: Some preliminary evidence*, Management Science, 29 (1), 1983, 33–51.
[11] Wyrwicka M.K., *Endogenne przesłanki organizacyjne rozwoju przedsiębiorstwa*, Rozprawy nr 374, Wydawnictwo Politechniki Poznańskiej, Poznań 2003, 45 –47.
[12] Doubience J., *Corporate entrepreneurship in organizational life–cycle*, Economics and management: 2013.18(3), 2013, 584–592.
[13] Greiner L., *Evolution and Revolution as Organizations Grow*, Harvard Business Review, 50(4), July– August, 1990, 37–46.
[14] IMD World Competitiveness Yearbook 2003, IMD, Lausanne, Switzerland, 2004.
[15] Porter M.E., *The Competitive Advantage of Nations*, New York: Free Press, 1990.
[16] Bossak J., Bieńskowski W., *International Competitiveness: Basic Concept*, Warszawa 1990.
[17] Henricsson J.P.E., Ericsson S., Flanagan F., Jewell C.A., *Rethinking competitiveness for the construction industry*, School of Construction Management and Engineering, University of Reading, PO Box 219, Reading, RG6 6AW, UK, 2004, 335–344.
[18] Scott B. R., Lodge G.C.,*US Competitiveness in the World Economy*, Boston: Harvard Business School Press, Boston, Massachussets, 1985, 13–70.
[19] Aldington Report Report from the Select Committee of the House of Lords on Overseas Trade. HMSO, London 1985.
[20] Šiškina A., Juodis A., Apanavičienė R., *Evaluation of the competitiveness of construction company overhead costs*, Journal of Civil Engineering and Management, 15(2), 2009, 215–224.
[21] Prahalad C.K., Hamel G., *The Core Competence of the Corporation*, Harvard Business Review, May–June 1990, 70–90.
[22] Mazurkiewicz A., Frączek P., *Kluczowe kompetencje a konkurencyjność przedsiębiorstw*, Zakład Ekonomiki Inwestycji i Zarządzania Strategicznego Uniwersytet Rzeszowski, Publikacja opracowana w ramach grantu nr N N115 408840, 96–97.

TECHNICAL TRANSACTIONS 8/2017
CZASOPISMO TECHNICZNE 8/2017
CIVIL ENGINEERING
DOI: 10.4467/2353737XCT.17.130.6881

Tadeusz Kasprowicz (tadeusz.kasprowicz@wat.edu.pl)
Faculty of Civil Engineering and Geodesy, Military University of Technology

Quantitative estimation of the impact of random confounding factors on the duration and cost of construction wor

Kwantytatywne szacowanie wpływu losowych czynników zakłócających na czas trwania i koszty robót budowlanych

Abstract

Random events may interfere with the execution process and results of the work. Then, the duration and cost of work are random variables. The random characteristics of these variables are described by using the β-PERT probability distribution and the simplified formulas. To determine the probable changes of the duration and cost of work, depending on the random factors, the coefficients of optimism and pessimism have been used. Additionally, the coefficients of improvement and deterioration of conditions of work implementation have been introduced. The values of these coefficients are calculated depending on the type, the probability of occurrence, the intensity of random perturbations and depending on the probable changes of the work duration as well as the probability and cost consequences of the price increase. Extreme random improvement and deterioration of the work execution conditions are analysed.

Keywords: construction, risk, coefficients of optimism and pessimism

Streszczenie

Zdarzenia losowe mogą zakłócać proces realizacji i wyniki robót, wówczas czas trwania i koszty robót są zmiennymi losowymi. Losowe charakterystyki tych zmiennych są opisywane za pomocą rozkładu prawdopodobieństwa β-PERT i uproszczonych formuł. Aby określić prawdopodobne zmiany czasu trwania i kosztów robót, w zależności od czynników losowych, zostały użyte współczynniki optymizmu i pesymizmu. Ponadto, wprowadzono współczynniki poprawy i pogorszenia warunków wykonywania robót. Wartości tych współczynników są obliczane w zależności od typu, prawdopodobieństwa wystąpienia i intensywności losowych perturbacji, prawdopodobnych zmian czasu trwania robót oraz prawdopodobieństwa i konsekwencji kosztowych wzrostu cen. Ekstremalna poprawa i pogorszenie warunków wykonywania robót są analizowane.

Słowa kluczowe: budowa, ryzyko, współczynniki optymizmu i pesymizmu

1. Introduction

Constructions work is carried out on building sites in actual surroundings and the natural environment. The technological and organizational conditions that characterize the requirements of the object structure execution can be described by using the design characteristics model of structure $\boldsymbol{S}$ as follows [1, 2]:

$$\boldsymbol{S}=\langle \boldsymbol{G},\boldsymbol{L}\rangle \tag{1}$$

$\boldsymbol{G}=\langle \boldsymbol{Y},\boldsymbol{U},\boldsymbol{P}\rangle$ – a coherent and a-cyclic unigraph with a single initial node and a single final node that describes the interdependence and permissible sequences of works,
$\boldsymbol{Y}=\{y_1, ..., y_i, ..., y_k, ..., y_m\}$ – set of the nodes of the graph representing: y_i initial event and y_i final event for each specific piece of work $u_j \in \boldsymbol{U}$;
$\boldsymbol{U}=\{u_1, ..., u_j, ..., u_1, ..., u_n\}$ – set of the arcs (arrows) of the graph representing relatively independent pieces of work constrained by initial $y_i \in \boldsymbol{Y}$ and final $y_k \in \boldsymbol{Y}$ nodes;
$\boldsymbol{P} \subset \boldsymbol{Y}\times\boldsymbol{U}\times\boldsymbol{Y}$, $\langle yi, uj, yk\rangle \in \boldsymbol{P}$ – a three-term relation that assigns to each arc $u_j \in \boldsymbol{U}$ the initial node $y_i \in \boldsymbol{Y}$ and final node $y_k \in \boldsymbol{Y}$;
$\boldsymbol{L}:\boldsymbol{U}\rightarrow \boldsymbol{R}^+$ – a function defined on the set $\boldsymbol{U}$ of arcs of the graph $\boldsymbol{G}$ determines the expected values $E[L_j]$ of the variables L_j and describes the size of works $u_j \in \boldsymbol{U}$.

The resource requirements and conditions for executing the work are described by using the construction technology model $\mathscr{L}$ as follows [1, 2]:

$$\mathscr{L}=\{\langle \boldsymbol{H},\boldsymbol{K},\boldsymbol{T}\rangle,\boldsymbol{S}\} \tag{2}$$

$\boldsymbol{H}=\{\boldsymbol{H}^1, ..., \boldsymbol{H}^r, ..., \boldsymbol{H}^S\}$ – the set of teams $\boldsymbol{H}^r$ for work $u_j \in \boldsymbol{U}$ execution,
$\boldsymbol{T}:(\boldsymbol{H}\times\boldsymbol{U})\rightarrow \boldsymbol{R}^+$ – a function defined on the set $\boldsymbol{H}$ of teams $\boldsymbol{H}^r$ determines the expected values $E[T_{j,r}]$ of random variables $T_{j,r}$ and describes the duration of work $u_j \in \boldsymbol{U}$,
$\boldsymbol{K}:(\boldsymbol{H}\times\boldsymbol{U})\rightarrow \langle \boldsymbol{R}^+\rangle$ – a function defined on the set $\boldsymbol{H}$ of teams $\boldsymbol{H}^r$ determines the expected values $E[K_{j,r}]$ of random variables $K_{j,r}$ and describes the cost of work $u_j \in \boldsymbol{U}$.

In the proposed approach, the expected values $E[T_{j,r}]$ and $E[K_{j,r}]$ of random variables $T_{j,r}$ and $K_{j,r}$ are calculated in accordance with the simplified formulas of the PERT method¨

$E[T_{j,r}]=\dfrac{\underline{T}+4\widehat{T}+\overline{T}}{6}$ and $E[K_{j,r}]=\dfrac{\underline{K}+4\widehat{K}+\overline{T}}{6}$ [1, 2]. The realistic or the most probable values

$\widehat{T}_{j,r}$ and $\widehat{K}_{j,r}$ for these formulas are estimated directly on the basis of the individual analysis of the technology, resources, and conditions of work execution, or determined on the basis of commonly used catalogues of standards of resource consumption and commonly used price lists. The optimistic values $\underline{T}_{j,r}$ and $\underline{K}_{j,r}$ as well as the pessimistic values $\overline{T}_{j,r}$ and $\overline{K}_{j,r}$ are calculated by using coefficients of optimism $\underline{p}^t_{j,r}$ and $\underline{p}^k_{j,r}$, and coefficients of pessimism $\overline{p}^t_{j,r}$ and $\overline{p}^k_{j,r}$ according to the

formulas: $\underline{T}_{j,r}=\widehat{T}_{j,r}-\underline{p}^t_{j,r}\ \widehat{T}_{j,r}$, $\underline{K}_{j,r}=\widehat{K}_{j,r}-\underline{p}^k_{j,r}\ \widehat{K}_{j,r}$, $\overline{T}_{j,r}=\widehat{T}_{j,r}+\overline{p}^t_{j,r}\ \widehat{T}_{j,r}$, $\overline{K}_{j,r}=\widehat{K}_{j,r}+\overline{p}^k_{j,r}\ \widehat{K}_{j,r}$.

Other approaches to the risk assessment, partly comparable to those described here, are presented in papers [3–5].

The above mentioned approach corresponds to standard or moderate conditions for the execution of the work. In practice, the conditions for the implementation of the work may be highly changeable. In terms of such conditions, the favourable and difficult conditions of the execution should be considered. Then, additionally it is proposed to apply the coefficient of conditions improvement and the coefficient of conditions deterioration of work execution, respectively.

2. The rules for determining the coefficients of optimism and pessimism

Coefficients of optimism $\underline{p}^t_{j,r}$ and pessimism $\overline{p}^t_{j,r}$ enable us to take into account the impact of random events on the duration of work $u_j \in \boldsymbol{U}$ carried out by the working team $\boldsymbol{H}^r \in \boldsymbol{H}$. They are estimated for each part of the project for particular perturbations in a similar way. In specific situations, the aggregate coefficients of optimism and pessimism should be estimated, which take into account the total influence of all random disturbances. In such cases coefficients $\underline{p}^t_{j,r}$ and $\overline{p}^t_{j,r}$ are estimated depending on the probability of disturbances $q_{j,r}$ and the time consequences of the disturbances $t_{j,r}$. The values $q_{j,r}$ and $t_{j,r}$ can be determined rmined using the description of the situation listed in the Tables 1 and 2.

Table 1. Probability of disturbances $q_{j,r}$

Level	Description	$q_{j,r}$
Level 1	The probability of disturbances is extremely small	0.00–0.20
Level 2	The probability of disturbances is little	0.20–0.40
Level 3	The probability of disturbances is medium	0.40–0.60
Level 4	The probability of disturbances is high	0.60–0.80
Level 5	The probability of disturbances is extremely high	0.80–1.00

Table 2. Time consequences of disturbances $t_{j,r}$

Level	Description	$t_{j,r}$
Level 1	Disturbances may have extremely small influence on continuity and the quality of works	0.00–0.20
Level 2	Disturbances may have small influence on continuity and slightly reduce pace but without affecting the quality of works	0.20–0.40
Level 3	Disturbances may slightly disrupt continuity and reduce pace, and cause small difficulties to ensure the quality of works	0.40–0.60
Level 4	Disturbances may highly disrupt continuity and reduce pace, and cause important difficulties to ensure the quality of works	0.60–0.80
Level 5	Disturbances may enforce periodic suspension and cause extremely high difficulties to maintain the quality of works	0.80–1.00

According to the probability of disturbances $q_{j,r}$, the probability of absence of disturbances $r_{j,r}=1-q_{j,r}$ can be estimated. If the scope and impact of disturbances may be highly variable, it is proposed to additionally use the coefficient of variation of disturbances v. Then $r_{j,r}=(1-q_{j,r})\,v$ and $v\in(0,1]$. Finally, the values of coefficients of optimism $\underline{p}^{t}_{j,r}$ and pessimism $\overline{p}^{t}_{j,r}$ for the random duration of the work can be calculated as follows:

$$\underline{p}^{t}_{j,r}=1-(1-r_{j,r}\,t_{j,r}) \text{ and } \overline{p}^{t}_{j,r}=1-(1-q_{j,r}\,t_{j,r}) \tag{3}$$

If there are random disturbances $f = 1, \ldots, g$ and some or all of them can strongly disrupt the run of work and such impact can be reliably estimated, their influence can be compiled separately. This means the factors $q^{f}_{j,r}$, $r_{j,r}$ and $t^{f}_{j,r}$ should be determined for each random factor also using the descriptions in tables (1) and (2). Then, the time coefficients of optimism $\underline{p}^{t}_{j,r}$ and pessimism $\overline{p}^{t}_{j,r}$ should be calculated according to the formulas:

$$\underline{p}^{t}_{j,r}=1-\prod_{f=1}^{g}(1-r^{f}_{j,r}\;t^{f}_{j,r}) \qquad \text{and} \qquad \overline{p}^{t}_{j,r}=1-\prod_{f=1}^{g}(1-q^{f}_{j,r}\,t^{f}_{j,r}) \tag{5}$$

Changes in duration of work also affect the costs of the work. This impact can be estimated using time coefficients of optimism $\underline{p}^{t}_{j,r}$ and pessimism $\overline{p}^{t}_{j,r}$. However, the costs of the work also depend on changes in the prices of labour, prices of machinery, and prices of products and building materials. From this perspective, it is necessary to estimate the probability of prices changes $\delta_{j,r}$ and $\varepsilon_{j,r}$ or $\varepsilon_{j,r}=(1-\delta_{j,r})v$, and cost consequences of the price changes $\kappa_{j,r}$. Factors $\delta_{j,r}$ and $\kappa_{j,r}$ are independent. Their values can be estimated using descriptions in Tables 3 and 4 respectively.

Table 3. Probability of price changes $\delta_{j,r}$

Level	Description	$\delta_{j,r}$
Level 1	The probability of price changes is extremely small	0.00–0.20
Level 2	The probability of price changes is little	0.20–0.40
Level 3	The probability of price changes is medium	0.40–0.60
Level 4	The probability of price changes is high	0.60–0.80
Level 5	The probability of price changes is extremely high	0.80–1.00

Table 4. Cost consequences of price changes $\kappa_{j,r}$

Level	Description	$\kappa_{j,r}$
Level 1	An increase of cost is extremely small	0.00–0.20
Level 2	An increase of cost is little	0.20–0.40
Level 3	An increase of cost is medium	0.40–0.60
Level 4	An increase of cost is high	0.60–0.80
Level 5	An increase of cost is extremely high	0.80–1.00

Based on the aforementioned factors, the direct influence of price changes on the cost of work can be calculated as follows:

$$\underline{k}_{j,r} = 1-(1-\varepsilon_{j,r}\,\kappa_{j,r}) \qquad \text{and} \qquad \overline{k}_{j,r} = 1-(1-\delta_{j,r}\,\kappa_{j,r}) \tag{6}$$

Then, the total impact of the disruptions and price changes on the cost of the work can be estimated using the coefficients of optimism $\underline{p}^{k}_{j,r}$ and pessimism $\overline{p}^{k}_{j,r}$. The coefficients can be calculated as follows:

$$\underline{p}^{k}_{j,r} = 1-(1-\underline{p}^{t}_{j,r}\,(1-\underline{k}_{j,r})) \qquad \text{and} \qquad \overline{p}^{k}_{j,r} = 1-(1-\overline{p}^{t}_{j,r})(1-\overline{k}_{j,r})) \tag{7}$$

The assumptions presented in the Tables 1–4, and the formulas (1)–(7) enable the random characteristics of the work to be estimated and, on this basis, to reliably analyse and assess the risk of time and risk of cost of construction project. All coefficients can be easily calculated using any spreadsheet.

3. Explanation examples

As an example, some varieties of work have been presented. They are part of a construction project. All estimations and calculations have been made using the formulae (1)–(7) and the assumption determined in Tables 1–4 and factor v=0,15.

Table 5. Land development and preconstruction works

f	**Descriptions of disturbances**	$r^{f}_{j,r}$	$q^{f}_{j,r}$	$t^{f}_{j,r}$		
1	Weather conditions	0.10	0.35	0.40		
$\underline{p}^{t}_{j,r}$		0.039	$\overline{p}^{t}_{j,r}$	0.140		
Description of cost		$\varepsilon^{f}_{j,r}$	$\delta^{f}_{j,r}$	$\kappa^{f}_{j,r}$	$\underline{k}^{f}_{j,r}$	$\overline{k}^{f}_{j,r}$
Characteristic of price changes		0.12	0.20	0.30	0.36	0.60
$\underline{p}^{k}_{j,r}$		0.038	$\overline{p}^{k}_{j,r}$	0.192		

Table 6. Abutment right

f	**Descriptions of disturbances**	$r^{f}_{j,r}$	$q^{f}_{j,r}$	$t^{f}_{j,r}$
1	Weather conditions	0.10	0.35	0.40
2	Failure of equipment	0.12	0.20	0.35
$\underline{p}^{t}_{j,r}$		0,079		

$\overline{p}^{t}_{j,r}$	0,200				
Description of cost	$\varepsilon^{f}_{j,r}$	$\delta^{f}_{j,r}$	$\kappa^{f}_{j,r}$	$\underline{k}^{f}_{j,r}$	$\overline{k}^{f}_{j,r}$
Characteristic of price changes	0,11	0,25	0,35	0,39	0,88
$\underline{p}^{k}_{j,r}$	0.076				
$\overline{p}^{k}_{j,r}$	0.270				

Table 7. Bridge span

f	**Descriptions of disturbances**	$r^{f}_{j,r}$	$q^{f}_{j,r}$	$t^{f}_{j,r}$
1	Precipitation	0.10	0.35	0.20
2	Temperature	0.11	0.25	0.15
	Wind	0.11	0.30	0.30
	Humidity	0.12	0.20	0.20
	Failure rate of equipment	0.14	0.10	0.40
	Disruption on the energy supply	0.11	0.25	0.04
$\underline{p}^{t}_{j,r}$		0.141		
$\overline{p}^{t}_{j,r}$		0.256		
Description of cost		$\varepsilon^{f}_{j,r}$	$\delta^{f}_{j,r}$	$\kappa^{f}_{j,r}$	$\underline{k}^{f}_{j,r}$	$\overline{k}^{f}_{j,r}$
Characteristic of price changes		0.13	0.15	0.25	0.32	0.38
$\underline{p}^{k}_{j,r}$		0.137				
$\overline{p}^{k}_{j,r}$		0.284				

4. Final conclusions

The presented approach is simple and easy to apply. The examples given are part of a test task. Analysis of the solutions to this task has confirmed the validity of the assumptions made. The method does not require any changes in standard operating procedures of scheduling and cost estimation. Thanks to this, it can be used as part of other risk analysis methods in which the β-PERT probability distribution is used.

Taking into account the results obtained, we can ascertain that in many cases it is worth considering whether the work should be executed in very difficult conditions. When the probabilities and the time consequences of disturbances and the probability of price changes and cost consequences of these changes are estimated at level 3, it is necessary to prepare additional measures to ensure the execution of work in accordance with the project design and technical

specifications for the execution of work. If disturbances and their consequences or the probability of price changes and cost consequences of these changes are estimated at the level 4 or 5, it is worth considering changing the period of implementation of work or, if possible, changing the technology of work to those more suitable for executing the work in a difficult situation. Moreover, when work is executed in spite of extremely difficult conditions or very large changes in the impact of random disturbances on the course and results of the work, it is reasonable to consider favourable, moderate and difficult conditions of implementation. To estimate the impact of such disturbances on the duration and cost of work, the coefficients of improvement and deterioration of conditions of work implementation are used. Coefficients of condition improvement are used for favourable conditions for work execution. They are used to correct optimistic values for the duration and cost of work. Coefficients of condition deterioration are applied to difficult conditions for work execution. They are used to correct pessimistic values of duration and cost of work. In both cases, the values of the coefficients can be estimated directly on the basis of an analysis of the change of strength and kind of random perturbations.

References

[1] Kasprowicz T., *Analiza ryzyka przedsięwzięć budowlanych*, Zeszyty Naukowe Politechniki Rzeszowskiej, seria Budownictwo i Inżynieria Środowiska Z.58 (3/11/III), Rzeszów 2011, 233–240.

[2] Kasprowicz T., *Inżynieria przedsięwzięć budowlanych*, [w:] *Metody i modele w inżynierii przedsięwzięć budowlanych*, red. naukowy Oleg Kapliński, Wyd. PAN KILiW, IPPT, 2007, 35–78.

[3] Skorupka D., *Method of Construction Projects Risk Assessment*, LAMBERT Academic Publishing GmbH & Licensors, Saarbrücken 2012.

[4] Skorupka D., *Identification and initial risk assessment of construction projects in Poland*, Journal of Management in Engineering, 2008, 120–127.

[5] Turskis Z., Gajzler M., Dziadosz A., *Reliability, Risk Management, and Contingency of Construction Processes and Projects*, Journal of Civil Engineering and Management, ISSN 1392-3730 print/ISSN 1822-3605 online, 2012 Volume 18(2): 290–298.

TECHNICAL TRANSACTIONS 8/2017
CZASOPISMO TECHNICZNE 8/2017
CIVIL ENGINEERING
DOI: 10.4467/2353737XCT.17.131.6882

Renata Kłaput
Agnieszka Kocoń
Andrzej Flaga (liwpk@windlab.pl)
Institute of Structural Mechanics, Faculty of Civil Engineering, Cracow University of Technology

Air flow formation in the inlet of a closed circuit boundary layer wind tunnel using the one-set guide vanes solution

Formowanie przepływu powietrza na wlocie tunelu aerodynamicznego z warstwą przyścienną o obiegu zamkniętym z użyciem jednostopniowego układu kierownic

Abstract

The paper presents tests of wind velocity distribution at the inlet to the working section of a wind tunnel. Unconventional guide vanes were introduced in the construction of the wind tunnel to obtain a uniform air flow in this area.

Keywords: wind tunnel, guide vanes, uniform wind velocity distribution

Streszczenie

W artykule przedstawiono wyniki badań rozkładu prędkości powietrza na wlocie do tunelu aerodynamicznego. W celu uzyskania jednorodnego strumienia powietrza w tym obszarze wprowadzono niekonwencjonalny układ kierownic.

Słowa kluczowe: tunel aerodynamiczny, kierownice, jednorodny rozkład prędkości powietrza

1. Introduction

Wind tunnels are commonly used in civil engineering to simulate natural conditions at a model scale [1]. The range of phenomena which can be tested there is broad. Types of investigations include: aerodynamics of structures and buildings, wind characteristics in a boundary layer, wind energy, pedestrian wind comfort and simulation of pollution dispersion.

The wind tunnel at the Cracow University of Technology is an example of such a tunnel. It has a mixed air circulation, open or closed. The basic dimensions of the working section of the wind tunnel are: width 2.20 m, height from 1.40 m at the inflow to 1.60 m at the end of the measurement space, length 10 m (Fig. 1). Four characteristic segments, each of 2.5 m length can be distinguished in the working section.

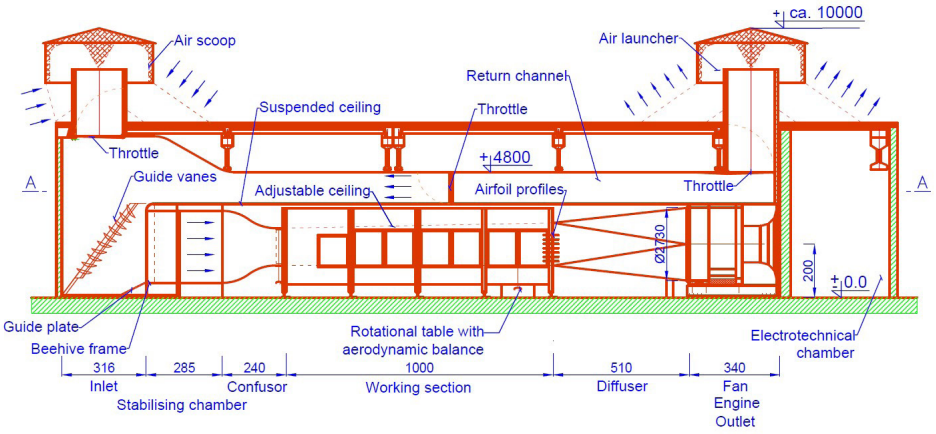

Fig. 1. Side view of the wind tunnel

a) b) c)

Fig. 2. Elements at the inlet to the wind tunnel: diagonal openwork shield (a), guide vanes (b), angle of the guide vane inclination (c)

The paper contains detailed tests of the redesign of the existing inlet to the working section. Elements forming an air flow in this part of the wind tunnel had been changed, so it was necessary to test this new configuration. In the previous solution diagonal, openwork shield, whose aim was to reduce undesirable vortexes, was applied (Fig. 2a). It had too slight an influence on the formation of uniform air flow, so this solution required improvement. Therefore unconventional guide vanes were introduced in the construction of the wind tunnel to obtain a uniform air flow at the inlet area of the working section (Fig. 2b). The set consists of 10 guide vanes of the same cross-section. The design of this solution is not the subject of this paper.

New elements in the wind tunnel demanded tests, so investigations were conducted for different arrangements of guide vanes. The final choice was the one which leads to a uniform flow at the inlet section. Trial and error was used to find the optimal arrangement of the guide vanes angles.

2. Inlet guide vane arrangement in the wind tunnel

The movement of air in the wind tunnel is caused by an axial fan which sucks it. Air goes back through the return channel and is then directed into the area of the working section by the guide vanes. It goes through a beehive frame, a stabilizing chamber and a confusor. Then – in the beginning of the working section – the mean velocity profile and the turbulence intensity profile characteristic for a specific terrain category are formed. Terrain categories reflect type of the terrain roughness and are defined according to specific standards [e.g. 2, 3] or by different authors [4].

To imitate real wind behaviour in a specific terrain roughness, respective turbulence elements (barriers, spires, blocks) are used. To execute this properly, it is necessary to obtain uniform distribution of wind flow at the starting point of the working section. Mean wind velocity at every point of the cross-section at the inlet to the wind tunnel should be the same. Hence, the essential thing is to direct the air stream in the right way. The key point is the proper arrangement of vanes. So, the main aim of these measurements was to establish uniform air flow distribution at the inlet section of the wind tunnel.

The solution of using guide vanes to direct air flow into the working section is not common in wind tunnels. There is little information concerning the influence of guide vanes arrangement on the distribution of the mean wind velocity [5], but these cannot be directly used in our case because of the specifics of the wind tunnel construction.

Problems of design optimization for wind tunnels have been discussed in many papers: from contraction design [6–8] to wind tunnel shape modification and CFD modelling of the air flow [9–11]. Particularly, wind tunnel configuration with respect to the blockage effect is considered in [12–14].

The solution presented in this paper is not commonly used in closed circuit wind tunnels. A typical construction is based on a few sets of guide vanes which direct the air flow (Fig. 3a). In the Wind Engineering Laboratory at the Cracow University of Technology only one set of guide vanes was applied, which is a new approach in this field (Fig. 3b).

Even though the construction of wind tunnels is discussed in many papers, the need to develop in this area still exists. This paper can provide a new method of forming uniform wind flow in a closed-circuit wind tunnel by using a special arrangement of guide vanes. Due to the lack of data concerning this solution, a wide range of experiments was conducted to select the suitable option for proper guide vanes arrangement.

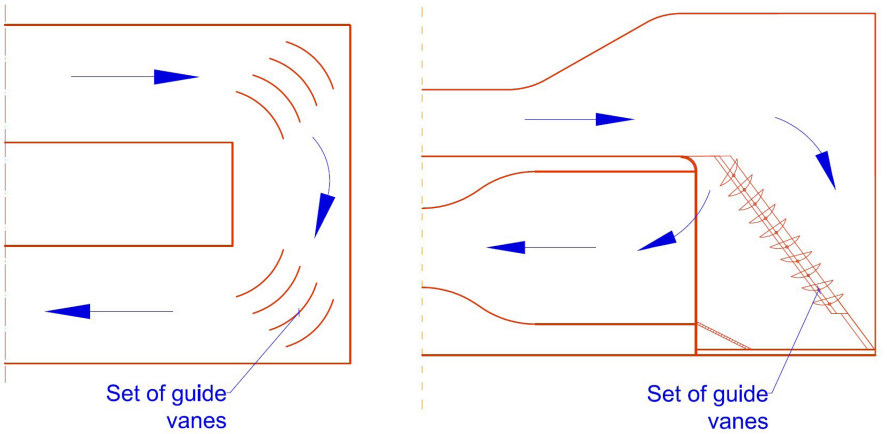

Fig. 3. Scheme of the air circulation in the closed circuit wind tunnel: typical solution of the air circulation with using a few sets of guide vanes (top view) (a); view of the inlet part of the Wind Engineering Laboratory at the Cracow University of Technology – solution of one-set guide vanes (side view) (b)

3. Experimental setup

Taking into consideration the set of different configurations, the angles of the guide vanes were changed in each experiment. Air stream velocities were measured at the inlet section of the wind tunnel at a set of measurement points. The purpose of this test was to obtain a uniform velocity distribution at the final configuration. Guide vane angles were measured in the manner illustrated in Fig. 2c.

The measurements were made using a system of pressure electronic scanners of parallel type allowing simultaneous measurements at 64 points. The scanner is built on the base of Motorola MPX2010 piezoresistive pressure sensors. The registration of the wind velocity pressure (dynamic) was made at taps regularly distributed at the inlet to the wind tunnel, at the inlet to the working section and in the working section (Fig. 4). The measured data were converted into the form of the mean wind velocity using the relationship:

$$q = \frac{1}{2}\rho \overline{V}^2 \tag{1}$$

where: q – dynamic pressure, ρ – air density; $\overline{V}$ – mean wind velocity.

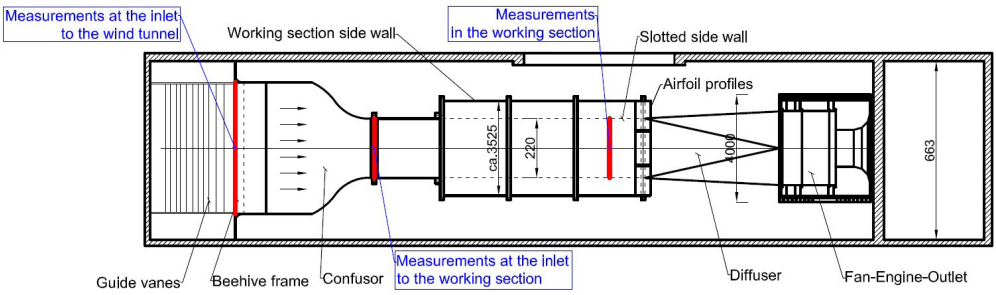

Fig. 4. Top view of the measuring areas in the wind tunnel

The tests were performed in the following conditions: period of signal sampling: 30 s, frequency of signal sampling: 200 Hz, number of time steps in sampling signal: 6000.

The mean wind velocity during experiments was set as equal to about 15 m/s with use of ATU2001 thermo-anemometers cooperating with a National Instruments NI-USB 6009 multifunction data acquisition system. This velocity was measured in the area of the wind tunnel working section.

3.1. Measurements at the inlet to the wind tunnel

The wind velocity was measured at 25 taps situated regularly from 50 cm above the floor at the inlet to the wind tunnel, every 40 cm vertically and 80 cm horizontally. The distribution of the measurement points is presented in Fig. 5. Taps were localized in the section of beehive frame (comp. Fig. 1, Fig. 4).

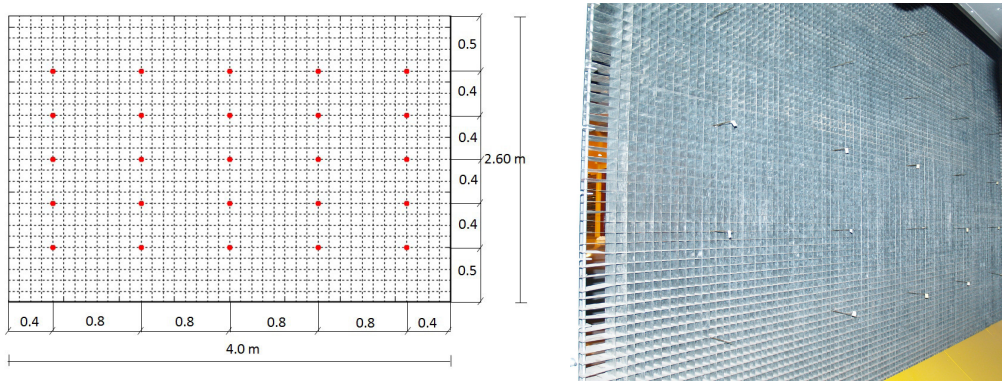

a) b)

Fig. 5. Distribution of the measurement points at the inlet to the wind tunnel scheme (a), view in the wind tunnel (b)

3.2. Measurements at the inlet to the working section

The mean wind velocity was measured at 42 taps situated regularly from 10 cm above the floor in the working section, every 20 cm vertically and 30 cm horizontally. The distribution of the measurement points at the inlet to the working section is presented in Fig. 6. Taps were localized in the section between the confusor and the working section (comp. Fig. 1, Fig. 4).

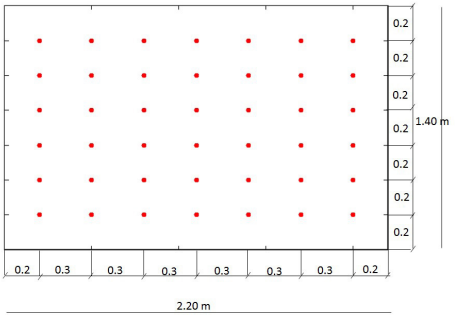

a)

b)

Fig. 6. Distribution of the measurement points at the inlet to the working section (view from the inlet side of the wind tunnel): scheme (a), view in the wind tunnel (b)

3.3. Measurements in the working section

The third series of tests were carried out in the fourth segment of the working section where models are situated during wind tunnel tests. The mean wind velocity was measured at 42 points situated regularly in the cross-section as in case 3.2. No turbulence elements (spires, barriers, blocks) were used in simulation of terrain roughness.

4. Results of experiments

In the further analysis, the situation before modification of the wind tunnel (without guide vanes) is called the initial state. In this case, there were no elements at the inlet section to the wind tunnel which could configure the direction of the air stream. The final state means the situation obtained after installing the guide vanes and its proper arrangement achieved by trial and error, when wind velocity distribution at the inlet section to the wind tunnel is uniform.

At first, the comparison of the mean wind velocity distributions in these two states – initial and final – is presented.

4.1. Measurements at the inlet to the wind tunnel

The distribution of the mean wind velocity at initial and final state at the inlet to the wind tunnel is presented in Figs 7, 8 respectively. Results of the measurements are presented

by two-dimensional distribution (a) and by values of the mean wind velocities in the measurement points (b).

The final guide vanes arrangement is presented in Fig.9. Angles of guide vanes inclination are designated on the left side of the guide vanes, while the guide vanes numbers are presented on the right. Distribution of the mean wind velocity at the final state at the inlet to the wind tunnel in the view of the whole tunnel space is also shown (Fig. 8 c).

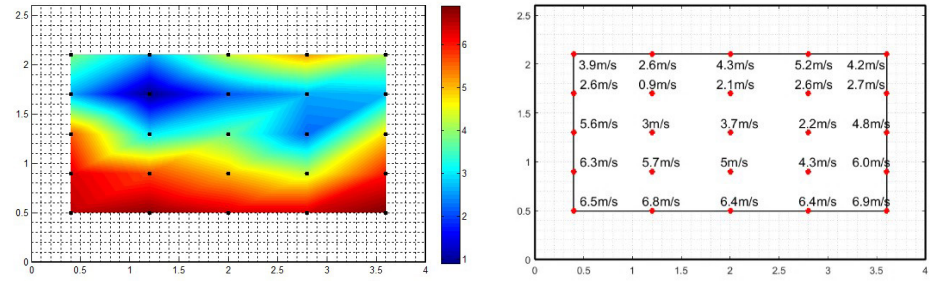

a) b)

Fig. 7. Distribution of the mean wind velocity [m/s] at the initial state at the inlet to the wind tunnel (before installing the guide vanes): 2D distribution (a), velocity values in the measurement points (b)

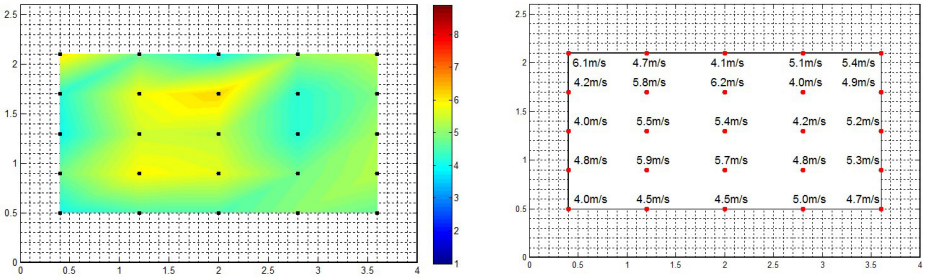

a) b)

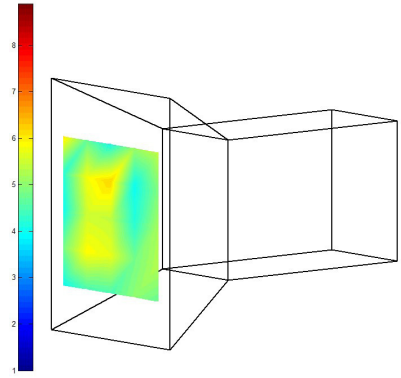

c)

Fig. 8. Distribution of the mean wind velocity [m/s] at the final state at the inlet to the wind tunnel (after installing the guide vanes): 2D distribution (a), velocity values in the measurement points (b), 2D distribution in the view of the whole tunnel space (c)

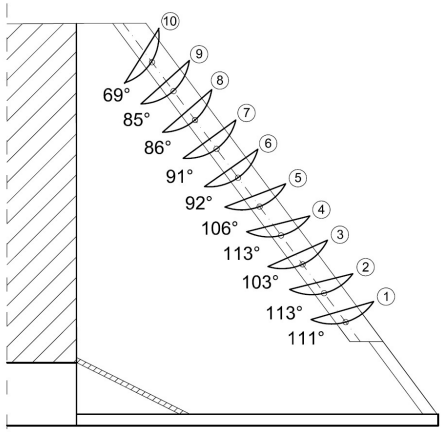

Fig. 9. The final setting of the inclination angles of guide vanes

Mean wind velocity distribution at the inlet area to the wind tunnel in the initial situation (Fig. 7) was not uniform. Velocities in the lower part of the measurement area were significantly higher than in the upper. This was a very undesirable situation and therefore changes aiming to improve it had to be made. After installing a set of guide vanes and their proper arrangement a uniform distribution of mean wind velocity can be observed (Fig. 8).

4.2. Measurements at the inlet to the working section

The distribution of the mean wind velocity in the initial and final states at the inlet to the working section is presented in Figs 10, 11 respectively. As before, two-dimensional distribution and values of the mean wind velocity in each measurement point are presented.

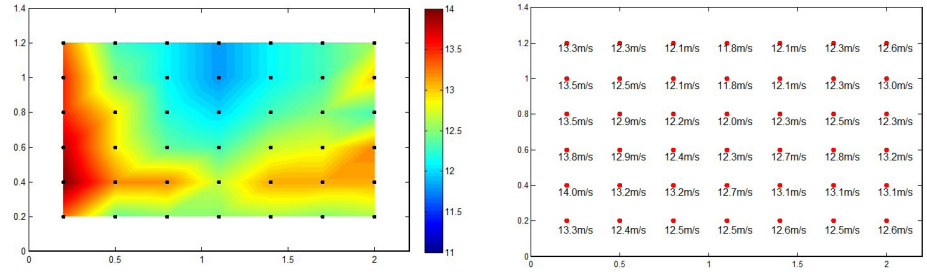

a) b)

Fig. 10. Distribution of the mean wind velocity [m/s] at the inlet to the working section (before installing the guide vanes): 2D distribution (a), velocity values in the measurement points (b)

Similarly to case 4.1, a significant difference between the distribution of the mean wind velocity before and after installing the set of guide vanes can be observed. We were able to achieve a uniform distribution, as can be seen in Fig.11. It must be pointed out that mean velocities in this case are higher than those measured at the inlet to the wind tunnel. The air stream flows through the confusor on its way from the inlet to the wind tunnel to the inlet to the working section. The confusor increases wind velocity and improves the uniformity of its distribution in the cross-section.

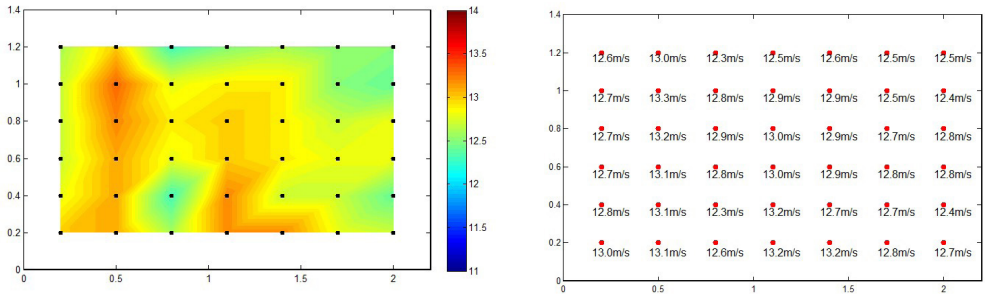

a) b)

Fig. 11. Distribution of the mean wind velocity [m/s] at the inlet to the working section (after installing the guide vanes): 2D distribution (a), velocity values in the measurement points (b)

4.3. Measurements in the working section

Fig.12 presents results of the mean wind velocity distribution in 4th segment of the working section of the wind tunnel in the final state in the form of two-dimensional distribution (a) and velocity values in the measurement points (b). Additionally, a two-dimensional distribution of the mean wind velocity in two cross-sections of the wind tunnel space (inlet to the working section, 4th segment of the working section) is also presented in Fig.12c.

The results show clearly that in the area where wind tunnel tests were carried out, the distribution of the mean wind velocity is uniform. Such situation takes place only in the case without turbulence elements. A simulation of e.g. urban terrain categories by using spires, barriers or blocks would provide a significantly different distribution of mean wind velocities in the working section of the wind tunnel to the presented results.

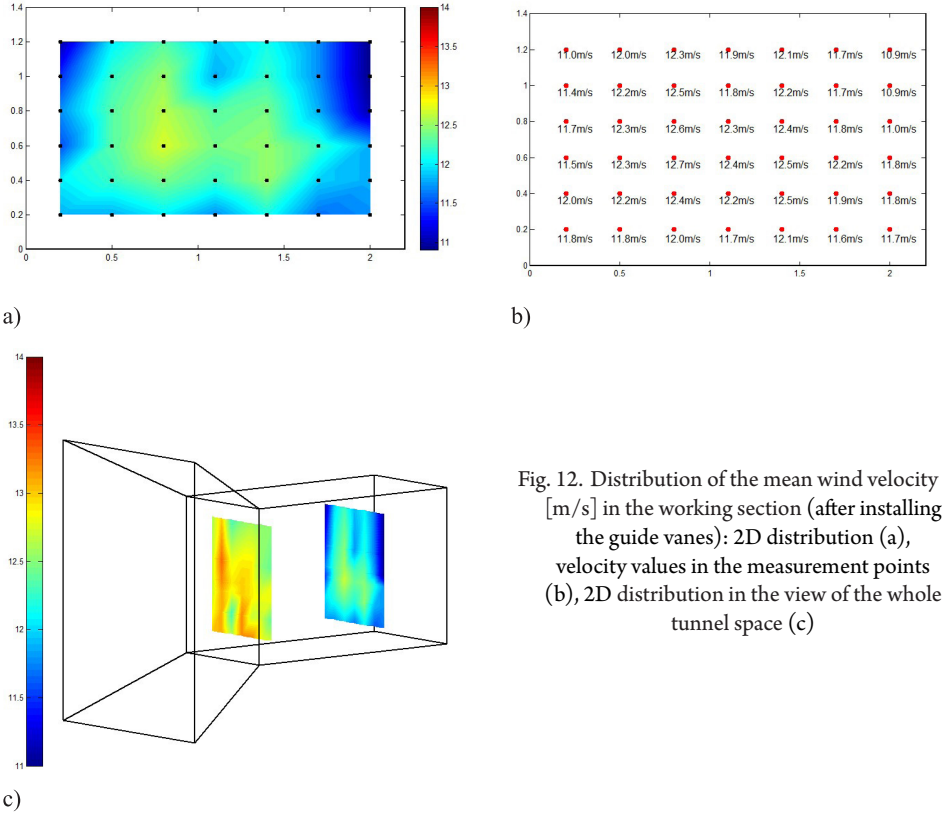

Fig. 12. Distribution of the mean wind velocity [m/s] in the working section (after installing the guide vanes): 2D distribution (a), velocity values in the measurement points (b), 2D distribution in the view of the whole tunnel space (c)

4.4. Selected cases of the guide vanes settings

In this section some measurement results which finally led to the proper guide vane arrangement and the uniform mean velocity distribution are presented. They were chosen to show the influence of guide vane angle of inclination on this distribution. Only the results of the measurements carried out at the inlet to the wind tunnel are presented.

Six measurement situations discussed further are summarized in Tab.1. Specific guide vane arrangement are assigned to the case (I-VI). Each of the guide vanes (1-10) has its own angle of inclination.

Table 1. Measurement cases of different guide vanes arrangements

Case	Guide vane number									
	1	2	3	4	5	6	7	8	9	10
	Inclination angle [°]									
I	76	76	76	67	74	71	57	49	50	39
II	76	76	76	67	74	71	57	49	50	68

III	111	113	96	102	94	80	91	86	85	69
IV	111	113	103	113	106	115	110	110	118	128
V	94	95	103	113	106	92	91	86	85	69
VI	111	113	103	113	106	92	91	86	85	69

Results of the measurements in the form as before – 2D distribution of the mean wind velocity, the mean wind velocity values in particular points in the cross-section at the inlet to the wind tunnel and guide vanes configuration corresponding to the specific case are shown in Figs 13–18.

Case I

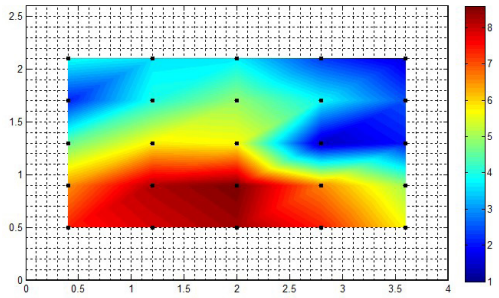

a)

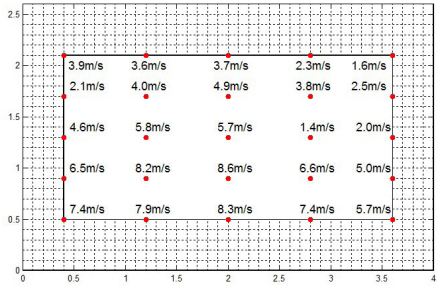

b)

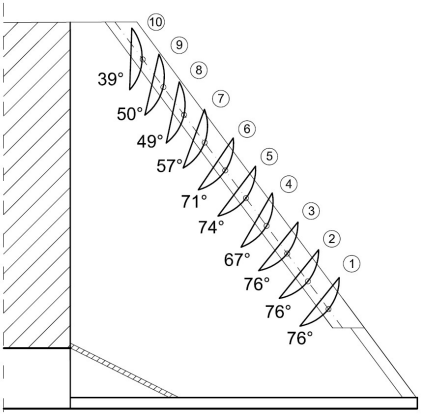

c)

Fig. 13. Case I: 2D distribution of the mean wind velocity [m/s] (a), velocity values in the measurement points [m/s] (b), guide vanes configuration (c)

In the case I, high mean wind velocities (6–8 m/s) at the bottom and low (2–4 m/s) at the top of the measurement area can be observed. It was considered whether the 10th guide vane may block air flow in the higher part, which could cause a decrease in velocity. Due to this fact it was decided to increase the inclination of 10th guide vane.

Case II

Inclination of 10th guide vane was increased while the angle of other guide vanes were as in Case I (Fig. 14). In this situation an increase in mean wind velocities at the top of the measurement area in comparison to Case I can be observed. It can be deduced that the change of the inclination angle of the guide vane enabled flow of the air stream into the inlet area. The inner side of the 10th guide vane directed it into the top part of the inlet to the wind tunnel.

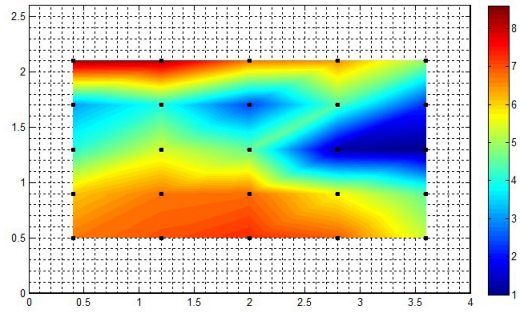

a)

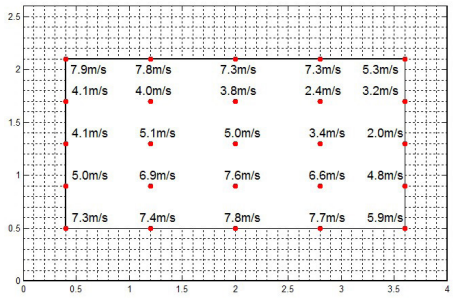

b)

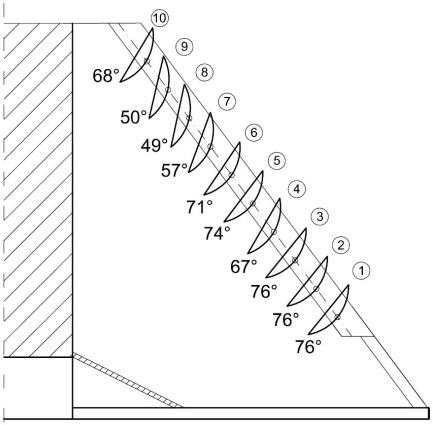

c)

Fig. 14. Case II: 2D distribution of the mean wind velocity [m/s] (a), velocity values in the measurement points [m/s] (b), guide vanes configuration (c)

The influence of the change of each guide vane angle on the mean wind velocity distribution was also investigated during wind tunnel tests. Investigations were carried out in the following way: the angle of only one guide vane was changed while other guide vanes were in configuration as in case I. It should be noted that the change of the angle of one guide vane has a negligible influence on velocity distribution at the inlet space to the wind tunnel. However, the results of these cases are not presented in this paper.

Case III

The inclinations of guide vanes 1–9 were increased while the angle of the 10th guide vane was as in Case II (Fig. 15). The significant change in guide vanes inclination angles caused improvement of the uniformity of the mean wind velocity distribution. Only at the top part of the inlet area on the left and the right side are the velocities lower (2–4 m/s).

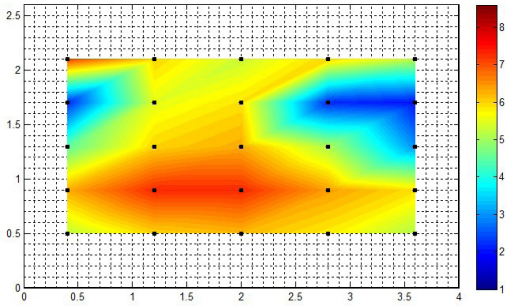

a)

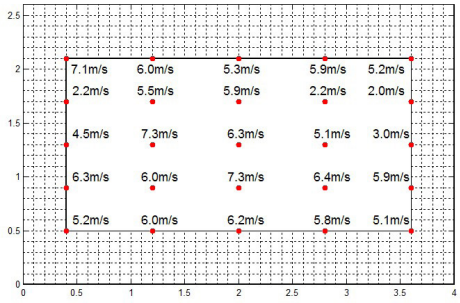

b)

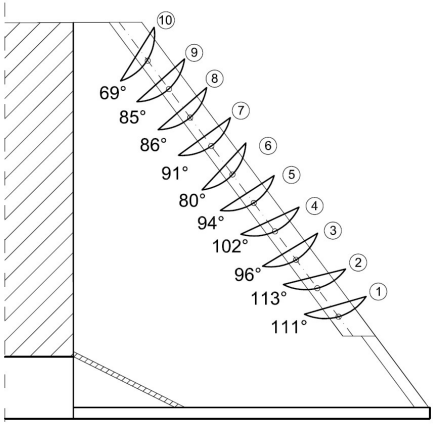

c)

Fig. 15. Case III: 2D distribution of the mean wind velocity [m/s] (a), velocity values in the measurement points [m/s] (b), guide vanes configuration (c)

The reason could be quite obvious – the inlet area of the wind tunnel is not built over on the left and right side (comp. Fig. 4). The air can inflow to this empty space if it is not properly directed into the space of the wind tunnel. Due to this fact it was decided to use temporary partition foils aimed at limiting the area of air flow.

Case IV

The inclination angles of guide vanes 3–10 were increased. Additionally, temporary partition foils were used over the height of the guide vanes set, starting from 0.5 m above floor level. These partition foils are marked in Fig. 16(c) as a dashed area.

These changes made an improvement in the uniformity of the mean wind velocity distribution. Regions of low wind velocity do not appear on both sides of the inlet area. There is only a slight difference in the velocities in the corners of the tested cross-section.

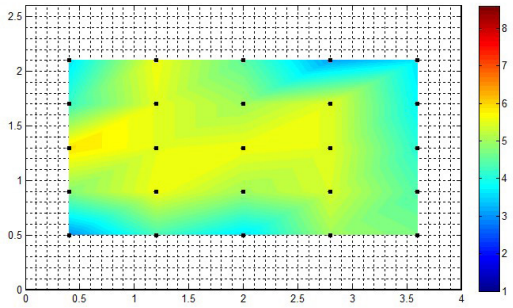

a)

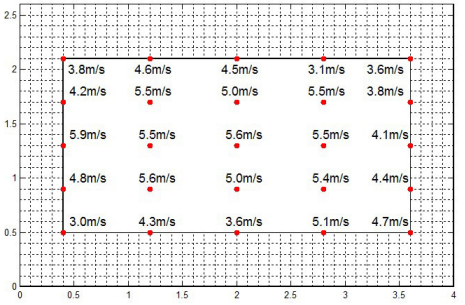

b)

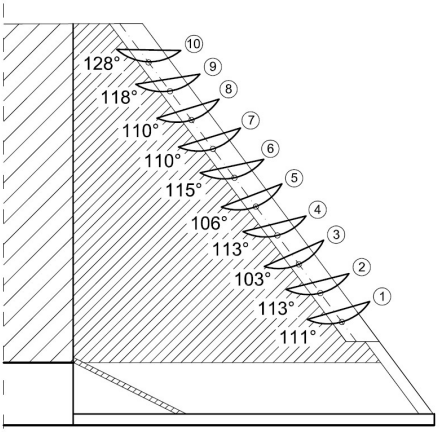

c)

Fig. 16. Case IV: 2D distribution of the mean wind velocity [m/s] (a), velocity values in the measurement points [m/s] (b), guide vanes configuration (c)

Case V

In this arrangement inclination angles of upper guide vanes (6–10) and lower guide vanes (1–2) (Fig. 17) were decreased.

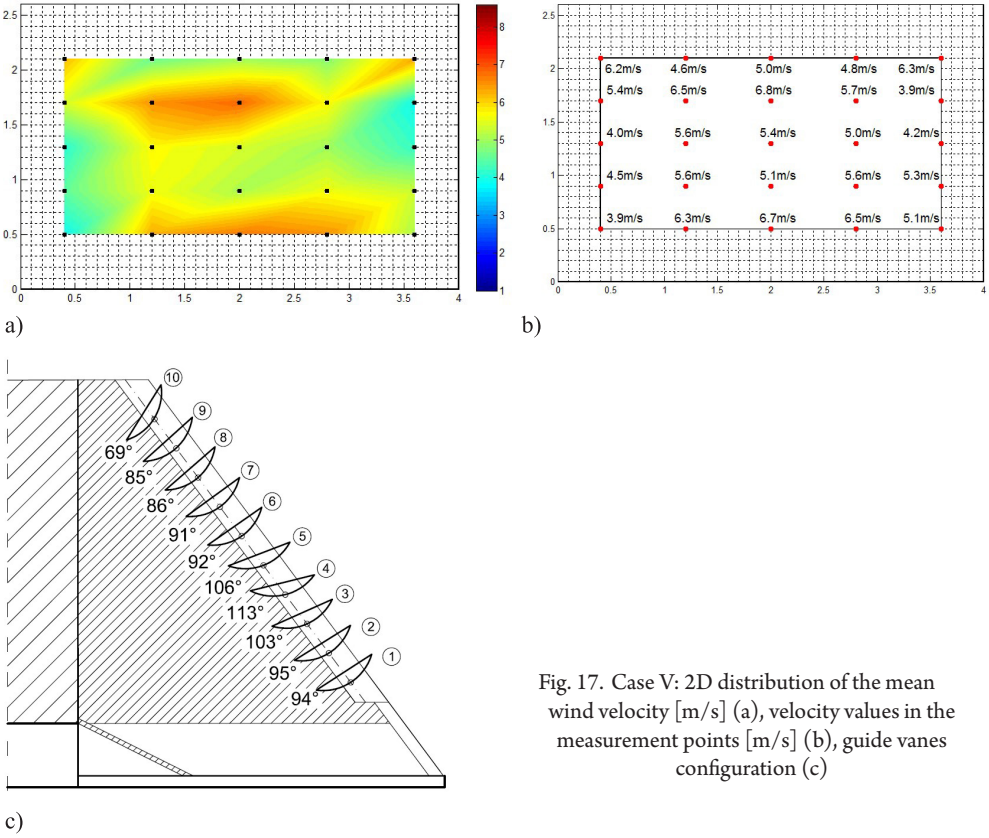

Fig. 17. Case V: 2D distribution of the mean wind velocity [m/s] (a), velocity values in the measurement points [m/s] (b), guide vanes configuration (c)

The improvement in the results in this case can be observed. The mean wind velocity in the corners of the wind tunnel inlet area is higher than in Case IV. Only the value in the left bottom corner is still slightly different to that in other measurement points.

Case VI

The inclination angles of the lower guide vanes (1–2) were increased (as in Case IV) (Fig. 18). The improvement in uniformity of the mean wind velocity distribution was achieved by an increase in the inclination angles of the lower guide vanes and a decrease in the inclination angles of the upper guide vanes (in comparison to Case IV).

It should be highlighted that the upper guide vanes influence the mean velocity distribution at the top level of the wind tunnel inlet area as well as at the bottom level, because the air stream is directed by their inner and outer sides in different ways.

The results presented in Case VI were obtained for the situation using partition foils. It was only a temporary solution which was used to determine the best guide vane arrangement. The results of the mean wind velocity distribution in the wind tunnel inlet area for this guide vanes arrangement but without foils was presented in Fig. 8.

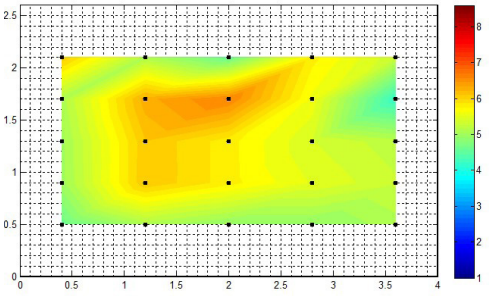

a)

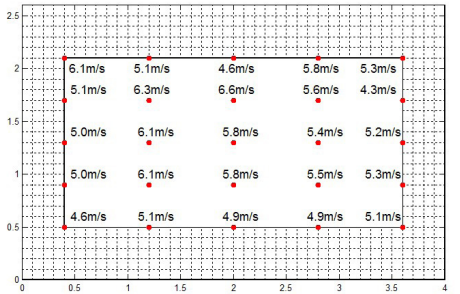

b)

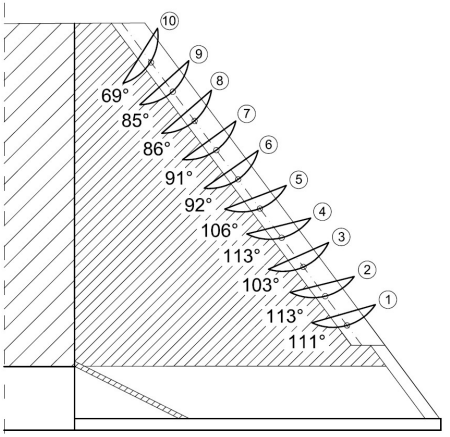

c)

Fig. 18. Case VI: 2D distribution of the mean wind velocity [m/s] (a), velocity values in the measurement points [m/s] (b), guide vanes configuration (c)

5. Conclusions

The optimum setting of the guide vanes (Case VI) was applied as the final solution, but without the partition foils. In this arrangement both sides of the guide vanes – inner and outer – take part in directing the air stream into the inlet area of the wind tunnel. This setting leads to obtaining a uniform mean wind velocity distribution, which was the aim of these tests.

Experiments show that one set of guide vanes is a good solution for obtaining a uniform distribution of the wind velocity at the inlet to the wind tunnel. Especially, it is very useful solution for tunnels where there is insufficient space to apply other types of constructions. The specific arrangement of guide vanes provides uniform wind flow in its inlet section. Then wind conditions can be modified optionally in the working section.

References

[1] Cermak J.E., *Wind-tunnel development and trends in applications to civil engineering*, Journal of Wind Engineering and Industrial Aerodynamics 91, 2003, 355–370.

[2] PN-EN 1991-1-4: Oddziaływania na konstrukcje. Oddziaływania ogólne. Oddziaływania wiatru.

[3] PN-77/B-02011: Obciążenia w obliczeniach statycznych. Obciążenie wiatrem.

[4] Flaga A., *Inżynieria wiatrowa. Podstawy i zastosowania*, Arkady, 2008.

[5] Moonen P., Blocken B., Carmeliet J., *Indicators for the evaluation of wind tunnel test section flow quality and application to a numerical close-circuit wind tunnel,* Journal of Wind Enginnering and Industrial Aerodynamics 95, 2007, 1289–1314.

[6] Fang F.-M., Chen J.C., Hong Y.T., *Experimental and analytical evaluation of flow in a square-to-square wind tunnel contraction*, Journal of Wind Engineering and Industrial Aerodynamics 89, 2001, 247–262.

[7] Abdelhamed A.S., Yassen Y.El-S., ElSakka M.M., *Design optimization of three dimensional geometry of wind tunnel contraction,* Ain Shams Engineering Journal 6, 2015, 281–288.

[8] Doolan C., Morgans R., *Numerical Evaluation and Optimization of Low Speed Wind Tunnel Contractions*, 18th AIAA Computational Fluid Dynamics Conference, 25–28 June 2007, Miami, FL.

[9] Moonen P., Blocken B., Roels S., Carmeliet J., *Numerical modeling of the low conditions in a closed-circuit low speed wind tunnel,* Journal of Wind Engineering and Industrial Aerodynamics 94, 2006, 699–723.

[10] Scotto di Perta E., Agizza M.A., Sorrentino G., Boccia L., Pindozzi S., *Study of aerodynamic performances of different wind tunnel configurations and air inlet velocities, using computational fluid dynamics (CFD)*, Computers and Electronics in Agriculture 125, 2016, 137–148.

[11] Atieh A., Al Shariff S., Ahmed N., *Novel wind tunnel*, Sustainable Cities and Society 25, 2016, 102–107.

[12] Chen T.Y., Liou L.R., *Blockage corrections in wind tunnel tests of small horizontal-axis wind turbines*, Experimental Thermal and Fluid Science 35, 2011, 565–569.
[13] Amrouche N., Dizene R., Laneville A., *Observations of the wind tunnel blockage effects on the mean pressure distributions around rectangular prisms in smooth and grid turbulent flows*, Revue des Energies Renouvelables SMEE'10 Bou Ismail Tipaza, 2010, 21–26.
[14] Anthoine J., Olivari D., Portugaels D., *Drag coefficient determination of bluff bodies – analysis of blockage effect*, COST Action C14, Impact of Wind and Storm on City Life and Building Environment, May 5-8 2004, Rhode Saint Genese, Belgium.

TECHNICAL TRANSACTIONS 8/2017
CZASOPISMO TECHNICZNE 8/2017
CIVIL ENGINEERING
DOI: 10.4467/2353737XCT.17.132.6883

Renata Kozik (rkozik@izbwit.wil.pk.edu.pl)
Institute of Construction and Transportation Engineering and Management, Faculty of Civil Engineering, Cracow University of Technology

Izabela Karasińska-Jaśkowiec
Institute for Computational Civil Engineering, Faculty of Civil Engineering, Cracow University of Technology

Green public procurement for water infrastructure in the context of sustainable development and respect for water

Zielone zamówienia publiczne dla infrastruktury ściekowej w kontekście zrównoważonego rozwoju i poszanowania wody

Abstract

The paper presents the results of research aimed at examining how public institutions implement sustainable development policy at the stage of preparation of tender documentation for construction and extension of wastewater treatment plants and water and wastewater infrastructure. The most important assumptions of sustainable development policy at national and European level are also briefly discussed.

Keywords: sustainable development, water infrastructure, green public procurement

Streszczenie

W artykule przedstawiono wyniki badań, których celem było sprawdzenie, w jaki sposób instytucje publiczne realizują politykę zrównoważonego rozwoju na etapie przygotowywania dokumentacji przetargowej na budowę i rozbudowę oczyszczalni ścieków i infrastruktury wodno-ściekowej. Krótko omówiono również najważniejsze założenia polityki zrównoważonego rozwoju w wymiarze krajowym i europejskim.

Słowa kluczowe: zrównoważony rozwój, infrastruktura wodno-ściekowa, zielone zamówienia publiczne

1. Introduction

The public procurement system, due to its role in the economy, forms the basis for policy-making in regard to public spending as well as is one of the elements of sustainable development and environmental policy, setting its trends.

This indicates that the development of civilization has lead among other things to improving the quality of life of its inhabitants. The topic of sustainable construction is discussed extensively in the literature and is mainly related to buildings [1, 2].

One of the criteria for assessing the standard of living of citizens is access to drinking water and providing ways of solving the problems of the sewage generated. The increase in well-being should not take place at the expense of the environment. Significant importance is attributed here to the transformation of environmental policy into a resource-efficient economy.

The condition for the proper functioning and development of water management is the appropriate development of water and sewage infrastructure. Hence, not only water management, understood as sharing water resources, is important, but also of water/sewage management, responsible for the efficient use of its resources.

It is estimated that only 2.5 percent of the Earth's water resources is fresh water, and only 0.6% constitutes water which could be a source of drinking water [14]

Only a small portion of fresh water, approx. 0.3%, is available in the form of rivers, lakes and swamps. As a result of various factors, mainly climatic and hydrological conditions, Poland is threatened by a water deficit [15]. Data from the National Water Management shows that Poland has an average of approx. 1580 m3 of water per year per capita (in times of drought this coefficient falls below 1000 m^3), and the average resources per capita in Europe are 4560 m3/year, while on Earth approx. 7300 m^3 [4].

In contrast, according to the Central Statistical Office (CSO) data [13], in Poland in 2009, approx. 88% of urban population and only 27% of rural residents used the collective wastewater treatment plants. In 2014, these numbers amounted to respectively 93.90% in urban areas and in rural areas 37.40% of the population. The reason for this is negligence, at the basis of which is a lack of sufficient funds for these types of investments.

In accordance with Article 7 of the Local Government Act [7], meeting the collective needs of the community in the area of water mains, supply in water and sewage disposal is the responsibility of municipalities, which is fulfilled within the financial capabilities by the local governments. Investments in infrastructure are particularly expensive, therefore local authorities are faced with the challenge of obtaining additional sources of financing and using it effectively, for example, through the public procurement system.

One of the most important documents allowing action in this direction was the "National Strategic Reference Framework – National Cohesion Strategy 2007–2013", adopted by the Council of Ministers on 1 August 2006, defining Poland's policy objectives in relation to EU policies. "The upgrade of technical and social infrastructure, which is crucial for the growth and competitiveness of Poland and its regions", is included in a group of specific cohesion policy objectives, and within it "construction and development of environmental protection infrastructure." The Act of 6 December 2006 on the principles of development

policy (Journal of Laws No. 277, item 1658) [8] indicates that the implementation of the development strategy is based on the operational programmes in the form of national operational programmes in relation to the development strategy of the country as well as sectoral strategies, and in the form of regional operational programmes co-financed from the state budget and foreign sources, and implementing development strategies of provinces. The development of municipal water and sewage management in 2007–2013 was included in the national operational programme "Infrastructure and Environment", adopted by the Council of Ministers on 29 November 2006, as well as in 16 regional operational programmes [3]. Operational programmes have enabled Poland to finance, among other things, sewage infrastructure projects, including sewage treatment plants, amounting to a very significant share of the cost, using European Union funds, and just a small part were to come from domestic sources. Public sector entities – the municipalities – were required to spend these funds in accordance with the provisions of the law on public procurement [9] (e.g. the public procurement act and the relevant sector regulations).

The European Union's approach to public procurement is based on respect for the environment. The European Commission has consistently supported initiatives to protect the environment, including promoting making procurement commissioned by public authorities more green. "Green public procurement" (GPP) [6] should be understood as a process whereby public authorities seek to procure goods, services and works whose impact on the environment during their life cycle is smaller compared to goods, services and works with the same primary function that would otherwise be procured. The current *Europe 2020* strategy is a long-term social and economic program of the EU. One of its three overarching priorities is sustainable development – promoting a sustainable, ecological, resource-efficient, more "green" and yet competitive economy. This means, among other things, the need to include this priority in all types of policies at EU and national level. Public bodies that purchase goods and services using public funds are obligated to adhere to the principles laid down in the Public Procurement Law [9] and the Public Finance Act [10]. In the case of the issue which interests us, public procurement procedures are being increasingly influenced by the provisions of environmental law, construction law [11] and water law [12]. With regard to public procurement, a regularity can be confirmed with satisfaction, according to which the basic rules specific to this branch of law are subject to modification under the influence of pro-environmental legislation.

Pro-environmental criteria, meeting the needs of environmental protection and sustainable development, can be included in the procurement process at each stage. The most effective is their inclusion in the terms of reference, hence the authors present several examples and options in tabular form:

1) Employer's requirements relating to water consumption in a sewage treatment plant (Tab. 1), and
2) Employer's requirements on the efficiency of sewage treatment (Tab. 2),

Which could make the contract and thus the sewage treatment plant more "green", corresponding in a greater extent to the concept of sustainable development, and the funds disbursed more effective. They are also proposals of solutions or best practices, which are more

environmentally friendly, and therefore meeting the objectives of the concept of sustainable development [5]. Results of studies showing a degree of understanding and "greening" of public procurement are also presented.

2. Application of environmental requirements and criteria in public procurement – own study

The study involved proceedings, the subject of which was the construction or expansion of water and sewage infrastructure, which were initiated between 2009 and 2015, and regarded investments co-financed from EU funds in 2007–2013. During this period, a total of 113,136 projects were completed, of which 3,077 were in the field of environmental protection. In 411 cases, the project was defined as the construction or expansion of a sewage treatment plant. The study was conducted using a questionnaire developed by the Authors as part of a request for disclosure of public information.

In total, the whole study included 70 projects (out of 411; i.e. approx. 17%) in 70 municipalities, and 172 related procedures – 88 procedures concerned construction work, 19 "design and build" projects, 25 concerned design, and others concerned services, supplies, etc. The cost of the surveyed projects amounted to more than 1.24 billion PLN. This paper presents only part of the results, the proceedings, the subject of which was a contract for the development of design documentation and for the design and execution of work. Environmental requirements are most applicable at the design stage, and therefore the authors decided to focus on this stage.

The research for the analysis of public procurement in the area of sewage infrastructure covered projects carried out in five provinces. This includes two provinces where the investments were the highest (Silesian and Greater Poland provinces) and two where the least funds were allocated for this purpose (Świętokrzyskie and Warmian-Masurian provinces) as well as one province with an average score (Western Pomeranian province).

Respondents answered a number of questions, whose main objective was to investigate whether the employers apply environmental requirements, mainly in the terms of reference, as well as in the evaluation of bids (question 12 and 14). A set of questions related to water consumption and the efficiency of sewage treatment is included in Tables 1 and 2. The employers had the following response choices: Yes (Y), No (N), Not applicable (N/A). The number of responses is shown in the graphs: Fig. 1 and Fig. 3 for procedures for the development of design documentation, Fig. 2 and Fig. 4 show the results of procedures for the design and execution of works. The set of questions was the same for both "development of design documentation" and for the "design and execution of works. In five cases, detailed answers have not been given. Most of the questions concerned the construction and expansion of sewage treatment plants. In both types of procedures, in more than 60% of cases it was indicated that the projects are never consulted with environmental protection specialists.

Table 1 presents the questions related to the requirements of the employers regarding the consumption of water in the sewage infrastructure facilities.

Table 1. Requirements of the employer relating to water consumption. Source: own study

No.	Questions – requirements related to water consumption
1	Overall consumption of drinking water in the sewage infrastructure facilities (excluding water consumption in office or administrative buildings), as defined in the documentation for the procurement procedure, should not exceed: Facilities for sewage treatment: x m^3 of water used per 1000 m^3 of sewage treated; Sewage systems – cleaning the pipes installed: m^3 of water used per 100 m of pipes installed
2	The contractor was required to submit documentation and grant guarantees relating to the annual consumption of water in the treatment plant, verified by summing the consumption of water in all major water-using facilities
3	Sanctions for breaching obligations for the guaranteed water consumption have been defined.
4	The contractor was required to submit documentation and grant guarantees relating to the annual consumption of water in the treatment plant and relating to the consumption of water by specific equipment depending on the type of bid, verified by summing the consumption of water in all major water-using facilities
5	The contractor was required to submit technical data sheets for the maximum allowable consumption of drinking water per 1 000 m^3 of treated sewage, confirming compliance with the specification, and had to specify the expected usage of grey water and rainwater, for example
6	The contractor was obligated to point out systems in the sewage treatment plant, where the drinking water is not used for treatment
7	If the bid covered plant operation, did the requirement of verifying consumption include conducting checks using water meters installed for the entire treatment plant
8	Contractors should quantify the expected savings of drinking water resulting from any proposed measures, with reference to the earlier designs or independent technical assessments
9	The contractor was required to propose how to maximise the use of rainwater and grey water
10	In order to verify, the contractor was required to present calculations and documentation in relation to the amount of rainwater and grey water used in sewage infrastructure facilities
11	The contractor was required to propose how to reduce consumption of fresh water to rinse the pipes prior to installation and afterwards
12	Classification of bids took place according to the following criteria: Number of rinses before installation and after its completion; Estimated water consumption expressed by the percentage of consumption of water amounting to ... m^3 per m of pipeline installed
13	In order to verify, the contractor was required to present calculations and documentation related to the consumption of water in relation to the piping
14	Extra points were awarded for measures to save water going beyond the specification as defined in the procurement procedure documentation in accordance with the basic criteria

Fig. 1 and 2 below list the number of responses to issues related to water consumption.

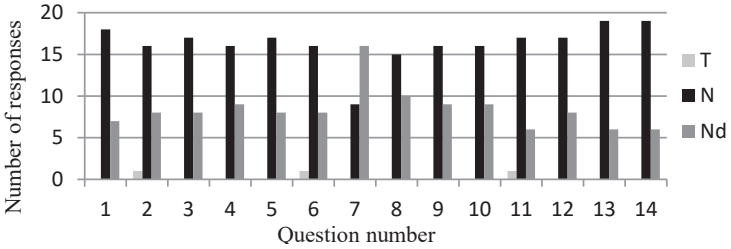

Fig. 1. Requirements for water consumption – design documentation. Source: own study

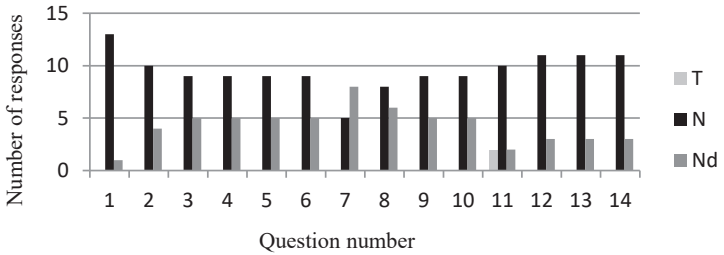

Fig. 2. Requirements for water consumption – design and execution of works. Source: own study

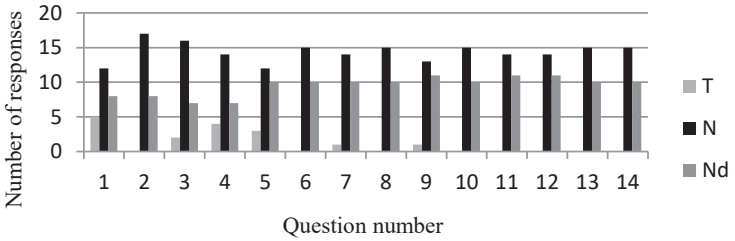

Fig. 3. Requirements for sewage treatment efficiency – design documentation. Source: own study

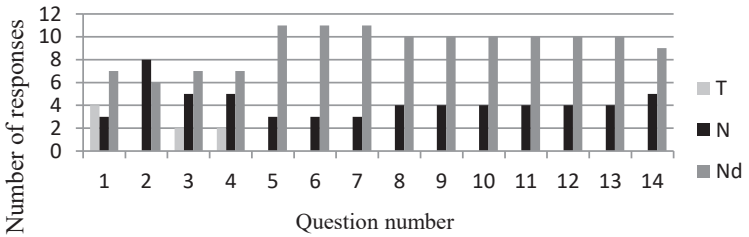

Fig. 4. Requirements for sewage treatment efficiency – design and execution of works. Source: own study

The research results shown in Fig. 1 and 2 show that the employers rarely used requirements that go beyond the basic requirements in the terms of reference at the stage of development of design documentation. In each question asked, negative questions prevail. Answers confirming the use of green requirements are practically none. Employers confirmed the use of environmental requirements in just a few cases, for example, in regard to the use of fresh water to rinse the piping.

Table 2. Requirements of the employer for the efficiency of sewage treatment. Source: own study

No.	Questions – requirements regarding the efficiency of sewage treatment
1	Contractors were required to submit documentation confirming that offered sewage treatment technology complies with the required standards for drainage
2	The employer appealed to the bidders to sign a detailed guarantee for the efficiency of the technological process
3	The procurement procedure documentation describes sanctions for breaching the above obligations
4	Methodology has been described to be used to control the efficiency of the sewage treatment plant
5	Requirements have been set out for the maximum use of chemicals used for precipitation (salts of iron or aluminium) per m^3 of sewage treated or chemicals used for precipitation per kilogram of phosphorus at the inlet
6	The contractor was required to submit approved calculations for the consumption of the precipitation agent or agents per m^3 of sewage treated or kg of total phosphorus at the inlet
7	The contractor has to calculate and document the consumption of precipitation agent or agents per kg of total phosphorus at the inlet, specifying the percentage with respect to the ratio between the traditional uses of a precipitation agent or agents divided by a phosphorus concentration at the outlet from the sewage treatment plant allowed under national legislation
8	The employer requires or promotes (e.g. by awarding additional points) increased cleaning efficiency for heavy metals
9	Contractors had to present documentation confirming the guaranteed level of heavy metals in effluent (µg/l)
10	The employer requires or promotes (e.g. by awarding additional points) increased cleaning efficiency in relation to the persistent organic pollutants, for example, nonylphenols and octylphenols; - benzo[a]pyrene
11	Contractors must submit documentation confirming the guaranteed level of the content of persistent organic pollutants (bis(2-ethylhexyl) phthalate (DEHP), naphthalene, nonylphenol and octylphenol or polycyclic aromatic hydrocarbons (PAH) in treated sewage, expressed in (µg/l)
12	The employer requires or promotes (e.g. by awarding additional points) increased cleaning efficiency for medicinal products (tramadol and primidone)
13	Contractors had to present documentation confirming the guaranteed level of tramadol and primidone in effluent (µg/l)
14	The employer requires or promotes (e.g. by awarding additional points) increased cleaning efficiency for pathogens

Fig. 3 and 4 below summarise in graphs the number of responses to issues related to water consumption.

A similar situation occurs in the case of questions concerning the effectiveness of sewage treatment. The research results shown in Fig. 3 and 4 show that the employers rarely used requirements that go beyond the basic requirements in the terms of reference at the stage of development of design documentation. A large number of "not applicable" responses is related to the fact that the subject of procedures for the "design and execution of work" mainly regarded infrastructure, e.g. construction of sewage piping. Therefore, the employers did not have to use all of the requirements.

3. Conclusion

The amount of water consumption is the sum of the necessary consumption and water losses. Rational consumption is the amount of water to meet all human needs. Other activities involving wasting water as a result of, for example, wasteful management, including unfriendly water/sewage infrastructure represent a loss.

Research has shown that too small requirements imposed mainly by municipalities in public tendering procedures for newly built water/sewage infrastructure, do not make full use of the role they could play as a very effective instrument, among other things, for measures aiming at saving drinking water and sustainable development.

At the moment, on the basis of legal possibilities and more often (though insufficiently) in the awareness of administrative authorities at various levels, initiatives to protect the environment are being consistently supported, and the relatively small resources of drinking water in Poland, force the need for further "greening" of public procurements for water/sewage infrastructure, for which the idea of environmental protection should be more natural. It is still necessary to promote knowledge about the admissibility of application of such criteria and the benefits of "green public procurement."

References

[1] Belniak S., Głuszak M., Zięba M., *Budownictwo ekologiczne. Aspekty ekologiczne*, PWN, Warszawa 2013.

[2] Belniak S., Głuszak M., Zięba M., *The Supply of Sustainable of office Space in Poland,* Świat Nieruchomości Nr 82 (4/2012).

[3] Czechowicz M., *Koncepcja rozwoju komunalnej gospodarki ściekowej w aspekcie standardów Unii Europejskiej,* Człowiek i Środowisko 31 (1–2), 2007, 61–92, https://www.igpim.pl/publikacje/str07_1–2/czechowicz.pdf (access:11.02.2017).

[4] Kądzielawski G., *Woda palący problem*, Wyd. Fundacja Energia dla Europy, 2013 (http://www.3xsrodowisko.pl/uploads/media/raport-07.pdf (access:11.02.2017).

[5] *Kryteria zielonych zamówień publicznych dotyczące infrastruktury ściekowej*, Polityka regionalna i miejska, July 2013; regio-publication@ec.europa.eu, http://ec.europa.eu/regional_policy/index_en.cfm ISBN : 978 92-79-40096-4 doi:10.2776/20992,http://

ec.europa.eu/regional_policy/sources/docgener/studies/pdf/green_public_procurement_pl.pdf (access: 11.02.2017).
[6] Public Procurement Office, https://www.uzp.gov.pl/baza-wiedzy/zrownowazone-zamowienia-publiczne/zielone-zamowienia/wprowadzenie (access: 11.02.2017).
[7] The Act of 8 March 1990 on the Local Government, Journal of Laws of 2001 No. 142 Item 1591, as amended).
[8] Act of 6 December 2006 on the principles of development policy (Journal of Laws of 2009 No. 277, Item 1658).
[9] Act of 29 January 2004 Public Procurement Law (Journal of Laws 2004 No. 19 Item 177 as amended).
[10] Act of August 27 on public finances, Journal of Laws 2009 No. 157, item 1240.
[11] Act of 7 July 1994 Construction Law Journal of Laws 1994 No. 89 item 414, as amended).
[12] Act of 18 July 2001 Water Law Journal of Laws 2001 No. 115 Item 1229.
[13] Główny Urząd Statystyczny (Central Statistical Office), Ochrona środowiska 2015, Warszawa,2015"http://stat.gov.pl/obszary-tematyczne/srodowisko-energia/srodowisko/ochrona-srodowiska-2015,1,16.html (access: 26.02.2017).
[14] (http://iche2002.pl/zasoby-wodne-na-swiecie.html (access: 24.02.2017).
[15] Polska Fundacja Ochrony Zasobów Wodnych http://www.pfozw.org.pl/zrodlo-wiedzy/w-budowie-3/ (access: 22.02.2017).

TECHNICAL TRANSACTIONS 8/2017
CZASOPISMO TECHNICZNE 8/2017
CIVIL ENGINEERING
DOI: 10.4467/2353737XCT.17.133.6884

Michał Krzemiński (mkrz@il.pw.edu.pl)
Institute of Building Engineering, Faculty of Civil Engineering, Warsaw University of Technology

Optimization of construction schedules with the assumed multi-tasking of working brigades

Optymalizacja harmonogramów budowlanych przy założonej wielozadaniowości brygad roboczych

Abstract

The paper presents a newly developed model aimed at minimizing the downtime in working brigades work. The developed method is dedicated to the construction planned using the stream method of work organization. The model focuses on the assumption of multi-tasking of working brigades. It has been possible to model the performance depending on the type of brigade and the type of work being performed. The article also shows an example illustrating the results of the model's operation.

Keywords: flowshop models, slack minimization, construction schedules

Streszczenie

W artykule zaprezentowano nowo opracowany model mający na celu minimalizację przestojów w pracach brygad roboczych. Opracowana metoda dedykowana jest dla budów planowanych z zastosowaniem potokowej metody organizacji robót. W modelu skupiono się na założeniu wielozadaniowości brygad roboczych. Przyjęto możliwość modelowania wydajności w zależności od typu brygady i rodzaju wykonywanego zadania. W artykule pokazano ponadto przykład ilustrujący wyniki działania modelu.

Słowa kluczowe: modele potokowe, minimalizacja przestoi, harmonogramy budowlane

1. Introduction

The issue of scheduling is the subject of many scientific papers. In the construction industry, there is also a lot of attention paid to this issue. However, this is quite a large area, even after limitation to the conditions of construction output. This article discusses the part of the issue related to scheduling the work organized using the stream method of work organization. The basic assumption is that a given field of operation can be divided into workspaces on which the schedule of operations should be performed. The following figure shows the schedule on the basis of which the new method of optimization proposed by the author will be discussed. For this schedule, the result of the optimization will also be shown.

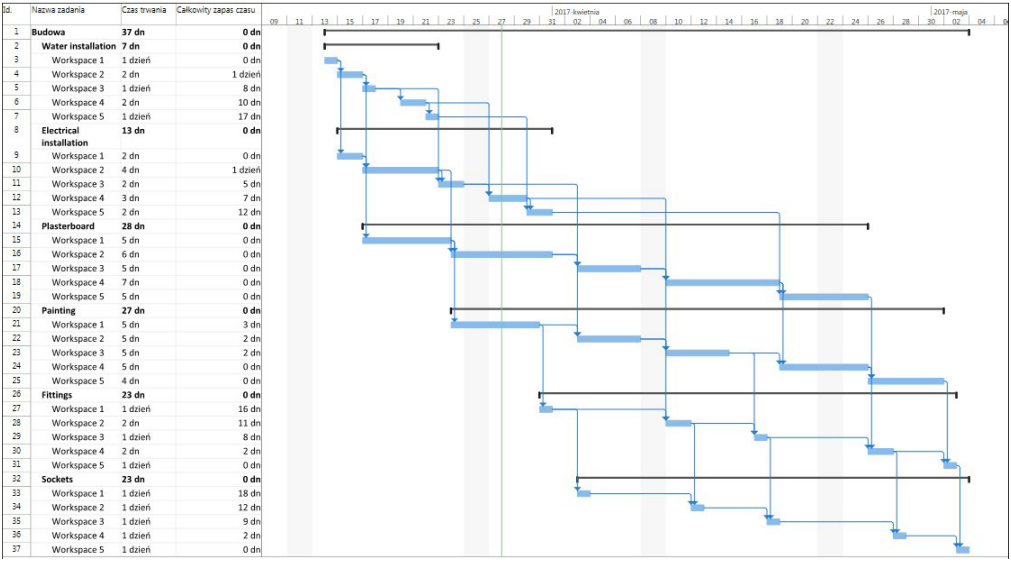

Id.	Nazwa zadania	Czas trwania	Całkowity zapas czasu
1	**Budowa**	**37 dn**	**0 dn**
2	**Water installation**	**7 dn**	**0 dn**
3	Workspace 1	1 dzień	0 dn
4	Workspace 2	2 dn	1 dzień
5	Workspace 3	1 dzień	8 dn
6	Workspace 4	2 dn	10 dn
7	Workspace 5	1 dzień	17 dn
8	**Electrical installation**	**13 dn**	**0 dn**
9	Workspace 1	2 dn	0 dn
10	Workspace 2	4 dn	1 dzień
11	Workspace 3	2 dn	5 dn
12	Workspace 4	3 dn	7 dn
13	Workspace 5	2 dn	12 dn
14	**Plasterboard**	**28 dn**	**0 dn**
15	Workspace 1	5 dn	0 dn
16	Workspace 2	6 dn	0 dn
17	Workspace 3	5 dn	0 dn
18	Workspace 4	7 dn	0 dn
19	Workspace 5	5 dn	0 dn
20	**Painting**	**27 dn**	**0 dn**
21	Workspace 1	5 dn	3 dn
22	Workspace 2	5 dn	2 dn
23	Workspace 3	5 dn	2 dn
24	Workspace 4	5 dn	0 dn
25	Workspace 5	4 dn	0 dn
26	**Fittings**	**23 dn**	**0 dn**
27	Workspace 1	1 dzień	16 dn
28	Workspace 2	2 dn	11 dn
29	Workspace 3	1 dzień	8 dn
30	Workspace 4	2 dn	2 dn
31	Workspace 5	1 dzień	0 dn
32	**Sockets**	**23 dn**	**0 dn**
33	Workspace 1	1 dzień	18 dn
34	Workspace 2	1 dzień	12 dn
35	Workspace 3	1 dzień	9 dn
36	Workspace 4	1 dzień	2 dn
37	Workspace 5	1 dzień	0 dn

Fig. 1. Base schedule of the undertaking

Numerous papers talk about how these workspaces can be sequenced. For example, well-known task sequencing rules such as SPT (shortest processing time) and LPT (longest processing time) [5]. The models from the collection of artificial intelligence methods can also be used here [2, 6]. The initial schedule discussed has been developed using the specialized KASS software allowing for analysis of all possible workspace sequencing [3]. As the sequencing criteria, the shortest lead times and minimal downtime were assumed in the work of the brigades.

The following table shows the execution times for all activities on each workspace.

Table 1. Performance times

W1		Workspace				
		W2	W3	W4	W5	
Working brigade	Water installation	1	2	1	2	1
	Electrical installation	2	4	2	3	2
	Plasterboard	5	6	5	7	5
	Painting	5	5	5	5	4
	Fittings	1	2	1	2	1
	Sockets	1	1	1	1	1

It should be noted that with this sequence of workspaces, there was a downtime in the work, mainly the fifth and sixth brigade. It should be noted that further optimization work on the schedule is possible.

The simplest way to do this would be to increase the employment in the third and fourth brigade. Such an operation would increase their productivity and, consequently, shorten the performance of tasks [4].

Another way would be to use a multi-variant work execution. Such an approach would involve proposing alternatives for the work, for third and fourth workspace the shorter variants should be given and longer variants for fifth and sixth workspace. This solution would probably result in obtaining a schedule that is characterized by continuity of work [1].

This article focuses on finding a solution to the problem, assuming that neither the number of means of production can be employed nor multi-variant work performance is possible. It is also not possible to relocate the workers to another construction site in periods when they are not employed. Such restrictions may, in practice, result from the characteristics of the contractor.

This paper focuses on the assumptions of the possibility of schedule optimization using the possible multitasking of work brigades. The brigades with downtime can assist the preceding brigades in order to minimize these downtimes. It was assumed that the preceding brigades cannot assist the subsequent brigades because it seems reasonable to assume that when they finish working on their workspace they may move on to the next field of operation or construction site. The performance of the assisting brigades is shown in a special matrix in which 1 means that the brigade has the same performance and 0 that it cannot perform the work, the intermediate values determine the performance coefficient. Later in this article there is a detailed description of the newly developed algorithm and a numerical example illustrating its operation.

2. The description of the brigades' downtime elimination model

The presented algorithm is iterative. It was developed on the assumption that only the subsequent brigades can assist the preceding brigades. The following figure shows the block diagram of the algorithm:

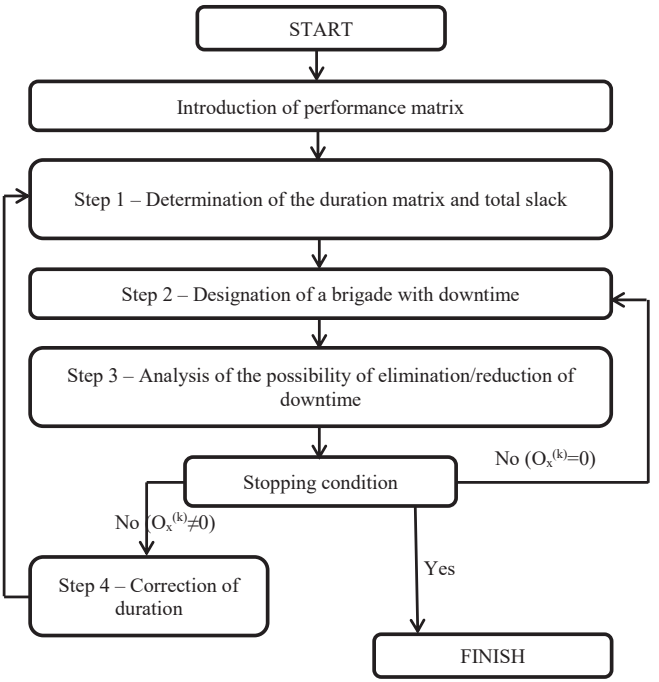

Fig. 2. The algorithm of brigades' downtime elimination model

2.1. Introduction of performance matrix

The assumption of the method is that when a brigade supports another brigade, its performance on the executed process may be the same as that of the basic brigade or less. The performance is characterized by performance matrix.

$$EC_{p,i}\begin{bmatrix} ec_{1,1} & \cdots & ec_{1,i} \\ \vdots & \ddots & \vdots \\ ec_{p,1} & \cdots & ec_{p,i} \end{bmatrix}; p=1, \ldots, m;\ i=1, \ldots, m \qquad (1)$$

where:

$ec_{p,i}$ – means the brigade performance when performing work on the process i,
p – number of assisted process,
i – (assisting) brigade number,
m – total number of working brigades.

The next steps in the algorithm will be described in the next section.

2.2. Step 1

Determination of the duration matrix and matrix of total slack. The matrices are determined by the analysis of the network model chosen to optimize the work schedule.

$$T_{i,j}^{(k)} = \begin{bmatrix} t_{1,1} & \cdots & t_{1,j} \\ \vdots & \ddots & \vdots \\ t_{i,1} & \cdots & t_{i,j} \end{bmatrix}; \; i=1, \ldots, m; \; j=1, \ldots, n \tag{2}$$

$$TF_{i,j}^{(k)} = \begin{bmatrix} tf_{1,1} & \cdots & tf_{1,j} \\ \vdots & \ddots & \vdots \\ tf_{i,1} & \cdots & tf_{i,j} \end{bmatrix}; \; i=1, \ldots, m; \; j=1, \ldots, n \tag{3}$$

where:

k – iteration number,

j – workspace number,

n – number of workspaces.

2.3. Step 2

The next step in the algorithm is to select the first brigade that has downtime in its work. To find such a brigade, use the following short algorithm:

1) $i = 1$,
2) Determine the value $tf_{i,1}^{(k)}$,
3) If the value $tf_{i,1}^{(k)} = 0$ then $i := i+1$ and return to step 2 of the algorithm. If, however, $tf_{i,1}^{(k)} \neq 0$ proceed to 4 point of the algorithm,
4) The value i for which $tf_{i,1}^{(k)} \neq 0$ determines the number of the brigade which has downtime in its work.

This condition allows the brigades that have downtime to be determined. In the case in which the condition $tf_{i,1}^{(k)} = 0; \; i=1, \ldots, m$ is met, we would have a schedule with no downtime.

Having selected the first brigade with downtime we can proceed to step 3 of the algorithm.

2.4. Step 3

From the previous step of the algorithm we know that the selected brigade has downtime at work. We know that these downtimes are caused by the prolonged working time of the preceding brigade. In this step of the algorithm, the first downtime should be identified, and then it should be checked if there is a possibility to eliminate it.

To identify the first downtime, use the following short algorithm:

1) The value is constant and determined on the basis of step 2 of the algorithm, $j = 1$,
2) Determine the value of $tf_{i,j}^{(k)} - tf_{i,j+1}^{(k)}$,

3) If $tf_{i,j}^{(k)} - tf_{i,j+1}^{(k)} = 0$ then $j := j+1$ and return to step 2 of the algorithm. If, however, $tf_{i,j}^{(k)} - tf_{i,j+1}^{(k)} \neq 0$ proceed to step 4 of the algorithm,
4) The value $tf_{i,j}^{(k)} - tf_{i,j+1}^{(k)} \neq 0$ for which determines the number of the workspace after which the brigade with number i has downtime.

The downtime is generated by the action of the preceding brigade. In order to eliminate the downtime, it is necessary to shorten the execution time of the preceding action by a value equal to $tf_{i,j}^{(k)} - tf_{i,j+1}^{(k)}$.

In order to determine all possible variants of elimination of the downtime, a set should be developed containing the days in which the given downtime can be eliminated, i.e. the dates from the beginning of the preceding action to finish. The boundaries of the set can be determined by the following dependency:

$$lower\ boundry - ES_{i-1,j+1}^{(k)}, \tag{4}$$

$$upper\ boundry - EF_{i-1,j+1}^{(k)}, \tag{5}$$

Having a determined the set proceed to determine the sets in which the information is provided concerning the downtimes of successive brigades. Downtime in the work of the subsequent brigades can be used to reduce the working time of the preceding brigade. Index gives the number of the next variant. The following dependencies should be used to define the boundaries of variants:

$$lower\ boundry - EF_{i-1,j+1}^{(k)},\ i = i, ..., n;\ j = 1, ..., n-1, \tag{6}$$

$$upper\ boundry - ES_{i-1,j+1}^{(k)},\ i = i, ..., n;\ j = 1, ..., n-1, \tag{7}$$

Having determined all sets $B_x^{(k)}$ it should be determined:

$$D_x^{(k)} = A^{(k)} \cap B_x^{(k)};\ x = 1, ..., z, \tag{8}$$

where:

z – number of predefined variants.

Then the value $\left|D_x^{(k)}\right|$ should be determined, which specifies the cardinal number of the set $D_x^{(k)}$. The penultimate element of the third step is to determine possible variants of the shortening of the preceding operation. These variants are determined on the basis of the following dependency:

$$X \wedge Y \wedge Z \tag{9}$$

where:

$$X = \left(\left|D_x^{(k)}\right| \leq \left\lfloor \frac{A^{(k)}}{2} \right\rfloor \rightarrow \begin{cases} O_x^{(k)+} = \left|D_x^{(k)}\right| \\ O_x^{(k)-} = \left\lfloor \left|D_x^{(k)}\right| * ec_{p,i} \right\rfloor \end{cases} \right) \tag{10}$$

where:
$|A^{(k)}|$ – specifies the cardinal number of the set.

The first component of the formula is responsible for the case where the possible shortening is less than or equal to half the length of the shortened operation. Rounding down in the formula, which is encrypted as "$\lfloor \ldots \rfloor$" is intended to preserve the basic unit of the schedule as an integer.

The second component of the formula is responsible for the case in which it is possible to exceed the duration of the operation. Such shortening would make no sense because by shortening the working time of the first brigade, we would increase the working time of the second brigade which would not shorten the work on the workspace anyway.

$$Y = \left(\left(\left| D_x^{(k)} \right| \leq \left\lfloor \frac{A^{(k)}}{2} \right\rfloor \rightarrow \begin{cases} O_x^{(k)+} = \left| D_x^{(k)} \right| \\ O_x^{(k)-} = \left\lfloor \left| D_x^{(k)} \right| * ec_{p,i} \right\rfloor \end{cases} \right) \wedge \left(O_x^{(k)-} = 0 \rightarrow O_x^{(k)+} = 0 \right) \right) \quad (11)$$

The second component contains two elements. The first is responsible for shortening the working time of the assisted brigade and increasing the working time of the assisting brigade. The second, responsible for elimination of the case of prolonging the working time of the assisted brigade without shortening the time of the assisting brigade.

The task of the last dependency component is to eliminate the case in which there will be an excessive reduction in working time of the assisted brigade due to the operation of the mathematical model. Such shortening would unnecessarily involve the assisting brigade.

$$Z = \left(O_x^{(k)-} > \left(tf_{i,j}^{(k)} - tf_{i,j+1}^{(k)} \right) \rightarrow \begin{cases} O_x^{(k)+} = \left\lceil \dfrac{\left(tf_{i,j}^{(k)} - tf_{i,j+1}^{(k)} \right)}{ec_{p,i}} \right\rceil \\ O_x^{(k)-} = tf_{i,j}^{(k)} - tf_{i,j+1}^{(k)} \end{cases} \right) \quad (12)$$

Rounding up in the formula ($\lceil \ldots \rceil$) is intended to preserve the basic unit of the schedule as an integer.

The last element of step three is choosing the optimal variant. In order to choose the best option, the following rules should be observed:

- A variant that allows for shortening the preceding action as quickly as possible should be chosen.
- If several variants of shortening allow for shortening the preceding action by the same value, then the one with the highest performance coefficient should be chosen.
- If, however, there is a case in which several variants are equivalent for shortening and have the same performance coefficient, there should be chosen the variant in which the assisting brigade has a smaller index , the brigade that occurs earlier.

There is also the case where no variant is available to shorten the brigade downtime. In that case, go back to the beginning of step 3 of the algorithm and look for the next downtime at work and repeat the third step of the algorithm.

2.5. Stopping condition

It is also possible to schedule a pattern in which, in the course of the work of the whole brigade no downtime can be shortened, in which case the downtime of the next brigade should be reconsidered, that is, the one with increased by one index and return to the second point of the algorithm.

If and are achieved and i no shortening occurs, it means that no further optimization of the schedule is possible and the model must be discontinued.

If the shortening occurs, then proceed to the fourth step of the algorithm.

2.6. Step 4

In the fourth step, the duration of activities should be adjusted, the adjustment is performed using the following dependency:

$$t_{i-1,j+1}^{(k+1)} = t_{i-1,j+1}^{(k)} - O_x^{(k)-} \tag{13}$$

Based on the selected $O_x^{(k)+}$ the working time of the brigade on the basis of which the set $B_x^{(k)}$ was determined should also be added.

3. Application examples

The optimized schedule is described in the introduction to the article. Below, the schedule after optimization is presented.

The hatched actions indicate an additional work of assisting brigades. The description contains information on which field they work in and what activities they perform.

The initial total time is 37 days, after optimization 33 days, the shortening was 11%. The total initial downtime is 37 days, after optimization 16 days, the decrease was 57%. The results obtained can therefore be considered as satisfactory.

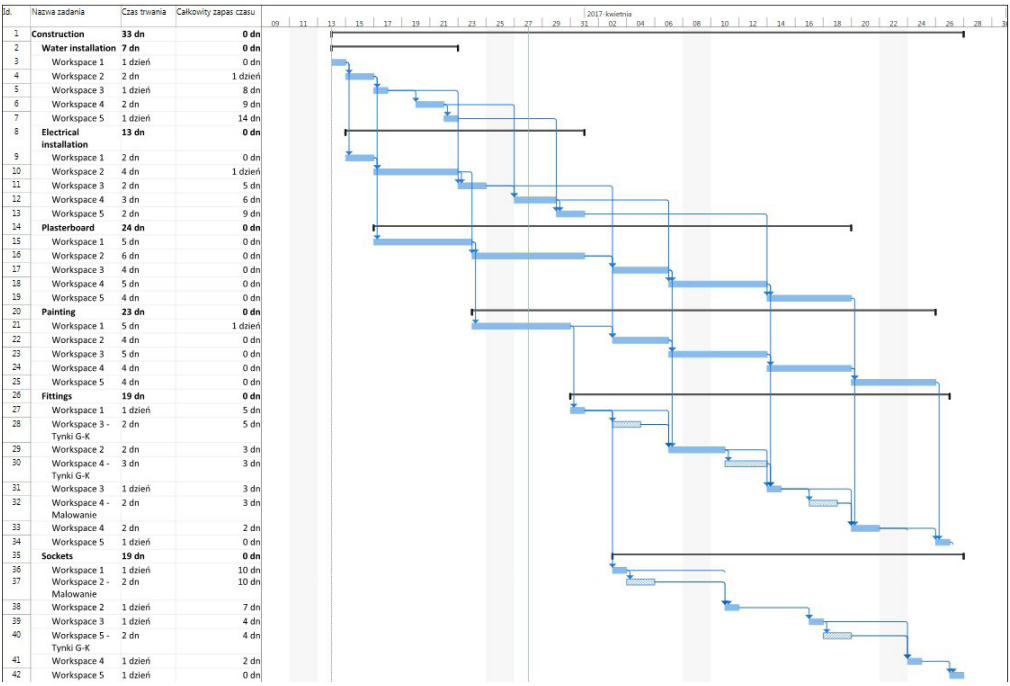

Id.	Nazwa zadania	Czas trwania	Całkowity zapas czasu
1	**Construction**	**33 dn**	**0 dn**
2	**Water installation**	**7 dn**	**0 dn**
3	Workspace 1	1 dzień	0 dn
4	Workspace 2	2 dn	1 dzień
5	Workspace 3	1 dzień	8 dn
6	Workspace 4	2 dn	9 dn
7	Workspace 5	1 dzień	14 dn
8	**Electrical installation**	**13 dn**	**0 dn**
9	Workspace 1	2 dn	0 dn
10	Workspace 2	4 dn	1 dzień
11	Workspace 3	2 dn	5 dn
12	Workspace 4	3 dn	6 dn
13	Workspace 5	2 dn	9 dn
14	**Plasterboard**	**24 dn**	**0 dn**
15	Workspace 1	5 dn	0 dn
16	Workspace 2	6 dn	0 dn
17	Workspace 3	4 dn	0 dn
18	Workspace 4	5 dn	0 dn
19	Workspace 5	4 dn	0 dn
20	**Painting**	**23 dn**	**0 dn**
21	Workspace 1	5 dn	1 dzień
22	Workspace 2	4 dn	0 dn
23	Workspace 3	5 dn	0 dn
24	Workspace 4	4 dn	0 dn
25	Workspace 5	4 dn	0 dn
26	**Fittings**	**19 dn**	**0 dn**
27	Workspace 1	1 dzień	5 dn
28	Workspace 3 - Tynki G-K	2 dn	5 dn
29	Workspace 2	2 dn	3 dn
30	Workspace 4 - Tynki G-K	3 dn	3 dn
31	Workspace 3	1 dzień	3 dn
32	Workspace 4 - Malowanie	2 dn	3 dn
33	Workspace 4	2 dn	2 dn
34	Workspace 5	1 dzień	0 dn
35	**Sockets**	**19 dn**	**0 dn**
36	Workspace 1	1 dzień	10 dn
37	Workspace 2 - Malowanie	2 dn	10 dn
38	Workspace 2	1 dzień	7 dn
39	Workspace 3	1 dzień	4 dn
40	Workspace 5 - Tynki G-K	2 dn	4 dn
41	Workspace 4	1 dzień	2 dn
42	Workspace 5	1 dzień	0 dn

Fig. 3. Project schedule after optimization

4. Summary

The article presents a newly developed method of optimizing construction schedules, performed assuming the organization by stream method. The work itself did not focus on sequencing the tasks, it was assumed that this issue had already been resolved earlier. The task of the new algorithm is to assign the work to brigades with downtimes that will reduce their total number. The developed model allows for the introduction of performance dependencies. The model, in its premise, first assigns the work to the brigades with the highest efficiency. The developed model can be successfully used in the construction industry. Further work is planned to verify the assumptions that have been adopted in the model.

References

[1] Biruk S., Jaśkowski P., *Scheduling construction of multi-object projects: problem of works continuity in consecutive units,* Zeszyty Naukowe WSOWL, 3 (157), 2010, 340–349.

[2] Hejducki Z., *Scheduling Model of Construction Activity with Time Couplings,* Journal of Civil Engineering and Management, 9:4, 2003, 284–291.

[3] Krzemiński M., *Use of the KASS Program in Scheduling,* Technical Transaction, 2-B(6), 2014, 217–224.

[4] Marcinkowski R., *Metody rozdziału zasobów realizatora w działalności inżynieryjno - budowlanej,* WAT, Warszawa 2002.
[5] Pinedo M.L., *Scheduling: Theory, Algorithms, and Systems,* Springer, 2012.
[6] Rogalska M., Bożejko W., Hejducki Z., *Time/Cost Optimization Using Hybrid Evolutionary Algorithm in Construction Project Scheduling,* Automotion in Construction, 18, 2008, 24–31.

TECHNICAL TRANSACTIONS 8/2017
CZASOPISMO TECHNICZNE 8/2017
CIVIL ENGINEERING
DOI: 10.4467/2353737XCT.17.134.6885

Zygmunt Orłowski
Aleksandra Radziejowska (aradziej@agh.edu.pl)
Department of Geomechanics, Civil Engineering and Geotechnics, Faculty of Mining and Geoengineering, AGH University of Science and Technology in Cracow

Model for assessing "accessibility" – the basic category in the evaluation of social performance of buildings according to standards PN-EN 16309+A1:2014-12

Model oceny kategorii „dostępność" – podstawowego czynnika w ocenie socjalnych właściwości użytkowych budynków wg normy PN-EN 16309+A1:2014-12

Abstract

The paper considers the assessment model of the category Accessibility, which is a basic element of the social aspect of sustainable construction. The model takes into account the standard PN-EN 16309+A1:2014-12, which generally provides methods and requirements for assessing the social performance of buildings. The authors, for the purposes of the model particularise the scope of the assessment category and set threshold values and the weight of particular social indicators. The model is treated as a contribution to developing a method for comprehensive assessment of the social characteristics of buildings.

Keywords: Technical Committee CEN / TC 350, the social aspect, accessibility, model

Streszczenie

W artykule rozpatrywany jest model oceny kategorii Dostępność będącej podstawowym elementem aspektu socjalnego zrównoważonego budownictwa. Model uwzględnia normę PN-EN 16309+A1:2014-12, która w sposób ogólny podaje metody i wymagania dotyczące oceny socjalnych właściwości użytkowych budynków. Autorzy dla potrzeb modelu uszczegóławiają zakres oceny rozpatrywanej kategorii oraz ustalają progowe wartości oraz wagi poszczególnych wskaźników społecznych modelu. Model traktowany jest jako przyczynek do opracowania metody umożliwiającej kompleksową ocenę socjalnych właściwości budynku.

Słowa kluczowe: Komitet Techniczny CEN/TC 350, aspekt socjalny, dostępność, model

1. Introduction

One of the basic standards developed by the Technical Committee CEN/TC 350 *Sustainability of construction Works* [3, p. 2010–2023] regarding the social aspect of sustainable development is the PN-EN 16309+A1:2014-12 Sustainability of construction works – Assessment of social performance of buildings – Calculation methodology published in English. In this standard six categories have been distinguished, which are used to assess the social performance of buildings: K_1 – *accessibility*; K_2 – *adaptability*; K_3 – *health and comfort*; K_4 – *impacts on the neighbourhood*; K_5 – *maintenance and maintainability*; K_6 – *safety and security*. The standard also includes methods and requirements for assessing social performance in buildings by taking into account the technical characteristics and functionality of the building. It should be noted that the standard [8] provides guidance for the assessment of the building, but does not include threshold values or weights of individual social indicators (category).

In this paper, the authors present a mathematical model for the assessment of the first category of social performance in buildings K_1 *Accessibility*. The authors treat the model as a contribution to the development of a model to enable a comprehensive assessment of the social characteristics of the building.

2. Assumptions for model

The proposed method, designed to assess the category *Accessibility*, covers the comparison of the solution features of the building tested (in terms of access to the building) with the characteristics of the reference object. The reference building is a hypothetical building designed according to current standards and practice with the same technological, structural and functional parameters as the building being evaluated. The reference building serves as a base of all possible theoretical analyses and is associated with a set of data defining the assess object. More information about the reference building is contained, among others, in paper [7].

In the constructed model, only the basic, in the authors' opinion, most important elements related to the categories $K_i (i = 1, 2, ..., m)$ describing the system (object) are included. In order to clarify the scope of given category *Ki* subcategories $K_{ij} (j = 1, 2, ..., n_i, i = 1, 2, ..., m)$ were specified that particularise $K_i (i = 1, 2, ..., m)$. Each of the subcategories is judged by the criteria $K_{ijk} (k = 1, 2, ..., n_{ij}, j = 1, 2, ..., n_i, i = 1, 2, ..., m)$. In order to formally describe the evaluation of the category K_i with components (subcategories) assessed by n_{ij} criteria shall be introduced the following scoring matrix $\mathbf{O}^i$:

$$\mathbf{O}^i = [o^i_{j,1}, o^i_{j,2}, ..., o^i_{j,n_{i,j}}] \text{ for } i = 1, 2, ..., m; j = 1, 2, ..., n_i \tag{1}$$

wherein the values $o^i_{j,n_{i,j}}$ for last $n'_{ij} - n_{ij}$ places will be zero,

where:
n_{ij} limiting values for the index k, $n'_{ij} = \max_{1 \le j \le n_i} n_{ij}$;

n_i limiting values for the index j, $n'_i = \max_{1 \le i \le m} n_i$;

The values of ratings criteria are determined on the basis of expert knowledge [5, p. 73-78].

For the evaluation of the considered factor (criterion), depending on finding the existing state, a discrete scale consisting of 1 ÷ p levels for p = 5 p with levels with the following meaning were adopted:

5 – *very good condition,*
4 – *good condition,*
3 – *satisfactory state,*
2 – *poor condition,*
1 – *very poor condition.*

The proposed scale enables the influence of factors that are difficult to measure to be taken into account.

In the multi-criteria analyses [1], and these we are dealing with, an important problem is the unequal validity of the criteria adopted, in varying degrees of fragmentation characteristics of the object (criteria), and including this in the assessment algorithm. For this purpose weights should be entered (hierarchical coefficients, standardized with regard to individual vectors of state assessment) which are correction values according to the preferences expressed by an expert:

$$\lambda_{ijk} \in [0,1] \quad \text{where} \quad \sum_{i=1}^{m} \lambda_{ijk} = 1 \quad \text{dla} \quad j = 1, 2, ..., n_i, \; k = 1, 2, ..., n_{ij} \tag{2}$$

The model assumes the scale of weights from 0.1 to 1.0 (0.1 – little important, ..., 1.0 - very important) [4, p. 4236–4240].

3. Construction of the model

In a complex system which a building is, a clear proposition of the evaluation index is extremely difficult, so the authors propose to deal with a qualified assessment. Using the qualified evaluation o_{jk}, for $j = 1, ..., n_i$; $k = 1, ..., n_{ij}$ we receive a rating matrix of category $\mathbf{O}^i$ and assigned to it the matrix of weights $\mathbf{\Lambda}^i$:

$$\mathbf{O}^i = \begin{bmatrix} O^i_{1,1} & \cdots & O^i_{1,n_{ij}} \\ \vdots & \ddots & \vdots \\ O^i_{n_i,1} & \cdots & O^i_{n_i,n_{ij}} \end{bmatrix} \quad \mathbf{\Lambda}^i = \begin{bmatrix} \lambda^i_{1,1} & \cdots & \lambda^i_{1,n_{ij}} \\ \vdots & \ddots & \vdots \\ \lambda^i_{n_i,1} & \cdots & \lambda^i_{n_i,n_{ij}} \end{bmatrix} \tag{3}$$

where:

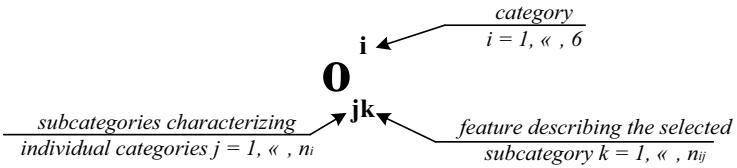

In the present case for K_1 *Accessibility* two subcategories K_{11} and K_{12} and the criteria by which they are assessed are specified. The tree of the assessment for category K_1 is shown in Fig. 1.

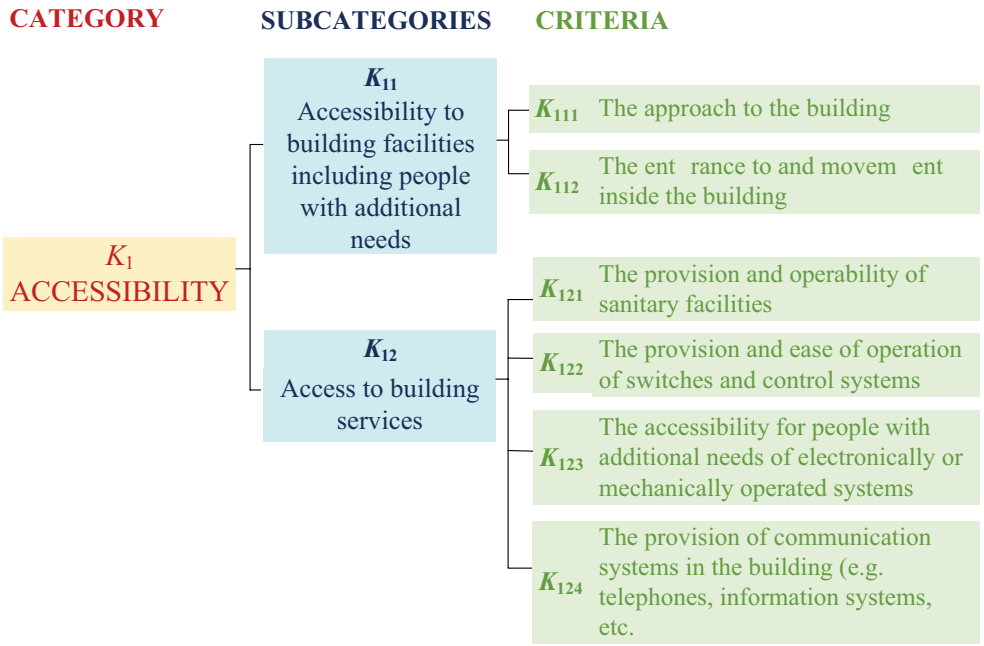

Fig. 1. Assessment tree of category K_1 *Accessibility*

Indexes for category K_1 *Accessibility* will take the following values (Fig. 1):
– n_i index values j: for $i = 1$, $n_i = 2$,
– n_{ij} index values k (when $i = 1$) for $j = 1$:$n_{1j} = 2$; for $j = 2$:$n_{1j} = 4$;

In paper [6, p. 55–61] the characteristics of the elements of the "tree assessments" juxtaposed in Fig.1, including the matched rating scale, have been presented. The matrix of assessment for *Accessibility* and the matrix of weights assigned to it will have the form:

$$\mathrm{O}^1 = \begin{bmatrix} o^1_{1,1} & o^1_{1,2} & 0 & 0 \\ o^1_{2,1} & o^1_{2,2} & o^1_{2,3} & o^1_{2,4} \end{bmatrix} \quad \Lambda^1 = \begin{bmatrix} \lambda^1_{1,1} & \lambda^1_{1,2} & 0 & 0 \\ \lambda^1_{2,1} & \lambda^1_{2,2} & \lambda^1_{2,3} & \lambda^1_{2,4} \end{bmatrix} \tag{4}$$

Based on presented in [6, p. 55–61] subcategories and the criteria describing them can be extracted from the matrix (4) assessments vectors and weight vectors for individual characteristics (criteria):

$$o^1_{1k} = [o^1_{1,1}, o^1_{1,2}] \quad \text{and} \quad o^1_{2k} = [o^1_{2,1}, o^1_{2,2}, o^1_{2,3}, o^1_{2,4}] \tag{5}$$

$$\lambda^1_{1k} = [\lambda^1_{1,1}, \lambda^1_{1,2}]^T \quad \text{and} \quad \lambda^1_{2k} = [\lambda^1_{2,1}, \lambda^1_{2,2}, \lambda^1_{2,3}, \lambda^1_{2,4}]^T \tag{6}$$

Taking into account vectors (5) and (6), by applying the adjusted index of summation [2, p. 2010-2023], a partial assessment for each of the two separate subcategories should be calculated:

- for K_{11} *Accessibility to building facilities including people with additional needs we obtained*:

$$o^1_1 = \sum\nolimits_{k=1}^{2} o^1_{1,k} \cdot \lambda^1_{1,k} = o^1_{1,1} \cdot \lambda^1_{1,1} + o^1_{1,2} \cdot \lambda^1_{1,2} \tag{7}$$

- for K_{12} *Access to building services* scalar function will have the form:

$$o^1_2 = \sum\nolimits_{k=1}^{4} o^1_{2,k} \cdot \lambda^1_{2,k} = o^1_{2,1} \cdot \lambda^1_{2,1} + o^1_{2,2} \cdot \lambda^1_{2,2} + o^1_{2,3} \cdot \lambda^1_{2,3} + o^1_{2,4} \cdot \lambda^1_{2,4} \tag{8}$$

The next stage is to determine the adjusted index of summation for the vector value received in the previous calculation: $\mathbf{O}^1_j = \left[O^1_1, O^1_2 \right]$. In addition, for each subcategory a weight vector in the form has also been designated (by survey):

$$\mathbf{L}^1_j = \left[L^1_1, L^1_2 \right]^T \tag{9}$$

For such a set value we calculate:

$$O^1_C = \sum\nolimits_{j=1}^{2} \mathbf{O}^1_j \cdot \mathbf{L}^1_j = O^1_1 \cdot L^1_1 + O^1_2 \cdot L^1_2 \tag{10}$$

The evaluation of K_1 for the social aspect of sustainable construction obtained in the above calculation should be compared with the assessment, previously determined, for the reference object. The difference between the obtained assessments gives us information about the state of the analysed object in relation to the current requirements for the category *Accessibility*.

4. Example

4.1. Building characteristics

A residential unit located in multi-family building on the housing complex "Pod Fortem" in Kraków has been assessed. The building was constructed using mixed technologies: ceilings between storeys, basement walls and pillars on each floor are monolithic, the interior brick walls are made of silicate blocks, external walls are three-layer. Building dimensions: 53.10 x 15.45 x 10.60 m^3. The housing estate was erected in the years from 2006 to 2008 and together nineteen residential blocks were created. The building is triple-staircase, three-storey and basement. In the basement storey there are 13 parking places for cars. The estate is located on the outskirts of Kraków, it is fenced and has an internal road infrastructure and parking spaces for cars in its area. The premises shown are a three-bedroom apartment, located on the first floor. The layout and location of the apartment are presented in Figures 2 and 3.

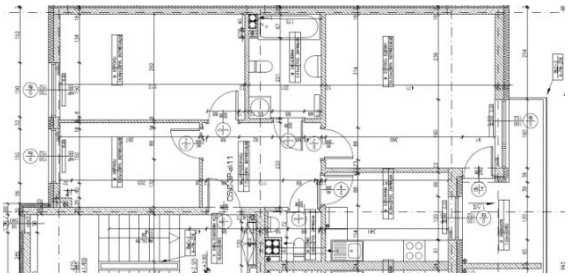

Fig. 2. Layout of assessed apartment

Fig. 3. View of housing estates on which the assessed apartment is situated

4.2. Determining the values of the criteria

After the local vision, the necessary information was collected from the occupants about the building and the surroundings and taking into account the rating scales proposed in paper [6, p. 55–61], the criteria characterizing the category K_1 *Accessibility* in the examined apartment were established. The results of the findings are presented in Table 1:

Table 1. The assessment of criteria characterizing the various subcategories

Subcategories		Criteria		Assessment o^1_{jk}
K_{11}	Accessibility to building facilities including people with additional needs	K_{111}	The approach to the building	5
		K_{112}	The entrance to and movement inside the building	3
K_{12}	Access to building services	K_{121}	The provision and operability of sanitary facilities	5
		K_{122}	The provision and ease of operation of switches and control systems	3
		K_{123}	The accessibility for people with additional needs of electronically or mechanically operated systems	4
		K_{124}	The provision of communication systems in the building (e.g. telephones, information systems, etc.)	5

The validity of the various criteria λ^1_{jk} established on the basis of expert preferences is shown in Table 2.

Table 2. Weights of each criteria (marking of subcategories and criteria according to Tab. 1)

Subcategories	Criteria	Weights λ^1_{jk}
K_{11}	K_{111}	0.559
	K_{112}	0.441
K_{12}	K_{121}	0.213
	K_{122}	0.246
	K_{123}	0.224
	K_{124}	0.317

Below are given the qualification data for evaluation of the *Accessibility* category in matrix form together with matrices assigned to the weights (determined on the basis of the survey):

$$\mathbf{O}^1 = \begin{bmatrix} 5 & 3 & 0 & 0 \\ 5 & 3 & 4 & 5 \end{bmatrix}, \qquad \mathbf{\Lambda}^1 = \begin{bmatrix} 0.559 & 0.441 & 0 & 0 \\ 0.213 & 0.246 & 0.224 & 0.317 \end{bmatrix} \tag{11}$$

$$\mathbf{L}^1_j = \begin{bmatrix} 0.489 \\ 0.511 \end{bmatrix} \tag{12}$$

By multiplying the matrices (shown in paragraph 3) the vector of ratings was yielded:

$$\mathbf{O}_j^1 = \begin{bmatrix} 4.118 \\ 4.284 \end{bmatrix}$$

Then multiplying the vector of ratings by the vector of weight, were obtained the evaluation of category K_1 for the investigated object:

$$\mathbf{O}_c^1 = O_j^1 \cdot L_j^1 = 4.203$$

In parallel, an assessment of the reference object for this type of building () should be performed. Next we examine the difference in assessments of category K_1 of the tested object and the reference object:

$$\Delta \mathbf{O}_c^1 = \mathbf{O}_c^{1R} - \mathbf{O}_c^1 \tag{13}$$

and quotient:

$$\delta = \frac{\Delta \mathbf{O}_c^1}{\mathbf{O}_c^{1R}} \tag{14}$$

The indicator δ shows how big the difference is between the category of *Accessibility* for the particular building, and the value of *Accessibility* for the reference building, which takes into account the current technical and construction regulations, contemporary logistics of towns and housing estates, new technologies of erection, etc.

5. Conclusions

Assessment of the social performance of buildings is a quite difficult process. A part of the assessed elements may be quantified, compared with standard parameters, while others, such as logistics solutions in the object, the degree of implementation of modern electronic devices (BMS) is difficult to quantify. The proposed model is characterized by a comprehensive approach to assessing the social performance of the building. It can provide significant simplification in the evaluation of real estate and indicate the manager / owner the need and scope of refurbishment for the approach to the building and functional solutions inside the building.

The work was done partly through a statutary research of AGH in Faculty of Mining and Geoengineering 11.11.100.197.

References

[1] Arroyo P., *Exploring decision-making methods for sustainable design in commercial buildings*, Dissertation in the University of California, Berkeley 2014.

[2] Bragança L., Mateus R., Koukkari H., *Building Sustainability Assessment*, Sustainability open access, 02.2010, 2010–2023.

[3] CEN/TC 350, *WG1*. Sustainability of Construction Works–Assessment of Environmental Performance of Buildings–Calculation Methods; CEN (European Centre for Standardization): Brussels, Belgium 2007, Working Draft N024.
[4] Koźniewski E., Orłowski Z., *Propozycja metody oceny rozwiązań logistycznych budynku mieszkalnego wielorodzinnego,* Logistyka, 04.2015, 4236–4240.
[5] Orłowski Z., Radziejowska A., *Socjalne właściwości użytkowe budynków mieszkalnych w* świetle *badań ankietowych,* Budownictwo i Architektura 15(2), 2016, 73–78.
[6] Orłowski Z., Radziejowska A., *Charakterystyka kategorii „Dostępność" – podstawowego elementu aspektu społecznego (socjalnego) budownictwa zrównoważonego,* Acta Sci. Pol. Architectura 16 (2), 2017, 55–61.
[7] Owczarek S., Orłowski Z., Szklennik N., *Budynek referencyjny – podstawa oceny stanu budynku*, Prace Naukowe Instytutu Budownictwa Politechniki Wrocławskiej 87, Studia i Materiały 18, Oficyna Wydawnicza Politechniki Wrocławskiej, Wrocław 2006.
[8] PN-EN 16309+A1, Sustainability of construction works – Assessment of social performance of buildings – Calculation methodology, 12.2014.

TECHNICAL TRANSACTIONS 8/2017
CZASOPISMO TECHNICZNE 8/2017
CIVIL ENGINEERING
DOI: 10.4467/2353737XCT.17.135.6886

Jakub Popławski (j.poplawski@doktoranci.pb.edu.pl)
Małgorzata Lelusz
Department of Construction Materials, Technology and Organization, Faculty of Civil and Environmental Engineering, Bialystok University of Technology

Utility assessment of biomass fly-ash for production of concrete products

Ocena przydatności popiołu lotnego ze spalania biomasy do produkcji wyrobów betonowych

Abstract

International agreements oblige our state to develop ecological sources of energy, one of which is biomass. During its combustion fly-ashes are produced. Several studies have shown that they might be useful in concrete production. The article presents a comparison of biomass fly-ash and coal fly-ash influence on the properties of cement composites. The replacement levels of cement by fly-ash (FA) were 20%, 40% and 60%. Biomass fly-ash FA(B) have replaced coal fly-ash by 0%, 50% and 100%. The compressive strength tests showed similarities in strength development of coal and biomass fly-ashes concretes. Specimens with biomass fly-ash presented similar or better abrasion resistance comparing to coal fly-ash samples.

Keywords: biomass fly-ash, cement, concrete

Streszczenie

Zobowiązania międzynarodowe obligują nasz kraj do produkcji energii z wykorzystaniem jej odnawialnych źródeł, jednym z nich jest biomasa. Podczas jej spalania powstają popioły lotne. Przeprowadzone dotychczas badania sugerują, że produkcja wyrobów betonowych może stanowić skuteczny sposób ich wykorzystania. Celem artykułu jest porównanie wpływu popiołu lotnego ze spalania biomasy i spalania węgla. Popioły (FA) stanowiły 20%, 40% lub 60% masy spoiwa. Popiół lotny z biomasy FA(B) dozowany był w ilości 0%, 50% lub 100% masy popiołów. Wyniki badań wytrzymałość na ściskanie wykazały podobny rozwój wytrzymałości betonów. Próbki z dodatkiem popiołów z biomasy charakteryzowały się zbliżoną lub większą odpornością na ścieranie od próbek z dodatkiem popiołów węglowych.

Słowa kluczowe: popioły lotne ze spalania biomasy, cement, beton

1. Introduction

The industrial-scale burning of carbon-based fossil fuels started at the turn of the 20th c. Nowadays, global coal production is estimated up to 7–8 billion t/year. In 2015 Poland produced 72 million t of that resource [1]. In the last decades of the 20th c. the awareness of global warming raised. The rise of the average temperature on Earth is a direct consequence of greenhouse gas emissions. One of these is carbon dioxide. Our economy produced 295.8 million t of CO_2 [2]. The cement industry is a significant source of carbon dioxide, its share of global emission is estimated at 7–8%. A variety of solutions ought to be considered to minimize industry's carbon footprint. One of these is reduction of the amount of cement in cement composite mixes. Some additives can partly substitute cement in the mix. V category fly-ash, rich in glassy silica and alumina, is an example of a pozzolanic additive. W category fly-ash is also considered a hydraulic additive, due to the presence of CaO. Both of them are a side-product of coal burning in combined heat and power plants. The utilization of fly-ash in cement composites raises the ecological value of the material [3]. The introduction of biomass fuel to Polish energy production began after its accession to the European Union. Since then the share of renewable sources in overall energy production has grown to the value of 11.25% in 2013, most of it derived from solid biomass firing. The dominant type of biomass in Poland is woody and herbal biomass from forest management and agricultural production. Further promotion of biomass fuels is planned in Ministry of Energy document "Energy policy of Poland until 2050" [4, 5]. The introduction of biomass fuels in power plants has created a new field of study in utilization of their combustion side-products. An insufficient amount of research prevents biomass fly-ash systematization in concrete standards [3, 6]. Various biomass fly-ashes have considerable activity and pozzolanic properties just like coal fly-ash [6, 7].

The PN-EN 450-1 standard defines fly-ash as "fine powder of mainly spherical, glassy particles, derived from burning of pulverized coal with or without co-combustion materials, which has pozzolanic properties and consists essentially of SiO_2 and Al_2O_3". Their colour is mostly light or dark grey, are alkaline, and have fineness similar to cement. The main physical properties are related to the combustion method in the heat or power plant [3, 6]. The biomass fly-ashes chemical composition varies with the source of combusted biomass. The combustion conditions and fuel influence the physical properties, the specific surface area, and loss on ignition percentage. Generally, the biomass fly-ashes have higher alkaline oxides and lower alumina percentages than coal fly-ashes [3, 6]. As mentioned, the current standards PN-EN 450-1 and PN-EN 206-1 allow utilization of coal and coal co-combusted fly-ashes. Siliceous and calcareous fly-ashes can become cement components if they meet the PN-EN 197-1 requirements. Siliceous fly-ashes are the most common type of fly-ash used in the Polish cement and concrete industry [3, 8]. The growing problem with biomass fly-ashes storage, and similarities in chemical composition between biomass fly-ashes and coal fly-ashes, are encouraging enough to research biomass fly-ash and its influence on cement composite properties. Some suitable ways of utilization in concrete technology have already been

proposed or discussed in the literature, including: dry-cast concrete, lower-class road pavements, heavy-metals immobilization, and self-compacted concrete. Any of these must take into consideration the unique properties of this type of fly-ash [9–11].

The addition of rice husk fly-ash is one of the best known biomass fly-ashes. It has an irregular shape of particles, with a slightly higher specific surface area than cement. Its consequently significant amount of silica is accompanied by pozzolanic properties [12, 13]. However, the ability to enhance the mechanical properties is also influenced by the crystalline structure of the material which is more dependent on the combustion process [14]. The comparative study of the filler-effect of sand and pozzolanic properties of rice husk fly-ash of the same size has shown that the pozzolanic reaction of the latter can be considerably more influential on compressive strength from 14 up to 90 days from casting [15]. It was reported that the replacement of 20% cement with rice husk fly-ash in concrete can result in the compressive strength results similar to results of cement specimens. Also barley husk fly-ash can also exhibit pozzolanic properties due to high content of silica [16]. The rice husk fly-ash can improve chlorine ions penetration resistance [12]. Regarding their properties, wood and woody material fly-ash is a more inconsistent material than e.g. rice husk fly-ash. Currently, wood waste fly-ash is mainly used for soil improvements in agriculture. Wood fly-ash has a bulk density ranging from 2.1 to 2.6 g/cm^3. Its particles are irregular in shape and porous [17, 18]. The d_{50} size is about 110–150 μm. The combustion temperature drastically influences the amount of unfired carbonate residue. A temperature of combustion above 1000°C significantly decreases the amount of carbonates and elevates the amount of quick lime in the chemical composition. After combustion in 750°C the LOI is 4.6–8.4%. Also, with increasing combustion temperature the amount of alkaline metals declines. Despite the contaminants, the sum of silica, alumina and ferric compounds can be up to 60–80% [17]. Some elevated levels of chlorines and sulphates were detected in some Polish biomass fly-ashes [5]. Generally, the amount of hydration heat decreases with the addition of woody fly-ash in a similar manner like in coal fly-ash. However, the addition of woody fly-ash up to 20% of mass can result in a similar heat of hydration like in pure cement binder [19]. The wood waste fly-ash influences the setting time. It delays the initial and final setting time of the concrete mix [20, 21]. The mechanical properties of cement composites can be enhanced with wood waste fly-ash with the replacement level up to 10% [19]. Other research suggests that a replacement of 25% of cement with wood waste fly-ash can result in similar compressive strength to coal fly ash up to 7 days from mixing which suggest a filler-effect [18]. An additional increase of strength between 28 day and 365 day compressive strength of concrete specimens was also reported [22], suggesting the presence of pozzolanic reaction. The addition of woody biomass fly-ash can reduce the workability of cement paste and increase its water demand. A similar effect was observed with fresh concrete samples. A 15% replacement of cement with sawdust fly-ash in concrete binder can reduce the slump test result by 32%. Other results suggest that an addition of 10% of woody fly-ash to the binder has no adverse effect on water demand of cement mortar [19, 23, 24]. Self-compacting mortars with addition of 10% of wood waste fly-ash can exhibit compressive strength higher than cement control mortars up to 90 days after

mixing [25]. Incorporation of woody material and rice-husk fly-ashes can improve alkali-silica mitigation. Those types of fly-ashes were reported to enhance chlorine penetration resistance in replacements levels up to 25%. The presence of wood fly-ash does not tend to change the freeze-thaw resistance [17]. Woody biomass fly-ash tend to have less heavy metals in their chemical composition than coal fly-ash and can present some potential in the process of immobilization [11].

The aim of this paper is to assess the utility of wood biomass fly-ash for cement composite production. The coal fly-ash was substituted with wood fly-ash in a blended binder. For comparison, cement control specimens were made. The experiment program consisted of compressive strength tests after 7, 28, and 90 days, a density and water absorption test, and an abrasion test of cement concrete. Workability test were performed on cement mortars. Hydration heat measurements in the first 48 hrs after mixing of cement binders were also performed.

2. Materials and test methods

2.1. Materials

As a binder material a commercial CEM I 42,5R cement was used. The material conformed to the requirements of the PN-EN 197-1 standard. The wood biomass fly-ash was taken from fluidized bed combustion (750°C) while the coal fly-ash was taken from conventional combustion (1100–1200°C). Both fly-ashes came from the local combined heat and power plant. The silica content, loss on ignition and pozzolanic activity index of both fly-ashes are presented in Table 1. The grain size distribution of both materials are presented in Table 2. Natural sand with a maximum aggregate diameter of 16 mm was used. Tap water was used in the mixing and curing.

Table 1. The properties of wood biomass fly-ash and coal fly-ash

Property	*PN-EN 450-1 requirements*	**Wood biomass fly-ash**	*Coal fly-ash*
SiO_2 content	≥ 25%	52%	63%
Loss on ignition	≤ 9%	12%	14%
Pozzolanic activity index after 28 days	≥ 75%	77.0%	77.2%
Pozzolanic activity index after 90 days	≥ 85%	80.3%	95.9%

Table 2. The grain size distribution of wood biomass fly-ash and coal fly-ash

Fly-ash type	2-1 mm [%]	1-0,5 mm [%]	0,5-0,25 mm [%]	0,25-0,125 mm [%]	0,125-0,63 mm [%]	0,63-0,01 mm [%]	<0,01 mm [%]
Coal fly-ash	0.0	0.0	1.1	15.4	25.7	41.2	16.6
Wood biomass fly-ash	0.3	0.2	0.4	6.7	11.2	45.4	35.8

2.2. Mixture composition and specimen preparation

The fly-ash amount changed between series of specimen. The percentage of fly-ash (FA) – understood as the sum of both fly-ashes – in the binder mass was 20%, 40% or 60%. The content of coal fly-ash replaced with biomass fly-ash (FA(B)) was 0%, 50% or 100% mass of FA. The proportions are presented in Table 3. The water to binder ratio (w/b) was 0.5. The mass of the binder was the same in the series, 380 kg/m^3. Table 4 presents the mixture composition of concrete specimens. In the calorimetric tests binder samples were used. The binders had also w/b equal 0.5.

Table 3. The content of fly-ash in the binder and the content of biomass fly-ash in fly-ash mass

Series code	Biomass fly-ash content in fly-ash mass FA(B) [%]	Fly-ash content (FA) [%]
FA(B)0-20%	0	20
FA(B)0-40%	0	40
FA(B)0-60%	0	60
FA(B)50-20%	50	20
FA(B)50-40%	50	40
FA(B)50-60%	50	60
FA(B)100-20%	100	20
FA(B)100-40%	100	40
FA(B)100-60%	100	60
CEM I	0	0

The concrete specimens were cast in 10x10x10 cm moulds and completely compacted by vibration. The specimens were stored in water at temperature of 20 ± 2°C and cured until test time. They were tested for compressive test after 7, 28, and 90 days. The density, water absorption and abrasion tests were performed after 28 days. The number of concrete samples in each series destined for a single test was 3. For the hydration heat measurements the binder sample was prepared before the test. A single binder sample was made for each series.

The workability test was performed on fresh cement mortars. The control cement mix was prepared in accordance to the PN EN 196-1 standard. In the two series with the addition of fly-ashes 30% by binder mass was replaced with either biomass fly-ash or coal fly-ash respectively.

Table 4. The proportions of concrete mixtures

Series code	The proportions for 1 m^3 of concrete mix [kg]							
	Cement	Biomass fly-ash	Coal fly-ash	Sand	Aggregate			Water
					2-4 mm	4-8 mm	8-16 mm	
FA(B)0-20%	304	0	76	590	220	220	780	190
FA(B)0-40%	228	0	152	590	220	220	780	190
FA(B)0-60%	152	0	228	590	220	220	780	190
FA(B)50-20%	304	38	38	590	220	220	780	190
FA(B)50-40%	228	76	76	590	220	220	780	190
FA(B)50-60%	152	114	114	590	220	220	780	190
FA(B)100-20%	304	76	0	590	220	220	780	190
FA(B)100-40%	228	152	0	590	220	220	780	190
FA(B)100-60%	152	228	0	590	220	220	780	190
CEM I	380	0	0	590	220	220	780	190

2.3. Test methods

The compressive strength tests were performed in accordance to the PN-EN 12390-3 standard. The abrasion test was performed using the Bohme test method in accordance with PN-EN 13892-3:2005. The water absorption was calculated as the percentage of absorbed water mass compared to the mass of a specimen dried to constant weight. The workability test was performed in accordance with PN-EN 1015-3 and was assessed by percentile change in water demand needed to achieve a slump test result similar to the control specimens. Three tests on fresh mortar were performed for each series. The 48 hr long heat of hydration measurements were performed on a conductive calorimeter. The calorimeter enabled the heat of hydration from the moment of binder and water mixing to be measured [26].

3. Test results and discussion

3.1. Results of hydration heat measurements

The calorimetric measurement results for the binder series with addition of biomass fly-ash are presented in Figure 1. The addition of biomass fly-ash has caused a diminishment of hydration peak and has delayed it in time. The replacement of 60% of cement with biomass fly-ash resulted in a reduction of hydration peak by 53% and its delay by 1.5 hr. There is a visible and significant peak in the first minutes from mixing water with binder.

With the growing replacement of coal fly-ash with biomass fly-ash the hydration peaks were bigger. Comparing the binders with 40% cement replaced with fly-ash, the binder with biomass fly-ash replacement was characterized with a higher hydration peak by 20% (Fig. 2). The growing addition of biomass fly-ash caused a delay in its occurrence.

The biomass and coal fly-ashes significantly diminished the peak of hydration. The coal fly-ashes generally have a similar effect [3]. The differences in outcomes between the fly-ashes might have been the result of different chemical composition. The grain size distribution also could have been influential. The biomass fly-ash has the grain size distribution shifted towards smaller particles and those can provide an additional surface for the seeding of the hydration process. The decrease in the peak of hydration of the 20% replacement of cement with biomass fly-ash is comparable with the result reported [19] – contrary to the results observed in this study, the addition of woody biomass fly-ash slightly increased the hydration speed.

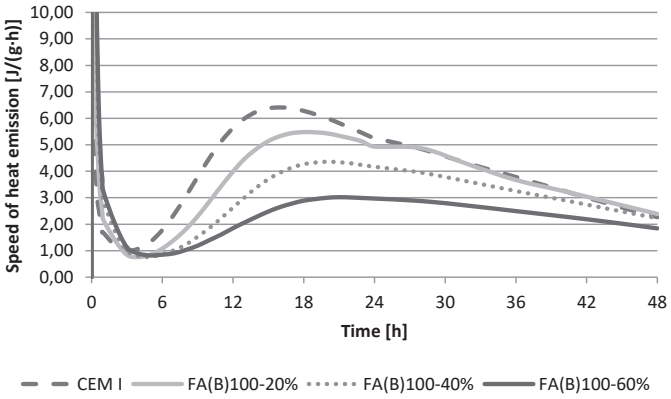

Fig. 1. The influence of biomass fly-ash addition on the calorimetric measurement results of cement binders

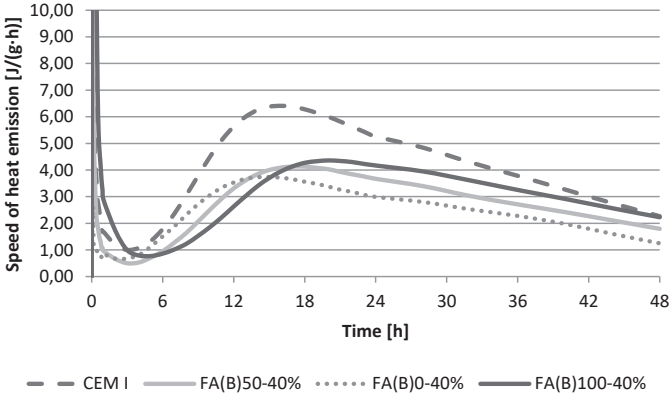

Fig. 2. The influence of 40% replacement of cement with biomass fly-ash addition, coal fly-ash addition and the mix of biomass fly-ash and coal fly-ash addition on the calorimetric measurement results of cement binders

3.2. Results of the workability tests

The workability test results of fresh mortar mixes with the addition of biomass and coal fly-ashes are presented in Table 5. The slump test result for the control specimens was 14 cm. To achieve this result coal fly-ash fresh mortar specimens needed an additional 13% water. The specimens of biomass fly-ash needed 17% of water in the mixture.

The result are similar to findings reported in the literature. A severe reduction of consistency was reported [22] and results comparable to this [18, 23]. The researchers attribute the increased water demand of woody biomass fly-ashes to either a higher specific surface of their irregularly-shaped particles or a higher content of unfired carbon. The coal fly-ashes with small percentage of LOI tend to increase workability and have small effect on water demand [3, 8].

Table 5. The results of cement mortar workability tests

Series code	Slump test result [cm]	Water content in the mortar mix [g]	Water content change [%]
CEM I	14.0	225	100
FA(B)0-30%	13.7	255	113
FA(B)100-30%	14.5	265	117

3.3. Results of the compressive strength tests

The compressive strength results of concretes with the addition of biomass and coal fly-ashes after 7, 28, and 90 days of curing are presented in Fig. 3–5.

The addition of coal fly-ash has caused a diminishment in the compressive strength of the concrete with rising dosage. Between 28 and 90 days of curing the compressive strength of control series did not change. The compressive strength of concrete with part

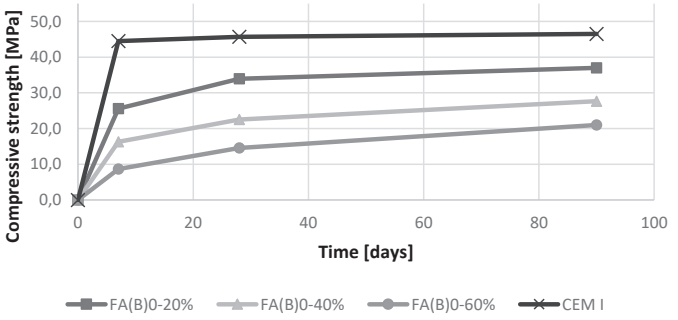

Fig. 3. Effect of coal fly-ash addition on compressive strength of concrete

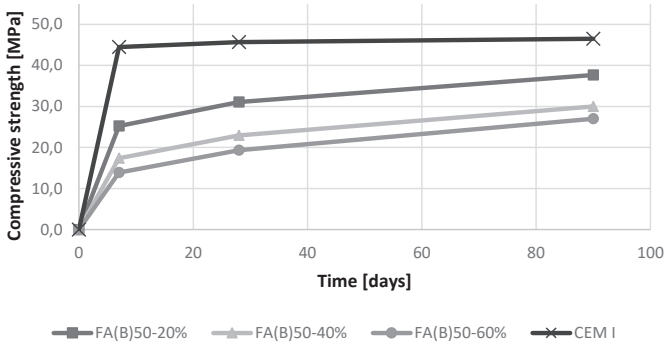

Fig. 4. Effect of coal fly-ash with 50% replacement with biomass fly-ash addition on compressive strength of concrete

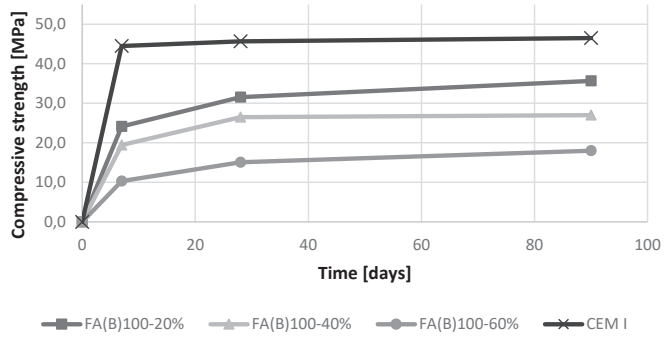

Fig. 5. The effect of biomass fly-ash addition on compressive strength of concrete

of cement replaced by coal fly-ash was significantly higher at 90 day than at 28 day. The 90 day compressive strength of FA(B)0-60% specimens was higher by 44,8% comparing to the series' 28 day results. In a similar manner, the addition of fly-ash with 50% replacement of biomass fly-ash influenced the development of compressive strength between 28 and 90 day of curing – the compressive strength of FA(B)50-20% raised by 21.6% between those test times (Fig. 4). Comparable results were visible in the series with full-replacement of coal fly-ash with biomass fly-ash addition (Fig. 5).

The half-replacement and full-replacement of coal fly-ash with biomass fly-ash did not change the compressive strength of the concrete significantly (Fig. 6). The development of compressive strength was similar with the addition of each fly-ash composition.

Coal fly-ash addition generally diminishes the strength of the concrete specimens, especially in its early increase [3, 8]. This was observed in this study. The compressive strength development of biomass fly-ashes specimens was similar. Also an additional gain in the compressive strength of coal fly-ash and biomass fly-ash can be seen between 28 and 90 days after casting. This may suggest the influence of a pozzolanic reaction from both fly-ashes. In

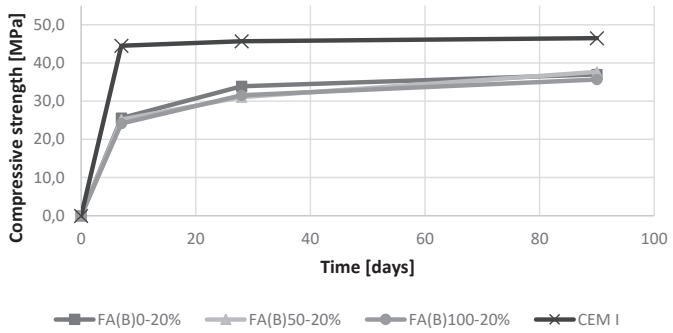

Fig. 6. The effect of 20% cement replacement with coal fly-ash addition, mixed coal and biomass fly-ash addition, and biomass fly-ash addition on compressive strength of concrete

other research the difference between 28 day and 90 days compressive strength of composites with the addition of woody biomass fly-ashes was not reported [18]. A comparable 6% gain of compressive strength of sawdust biomass fly-ash cement concrete was reported [22].

3.4. Results of the abrasion tests

The abrasion tests results for concretes with the addition of fly-ashes are presented in Figure 7. The 20% replacement of cement with either coal, mixed coal and biomass, or biomass fly ash did not influence the abrasion results. The replacement of 40% or 60% cement with coal fly-ash reduced the abrasion resistance by about 40%. The replacement of coal fly-ash with biomass fly-ash resulted in a smaller loss due to abrasion. The full-replacement of coal fly-ash with biomass fly-ash has resulted in a 24% reduction in abrasion loss of volume.

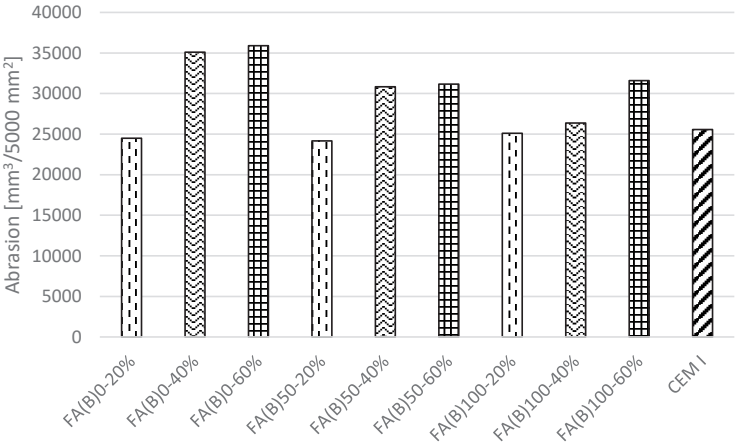

Fig. 7. The effect of cement replacement with coal fly-ash addition, mixed coal and biomass fly-ash addition, and biomass fly-ash addition on abrasion test results

3.5. Results of density and water absorption tests

According to [20] tests on cement mortar with and without 15% replacement of cement with wood waste fly-ash have shown little effect on water absorption. In another study [27] the increase of wood waste fly-ash from 5% to 30% of binder mass in cement concrete resulted in a less than 1% increase in water absorption. The increase in dosage of woody biomass fly-ash in this study also marginally influenced this property, but the difference between water absorption measured on control specimens and fly-ash specimens was significantly greater.

The water absorption and density test results are presented in Table 6. All the series with cement replaced partly by the fly-ashes were characterized by higher water absorption compared to control specimens. Slightly lower water absorption results were measured on biomass fly-ash concretes. A significant difference between densities of specimens with an addition of fly-ash and control specimens was not observed.

Table 6. The results of density and water absorption tests

	Water absorption [%]	**Density** [g/cm^3]
FA(B)0-20%	7.22	2.16
FA(B)0-40%	8.18	2.10
FA(B)0-60%	8.52	2.07
FA(B)50-20%	7.19	2.18
FA(B)50-40%	7.60	2.15
FA(B)50-60%	7.09	2.14
FA(B)100-20%	6.90	2.19
FA(B)100-40%	7.11	2.19
FA(B)100-60%	7.36	2.16
CEM I	4.84	2.29

4. Conclusions

The analysis of the test results shows that the influence of biomass fly-ash and coal fly-ash on cement concrete and cement binder can be similar. The addition of biomass fly-ash resulted in a slightly bigger peak of hydration. This could be attributed to the larger specific surface of biomass fly-ash or its chemical composition. The development of compressive strength was similar comparing specimens with the addition of coal fly-ash and biomass fly-ash. This may suggest that the hydration and pozzolanic capabilities of both types of blended binders were similar. The addition of biomass fly-ash resulted in a similar or up to 24% better abrasion resistance compared to concrete specimens with the addition of coal fly-ash. There

were no significant differences between the influences of the addition of biomass fly-ash and coal fly-ash considering the density and water absorption of concrete.

This study has shown that it is possible to produce concrete with an addition of biomass fly-ash that has similar properties to concrete with an addition of coal fly-ash. Biomass fly-ashes vary in chemical composition. Even different batches of fly-ash from the same source may present different levels of contained oxides. The issue of elevated LOI percentage can be sufficiently addressed by modern technical means in power plants or fly-ash treatment. Electrostatic separation of positively charged coal particles from negatively charged minerals can downsize the LOI percentage of treated fly-ashes below 5%. The separated coal particles can be reused in the burning chamber [28]. It is tremendously important to check biomass fly-ashes before adding it to cement composites mixes to maintain their utility. For a better understanding of the results, more chemical analysis of fly-ashes ought to be performed. Moreover, for a better assessment of the biomass fly-ash cement composite utility, more studies should be performed. In particular, there is a lack of sufficient knowledge on the durability of such composites.

Studies have been carried out in the framework of work no. MB/WBiIŚ/8/2016 and work no. S/WBiIŚ/1/2016 financed from the funds for science from Ministry of Science and Higher Education.

References

[1] *Rocznik statystyczny przemysłu 2015,* eds. Witkowski J., Dmochowska H., Główny Urząd Statystyczny, Warszawa 2015, 119–442.
[2] *BP Statistical Review of World Energy,* eds. Dale S. British Petroleum, London 2016.
[3] Giergiczny Z., *Popiół lotny w składzie cementu i betonu – monografia*, Wydawnictwo Politechniki Śląskie, Gliwice 2013.
[4] Ministerstwo Gospodarki, *Projekt Polityki energetycznej Polski do 2050 roku*, Warszawa 2015.
[5] Uliasz-Bocheńczyk A., Mokrzycki E., *Biomasa jako paliwo w energetyce,* Rocznik Ochrona Środowiska, Vol. 17, 2015, 900–913.
[6] Ahmaruzzaman M., *A review on the utilization of fly ash*, Progress in Energy and Combustion Science, Vol. 36, 327–363.
[7] Baran T., Ostrowski M., Giergiczny Z., *Wykorzystanie mieszanych popiołów lotnych z oddzielnego spalania pyłu węglowego i paliw wtórnych w produkcji spoiw wiążących*, Materiały Budowlane, Vol. 12, 2015, 37–40.
[8] Giergiczny Z., *Właściwości popiołu lotnego a trwałość betonu,* Budownictwo Technologie Architektura, Vol. 39, 2007, 44–48.
[9] Cuenca J., Rodriguez J., Martín-Morales M., Sánchez-Roldán Z., Zamorano M., *Effects of olive residue biomass fly ash as filler in self-compacting concrete,* Construction and Building Materials, Vol. 40, 2013, 702–709.

[10] Lessard J.-M., Omran A., Tagnit-Hamou A., Gagne R., *Feasibility of using biomass fly and bottom ashes in dry-cast concrete production,* Construction and Building Materials, Vol. 132, 2017, 565–577.
[11] Gawlicki M., Graur Z., Ślęzak E., *Popioły lotne ze spalania biomasy jako składniki spoiw drogowych,,* Scientific Works of Institute of Ceramics and Building Materials, Vol. 19, 2014, 34–46.
[12] Madandoust R. Ranjbar M.M., Maghadam H.A., Mousavi S.Y., *Mechanical properties and durability assessment of rice husk ash concrete*, Biosystems Engineering, Vol. 110, 144–152.
[13] Sua-Iam G., Makul N., *Utilization of coal- and biomass-fired ash in the production of self-consolidating concrete: a literature review*, Journal of Cleaner Production, Vol. 100, 2015, 59–76.
[14] Rodriguez de Sensale G., *Strength development of concrete with rice-husk ash*, Cement and Concrete Composites, Vol. 28, 2006, 158–160.
[15] Jamil M., Khan M.N.N., Karim M.R., Kaish A.B.M.A., Zain M.F.M., *Physical and chemical contributions of Rice Husk Ash on the properties of mortar*, Construction and Building Materials, Vol. 128, 2016, 185–198.
[16] Khalil N.M., Hassan E.M., Shakdofa M.M.E., Farahat M., *Beneficiation of the huge waste quantities of barley and rice husks as well as coal fly ashes as additives for Portland cement*, Journal of Industrial and Engineering Chemistry, Vol. 20, 2014, 2998–3008.
[17] Cheah C.B., Ramli M., *The implementation of wood waste ash as a partial cement replacement material in the production of structural grade concrete and mortar: An overview*, Resources, Conservation and Recycling, Vol. 55, 2011, 669–685.
[18] Wang S., Miller A., Llamazos E., Fonseca F., Baxter L., *Biomass fly ash in concrete: Mixture proportioning and mechanical properties*, Fuel, Vol. 87, 2008, 365–371.
[19] Rajamma R., Ball R.J., Tarelho L.A.C., Allen G.C., Labrincha J.A., Ferreira V.M., *Characterisation and use of biomass fly ash in cement-based materials*, Journal of Hazardous Materials, Vol. 172, 2009, 1049–1060.
[20] Elinwa A.U., Ejeh S.P., *Effects of incorporation of sawdust incineration fly ash in cement pastes and mortars,* Journal of Asian Architecture and Building Engineering, Vol. 3, 2004, 1–7.
[21] Abdullahi M., *Characteristics of wood ash/OPC concrete*, Leonardo Electronic Journal of Practices and Technologies, Vol. 8, 2006, 9–16.
[22] *Demonstration of manufacturing technology for concrete and CLSM utilizing wood ash from Wisconsin*, eds. Naik T.R., Kraus R.N., Siddique R., Department of Civil Engineering and Mechanics, University of Wisconsin-Milwaukee, Milwaukee 2002.
[23] Elinwa A.U., Mahmood Y.A., *Ash from timber waste as cement replacement material*, Cement & Concrete Composites, Vol. 24, 2002, 219–222.
[24] Berra M., Mangialardi T., Paolini A.E., *Reuse of woody biomass fly ash in cement-based materials*, Construction Building Materials, Vol. 76, 2015, 286–296.
[25] Elinwa A.U., Ejeh S.P., Mamuda A.M., *Assessing of the fresh concrete properties of self-compacting concrete containing sawdust ash*, Construction Building Materials, Vol. 22, 2008, 1178–1182.

[26] Zielenkiewicz W., Kamiński M., *A conduction calorimeter for measuring the heat of cement hydration in the initial hydration period*, Journal of Thermal Analysis and Calorimetry, Vol. 65, 2001, 335–340.
[27] Udoeyo F.F., Inyang H., Young D.T., Oparadu E.E., *Potential of wood waste ash as an additive in concrete, Journal of Materials in Civil Engineering*, Vol. 18, 2006, 605–611.
[28] Bittner J.D., Gąsiorowski S.A., *Separacja popiołów lotnych i usuwanie amoniaku w Tampa Electric Big Bend*, International Conference EuroCoalAsh, Warsaw, 6–8 October 2008.

TECHNICAL TRANSACTIONS 8/2017
CZASOPISMO TECHNICZNE 8/2017
CIVIL ENGINEERING
DOI: 10.4467/2353737XCT.17.136.6887

Daniel Wałach (walach@agh.edu.pl)
Joanna Sagan
Justyna Jaskowska-Lemańska
Faculty of Mining and Geoengineering, Department of Geomechanics, Civil Engineering and Geotechnics, AGH University of Science and Technology

Environmental assessment in the integrated life cycle design of buildings

Ocena środowiskowa w zintegrowanym procesie projektowania obiektów budowlanych

Abstract

The paper discusses the issue of building environmental assessments carried out as part of an integrated life cycle design process. The paper presents the methods used to evaluate environmental impact based on CEN and ISO standards. The paper concludes with an excerpt from an environmental assessment of a reinforced concrete structural frame in an office building.

Keywords: sustainable construction, ILCD, LCA

Streszczenie

Artykuł dotyczy problematyki przeprowadzania oceny środowiskowej budynku, będącej elementem zintegrowanej oceny obiektu budowlanego. Przedstawiono metodykę oceny aspektów środowiskowych, opartą na standardach CEN i ISO. Całość opracowania podsumowuje przykład będący fragmentem oceny środowiskowej żelbetowej konstrukcji szkieletowej budynku biurowego.

Słowa kluczowe: zrównoważone budownictwo, ILCD, LCA

1. Introduction

Up till now, functional and structural issues have taken priority in construction design, with the main objective being the development of structural solutions that possess the required characteristics, at the same time keeping the investment outlays as low as possible. The basic aim of design work was to adopt a solution that is optimal for the particular conditions, taking account of the needs of the investor and users of the building. The time-frame for analysing the efficiency of the solutions adopted was usually limited to the execution phase and the warranty period. However, on the basis of the sustainable development concept, a new approach to design was born, taking account of all requirements imposed on sustainable construction within a single design process, known as integrated life cycle design (ILCD). This new approach combines all aspects of design at the material, component and structural level, and analyses the selected criteria relating to sustainable development on all of those levels – including criteria which reflect the impact of the work on the environment. Therefore, the new concept of design is based on a complex, three-dimensional model [5] (Fig. 1).

The basis for assessing construction sustainability is the PN-EN 15643-1:2011 standard [9], which outlines general principles and requirements with regard to building assessment in terms of its environmental, social and economic properties, taking into account the technical and functional parameters of the building – by referring to the so-called functional equivalent.

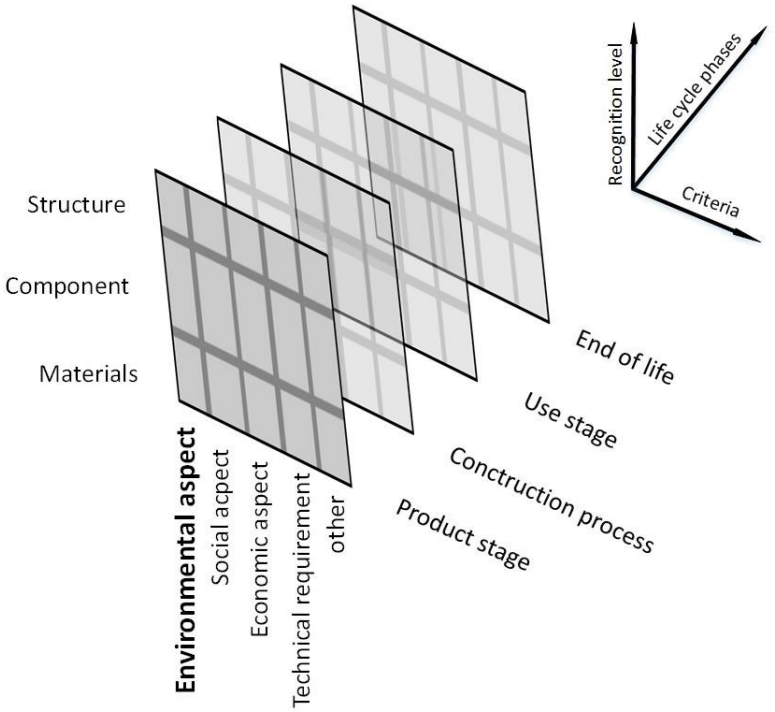

Fig. 1. 3D model of integrated design [5]

It should be noted that while the first part of the title of the integrated design standard refers to construction work, the currently applicable standards actually concern buildings. However, the methods developed are also useful for other engineering structures, even more so that the set of norms referred to above is based on general standards taken from the manufacturing sector and adapted accordingly.

The purpose of this article is to exhibit a synthesis of the environmental impact assessment methods. Based on an example, the adaptation of the LCA result to the structure design is presented. Both methodology and example analysis allowed for a qualitative assessment of the approach.

2. Methods used to assess environmental impact of buildings

Environmental impact assessment (EIA) is a systemized assessment involving interdisciplinary identification and evaluation of the impact of planned construction projects and their alternative variants on a specific area and the processes occurring therein [1]. The method used for carrying out environmental assessment of buildings is LCA – it is one of the most objective and accurate environmental assessment methods due to its multi-dimensional and comprehensive character [8]. The general environmental assessment method applicable to the entire life cycle is defined by the international ISO 14040:2006 standard [6] as a "*collection or estimation of initial data and results and the potential environmental impact of the designed system during its entire life cycle*". Therefore, the principles and methods of assessing building environmental characteristics found in PN-EN 15643-2:2011 [10] and PN-EN 15978:2012 [11] are based on the abovementioned ISO standards. However, the standards only cover the analytical part of the assessment, which means that they do not provide information about environmental indicator valuation methods.

Valuation systems and indicator aggregate calculation methods linked to those systems may be determined by national standards or separate legislation of varying scopes of application, or – if there are none – can be adopted according to individual preferences.

2.1. Determination of the purpose and scope of the assessment

Even though the EN 15643-2:2011 standard [2] stipulates that the scope of assessment covers the building with foundations and landscape features within the plot, as well as temporary structures related to the construction works during the entire life cycle, it allows for certain limitations in the assessment with regard to parts of the building and to part of its life cycle. The construction work life cycle (system), according to the PN-EN 15643-1:2011 standard [9], is divided into individual information modules corresponding to subsequent stages of its life (Fig. 2) – from obtaining raw materials required to manufacture construction products, to modules related to the final phase of the building's life cycle. The EN 15978:2011 standard [3], item 7.4, clearly determines the beginning and end of each of those phases. All types of impact of the construction work should be assigned to the relevant modules.

The purpose of an environmental assessment carried out as part of ILCD process is to obtain reliable environmental impact indicators for the construction design options considered or for their components at selected stages of the life cycle. The environmental indicators are then valued at a subsequent stage of the integrated life cycle design process, together with financial and social indicators obtained through appropriate assessments.

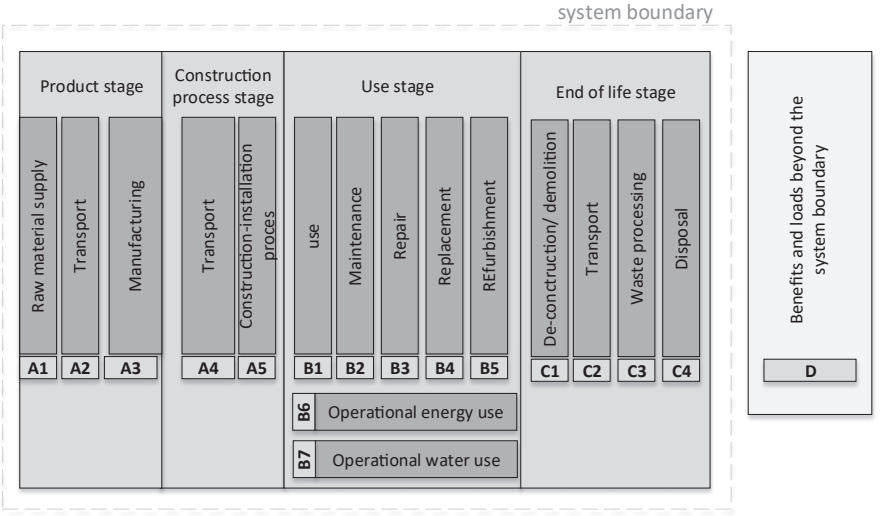

Fig. 2. Information modules of building life cycle [9]

2.2. Input and output analysis – LCI

LCI (Life Cycle Inventory) is a material balance used to collect and organize data on most types of environmental impact, i.e. to establish a set of system inputs from the environment, technosphere, etc., and to inventory environment-related outflow (emissions, waste) for a given process (Fig. 3).

The systemic approach suggested by the EN 15643-2:2011 standard [2], together with the aggregated set of individual processes at individual stages of the construction work life cycle facilitates analysis of the input and output data set, as well as its further interpretation. The information needed to develop an inventory may be found in the literature and ready databases – for example such collections as: ELCD, Ecoinvent, NEEDS, etc. or obtained directly from the product manufacturers. We should remember that collecting data these days is a very time-consuming and costly process. However, the standard allows the use of average and general values for construction work environmental assessment purposes. While selecting data for the assessment, their quality should be specified, i.e. it is necessary to provide information about their correlation in time, geographical and technological correlation, reliability and completeness. An important aspect of LCI is also data significance assessment based on sensitivity analysis; as well as data uncertainty analysis and its impact on the results obtained [7].

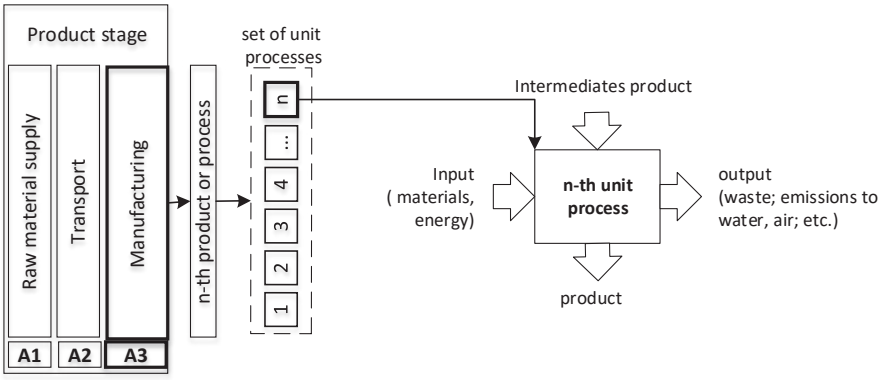

Fig. 3. Aggregation of units processes in information modules [own source]

2.3. Determination of environmental indicators

The following indicators should be used to examine a building's environmental impact:

- environmental impact indicator – LCIA categories,
- resource usage indicator,
- indicators referring to other environmental data.

The life cycle environmental impact assessment – LCIA, constitutes the third step of LCA assessment, which involves quantification of the correlations between the input and output data set and its environmental impact expressed in the input category. In order to convert LCI results into category indicators, according to (International Standard ISO 14040:2006 [6]), we should:

- select the input category, category indicators and characterization models,
- allocate LCI results (classification) to individual input categories,
- calculate the category indicator value (characterization).

There is now a range of environmental impact categories representing different approaches. Table 1 shows LCIA categories requested by the PN-EN 15643-2:2011 standard [2].

Table 1. LCIA categories [2]

Category	Examples of classification	Unit
Global warming (GWP)	CO_2, NO_2, CH_4, CFC, HCFC, CH_3Br	kg CO_2
Ozone depletion (ODP)	CFC, HCFC, CH_3Br	kg CFC 11
Soil and water acidification (AP)	SO_x, NO_x, HCL, HF, NH_4	kg SO_2
Eutrophication (EP)	HNO_3, NO_2, NO	kg $(PO_4)^{3-}$
Photochemical ozone production (POCP)	NMHC	kg ethylene
Resource depletion – ADP elements	Quantity of minerals used	kg Sb
Resource depletion – ADP – fossil fuels	Quantity of fossil fuels used	MJ, (net)

Apart from environmental impact indicators arising from LCIA, the PN-EN 15643-2:2011 standard [2] requires that the environmental assessment also covers resource use indicators and other indicators which represent important environmental information – they are summarized in Table 2.

Table 2. Other indicators of environmental assessment [2]

Indicator of resource use	Unit
Use of renewable primary energy excluding energy resources used as raw material	MJ
Use of non-renewable primary energy excluding primary energy resources used as raw material	MJ
Use of non-renewable primary energy resources used as raw material	MJ
Use of renewable primary energy resources used as raw materials	MJ
Use of secondary materials	kg
Use of renewable secondary fuels	MJ
Use of non-renewable secondary fuels	MJ
Net use of fresh water	m^3
Indicators of other environmental information	
Reusable components	kg
Recycling materials	kg
Materials for energy recovery	kg
Non-hazardous waste for disposal	kg
Hazardous waste for disposal	kg
Radioactive waste for disposal	kg
Exported energy	MJ

It is required that the result of environmental assessment is presented in the form of a summary of environmental indicators (Table 1 and 2) for individual information modules as vectors, while the following formula is used to determine their value:

$$\begin{bmatrix} GWP_{a_{1,i}} & GWP_{a_{2,i}} & GWP_{a_{3,i}} & GWP_{a_{...i}} & GWP_{a_{n,i}} \\ AP_{a_{1,i}} & AP_{a_{2,i}} & AP_{a_{3,i}} & AP_{a_{...i}} & AP_{a_{n,i}} \\ ODP_{a_{1,i}} & ODE_{a_{2,i}} & ODP_{a_{3,i}} & ODP_{a_{...i}} & ODP_{a_{n,i}} \\ ... & ... & ... & ... & ... \end{bmatrix} \cdot \begin{bmatrix} a_{1,i} \\ a_{2,i} \\ a_{3,i} \\ a_{...,i} \\ a_{n,i} \end{bmatrix} = \begin{bmatrix} GWP_i \\ AP_i \\ ODP_i \\ ... \end{bmatrix} \quad (1)$$

where:

$GWP_{an,i}$, $AP_{an,i}$, $ODP_{an,i}$ – values of environmental impact indicators (per unit) for *n*-th products or processes (labour) in *i*-th information module,

$a_{1\text{-}n,i}$ – vector comprising the total use *n* of products and/or processes (labour) n *i*-th module,

GWP_i, AP_i, ODP_i – value of environmental impact indicators for *i*-th information module, where: $i = [A_1{:}A_3, B_1{:}B_7, C_1{:}C_4, D]$.

3. Example environmental assessment at the engineering stage

In order to demonstrate the selected components of construction work environmental assessment, an analysis of a 12-storey office building is presented here. The building – built on a plan of 50×20 m, with single storey height of 3.7 m – was designed as a slab and column structure with an internal core. For the purpose of this analysis it was verified whether two concrete classes, C30/37 and C70/85, could be used in its construction while assuming the same usage of reinforcing steel in individual projects. The scope of the analysis presented includes determination of LCIA category indicators for the product stage (A1÷A3). Three variants of the structure were analysed: the ultimate limit and serviceability states were verified for all three variants to determine the use of concrete in each scenario:

- variant I – C30/37 concrete used on slabs and columns (2643.0 m^3),
- variant II – C70/85 concrete used on slabs and columns (2348.0 m^3),
- variant III – C30/37 concrete used on slabs (2436 m^3), C70/85 concrete used on columns (140.0 m^3).

A summary of the input and output data set was prepared for each concrete class, database was used for inventorying: EU27: Sand 0/2, EU-27-Diesel mix at refinery , EU-27: Gravel 2/32, EU-27: Tap water, GLO:Truck, Portland Cement (CEM I) ELCD/CEMBUREAU. An LCI for superplasticizer manufacture was prepared on the basis of Environmental Consultant INTRON B.V [4]. The classification and characterisation stage was carried out based on the CML method, which ultimately led to determining environmental indicators (LCIA) – Fig.4.

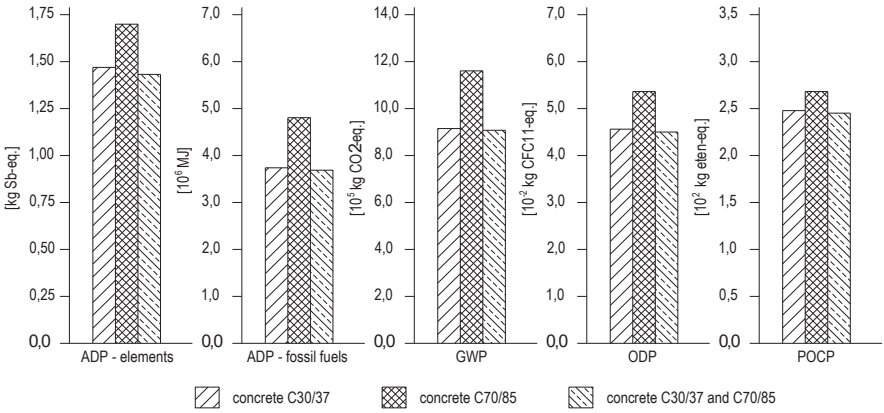

Fig. 4. Selected environmental impact indicators for individual variants [own source]

It should be stressed that the results presented above only refer to the engineering stage (A1÷A3), therefore, in order to carry out a comprehensive environmental impact assessment similar calculations would have to be made for the other phases of the life cycle and supplemented with other indicators. However, the analysis enables us to draw certain

conclusions valuable to the architect, namely that the use of high-strength concrete in this case reduces concrete usage only insignificantly (due to the bending of the slabs), therefore, due to an increased use of cement used in high-strength concrete, the use of such materials increases environmental impact at the engineering stage. A small improvement is seen in case of using HSC in compression components (columns) due to significant cross-section reductions.

4. Summary and final conclusions

There is no doubt that integrated construction design seems a proper and valuable approach to the design process. However, it requires knowledge of new methods of structural and material analysis, including environmental assessment methods. The assessment is a complex, interdisciplinary process. It requires close cooperation between the construction engineer and environmental engineer, otherwise the construction engineer needs to become familiar with additional methods and tools used to determine environmental impact indicators. The assessment process could be somewhat simplified by using a ready-made wide set of individual environmental impact indicators for construction products and processes, sensitive to the parameters that determine them to a great extent. Currently, the lack of free access to databases and a limited number of available databases leads to prolongation of the design process, increasing the related costs and limiting the scope of assessment, also resulting in a suggestive assessment.

References

[1] Adamczyk W., *Ekologia Wyrobu – jakość, cykl życia, projektowanie*, PWE, Warszawa 2004.
[2] EN 15643-2:2011 Sustainability of construction works. Assessment of buildings. Framework for the assessment of environmental performance.
[3] EN 15978:2011 Sustainability of construction works. Assessment of environmental performance of buildings. Calculation method.
[4] Environmental Consultant INTRON B.V, Environmental declaration Superplasticizing admixtures, EFCA, 2002.
[5] Hajek P., *Integrated life cycle assessment of concrete structures*, State-of-art report prepared by Task Group 3.7., fib, Prague 2013.
[6] International Standard ISO 14040:2006. Environmental management – Life cycle assessment – Principles and framework. International Standard Organization.
[7] Kowalski Z., Kulczycka J., Góralczyk M., *Ekologiczna ocena cyklu życia procesów wytwórczych (LCA)*, PWN, Warszawa 2007.
[8] Lesiuk, A., Oleszczuk, P., Kuśmierz, M., *Zastosowanie techniki LCA w ekologicznej ocenie produktów, technologii i gospodarce odpadami*, [w:] J. Ryczkowski, *Adsorbenty i katalizatory, Wybrane technologie a środowisko,* Uniwersytet Rzeszowski, Rzeszów 2012, 453–466.
[9] PN-EN 15643-1:2011. Zrównoważoność obiektów budowlanych – Ocena budynków – Część 1: Zasady ogólne.

[10] PN-EN 15643-2:2011. Zrównoważoność obiektów budowlanych – Ocena budynków – Część 2: Zasady oceny właściwości środowiskowych.
[11] PN-EN 15978:2012. Zrównoważone obiekty budowlane – Ocena środowiskowych właściwości użytkowych budynków – Metoda obliczania.

TECHNICAL TRANSACTIONS 8/2017
CZASOPISMO TECHNICZNE 8/2017
ENVIRONMENTAL ENGINEERING
DOI: 10.4467/2353737XCT.17.137.6888

Dorota Skrzyniowska (skdorota@pk.edu.pl)
Institute of Thermal Engineering and Air Protection, Faculty of Environmental Protection, Cracow University of Technology

Contaminants in circulating refrigerant

Zanieczyszczenia w czynniku ziębniczym

Abstract

Contaminants are inventible in the refrigeration cycle. Lubricant, water and moist air are the main contaminants in circulated refrigerant. This paper attempts to show how the presence of such contaminants influences the thermodynamic parameters of the refrigerating cycle and the mixture, which comes at the beginning..

Keywords: refrigerant, contaminants, mixture, specific enthalpy, thermodynamic cycle, refrigerating cycle, positive-displacement compressor

Streszczenie

Zanieczyszczenia w czynniku ziębniczym obiegu ziębniczego są nieuniknione. Obecność substancji smarnej, wody, powietrza wilgotnego to główne zanieczyszczenia czynnika obiegowego obiegu ziębniczego. W artykule przedstawiono wpływ obecności wymienionych zanieczyszczeń na podstawowe parametry obiegu ziębniczego, a w szczególności na entalpię właściwą powstałej mieszaniny.

Słowa kluczowe: czynnik chłodniczy, czynnik ziębniczy, zanieczyszczenia obiegu ziębniczego, mieszanina, entalpia właściwa, obieg termodynamiczny, obieg chłodniczy, obieg ziębniczy, sprężarka wyporowa

1. Introduction

Along with refrigerant, contaminants[1] can also circulate in the refrigeration cycle with a lubricated reciprocating compressor. These contaminants are very problematic. They can include inert gases (such as air), moisture (in vapour, aerosol and drop) and lubricant (in bulk liquid, aerosol and vapour [7]). Therefore, there is refrigerant, lubricant and moist air in the mixture in the refrigerating cycle (refrigerating- air-vapour-oil mixture).

The refrigeration cycle needs an almost sterile environment to survive.

Contaminants in the refrigerant have an influence on thermodynamic parameters, heat exchange and compressor work as well as the throttle valve (change in flow, pressure drop, change of refrigerants parameters, such as specific enthalpy, viscosity, surface tension, etc.). Therefore, the presence of contaminants in refrigerant should be considered in thermodynamic calculations.

Additionally, the refrigerant in the refrigeration cycle is considered as an ideal one, but indeed, it should be treated as a real gas.

2. Air in refrigerant – non-condensable contaminant (NCG)

Air is one of the most difficult contaminants in refrigerant. This contaminant can cause excessive head pressure and increased operating temperature [2, 9]. The result is higher utility costs, degradation of lubricant effectiveness, and premature compressor problems [6, 8, 13].

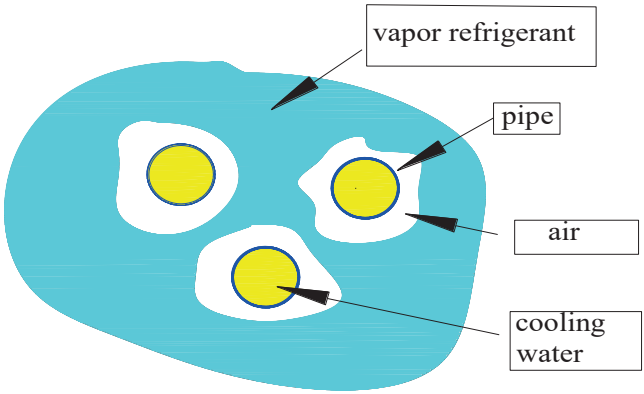

Fig. 1. Configuration of layer around coil pipe

Many studies talk about, for example in [10], the author presenting the temperature profile of R404A in a coil pipe for three air volume contents of 0%, 1,5% and 3%.

[1] Ingredient which is not refrigerant in refrigerating cycle, is contaminant.

According to the author, up to 5 % volume fraction of air overall heat-transfer coefficient increases up to 50 % in the water-cooled refrigerating unit.

Refrigerant only condenses during condensation, whereas air remains gaseous, aggravating near the heat exchange surface in the condenser [3] (even smattering of air around or inside the pipe causes a decrease of the heat exchange coefficient, causing an increase of pressure in the heat exchanger above the saturation pressure [2]).

3. Moisture in refrigerant

Another contaminant in the refrigeration system is moisture. Refrigeration systems are very sensitive to moisture in the refrigerant side of the system. If moisture gets into the system, failure may occur due to ice formation in expansion valves, capillary tubes or evaporators, corrosion of metals, copper plating, chemical damage to insulation in hermetic compressors or other system materials.

Sources of moisture in the refrigeration system include:

- Faulty equipment drying in factories and service operations,
- Introduction of moisture during installation or service operations in the field,
- Low-side leaks (resulting in entrance of moisture-laden air),
- Leakage of water-cooled condenser,
- Oxidation of certain hydrocarbons of oil to produce moisture,
- Wet oil, refrigerant or both,
- Decomposing cellulose insulation in hermetically sealed units.

Water freely absorbs into refrigerant as if being soaked up by a dry sponge. Due to its solubility characteristics, water will continue to absorb into refrigerant until saturation is achieved. Once saturation is exceeded, a flooded condition is created and the actual amount of water in the system cannot be determined by refrigerant analysis.

Refrigerant moisture directly causes the formation of acids resulting in metal corrosion copper plating and chemical damage to the insulation in hermetic compressors and other system materials. Metal corrosion may lead to rust and pitting of motor bearings and copper plating may form on bearings causing a reduction in tolerance. Moisture contamination occurs when moisture enters the refrigeration system. Moisture can exist in three forms: water, solid and gas. Therefore, if contaminants are introduced into the system, they act to reduce compressor efficiency, effectiveness and durability. If moisture enters in to a refrigeration system, it combines with the refrigerant to form an acidic solution, which may erode internal compressor components. Moisture does not actually cause direct compressor failure; the failure results from the failure of a part, which has been weakened as a result of the effects of rust and corrosion [4]. Any amount of water above 50 ppm is potentially dangerous and should be removed [8].

4. Lubricant in refrigerant

A lubricant is necessary in almost all the vapour compression systems, particularly for the right operation of the positive displacement compressor. The cylinder – piston assembly, the reciprocating movement and friction of piston give the main characteristic of a positive displacement compressor. The main role of lubricant is to ensure the existence of a thin lubricant film allowing the lubrication of the mechanical moving elements (pistons, connecting rod/crank, valves, …) in order to protect them against wear. Lubricant is used in order to reduce the friction.

It assures a correct compressor operation and cylinder – piston unit performance. The sliding mechanism with a cylinder and a piston compressor is shown in Fig. 2.

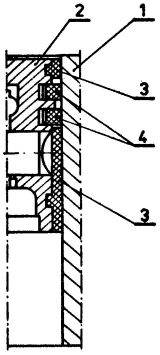

Fig. 2. Sliding mechanism of cylinder and piston in compressor 1 – cylinder, 2 – piston, 3 – oil ring rails, 4 – piston packing rings

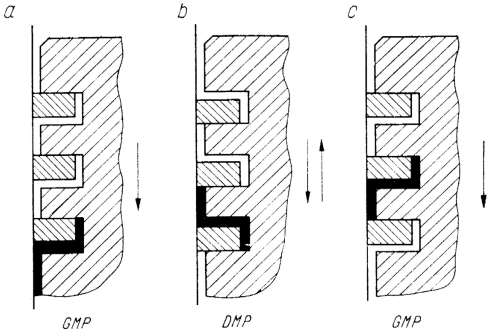

Fig. 3. Scheme blow up of operation of piston ring

The mechanism of movement of lubricant is shown in Fig. 3.

Because of a shortage of data about the amount of oil circulating in the cycle, it is exemplified contained in ISO deal with the amount of oil in the compressor. Inside the lubricated compressor, the refrigerant, unavoidably, picks up some mineral oil or synthetic lubricant. In addition, the refrigerant from the non-lubricated (dry) compressor may contain oil.

Lubricant, according to ISO 8573 (which pertain to compressed air and air in refrigeration cycle also exists) in compressed air can belong to one of the three following categories:

a) bulk liquid,
b) aerosol,
c) vapour [7].

The amount of oil (concentration) in air is presented in ISO 8573 [7].

Lubricant circulates in whole refrigeration cycle, which is presented in Fig. 4.

Table 1. Maximum oil content [7]

Class	Maximum concentration [mg/m³]
1	0,01
2	0,1
3	1
4	5
5	25

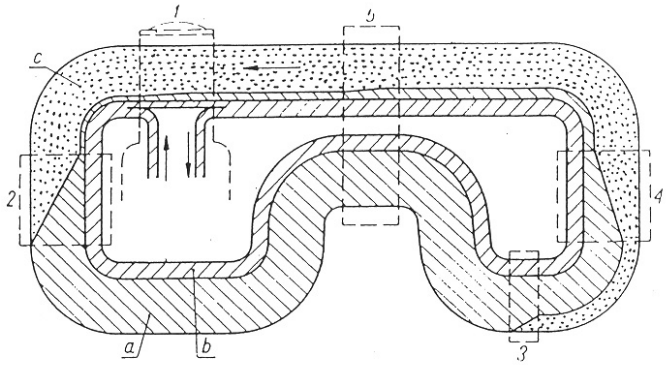

Fig. 4. Scheme of cycle of refrigerant and oil in refrigerant cycle (origin unknown)
a-liquid oil, b-vapor oil, c – refrigerant, 1 – compressor, 2 – condenser, 3 – throttling valve, 4 – evaporator, 5 – heat exchanger

ASHRAE research demonstrates a content of oil in refrigerant sampled from 10 randomly selected chillers. All samples contained excess oil (from 1% to 8 %). It caused a decline of energy efficiency depending on the increase of oil in cycle (from 2 % to 15 %).

Table 2. Efficiency lost according to percent oil content in evaporator [9]

Percent oil in evaporator	Efficiency loss
1–2 %	2 – 4 %
3 – 4 %	5.5 – 8 %
5 – 6 %	9.5 – 11 %
7 – 8 %	13.5 – 15 %

Although oil, moisture and air are existent in refrigeration systems, they do not provide for in the thermodynamic calculation. In this article, the first part of the thermodynamic calculation for a mixture consists of oil, moisture and air (oil and moist air). It could help to describe the mixture consisting of refrigerant with oil, moisture and air.

5. Other refrigerants in refrigerant – impurities (remains)

Remains of refrigerants sometimes can exist in working refrigerant. Chemical analysis of the refrigerant is required to determine that appropriate product specifications are met. The identification of contaminants, required chemical analysis (gas chromatography [11]), and acceptable contaminant level, will be published in ARI Standard 700 [1]. Maximum allowable levels of contaminants are shown in Tables 3.

Table 3. Characteristic of zeotropic blends and their maximum allowable levels of contaminants [1]

	Reporting Units	Reference Section	R-408A	R-409A	R-409B	R-410A	R-410B	R-411A	R-411B
CHARACTERISTICS[1]:									
Refrigerant Components	N/A	N/A	R-125/ 143a/22	R-22/ 124/142b	R-22/124/142b	R-32/125	R-32/125	R-1270/ 22/152a	R-1270/ 22/152a
Nominal Comp	% by weight	N/A	7/46/47	60/25/15	65/25/10	50/50	45/55	1.5/87.5/11.0	3/94/3
Allowable Comp	% by weight	N/A	5-9/45-47/ 45-49	58-62/23-27/14-16	63-67/23-27/ 9-11	48.5-50.5/ 49.5-51.5	44-46/54-56	0.5-1.5/87.5-89.5/10-11	2-3/94-96/ 2-3
Bubble Point[1]	°C @ 101.3 kPa °F @ 14.70 psia	N/A	-44.6 -48.2	-34.7 -30.4	-35.6 -32.1	-51.4 -60.6	-51.3 -60.4	-39.5 -39.1	-41.6 -42.8
Dew Point[1]	°C @ 101.3 kPa °F @ 14.70 psia	N/A	-44.1 -47.4	-26.4 -15.5	-27.9 -18.2	-51.4 -60.5	-51.6 -60.2	-36.6 -33.9	-40.0 -40.0
Critical Temperature[1]	°C °F	N/A	83.10 181.6	106.9 224.4	106.9 224.4	71.40 160.5	70.80 159.4	99.10 210.4	96.00 204.8
VAPOR PHASE CONTAMINANTS:									
Air and Other Non Condensables	% by volume @ 23.9°C	5.10	1.5	1.5	1.5	1.5	1.5	1.5	1.5
LIQUID PHASE CONTAMINANTS:									
Water	ppm by weight	5.4	10	10	10	10	10	10	10
All Other Volatile Impurities	% by weight	5.11	0.5	0.5	0.5	0.5	0.5	0.5	0.5
High Boiling Residue	% by volume	5.8	0.01	0.01	0.01	0.01	0.01	0.01	0.01
Particulates/Solids	Visually clean to pass	5.9	pass	pass	pass	pass	pass	pass	pass
Acidity	ppm by weight (as HCl)	5.7	1.0	1.0	1.0	1.0	1.0	1.0	1.0
Chloride[2]	No visible turbidity	5.6	pass	pass	pass	pass	pass	pass	pass

[1] Bubble points, dew points and critical temperatures, although not required, are provided for informational purposes.
[2] Recognized chloride level for pass/fail is about 3 ppm.
N/A Not Applicable
-- Data Not Available
Refrigerant data compiled from Refprop 7.0.

Volatile Impurities including other refrigerants

Although oil, moisture and air are existent in refrigeration systems, it does not provide for in the thermodynamic calculation. In this calculation, the first part of the thermodynamic calculation for a mixture consists of oil, moisture and air (oil and moist air). It could help to describe the mixture consists of refrigerant with oil, moisture and air [13].

6. The mathematics modelling of a mixture of moist air and lubricant in the vertical cylinder

In thermodynamics, humid air is considered a mixture of ideal gases. However, such an approach is not entirely appropriate, when taking into account an influence of higher pressures and temperatures in the compressor. The lubricating substances could be divided into natural (mineral oil), synthetic oil and half-synthetic oil.

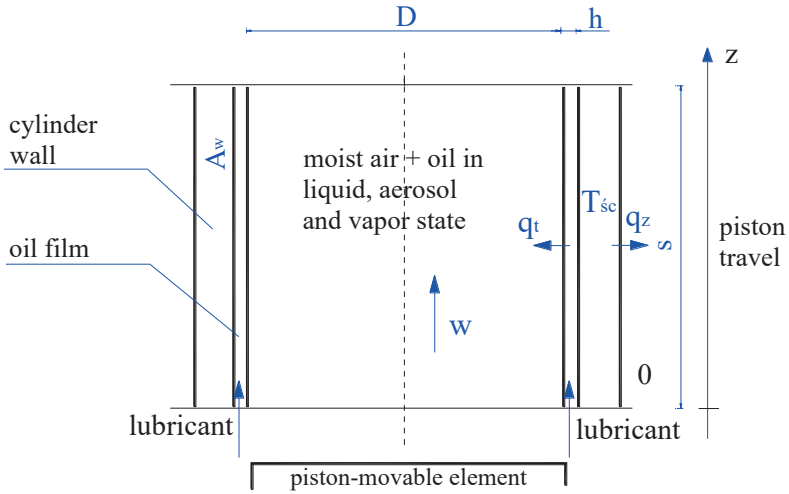

Fig. 5. Piston-cylinder arrangement with mixture inside cylinder

During lubrication of the cylinder's smooth surface, an oil-film is emerging on the cylinder's wall (further on, a partial dispersion of lubricating substance takes place in the working space of the compressor that results in appearance of aerosol). As a consequence of the piston's forward-backward movement and its friction against the cylinder's wall, the wall's temperature rises. If the temperature is high enough, the wall "dries out". The oil takes over the heat from the cylinder's wall (cooling function) and turns into vapour. In the compressors' cylinder, a structure of flux of the air and lubricating substance mixture in the form of liquid, steam and aerosol is emerging. The heat that is transferred during the exchange between the air and external environment is described as the external heat of transformation $\dot{q}_z$ (Fig. 5, 6). The value of this heat and its sign directly influence the pace of thermodynamic transformation taking place in the compressor. It is assumed in the paper that the process of compression is accompanied of exchange of the heat with the environment. Thus, in order to solve equation systems constituting a mathematical model of the compression process, what is needed is knowledge of the density of the stream of heat relating to the length of piston stroke.

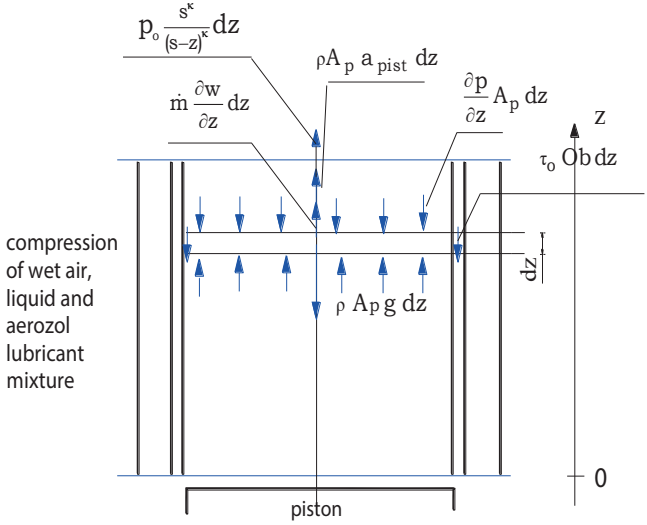

Fig. 6. Forces operative on elementary layer of fluid

Mass conservation low, momentum conservation, energy conservation law

In the analysed case of the compression air-lubricant mixture, we are dealing with the "haze" system. The phenomenological method has been adopted here to describe the model. This method assumes that it is justified to treat two-phase liquid as the two penetrating and interacting continuous units.

The two-phase as well as one-phase flux is governed by the mass, momentum conservation and energy conservation laws supplemented by constitutive equations (i.e. equations of state, strain, momentum transport and energy transport as well as chemical features of the liquid). The governing equations of the flow (continuity, momentum and energy) can be displayed either in the form of integral or in differential.

The mass conservation law adapted to the flowing mixture is given by equation:

$$A_p\left(\frac{\partial \rho}{\partial \tau}\right)+\frac{\partial \dot{m}}{\partial z}=0$$

Consider the force balance an elementary layer of mixture in the flow field is given by equation:

$$\frac{\partial \dot{m}}{\partial \tau}-A_p\frac{dp}{dz}=\tau_0 * Ob+A_p\rho\frac{wdw}{dz}-A_p\rho g+A_p a_{pist}+p_o\frac{s^\kappa}{(s-z)^\kappa}$$

The energy conservation law (I principal of thermodynamics):

$$\rho A_p \frac{\partial h}{\partial \tau} + \frac{d\left[\dot{m}\left(h + \frac{w^2}{2}\right)\right]}{dz} = \pi D_{in} \dot{q}_z - A_p \rho g w$$

Nomenclature

a_{pist} – acceleration of piston [m/s^2],
A_p – cross sectional area of cylinder [m^2],
D_{in} – inside diameter of cylinder [m],
ρ – gravitational acceleration [m/s^2],
h – specific enthalpy [J/kg],
$\dot{m}$ – mass flux[kg/s],
Ob – cross–sectional circumference of cylinder [m],
p, p_o, p_k, p_r – pressure, inlet pressure, outlet pressure, reduced pressure [Pa],
$\dot{q}_z$ – rate of heat flow [W/m^2],
s – piston stroke [m],
T, t – temperature [K], [°C],
v – molar volume of the mixture [m^3/kg],
w – velocity [m/s],
κ – polytropic exponent [–]
τ – time [s].

A method of the solution of an example

The presented mathematics model of the compression process takes the form of differential equations, depicting a change of the selected parameters along the cylinder's length in the form, which is directly useful for computer programs:

The initial values used for the mathematic model solution is: 1.initial air pressure equal to atmospheric pressure, 2. initial specific enthalpy value of the air in the compressors' entrance.

The presented system of differential equations can be solved by numeric integration methods. The Runge-Kutty fifth range method has been adopted in order to solve the above-mentioned differential equations [12].

7. Conclusions

initial calculations show differences in specific enthalpy between the specific enthalpy of dry air, wet air and a mixture of wet air and lubricant in liquid and aerosol state in the elevated pressure and temperature (Table 4).

Table 4. Specific enthalpy of mixture

T	Specific enthalpy of wet air*)	Specific enthalpy of lubricant*)	Specific enthalpy of mixture*)
[K]	[kJ/kg]	[kJ/kg]	[kJ/kg]
298	809,26	46,16	809,73
308	822,42	65,54	823,083
318	835,55	85,45	836,40
328	848,64	105,92	849,70
338	861,76	126,94	863,03
353	881,49	159,54	883,08

*) Example results of testing, when the pressure of compressed air is 0,2 MPa

References

[1] ARI Standard 700, *Standard for specifications for fluorocarbon refrigerant*, Air Conditioning and Refrigeration Institute, Arlington, Virginia 22203.

[2] Butrymowicz D., *Wpływ gazów inertnych oraz przegrzania pary na pracę skraplacza chłodniczego*, Technika Chłodnicza i Klimatyzacyjna 3/2003.

[3] Cooper K. W., Mount A. G., *Oil circulation – its effect on compressor capacity, theory and experiment*, Proceedings of the International Compressor Engineering Conference at Purdue 1972.

[4] Dutta A. K., Yanagisawa T., Fukuta M., *A study on compression characteristic of wet vapor refrigerant*, International Compressor Engineering Conference, 1996.

[5] Gurewicz I. L., *Własności i przeróbka pierwotna ropy naftowej i gazu*, WNT, Warszawa 1975.

[6] Hajduk T., Bonca Z., *Gazy nieskraplające się w urządzeniu chłodniczym*, Technika Chłodnicza i Klimatyzacyjna 3/2003.

[7] ISO 8573-1: Compressed air for general use, 1991.

[8] Key M., *How to eliminate the worst refrigerant contaminants*, contracting business 2006.

[9] Maczek K., Schnotale J., Skrzyniowska D., Sikorska-Bączek R., *Uzdatnianie powietrza w inżynierii środowiska dla celów wentylacji i klimatyzacji*, Politechnika Krakowska, podręcznik dla studentów wyższych szkół technicznych, drugie wydanie poprawione i uzupełnione, Kraków 2010.

[10] Matysko R., *Eksploatacja agregatów skraplających*, Chłodnictwo i Klimatyzacja 2011.

[11] Myłek A., et al., *Analiza rozwoju chromatograficznej metody oznaczania chlorofluorowodorów stosowanych w chłodnictwie*, Chłodnictwo 8/2009.

[12] Skrzyniowska D., *Model obliczeniowy mieszaniny powietrza i substancji smarnej wytłaczanej przez sprężarkę wyporową*, Politechnika Krakowska, praca doktorska, 2000.

[13] Skrzyniowska D., Zanieczyszczenia czynnika ziębniczego i ich jakościowa i ilościowa identyfikacja, Ciepłownictwo, Ogrzewnictwo, Wentylacja 12/47/2016, 517
[14] Tyczewski P., *Stanowisko do badania uszkodzeń sprężarek chłodniczych*, Problemy Eksploatacji 4-2011.

TECHNICAL TRANSACTIONS 8/2017
CZASOPISMO TECHNICZNE 8/2017
MATHEMATICS
DOI: 10.4467/2353737XCT.17.138.6889

Ludwik Byszewski (lbyszews@pk.edu.pl)
Institute of Mathematics, Faculty of Physics, Mathematics and Computer Science, Cracow University of Technology

Tadeusz Wacławski
Institute of Electrical Engineering and Computer Science, Faculty of Electrical and Computer Engineering, Cracow University of Technology

Uniqueness of solutions to inverse parabolic semilinear problems under nonlocal conditions with integrals

Jednoznaczność rozwiązań odwrotnych parabolicznych semiliniowych zagadnień z nielokalnymi warunkami z całkami

Abstract

The uniqueness of classical solutions to inverse parabolic semilinear problems together with nonlocal initial conditions with integrals, for the operator $\sum_{i,j=1}^{n}\frac{\partial}{\partial x_i}\left(a_{ij}(x,t)\frac{\partial}{\partial x_j}\right)+v(x,t)-\frac{\partial}{\partial t}$, $x=(x_1,...,x_n)$, in the cylindrical domain $D:=D_0\times(t_0,t_0+T)\subset\Re^{n+1}$, where $t_0\in\Re$, $0<T<\infty$ are studied. The result consists in the introduction of nonlocal conditions with integrals.

Keywords: inverse problems , parabolic problems, semilinear equation, nonlocal condition with integral, cylindrical domain, uniqueness of solutions

Streszczenie

W artykule studiowana jest jednoznaczność klasycznych rozwiązań odwrotnych parabolicznych semiliniowych zagadnień z nielokalnymi początkowymi warunkami z całkami dla operatora $\sum_{i,j=1}^{n}\frac{\partial}{\partial x_i}\left(a_{ij}(x,t)\frac{\partial}{\partial x_j}\right)+v(x,t)-\frac{\partial}{\partial t}$, $x=(x_1,...,x_n)$, w walcowym obszarze $D:=D_0\times(t_0,t_0+T)\subset\Re^{n+1}$, gdzie $t_0\in\Re$, $0<T<\infty$. Wynik polega na tym, że zostały wprowadzone warunki nielokalne z całkami.

Słowa kluczowe: zagadnienia odwrotne, zagadnienia paraboliczne, równanie semiliniowe, nielokalny warunek z całką, obszar walcowy, jednoznaczność rozwiązań

1. Introduction

In this paper, we prove two theorems on the uniqueness of classical solutions to inverse parabolic semilinear problems, for the equation:

$$\sum_{i,j=1}^{n}\frac{\partial}{\partial x_i}\left(a_{ij}(x,t)\frac{\partial u(x,t)}{\partial x_j}\right)+v(x,t)u(x,t)-\frac{\partial u(x,t)}{\partial t} \tag{1}$$

$$=f(x,t,u(x,t)),$$

$$(x,t)\in D:=D_0\times(t_0,t_0+T)\subset\Re^{n+1},$$

where $t_0\in\Re$, $0<T<\infty$. The coefficients $a_{ij}(i,j=1,\ldots,n)$ and the function f are given. By the solution of the inverse problem, for equation (1), we mean a pair of functions (u,v) satisfying equation (1) and suitable conditions. The nonlocal initial condition considered in the paper is of the form:

$$u(x,t_0)+\frac{h(x)}{T}\int_{t_0}^{t_0+T}u(x,\tau)d\tau=f_0(x),\quad x\in D_0,$$

where $|h(x)|\le 1$ for $x\in D_0$.

The obtained result is a continuation of the results given by Rabczuk in [6], by Beznohchenko and Prilenko in [1], by Chabrowski in [4], by Brandys in [2] and by the first author in [2] and [3].

2. Preliminaries

The notation, definitions and assumptions from this section are valid throughout this paper.

We will need the set $\Re_-:=(-\infty,0)$.

Let t_0 be a real finite number, $0<T<\infty$ and $x=(x_1,\ldots,x_n)\in\Re^n$.

Define the domain (see [2] or [3])

$$D:=D_0\times(t_0,t_0+T),$$

where D_0 is an open and bounded domain in $\Re^n$ such that the boundary ∂D_0 satisfies the following conditions:

If $n\ge 2$ then ∂D_0 is a union of a finite number of surface patches of class C^1, which have no common interior points but have common boundary points.

If $n \geq 3$ then all the edges of ∂D_0 are sums of a finite numbers of $(n-2)$ – dimensional surface patches of class C^1.

Assumption (A_1).

a_{ij}, $\frac{\partial a_{ij}}{\partial x_s} \in C(\overline{D},\Re)$ $(i,j,s=1,...,n)$, where $a_{ij}=a_{ij}(x,t)$ for $(x,t)\in\overline{D}$ $(i,j=1,...,n)$; $a_{ji}(x,t)=a_{ij}(x,t)$ for $(x,t)\in D$ $(i,j=1,...,n)$ and $\sum_{i,j=1}^{n} a_{ij}(x,t)\lambda_i\lambda_j \geq 0$ for arbitrary $(x,t)\in D$ and $(\lambda_1,...,\lambda_n)\in\Re^n$.

Assumption (A_2).

(i) $f: \overline{D}\in\Re\ni(x,t,z)\to f(x,t,z)\in\Re$, $f\in C(\overline{D}\times\Re,\Re)$, $f(x,t,0)\neq 0$ for $(x,t)\in D$,

$\frac{\partial f}{\partial z} \in C(\overline{D}\times\Re,\Re)$ and $\frac{\partial f(x,t,z)}{\partial z} > 0$ for $(x,t)\in\overline{D}$, $z \in \Re$;

(ii) $f_1:\partial D_0 \times [0,T]\to\Re$;

(ii') $k\in C(\partial D_0 \times [0,T],\Re)$ and $k(x,t)\leq 0$ for $(x,t)\in\partial D_0 \times [0,T]$;

(iii) $f_0:D_0\to\Re$.

Assumption (A_2). $h\in C(\overline{D}_0,\Re)$ and $|h(x)|\leq 1$ for $x\in D_0$.

Let $C^{2,1}(\overline{D},\Re)$ be the space of all $w\in(\overline{D},\Re)$ such that $\frac{\partial w}{\partial x_i}$, $\frac{\partial^2 w}{\partial x_i \partial x_j} \in C(\overline{D},\Re)$ for $i,j=1,...,n$ and $\frac{\partial w}{\partial t} \in C(\overline{D},\Re)$.

The symbol L is reserved for the operator given by the formula:

$$(Lw)(x,t) := \sum_{i,j=1}^{n} \frac{\partial}{\partial x_i}\left(a_{ij}(x,t)\frac{\partial w(x,t)}{\partial x_j}\right) \tag{2}$$

for $w\in C^{2,1}(\overline{D},\Re)$, $(x,t)\in\overline{D}$.

By n_x, where $x\in\partial D_0$, we denote the interior normal to ∂D_0 at x. Shortly, we denote, also, n_x by n.

Let $u\in C^{2,1}(\overline{D},\Re)$, $x_0\in\partial D_0$ and $t\in[t_0, t_0+T]$. The expression:

$$\frac{du(x,t)}{d\upsilon(x_0,t)} := \sum_{i=1}^{n} \frac{\partial u(x_0,t)}{\partial x_i} \sum_{j=1}^{n} a_{ij}(x_0,t)\cos(n_{x_0},x_j) \tag{3}$$

is called the transversal derivative of the function u at the point (x_0,t). Shortly, we denote, also

$\frac{du(x,t)}{d\upsilon(x_0,t)}$ by $\frac{d}{d\upsilon}u(x_0,t)$ or by $\frac{du}{d\upsilon_{x_0}}$.

For the given functions $a_{ij}(i, j=1, ..., n)$ satisfying Assumption (A_1) and for the given functions f, f_1, f_0 and h satisfying Assumptions (A_2) (i) – (iii) and (A_3), the first Fourier's inverse semilinear problem in D together with a nonlocal initial condition with integral consists in finding a pair of functions $u\in C^{2,1}(\overline{D},\Re)$, $v\in C(\overline{D},\Re\_)$ satisfying the equation

$$(Lu)(x,t)+v(x,t)u(x,t)-\frac{\partial u(x,t)}{\partial t}=f(x,t,u(x,t)) \quad \text{for} \quad (x,t)\in D, \tag{4}$$

the nonlocal initial condition:

$$u(x,t_0)+\frac{h(x)}{T}\int_{t_0}^{t_0+T}u(x,\tau)d\tau=f_0(x) \quad \text{for} \quad x\in\bar{D}_0, \tag{5}$$

the boundary condition:

$$u(x,t)=f_1(x,t) \quad \text{for} \quad x\in\partial D_0\times[t_0,\, t_0+T] \tag{6}$$

and the condition:

$$\int_{t_0}^{t_0+T}\left[\int_{D_0}v(x,t)u^2(x,t)dx\right]dt=C, \tag{7}$$

where C is a negative constant independent of u and v.

A pair (u,v) of functions possessing the above properties is called a solution of the first Fourier's inverse semilinear problem (4)–(7) in D.

Remark 2.1. The assumption that $f(x,t,0)\neq 0$ for $(x,t)\in D$ (see Assumption $(A_2)(i)$) implies that $u = 0$ cannot satisfy equation (4). Consequently, the above assumption implies that only $u \neq 0$ is considered in the paper.

If condition (6) from the first Fourier's inverse semilinear nonlocal problem (4)–(7) is replaced by the condition

$$\frac{d}{d\upsilon_x}u(x,t)+k(x,t)u(x,t)=f_1(x,t) \quad \text{for} \quad (x,t)\in\partial D_0\times[t_0,t_0+T], \tag{8}$$

where k is the given function satisfying Assumption $(A_2)(ii')$ then problem (4), (5), (8) and (7) is said to be the mixed inverse semilinear problem in D together with a nonlocal initial condition with integral. A pair of functions $u\in C^{2,1}(\overline{D},\Re)$, $v\in(\overline{D},\Re\_)$ satisfying equation (4) and conditions (5), (8), (7) is called a solution of the mixed inverse semilinear problem (4), (5), (8) and (7) in D.

Assumption (A_4). For every two solutions (u_1,v_1) and (u_2,v_2) of problem (4) – (7) or of problem (4), (5), (8) and (7) the following formulas hold:

$$\int_{t_0}^{t_0+T}\left[\int_{D_0}v_i(x,t)u_j^2(x,t)dx\right]dt=C \quad (i,j=1,2;i\neq j).$$

Remark 2.2. The reason for which Assumption (A_4) is introduced is that the considered problems are inverse.

Assumption (A_5). For each two solutions (u_1,v_1) and (u_2,v_2) of problem (4)–(7) or of problem (4), (5), (8) and (7) the following inequality:

$$\left[\frac{1}{T}\int_{t_0}^{t_0+T}\left(u_1(x,\tau)-u_2(x,\tau)\right)d\tau\right]^2 \le\left[u_1(x,t_0+T)-u_2(x,t_0+T)\right]^2 \quad \text{for} \quad x\in D_0$$

is satisfied.

Remark. 2.3. The reason for which Assumption (A_5) is introduced is that the considered problems are nonlocal.

3. Theorems about uniqueness

In this section, we shall prove two theorems about the uniqueness of solutions of inverse parabolic semilinear problems together with nonlocal initial conditions.

Theorem 3.1. *Suppose that coefficients $a_{ij}(i, j=1, ..., n)$ of the differential equation satisfy Assumption (A_1) and the functions f, f_1, f_0 and h satisfy Assumptions (A_2) (i) – (iii) and (A_3). Then, the first Fourier's inverse semilinear problem (4) – (7) admits at most one solution in D in the class of the solutions satisfying Assumptions (A_4) and (A_5).*

Proof. Suppose that (u_1,v_1) and (u_2,v_2) are two solutions of problem (4) – (7) in D and let

$$w:= u_1 - u_1 \text{ in } \overline{D}. \tag{9}$$

Then, the following formulas hold:

$$(Lw)(x,t)+v_1(x,t)u_1(x,t)-v_2(x,t)u_2(x,t)-\frac{\partial w(x,t)}{\partial t} \tag{10}$$

$$=f(x,t,u_1(x,t))-f(x,t,u_2(x,t)) \quad \text{for} \quad (x,t)\in\overline{D},$$

$$w(x,t_0)+\frac{h(x)}{T}\int_{t_0}^{t_0+T} w(x,\tau)d\tau=0 \quad \text{for} \quad x\in\overline{D}_0, \tag{11}$$

$$w(x,t)=0 \quad \text{for} \quad (x,t)\in\partial D_0\times[t_0,t_0+T], \tag{12}$$

$$\int_{t_0}^{t_0+T}\left[\int_{D_0} v_i(x,t)u_i^2(x,t)dx\right]dt=C \qquad (i=1,2). \tag{13}$$

From the assumption that $u_1, u_2 \in C^{2,1}(\overline{D}, \Re)$ from the second and fourth part of Assumption $(A_2)(i)$ and from the mean value theorem, there exists $\theta \in (0,1)$ such that:

$$f(x,t,u_1(x,t)) - f(x,t,u_2(x,t)) \tag{14}$$
$$= w(x,t)\frac{\partial f(x,t,u_2(x,t)+\theta w(x,t))}{\partial z} \quad \text{for} \quad (x,t) \in \overline{D}.$$

By (14), (10), by Assumption (A_1), by (2) and by [5] (Section 17.11),

$$\int_{t_0}^{t_0+T}\left[\int_{D_0} w^2 \frac{\partial f(x,t,u_2+\theta w)}{\partial z}dx\right]dt \tag{15}$$
$$= -\int_{t_0}^{t_0+T}\left[\int_{\partial D_0} w\sum_{i=1}^{n}\cos(n,x_i)\sum_{j=1}^{n}a_{ij}\frac{\partial w}{\partial x_j}d\sigma_x\right]dt$$
$$-\int_{t_0}^{t_0+T}\left[\int_{D_0} a_{ij}\frac{\partial w}{\partial x_i}\frac{\partial w}{\partial x_j}dx\right]dt$$
$$-\int_{t_0}^{t_0+T}\left[\int_{D_0}\frac{\partial w}{\partial x_i}w dx\right]dt + \int_{t_0}^{t_0+T}\left[\int_{D_0} v_1 u_1^2 dx\right]dt$$
$$+\int_{t_0}^{t_0+T}\left[\int_{D_0} v_2 u_2^2 dx\right]dt$$
$$-\int_{t_0}^{t_0+T}\left[\int_{D_0} v_1 u_1 u_2 dx\right]dt$$
$$-\int_{t_0}^{t_0+T}\left[\int_{D_0} v_2 u_1 u_2 dx\right]dt,$$

where $d\sigma_x$ is a surface element in $\Re^n$.

From (15), (12), from the last part of Assumption (A_1) and from the inequalities

$$-\int_{t_0}^{t_0+T}\left[\int_{D_0} v_i u_1 u_2 dx\right]dt \le -\frac{1}{2}\int_{t_0}^{t_0+T}\left[\int_{D_0} v_i(u_1^2+u_2^2)dx\right]dt \quad (i=1,2) \tag{16}$$

we have

$$\int_{t_0}^{t_0+T}\left[\int_{D_0} w^2 \frac{\partial f(x,t,u_2+\theta w)}{\partial z}dx\right]dt \le -\int_{t_0}^{t_0+T}\left[\int_{D_0}\frac{\partial w}{\partial t}w dx\right]dt \tag{17}$$

$$+\int_{t_0}^{t_0+T}\left[\int_{D_0} v_1 u_1^2 dx\right]dt+\int_{t_0}^{t_0+T}\left[\int_{D_0} v_2 u_2^2 dx\right]dt$$

$$-\frac{1}{2}\int_{t_0}^{t_0+T}\left[\int_{D_0} v_1(u_1^2+u_2^2)dx\right]dt$$

$$-\frac{1}{2}\int_{t_0}^{t_0+T}\left[\int_{D_0} v_2(u_1^2+u_2^2)dx\right]dt.$$

Using integration by parts, we obtain:

$$\int_{t_0}^{t_0+T}\left[\int_{D_0}\frac{\partial w}{\partial t}w dx\right]dt=\frac{1}{2}\int_{D_0} w^2(x,t_0+T)dx-\frac{1}{2}\int_{D_0} w^2(x,t_0)dx. \tag{18}$$

Formulas (17), (18) and (11) imply the inequality:

$$\int_{t_0}^{t_0+T}\left[\int_{D_0} w^2\frac{\partial f(x,t,u_2+\theta w)}{\partial z}dx\right]dt \tag{19}$$

$$\le-\frac{1}{2}\int_{D_0} w^2(x,t_0+T)dx+\frac{1}{2}\int_{D_0} h^2(x)\left[\frac{1}{T}\int_{t_0}^{t_0+T} w(x,\tau)d\tau\right]^2 dx$$

$$+\frac{1}{2}\int_{t_0}^{t_0+T}\left[\int_{D_0} v_1 u_1^2 dx\right]dt-\frac{1}{2}\int_{t_0}^{t_0+T}\left[\int_{D_0} v_1 u_2^2 dx\right]dt$$

$$+\frac{1}{2}\int_{t_0}^{t_0+T}\left[\int_{D_0} v_2 u_2^2 dx\right]dt-\frac{1}{2}\int_{t_0}^{t_0+T}\left[\int_{D_0} v_2 u_1^2 dx\right]dt.$$

From (19) and (13), and Assumptions (A_4) and (A_5),we have:

$$\int_{t_0}^{t_0+T}\left[\int_{D_0} w^2\frac{\partial f(x,t,u_2+\theta w)}{\partial z}dx\right]dt \tag{20}$$

$$\le-\frac{1}{2}\int_{D_0} w^2(x,t_0+T)[1-h^2(x)]dx.$$

By (20) and by Assumption (A_3) we obtain:

$$\int_{t_0}^{t_0+T}\left[\int_{D_0} w^2\,\frac{\partial f(x,t,u_2+\theta w)}{\partial z}\,dx\right]dt\le 0.$$

From the above inequality and from the last part of Assumption $(A_2)(i)$:

$$w^2\le 0 \quad \text{in} \quad D$$

and therefore:

$$w=0 \quad \text{in} \quad D.$$

The above formula implies that:

$$u_1=u_2 \quad \text{in} \quad D.$$

Consequently, by (10):

$$(v_1-v_2)\,u_1=0 \quad \text{in} \quad D.$$

Therefore, from Remark 2.1, we have that:

$$v_1=v_2 \quad \text{in} \quad D.$$

The proof of Theorem 3.1 is thereby complete.

Theorem 3.2. *Suppose that the assumptions of Theorem 3.1, concerning to the coefficients* $a_{ij}(i, j=1, ..., n)$ *and the functions* f, f_1, f_0 *and* h *are satisfied and that the function* k satisfies *Assumption* $(A_2)(ii')$. *Then, the mixed inverse semilinear problem (4), (5), (8) and (7) admits at most one solution in* D *in the class of the solutions satisfying Assumptions* (A_4) and (A_5).

Proof. Suppose that (u_1,v_1) and $(u_2,v_2)$are two solutions of problem (4), (5) , (8) and (7) in D and let

$$\mathrm{w}:=v_1-v_1 \text{ in } \overline{D}. \tag{21}$$

Then, the following formulas hold:

$$(Lw)(x,t)+v_1(x,t)u_1(x,t)-v_2(x,t)u_2(x,t)-\frac{\partial w(x,t)}{\partial t} \tag{22}$$

$$=f(x,t,u_1(x,t))-f(x,t,u_2(x,t)) \quad \text{for} \quad (x,t)\in\overline{D},$$

$$w(x,t_0)+\frac{h(x)}{T}\int_{t_0}^{t_0+T} w(x,\tau)d\tau=0 \quad \text{for} \quad x\in\overline{D}_0, \tag{23}$$

$$\frac{d}{d\upsilon_x}w(x,t)+k(x,t)w(x,t)=0 \quad \text{for} \quad (x,t)\in\partial D_0\times[t_0,t_0+T], \tag{24}$$

$$\int_{t_0}^{t_0+T}\left[\int_{D_0} v_i(x,t)u_i^2(x,t)dx\right]dt = C \qquad (i=1,2). \tag{25}$$

Applying a similar argument as in the proof of Theorem 3.1 and using the definition of $\frac{\partial u}{\partial \upsilon_x}$ (see (3)), we have:

$$\int_{t_0}^{t_0+T}\left[\int_{D_0} w^2 \frac{\partial f(x,t,u_2+\theta w)}{\partial z}dx\right]dt \tag{26}$$

$$= -\int_{t_0}^{t_0+T}\left[\int_{\partial D_0} w\frac{d}{\partial \upsilon_x} w d\sigma_x\right]dt$$

$$-\int_{t_0}^{t_0+T}\left[\int_{D_0}\sum_{i,j=1}^{n} a_{ij}\frac{\partial w}{\partial x_i}\frac{\partial w}{\partial x_j}dx\right]dt$$

$$-\int_{t_0}^{t_0+T}\left[\int_{D_0}\frac{\partial w}{\partial x_i}w dx\right]dt$$

$$+\int_{t_0}^{t_0+T}\left[\int_{D_0} v_1 u_1^2 dx\right]dt + \int_{t_0}^{t_0+T}\left[\int_{D_0} v_2 u_2^2 dx\right]dt$$

$$-\int_{t_0}^{t_0+T}\left[\int_{D_0} v_1 u_1 u_2 dx\right]dt$$

$$-\int_{t_0}^{t_0+T}\left[\int_{D_0} v_2 u_1 u_2 dx\right]dt.$$

From (26), (24), and as in the proof of Theorem 3.1, we obtain:

$$\int_{t_0}^{t_0+T}\left[\int_{D_0} w^2 \frac{\partial f(x,t,u_2+\theta w)}{\partial z}dx\right]dt \tag{27}$$

$$\le \int_{t_0}^{t_0+T}\left[\int_{\partial D_0} k w^2 d\sigma_x\right]dt - \frac{1}{2}\int_{D_0} w^2(x,t_0+T)[1-h^2(x)]dx$$

$$+\frac{1}{2}\int_{t_0}^{t_0+T}\left[\int_{D_0} v_1 u_1^2\,dx\right]dt-\frac{1}{2}\int_{t_0}^{t_0+T}\left[\int_{D_0} v_1 u_2^2\,dx\right]dt$$

$$+\frac{1}{2}\int_{t_0}^{t_0+T}\left[\int_{D_0} v_2 u_2^2\,dx\right]dt-\frac{1}{2}\int_{t_0}^{t_0+T}\left[\int_{D_0} v_2 u_1^2\,dx\right]dt.$$

By (27), by Assumption $(A_2)(ii')$ and (A_3), and by (25) and Assumption (A_4), we obtain the inequality:

$$\int_{t_0}^{t_0+T}\left[\int_{D_0} w^2\,\frac{\partial f(x,t,u_2+\theta w)}{\partial z}\,dx\right]dt\le 0.$$

From the above inequality and from the last part of Assumption $(A_2)(i)$,

$$w^2\le 0 \quad \text{in} \quad D$$

and, therefore, the same argument as in the proof of Theorem 3.1 implies that the proof of Theorem 3.2 is complete.

4. Physical interpretation of the nonlocal condition (5)

Theorems 3.1 and 3.2 can be applied to description of physical problems in the heat conduction theory, for which we cannot measure the temperature at the initial instant, but we can measure the temperature in the form of the nonlocal condition (5).

Also, observe that the nonlocal condition (5) considered in Theorem 3.1 and 3.2 is more general than the classical initial condition and the integral periodic condition and the integral antiperiodic condition. Namely, if the function h from condition (5) satisfies the relation:

$$h(x)=0 \quad \text{for} \quad x\in\overline{D}_0$$

then condition (5) is reduced to the initial condition:

$$u(x,t_0)=f_0(x) \quad \text{for} \quad x\in\overline{D}_0.$$

Instead, if the function h and f in (5) satisfy the conditions:

$$h(x)=-1\ [h(x)=1] \quad \text{for} \quad x\in\overline{D}_0,$$

$$f_0(x)=0 \quad \text{for} \quad x\in\overline{D}_0$$

then condition (5) is reduced, respectively, to the integral periodic [antiperiodic] initial condition:

$$u(x,t_0)=\frac{1}{T}\int_{t_0}^{t_0+T} u(x,\tau)d\tau \quad [\, u(x,t_0)=-\frac{1}{T}\int_{t_0}^{t_0+T} u(x,\tau)d\tau \,] \text{ for } x\in\bar{D}_0$$

References

[1] Beznoshchenko N. J., Prilenko A. I., *Inverse problems for parabolic equation,* Problems of Mathematical Physics and Computational Mathematics, Nauka, Moscow 1977, 51–63 (in Russian).

[2] Brandys J., Byszewski L,. *Uniqueness of solutions to inverse parabolic problems,* Comment. Math. Prace Matem. 42.1, 2002, 17–30.

[3] Byszewski L., *Uniqueness of solutions of parabolic semilinear nonlocal-boundary problems,* J. Math. Anal. Appl. 165.2, 1992, 472–478.

[4] Chabrowski J., *On nonlocal problems for parabolic equations,* Nagoya Math. J. 93, 1984, 109–131.

[5] Krzyżański M., *Partial Differential Equations of Second Order,* Vol. 1, PWN (Polish Scientific Publishers), Warsaw 1971.

[6] Rabczuk R., *Elements of Differential Inequalities,* PWN (Polish Scientific Publishers), Warsaw 1976 (in Polish).

TECHNICAL TRANSACTIONS 8/2017
CZASOPISMO TECHNICZNE 8/2017
MECHANICS
DOI: 10.4467/2353737XCT.17.139.6890

Monika Czernilewska
Andrzej Ryniewicz(andrzej@ryniewicz.pl)
Laboratory of Coordinate Metrology, Faculty of Mechanical Engineering, Cracow University of Technology

Application of cone beam computed tomography for detection of periapical lesions – clinical case

Zastosowanie tomografii wiązki stożkowej do detekcji zmian okołowierzchołkowych – przypadek kliniczny

Abstract

The purpose of the thesis is to show the dental imaging capability of Cone Beam Computed Tomography (CBCT) in comparison with intraoral X-ray images for detection and assessment of periapical lesions before and during treatment as well as to present the use of diagnostic functions in the available software. The thesis presents two clinical cases.

Keywords: CBCT, volumetric tomography, periapical lesions, dental imaging

Streszczenie

Celem artykułu jest pokazanie możliwości obrazowania stomatologicznego za pomocą tomografii wiązki stożkowej w porównaniu ze zdjęciami RTG wewnątrzustnymi do detekcji oraz oceny rozległości zmian okołowierzchołkowych przed i w trakcie leczenia. Omówiono dwa przypadki kliniczne.

Słowa kluczowe: tomografia wiązki stożkowej, tomografia wolumetryczna, zmiany okołowierzchołkowe, obrazowanie stomatologiczne

1. Introduction

In dentistry, a precise analysis of dental imaging is very important to make a diagnosis and determine a treatment plan. The imaging possibilities offered by volumetric tomography CBCT in most pathological cases are invaluable compared to traditional X-ray images. CBCT is used in the diagnosis, treatment planning, as well as its monitoring and evaluation of treatment results in such diverse fields of dentistry as implantology, surgery, orthodontics and more often, even in difficult endodontic cases [1–5]. But, of course, quality is connected with higher costs, for example, of purchase of CBCT equipment and its use. The cost of X-ray image is cheaper in comparison with the performance of imaging using Cone Beam Computed Tomography, but in many cases insufficient to detect changes even by an experienced dentist.

2. Cone beam computed tomography

2.1. The principles

CBCT – *cone beam computed tomography* is a compact, faster and safer version of the regular CT. Through the use of a cone shaped X-Ray beam, the size of the scanner, radiation dosage and time needed for scanning are all dramatically reduced. Most CBCT scanners are square like machines with a chair. You will sit upright while a C-arm rotates around your head. Within the arm there is an X-ray source and detector (X-ray receiver), which will make one complete 360° rotation for each scan. While the arm is rotating, it captures multiple images of your head from different angles. These images are then reconstructed to create a 3D image of

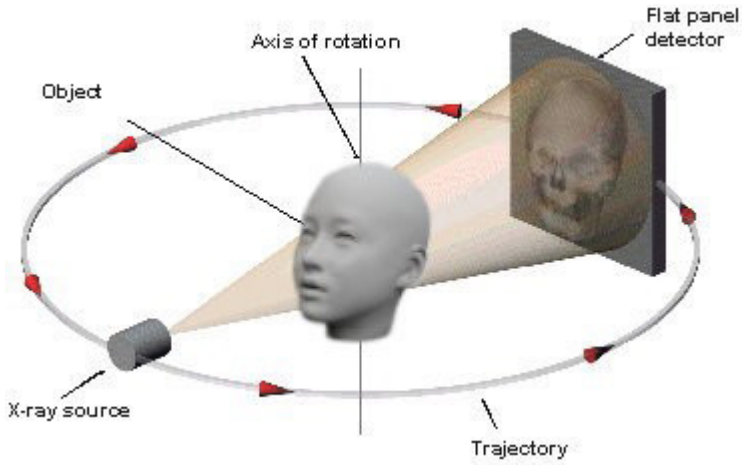

Fig. 1. Principle of CBCT working [7]

your internal anatomy. Some CBCT scanners have you lay down on a table that can move up or down, and slide into and out of the center of a hole, while a gantry makes a 360° rotation. CT imaging of the head can provide clear images not only of soft tissue, but also of bones and blood vessels [6]. To see how CBCT works, go to Fig. 1.

2.2. Application in dental imaging

There is a justified and wide application of volumetric tomography in the diagnostic imaging of teeth diseases of different etiology. Dental imaging focuses on the analysis of the alveolar bone and the surrounding tissues, volumetric tomography in contrast to 2D dental X-ray imaging allows us to view three-dimensional anatomical structures in real size without overlapping and also, in various projections which you can operate on your own [1]. This is the basis for assessing the extent of periapical lesions, which are dependent on both the location of the tooth in dental arches as well as the plain, and the angle at which the sections are analyzed. For example, periapical lesions are usually barely visible in the X-ray image, whereas CBCT imaging gives us a much better image quality, inter alia, thanks to no layers overlapping 3d anatomical structures. Unfortunately, accurate diagnosis of inflammatory changes around the apex of the tooth root is not an easy task. Some cases are complex and often confusing, even for an experienced dentist [8]. In one of the publications [2] it was proved that CBCT examination allows for earlier detection of periapical lesions than intraoral images, up to 38% of periapical lesions and 56% of fistulas detected on 3D imaging was not visible in the intraoral image. The drawback of volumetric tomography can be higher radiation dose than in conventional X-ray, but still it is less than e.g. in a spiral computed tomography. It should be noted that in many cases it is necessary to perform more than one X-ray image and sometimes even that is not enough for proper radiological assessment. Then, the total dose of radiation from the resulting dose of X-ray images exceeds the volumetric imaging dose of radiation from one shot. But on the other hand, the advantage of volumetric tomography is possibility to set the FOV - *field of view* so that the resolution is sufficiently high with radiation dosage which is as low as one can possibly achieve [5]. Depending on treatment plans that relate to maxillo-facial surgery, implantology and endodontics, we choose the most suitable FOV [9]. Comparing CBCT with a regular CT, patients receive a lower effective dose of radiation than that of CT scanners, by adjusting field of view, time scanning and the voxel size. In both cases, the image of hard structures – bones – is very good, but teeth are perfect in CBCT, while in CT just moderate.

3. Periapical lesion – clinical case

The research was conducted in dental clinic "NZOZ SPS Dentist" in Cracow using CBCT scanner Gendex, model GXCB-500 and GXDP-700, and intraoral X-ray system Gendex - Oralix 65S. The patients were tested through dental X-ray and CBCT, in an initial test when symptoms of the inflammation of the periapical tissue were noticed and a repeat test carried out a while after treatment.

The surface area of the periapical lesion was selected 10 times in an intraoral X-ray image, the values were averaged and standard deviation was calculated. In 3D imaging the projection was set as close as possible to view on the tooth in an intraoral X-ray image and the surface area of the periapical lesion was also selected 10 times, the values were averaged and standard deviation was calculated. The mean values of surface area of the periapical lesion visible in the intraoral X-ray image and volumetric imaging were compared.

The software used for analysis of intraoral images was Fiji Is Just ImageJ 1.48a and for 3D scans – Onis 2.4 Free Edition. Function, which allows for the selection of irregularly shaped surface area was crucial in choosing suitable software.

3.1. Case 1

A 35 year old male during the first examination. Tooth 46. The second complex examinations were done after the treatment – 2 and a half year later. Periapical lesion did not heal after 2,5 years.

Figure 2 and Table 1 show periapical lesions measurements on an intraoral X-ray image before the treatment and Figure 3 and Table 2 on 3D imaging.

Fig. 2. Intraoral X-ray image of tooth 46 – before the treatment with marked periapical lesions (case 1)

Table 1. Results of the measurement of the surface area of the periapical lesions in intraoral X-ray image of tooth 46 – before the treatment (case 1)

MEASUREMENT	SURFACE AREA OF PERIAPICAL LESION [mm^2]	
1	3,4	5,3
2	3,8	5,1
3	4,1	5,1
4	4,3	5,5
5	3,3	5,3
6	3,5	5,2
7	4,2	5,0
8	3,6	5,2
9	3,8	5,4

10	3,5	5,0
Average value:	3,8	5,2
Standard deviation:	0,35	0,17
Sum of 2 average values:	9,0	

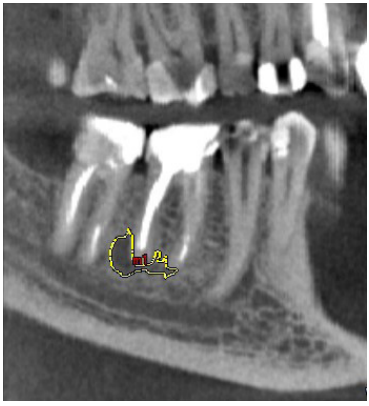

Fig. 3. View from CBCT on tooth 46 before healing period (case 1)

Table 2. Results of the measurement of the surface area of the periapical lesions in CBCT imaging of tooth 46 – before the period of healing (case 1)

MEASUREMENT	SURFACE AREA OF PERIAPICAL LESION [mm^2]
1	21,4
2	21,0
3	22,8
4	21,2
5	20,5
6	20,5
7	20,9
8	22,4
9	21,7
10	21,6
Average value:	21,4
Standard deviation: 0,76	

Comparing the average value of the surface area of the visible periapical lesions in the intraoral X-ray image with the 3D scan, this inflammation is visibile over 2 times better in 3D imaging in the first stage of treatment.

Figure 4 below and Table 3 show measurements in 2D images after 2,5 years of treatment and in CBCT, see Figure 5 and Table 4.

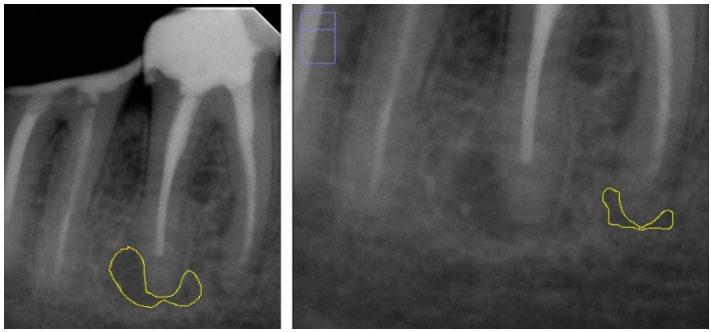

Fig. 4. Intraoral X-ray image of tooth 46 – during the treatment with marked periapical lesions (case 1)

Table 3. Results of the measurement of the surface area of the periapical lesions in intraoral X-ray image of tooth 46 – during treatment (case 1)

MEASUREMENT	SURFACE AREA OF PERIAPICAL LESION [mm^2]	
1	12,1	2,0
2	11,3	1,7
3	10,5	2,0
4	10,7	2,0
5	11,8	2,1
6	12,3	2,2
7	12,3	2,5
8	11,4	2,0
9	11,5	2,4
10	11,2	2,4
Average value:	11,5	2,1
Standard deviation: 0,62 0,25		
Sum of 2 average values:	13,6	

Fig. 5. View from CBCT on tooth 46 during treatment (case 1)

Table 4. Results of the measurement of the surface area of the periapical lesions in CBCT imaging of tooth 46 – during treatment (case 1)

MEASUREMENT	SURFACE AREA OF PERIAPICAL LESION [mm²]
1	20,5
2	22,0
3	21,1
4	20,5
5	22,6
6	19,9
7	20,2
8	22,6
9	20,7
10	20,5
Average value:	21,1
Standard deviation: 0,99	

Comparing the average value of the surface area of the visible periapical lesions in the intraoral X-ray image with the 3D scan, this inflammation is still visibile over 2 times better in 3D imaging after 2 and half year of treatment.

3.2. Case 2

A 50 year old male during the first examination. Tooth 11. The extraction of the tooth was done after more than a month of re-treatment, and after the next 8 months the patient got an implant. Figure 6 and Table 5 show periapical lesions measurements in an intraoral X-ray image before the treatment and Figure 7 and Table 6 in 3D imaging.

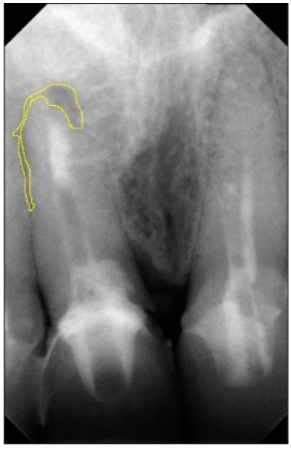

Fig. 6. Intraoral X-ray image of tooth 11 - before the treatment with marked periapical lesions (case 2)

Table 5. Results of the measurement of the surface area of the periapical lesions in intraoral X-ray image of tooth 11 – before the treatment (case 2)

MEASUREMENT	SURFACE AREA OF PERIAPICAL LESION [mm²]
1	7,2
2	7,7
3	7,0
4	7,1
5	7,6
6	7,9
7	7,8
8	8,0
9	7,6
10	7,5
Average value:	7,5
Standard deviation: 0,34	

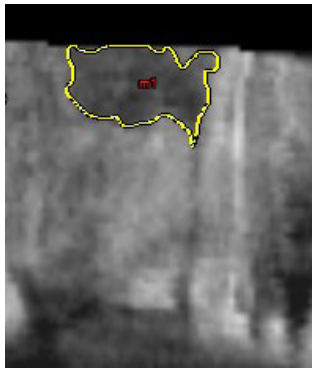

Fig. 7. CBCT image of tooth 11 – before the treatment with marked periapical lesions (case 2)

Table 6. Results of the measurement of the surface area of the periapical lesions in CBCT image of tooth 11 – before the treatment (case 2)

MEASUREMENT	SURFACE AREA OF PERIAPICAL LESION [mm²]
1	33,1
2	34,8
3	32,7
4	32,1
5	33,3
6	32,2
7	33,9
8	32,6

9	33,7
10	37,5
Average value:	33,6
Standard deviation: 1,60	

The surface area of periapical lesions visible in 3D imaging is more than 4 times bigger than in the 2D intraoral image. In volumetric imaging, due to the fact that there is no overlapping of anatomical structures and due to the ability to view the image from different angles, periapical lesion is very clearly visible.

4. Conclusion

Application of Cone Beam Computed Tomography in dental imaging is very useful in detection and assessment of periapical lesions. Volumetric tomography in contrast to X-ray allows us to view three-dimensional anatomical structures in real size without overlapping. This is the basis for assessing the extent of periapical lesions. Volumetric tomography is an excellent technique for dental use in endodontics and implantology.

References

[1] Bagińska J., Piszczatowski S., *Możliwości zastosowania różnych metod rentgenowskiej tomografii komputerowej w endodoncji – przegląd piśmiennictwa*, Czasopismo Stomatologiczne, 63,1, 2010, 41–50.

[2] Różyło-Kalinowska I., Różyło T.K., *Tomografia wolumetryczna w praktyce stomatologicznej*, Wydawnictwo Czelej Sp.z.o.o. Wydanie I, Lublin 2011.

[3] Kau C.H., Abramovitch K., Kamel S.G., Bozic M., *Cone Beam CT of the Head and Neck, An Anatomical Atlas*, Springer-Verlag, Berlin Heidelberg 2011.

[4] Krzyżostaniak J., Surdacka A., *Rozwój wybranych technik radiologicznych w aspekcie obrazowania szczękowo-twarzowego*, Nowiny Lekarskie 2010, 79, 3, 249–253.

[5] Krzyżostaniak J., Surdacka A., *Rozwój i zastosowanie tomografii wolumetrycznej CBCT w diagnostyce stomatologicznej – przegląd piśmiennictwa*, Klinika Stomatologii Zachowawczej i Periodontologii Uniwersytetu Medycznego im. Karola Marcinkowskiego w Poznaniu, Dental Forum 2/2010/XXXVIII.

[6] www.conebeam.com

[7] http://doctorspiller.com/radiation-course-page-20-cone-beam/ (access: 15.02.2017).

[8] Pandolfo I., Mazziotti S., *Orthopantomography, 5 - Periapical Lesions*, Springer-Verlag, Italia, 2013

[9] http://www.dentaleconomics.com/articles/print/volume-101/issue-1/features/cone-beam-computed-tomography-how-safe-is-cbct-for-your-paitents.html (access: 15.02.2017).

TECHNICAL TRANSACTIONS 8/2017
CZASOPISMO TECHNICZNE 8/2017
MECHANICS
DOI: 10.4467/2353737XCT.17.140.6891

Piotr Duda (pduda@mech.pk.edu.pl)
Łukasz Felkowski
Department of Thermal Power Engineering, Faculty of Mechanical Engineering, Cracow University of Technology

An analysis of the steam superheater coil operation depending on different methods of coil support

Analiza pracy wężownicy przegrzewacza pary przy różnych metodach jej utwierdzenia

Abstract

The paper presents the main types of power boiler steam superheater loads together with relevant standards applicable to superheater calculations. In the case of horizontal superheaters, due to their thermal expansion and assembly errors which are the effect of non-uniform support of the hanger tubes, extra loads are generated on the coil pipes. An FEM analysis performed for a selected superheater structure indicates that maximum stress values and the location where the stresses occur depend on the method of support of the superheater tubes. It is shown that maximum stresses in this structural element can be reduced by introducing appropriate tension of hanger bars supporting the superheater hanger tubes.

Keywords: power boiler, creep, stress, FEM analysis

Streszczenie

W artykule przedstawiono główne rodzaje obciążeń przegrzewaczy pary kotłów energetycznych oraz normy obowiązujące przy ich obliczeniach wytrzymałościowych. W przypadku przegrzewaczy poziomych, ze względu na ich rozszerzalność cieplną oraz błędy montażowe spowodowane nierównomiernym zawieszeniem rur przegrzewacza następuje generowanie dodatkowych obciążeń na rurach wężownicy. Wykonana analiza MES dla wybranej konstrukcji przegrzewacza wykazała zależność maksymalnych naprężeń i ich miejsca występowania od sposobu zawieszenia rur przegrzewacza. Pokazano, że wprowadzenie odpowiednich naciągów w prętach wieszakowych podtrzymujących rury wieszakowe przegrzewacza może obniżyć maksymalne naprężenia w tym elemencie konstrukcyjnym.

Słowa kluczowe: kotły energetyczne, pełzanie, naprężenia, analiza MES

1. Introduction

A large proportion of damage to boiler heating surfaces, including superheater steam coils, is due to material overheating and corrosion. But the coil fixing method is an equally important factor generating concentration of stresses, which has a substantial impact on the structural element time of a failure-free operation. Pressure and high temperatures lead to creep-related damage, changes in material structure and cracks, thus making further operation of the superheater impossible. Experience shows that after the assumed period of operation, individual elements – though operated in conditions which comply with design calculations – are also affected by slight, safe, creep-related strains in areas where no concentration zones arise [1]. In places with the highest stresses and strains, on the other hand, deformations caused by the creep phenomenon are difficult to predict.

The paper presents results of thermal and strength calculations performed for a horizontal superheater whose task is to dry steam and raise its temperature to a required level. In this type of structure, superheater coils need to be supported using hanger tubes. Superheater heating surfaces are made of a large number of coils with pipes made of austenitic steel (due to their exposure to high temperatures exceeding 550 [°C]) [2]. The results of numerous calculations and experiments indicate that for such a temperature range the use of austenitic steels is justified as, unlike most other steel grades, they ensure acceptable values of the superheater coil wall thickness [3, 4].

2. Requirements of European standards

The standards concerning boiler pressure element calculations are usually specified for loads resulting from pressure. But the impact of other loads should also be taken into consideration by the designer. In the case of horizontal superheaters, due to thermal expansion affecting them and the hanger tubes, and due to assembly irregularities which are the effect of non-uniform support of the superheater tubes, extra loads are generated on the coil pipes. These loads must be taken into account both at the design and the operation stage [5].

If pipelines operate in creep conditions, longitudinal stresses caused by calculation pressure P, resultant moment M_A related to mass and other long-term loads, and resultant moment M_C related to thermal elongation should satisfy the following equation [6]:

$$\sigma_S = \frac{p\,d_o}{4\,e_{ord}} + \frac{0.75\,i\,M_A}{Z} + \frac{0.75\,i\,M_C}{3\,Z} \le f \qquad (1)$$

The stresses calculated according to formula (1) are used to present the results of a thermal and strength analysis performed in the Bentley AutoPipe program. According to the EN 13480-3 Standard (for the creep range), only a third of stresses arising due to thermal elongation is taken into consideration because it is assumed that the other two thirds are released in the relaxation process [6]. The values of the stress increase factor i (including the reduction factor of 0.75) should be higher than or equal to 1.0 ($0.75\,i \ge 1.0$).

The allowable stress after an extended period of operation – f_{CR} – should take account of the creep phenomenon. It depends on the temperature and time of operation. The allowable stress value for creep is established according to Standard EN 13480-3 [6] or Standard EN 12952-3 [7], and it is calculated as $f_{CR} = S_{RtTc}/ Sfcr$, where S_{RtTc} is the creep rupture strength and *Sfcr* is the safety factor. If the design service life is specified as a period of 100,000 h to 200,000 h, and if a service life monitoring system is provided, the safety factor *Sfcr* value of 1.25 may be used.

3. Numerical analysis

The SH3 steam superheater under analysis is an element of the boiler installation presented in Fig. 1, where all 44.5x6.3 pipes of steam coil 1 are supported on 44.5x6.3 hanger tubes 2 by means of hanger straps [8]. The pipes of the steam coils are anchored in membrane wall 3 in all directions: *DX*, *DY*, *DZ*, φ*X*, φ*Y*, φ*Z*.

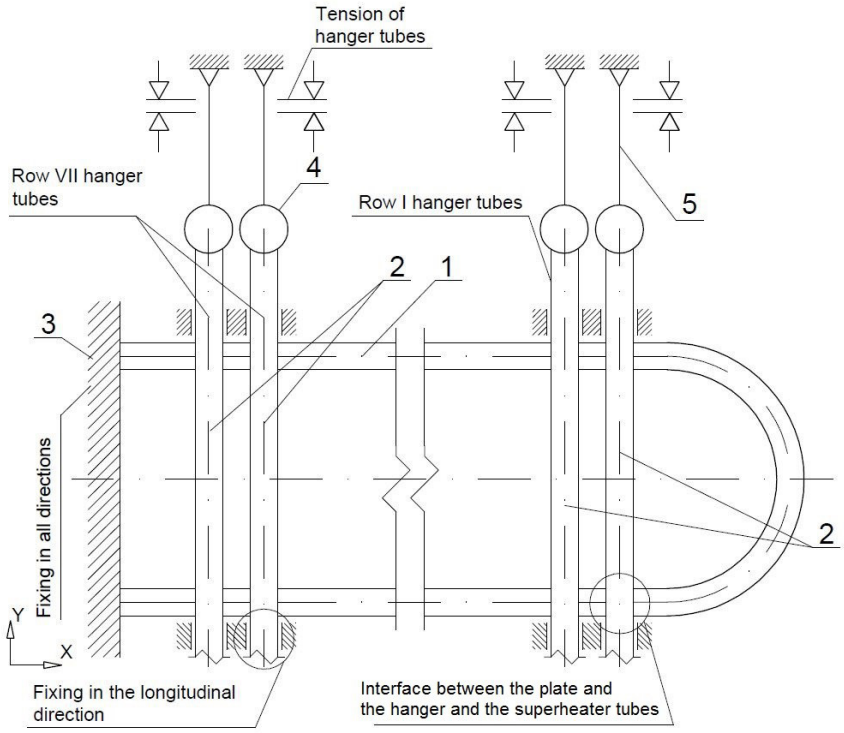

Fig. 1. Diagram of superheater SH3

Hanger tubes 2 are welded to chambers 4 hanging from hanger bars 5 in the structure grid. Tension of the bars can be adjusted to compensate for thermal elongation of the hanger tubes and to remove possible assembly irregularities. The adjustment and the measuring

methods depend on the technical solution adopted by the designer [2, 8, 9]. Superheater SH3 calculation temperature T is 604 °C, whereas calculation pressure P acting on the inner surface of the tubes is 284 bar.

The numerical analysis in the Bentley AutoPipe program is performed for two combinations of loads. The first enables an assessment of the coil stress-and-strain state for conditions in which the boiler is not operating, taking account of assembly irregularities. The second combination of loads makes it possible to assess stress concentration assuming a complete set of loads for an operating boiler with a variant with and without adjustment of the hanger bars.

3.1. First combination of loads

The analysis results are presented for loads resulting from the mass of the coil and the hanger tubes, and they take account of assembly irregularities introduced into the model in the form of preliminary displacement of the hanger tubes in direction DY = –58mm. The maximum stresses occur in point A shown in Fig. 2. They do not exceed allowable values in ambient temperature: f = 312/1.5 = 208 MPa, and for point A they total σ_A = 202 MPa.

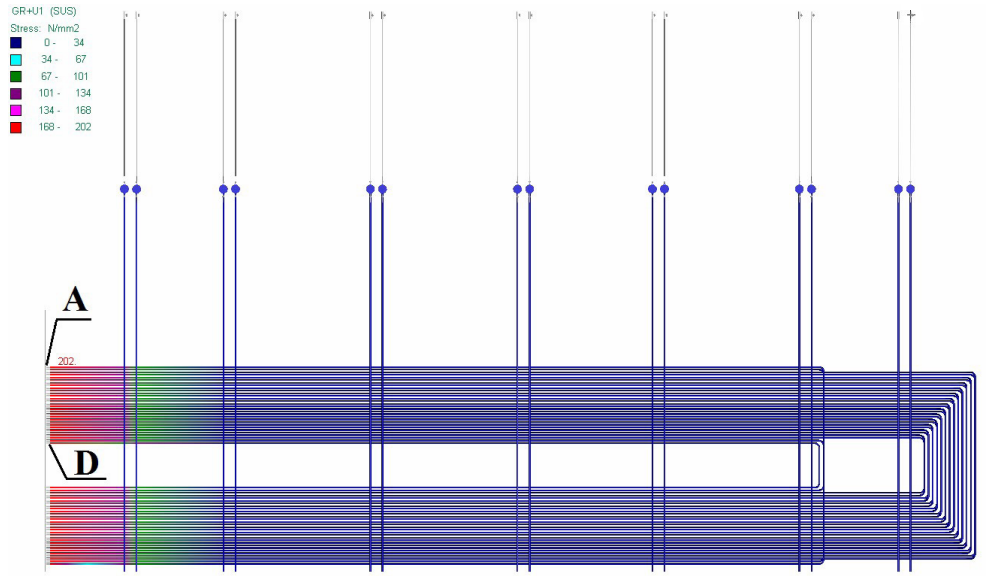

Fig. 2. Longitudinal stresses for the first combination of loads MPa

3.2. Second combination of loads

Fig. 3 presents the results of an analysis which takes account of the mass of the coil and the hanger tubes, calculation pressure P = 284 bar, temperature T = 604 °C, assembly irregularities and the variant with no tension of the hanger bars. The maximum stresses occur in point B: σ_B = 190 MPa and exceed the allowable value of f_{CR} = 209.4/1.25 = 167.5 MPa.

Stress concentration in point B is caused by the bending moment generated on the interface between the coil pipes and the membrane wall. The moment is an effect of thermal elongation of the hanger tubes of row VII (cf. 1) and a consequence of assembly irregularities taken into account in the analysis.

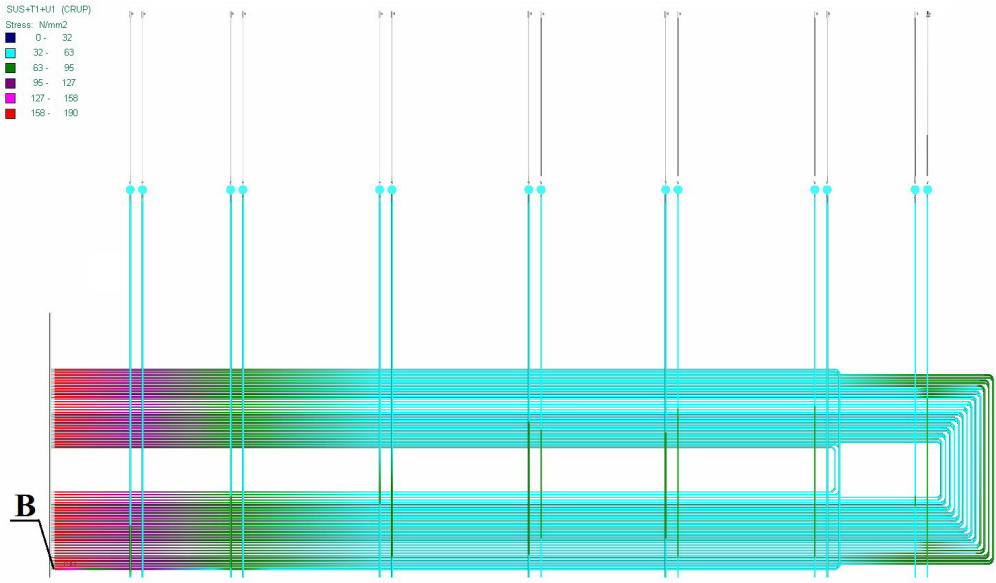

Fig. 3. Longitudinal stresses for the second combination of loads MPa; no tension of the hanger bars

If the calculations are performed taking account of the hanger bars tension as listed in Table 1, stress concentration in the superheater coil appears also in point B, as presented in Fig. 3.

Table 1. Tension adjustment values for the hanger bars

	Hanger tube rows						
	I	II	III	IV	V	VI	VII
Tension DY [mm]	27	29	29	29	29	30	40
	27	29	29	29	29	30	40

However, stresses in point B are lower and total $\sigma_{B1} = 73$ MPa, which is 44% of the allowable value ($\sigma_{B1} / f_{CR} = 0.44$). Stresses in the coil other areas are at the level of $\sigma = 44 \div 75$ MPa and are also lower than the allowable value.

Introduction of tension of the hanger tubes has an impact on the stress state also if the coil is not loaded with pressure and temperature. Compared to the results obtained for the first combination of loads, the maximum stresses occur in point D (cf. Fig. 2) and total $\sigma_D = 181$ MPa. The reduced concentration of stresses is the effect of adjustment of the hanger bars tension. The tension eliminates the non-uniform distribution of loads in the entire steam coil.

4. Conclusion

The paper presents a thermal and strength analysis of a steam superheater coil. It is shown that high stresses arise in this element mainly due to raised temperatures and assembly irregularities. The results indicate that the maximum stress values and the location where the stresses occur depend on the method of support of superheater tubes. It is shown that maximum stresses in this structural element can be reduced by introducing appropriate tension in the hanger bars which support superheater hanger tubes. The stress concentration zones indicated in the paper can be of help to make the decision which areas should be checked while operating horizontal superheater coils.

This research was financed by National Science Centre, Poland, UMO-2015/19/B/ST8/00958.

References

[1] Dobosiewicz J., Zbroińska-Szczechura E., *Ocena stopnia zużycia ciśnieniowych elementów kotłów pracujących w warunkach pełzania,* Energetyka, 12/2007, 917–922.
[2] Laudyn D., Pawlik M., Strzelczyk F., *Elektrownie,* WNT, 1997.
[3] Dobrzański J., Zieliński A., Pasternak J., Hernas A., *Doświadczenia z zastosowania nowych stali do wytwarzania elementów kotłów na parametry nadkrytyczne,* Prace IMŻ 62/1, 2010, 51–60 .
[4] Wala T., Hernas A., *Dobór materiałów na przegrzewacze referencyjnego kotła nadkrytycznego,* Prace IMiUE Politechniki Śląskiej, Book 23, Vol. III, 2009, 221–237.
[5] Sertić J., Kozak D., Konjatić P., Kokanović M., *Analytical and numerical investigation of elastic-plastic behaviour of the connecting pipes between header and steam superheater,* Proceedings of the 6th International Congress of the Croatian Society of Mechanics, Edited by Smojver, I., Sorić, J., Zagreb the Croatian Society of Mechanics, 2009. 119.
[6] EN 13480-3 Metallic industrial piping. Design and calculation.
[7] EN 12952-3 Water-tube boilers and auxiliary installations.
[8] Felkowski Ł., Duda P., *Analiza cieplno wytrzymałościowa wężownicy przegrzewacza pary, Analiza systemów energetycznych,* edited by: Węglowski B., Duda P., Wydawnictwo Politechniki Krakowskiej, Kraków 2013, 387–401.
[9] Renowicz D., Plaza M., Plaza B., Renowicz E., *Measurement and force adjustment in boiler suspensions and other statically indeterminate mechanical systems,* the 14th International Research/Expert Conference, Trends in the Development of Machinery and Associated Technology TMT 2010, Mediterranean Cruise, 11-18 September 2010.

TECHNICAL TRANSACTIONS 8/2017
CZASOPISMO TECHNICZNE 8/2017
MECHANICS
DOI: 10.4467/2353737XCT.17.141.6892

Joanna Fabiś-Domagała(fabis@mech.pk.edu.pl)
Institute of Applied Informatics, Faculty of Mechanical Engineering, Cracow University of Technology

Application of ishikawa diagram for failure analysis of a car water pump

Zastosowanie diagramu ishikawy do analizy uszkodzeń pompy cieczy chłodzącej

Abstract

The paper presents an identification of potential causes and effects of failures of a coolant pump for internal combustion engines. Ishikawa's quality improvement tools have been used to analyze the defects. The main causes of pump failures and cause-effect relationships have been identified. The main causes were identified and classified in order to select those which have the greatest influence on pump damage during operation.

Keywords: Ishikawa diagram, coolant pump

Streszczenie

W artykule przedstawiono identyfikację potencjalnych przyczyn i skutków powstawania uszkodzeń dla pompy cieczy chłodzącej silnika spalinowego. Do analizy uszkodzeń wykorzystano jedno z narzędzi doskonalenia jakości jakim jest diagram Ishikawy. Dokonano określenia głównych przyczyn problemu, identyfikacji związków przyczynowo-skutkowych oraz sklasyfikowania i hierarchizacji przyczyn głównych w celu wskazania przyczyn, które mają największy wpływ na uszkodzenia analizowanej pompy w czasie jej eksploatacji.

Słowa kluczowe: diagram Ishikawy, pompa cieczy, uszkodzenie

1. Introduction

A cooling system is one of the most important systems of combustion engines which maintains the engine temperature at the appropriate level. The key component of a cooling system is a coolant pump, which is subjected to variable and extreme loads during the engine operation. Therefore, the identification of possible failures and their causes and effects is as well an important issue. More and more effort is put into the identification of possible failures at the design and manufacturing stages, which allows for eliminating the reasons of failure or introduce preventing actions. On the other hand, identification of failures is a half way of solving the problem. Identified failures have to be classified and organized in an appropriate way. Then, those that have the greatest influence on reliability have to be selected and cause-effect relationships has to be determined. Various methods and tools are used for quality improvement. One of them is the Ishikawa diagram. It allows for identification of the problem, determining the cause-effect relationship and classifying it in a correct way in order to undertake preventive and corrective actions. This tool may also be used in further qualitative analyses such as cause-effect, SWOT, PDCA or risk and decision management. The Ishikawa diagram allows for visualizing a problem clearly and easily along with possible areas of its causes. It also allows for solving problems during brainstorming sessions where various causes of failures may be presented within different groups.

2. The Ishikawa diagram principles

The Ishikawa diagram was used in Japan at Sumitomo Electric for the first time. It was developed by Kaoru Ishikawa, a professor at Tokyo University, who published the principles of the diagram in 1962. Initially, the diagram was used only during the manufacturing process, but in a short time it appeared to be useful also in other areas. It was successfully used in administration, project management and functionality analysis. The diagram is a graphical representation of the relationships between effects and possible causes [1]. It is an analysis of the top-down category, which means that the analysis is carried out from the general to the detail. A group of primary and secondary causes are determined in a hierarchical way. The procedure of solving problem (effect) in the Ishikawa diagram includes problem identification, determining the main categories of causes (selection of causes that have the greatest impact on problem which may occur) [2]. An example of the Ishikawa diagram is presented in Fig. 1.

The Ishikawa diagram is represented by a graph in which the main elements can be found:

- element 0 – indicates problem/effect,
- element 1,2,.. – indicates the main categories of the causes that have influence on problem/effect. The concept of 5M + E: Man, Machine, Material, Method, Management, Environment is usually used to prepare a group of causes,
- element A - indicates the causes identified within the main categories (for each cause a sub-cause (a) may be described, which allows for a detailed analysis of the problem/effect to be performed).

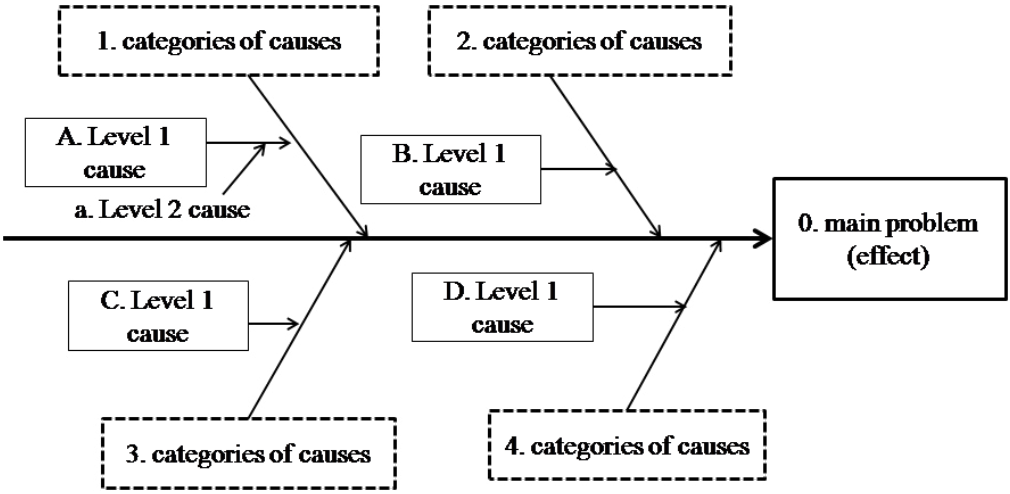

Fig. 1. The Ishikawa diagram

In the literature [3], three approaches may be found for causes of the considered problem:

- subject approach the causes are related to the components of the analyzed situation (categories are the components of the object, and the causes elements of these components),
- technological approach is considered as functional, because it depends on finding the causes within processes associated with the problem (technological processes and operations in these processes),
- approach of the factors involved the causes are presented in the form of so-called meta causes.

The created Ishikawa diagram allows for developing a numerical system of defect classification. The code characters can be specified depending on the level of details of identified causes. Accordingly, the code may consist of two or three characters. The code consisting of three characters 1Aa presented in Fig. 1, describes:

- the first character: 1 means a category of causes (100),
- the second character is the cause (1A0),
- the third character is a sub-cause (1Aa).

3. The Ishikawa diagram of coolant pump

A coolant pump which is a component of the engine cooling system is the object of the research. The main task of the pump is to circulate the coolant inside the engine, the cooler and the heater. The investigated coolant pump is a centrifugal pump with a belt drive which consists of housing (1), a rotor (2) mounted on a shaft (3), bearings (4) and a sealing ring (5).

The analyzed pump is shown in Fig. 2.

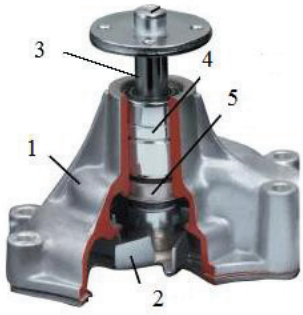

Fig. 2. Coolant pump [8]

The coolant is axially delivered to the pump where it is directed by the rotating rotor at the side to the outlet port [4]. The coolant pump is exposed to damages, whose symptoms can be noisy operation and leakage. Pump failure can be caused by many reasons, which may lead to overheating or even engine damage. Therefore, it is important to identify as many causes as possible and indicate those that are most likely to occur and have the greatest influence. The Ishikawa Cause and Effect Diagram was implemented for identification, classification, and ranking of potential causes of pump failures. Mechanical and operating damages as well as pump leaks were identified as the main problems for which a detailed identification of potential causes was made using both the technological and the subject approach. The use of the Ishikawa Diagram allows for linking the causes of a specific problem and assigning them to six main categories of causes:

- 100: assembly/disassembly,
- 200: medium,
- 300: exploitation,
- 400: maintenance,
- 500: sealing,
- 600: cooperating elements.

During the analysis, own categories have been developed, in which more than twenty reasons have been identified. On the basis of the Ishikawa Diagram, a numerical classification of causes has been proposed taking into account three levels of detail. Additionally, five main reasons have been identified from three categories with numbers: 100, 200 and 600. These causes are marked with the following code:

- 110: improper assembly/disassembly for category assembly/disassembly,
- 221: contaminated coolant for medium category,
- 240: low coolant level for medium category,
- 620: damaged impeller blades for category cooperating elements,
- 640: incorrect belt tension, worn belt,
- 650: sealing wear, seized bearing.

Those causes have significant influence on pump malfunction, noisy operation and leakages. Then, the causes were selected hierarchically depending on the probability of appearance. Therefore, the most important cause was considered to be code 221. The next

order is: 110, 640, 650, 620 and 240. Table 1 shows four main causes of pump damage with description and associated damage type.

Table 1. Main reasons of pump damages

cause	failure	description
221	exploitation	Pump corrosion, rust, salt or lime deposits are in the cooling system, the coolant does not meet the manufacturer's requirements.
110 640	mechanical leak tightness	Deformation, gasket or casing breakage, impeller crack, no engine cooling; belt breaking, visible rubber tracks on the pulley, squeaking of the belt due to wear, damage and seizure of the pump bearings, impeller contact with the pump housing.
650	mechanical leak tightness	The use of improper or excessively contaminated coolant leads to deterioration of its lubricating properties; improper pump assembly with inappropriate tools, hitting the pump housing leads to distortion of the bearing seat and seizure, improper belt tension or settings.

A graphical presentation of the analysis and identified cause-effect relationships for pump failure [5, 6] is presented in Fig. 3.

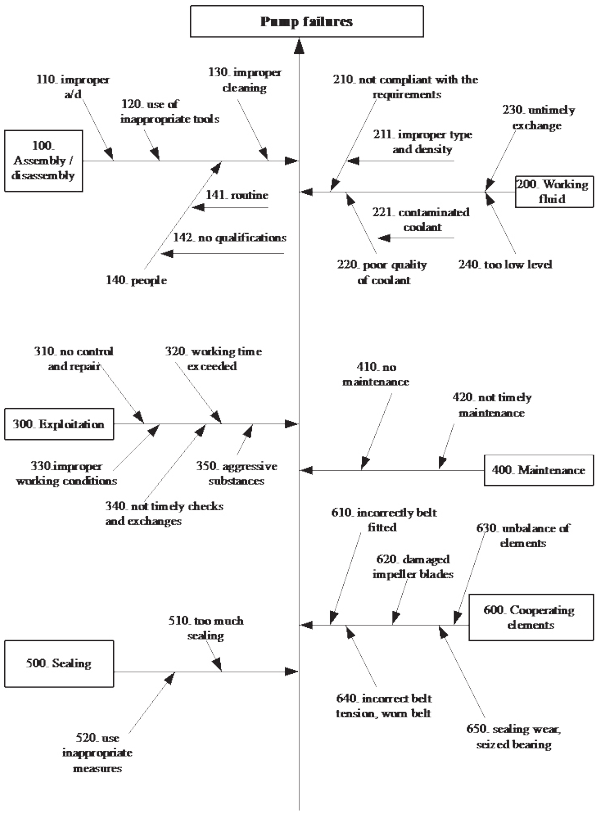

Fig. 3. The Ishikawa Diagram for the pump

4. Summary

The analysis of a pump by means of the Ishikawa Diagram proved that it can be a useful tool in identifying relationships between cause and effect for the during pump malfunction or its damage. The Ishikawa Diagram allowed for identifying the main problems and four most important causes that have influence on operational and mechanical damages and leaks as well. The selected main causes were categorized and sorted according to the considered problem. The clue of the cause-and-effect relationships was identification of problem location and reasons that have influence on efficiency of the engine cooling system.

References

[1] Gołaś H., Mazur A., *Zasady, metody i techniki wykorzystywane w zarządzaniu jakością,* Wydawnictwo Politechniki Poznańskiej, 2010.
[2] www.jakosc.biz., *Diagram-ishikawy,* 2009.
[3] Kindlarski E., *Wykres Ishikawy,* Warszawa 1995.
[4] www.terminalczesci.pl, *Pompa wody – funkcja, budowa, zasada działania,* 2012.
[5] Rybicki R., *Pompa wodna*, www.auto-swiat.pl, 2010.
[6] Hańczka W., *Pompy wody w napędach rozrządu – problemy,* motofocus.pl, 2013.
[7] Tabor A., Rączka M., Kowalski M., *Nowoczesne zarządzanie jakością: praca zbiorowa. T. 2, Metody i narzędzia jakości, normalizacja, akredytacja, certyfikacja,* Centrum Szkolenia i Org. Systemów Jakości, Kraków 2004.
[8] www.aa1car.com/library/water pump, *Water Pump Diagnosis & Replacement.*

TECHNICAL TRANSACTIONS 8/2017
CZASOPISMO TECHNICZNE 8/2017
MECHANICS
DOI: 10.4467/2353737XCT.17.142.6893

Artur Krowiak (krowiak@mech.pk.edu.pl)
Institute of Computer Science, Mechanical faculty, Cracow University of Technology
Jordan Podgórski
Student of Applied Informatics, Mechanical faculty, Cracow University of Technology

Hermite interpolation of multivariable function given at scattered points

Interpolacja hermite'a funkcji wielu zmiennych na nieregularnej siatce

Abstract

The paper shows the approach to the interpolation of scattered data which includes not only function values, but also values of derivatives of the function. To this end, an interpolant composed of radial basis functions is used and extended by terms possessing appropriate derivative terms. The latter match the given derivatives. Special attention is paid to the problem of choosing the value of the shape parameter, which is included in radial functions and influences the accuracy and stability of the solution. To validate the method, several numerical tests are carried out in the paper.

Keywords: scattered data interpolation, Hermite interpolation, radial basis functions

Streszczenie

W artykule przedstawiono podejście do interpolacji danych na nieregularnie rozłożonych węzłach. Dane te zawierają nie tylko wartości funkcji, ale również ich pochodne. Do rozwiązania zagadnienia użyto funkcję interpolacyjną złożoną z radialnych funkcji bazowych, powiększoną o człony zawierające odpowiednie pochodne tych funkcji. Pochodne te odpowiadają zadanym pochodnym. Szczególną uwagę położono na problem wyznaczania współczynnika kształtu w funkcjach radialnych. Współczynnik ten warunkuje dokładność i stabilność rozwiązania. Dla sprawdzenia metody przeprowadzono kilka testów numerycznych.

Słowa kluczowe: interpolacja na nieregularnie rozmieszczonych węzłach, interpolacja Hermite'a, radialne funkcje bazowe

1. Introduction

Interpolation methods play an important role in many areas of science, where there exists the need of a prediction on the basis of discrete data. Interpolating functions are also the main point in derivation of numerical schemas for various methods of solving differential equations. Conventional approximation methods allow to interpolate discrete data given on a regular grid or on structured mesh. Moreover, they enable to easily approximate data in two or three dimensions only. To overcome these drawbacks, the so-called meshfree approaches have appeared in recent years [1–3]. They allow to find an interpolating function for data given at scattered nodes, significantly increasing the possibilities of application of such methods.

Instead of polynomials that have been widely used as the basis functions in the interpolation on a mesh-based grid, a kind of functions which depend on data has been introduced in meshfree approaches. They are called radial basis functions (RBFs) since their values depend on the distance between two points in the space. These points can be easily defined in higher dimensional spaces, which does not change the general approach to the solution of the problem. It is a great advantage of the methods based on RBF, which allows to treat multidimensional problems in the same way as in two or three dimensions. An interesting information on this type of functions can be found in [4, 5].

In the present paper, the interpolation of multivariable discrete function is extended according to Hermite idea. We assume that at a node, not only the function value can be given, but also some derivatives can be known. This formulation differs from others that can be found in literature [1, 6], where it has been assumed that at one node there can exist only one degree of freedom, in the form of function value or its derivative. The approach presented in the paper can be especially useful to derive some meshfree methods for the solution of differential equations possessing multiply boundary conditions [7].

2. Hermite interpolation with RBFs

Let us consider a set of scattered nodes $\mathbf{x}_i \in \mathbb{R}, i=1,...,N$. At each of these nodes a function value $f(\mathbf{x}_i) = f_i$ is given. Moreover, at some of these nodes $\mathbf{x}_k^D, k=1,...,N^D$ there are values of derivatives of the function generally denoted by $(D_k f)(\mathbf{x}_k) = Df_k$, where D_k is a differential operator imposed on the function at kth node. For simplicity of the presentation we assume that there can be one derivative value at one node, although one can easily extend the problem to more than one derivative. To find an approximate value of the function at any point different from the given nodes or to analyze the function by tools available in mathematical analysis, an interpolation series involving RBF is introduced in the following form:

$$u(\mathbf{x}) = \sum_{j=1}^{N} \alpha_j \varphi\left(\|\mathbf{x}-\xi\|\right)\Big|_{\xi=\mathbf{x}_j^I} + \sum_{j=1}^{N^d} \beta_j \left[D_j^{\xi} \varphi\left(\|\mathbf{x}-\xi\|\right)\right]_{\xi=\mathbf{x}_j^D} \tag{1}$$

where $\varphi(\|\mathbf{x}-\xi\|)$ denotes RBF function, whose value is depended on the distance between an interpolation point $\mathbf{x}$ and a point ξ, called the center. In the paper the centers coincide with nodes $\mathbf{x}_i$. In Eq. (1) α_j, β_j are interpolation coefficients and D_j^{ξ} denotes the differential operator imposed on the function at $\mathbf{x}_j^d$ node. In this case, the function is considered as the function of ξ variable.

In order to determine the interpolation coefficients, the interpolation conditions are applied for the function:

$$\sum_{j=1}^{N}\alpha_j\varphi(\|\mathbf{x}_i-\xi\|)\Big|_{\xi=\mathbf{x}_j}+\sum_{j=1}^{N^D}\beta_j\left[D_j^{\xi}\varphi(\|\mathbf{x}_i-\xi\|)\right]_{\xi=\mathbf{x}_j^D}=f_i,\ i=1,...,N \tag{2}$$

as well as for its derivatives:

$$\sum_{j=1}^{N}\alpha_j\left[D_j^{\mathbf{x}}\varphi(\|\mathbf{x}-\xi\|)\right]_{\substack{\xi=\mathbf{x}_j\\ \mathbf{x}=\mathbf{x}_i^D}}+\sum_{j=1}^{N^D}\beta_j\left[D_j^{\mathbf{x}}\left[D_j^{\xi}\varphi(\|\mathbf{x}-\xi\|)\right]_{\xi=\mathbf{x}_j^D}\right]_{\mathbf{x}=\mathbf{x}_i^D}=Df_i,\ i=1,...,N^D \tag{3}$$

In Eq.(3) $D_j^{\mathbf{x}}$ denotes the same differential operator as D_j^{ξ} but acting on the radial function viewed as a function of $\mathbf{x}$ variable. It makes the coefficient matrix of the system (2)–(3) a symmetric one, which facilitates its assembling and solution of the problem. This system can be written in a more convenient manner using the following matrix notation:

$$\begin{bmatrix}\mathbf{\Phi} & \mathbf{\Phi}_{D^{\xi}}\\ \mathbf{\Phi}_{D^{\mathbf{x}}} & \mathbf{\Phi}_{D^{\mathbf{x}}D^{\xi}}\end{bmatrix}\cdot\begin{bmatrix}\boldsymbol{\alpha}\\ \boldsymbol{\beta}\end{bmatrix}=\begin{bmatrix}\mathbf{f}\\ \mathbf{Df}\end{bmatrix} \tag{4}$$

where:

$$\mathbf{\Phi}_{ij}=\varphi(\|\mathbf{x}_i-\xi\|)\Big|_{\xi=\mathbf{x}_j},\quad i,j=1,...,N$$

$$\left(\mathbf{\Phi}_{D^{\xi}}\right)_{ij}=\left[D^{\xi}\varphi(\|\mathbf{x}_i-\xi\|)\right]_{\xi=\mathbf{x}_j^D},\quad i=1,...,N,\ j=1,...,N^D$$

$$\left(\mathbf{\Phi}_{D^{\mathbf{x}}}\right)_{ij}=\left[D^{\mathbf{x}}\varphi(\|\mathbf{x}-\xi\|)\right]_{\substack{\xi=\mathbf{x}_j\\ \mathbf{x}=\mathbf{x}_i^D}},\quad i=1,...,N^D,\ j=1,...,N$$

$$\left(\mathbf{\Phi}_{D^{\mathbf{x}}D^{\xi}}\right)_{ij}=\left[D^{\mathbf{x}}\left[D^{\xi}\varphi(\|\mathbf{x}-\xi\|)\right]_{\xi=\mathbf{x}_j^D}\right]_{\mathbf{x}=\mathbf{x}_j^D},\quad i=1,...,N^D,\ j=1,...,N^D$$

α, β and $\mathbf{f}$, $\mathbf{Df}$ are vectors containing appropriate interpolation coefficients, function values and the derivatives, respectively.

To determine interpolation coefficients, the system (4) has to be solved yielding

$$\begin{bmatrix}\boldsymbol{\alpha}\\ \boldsymbol{\beta}\end{bmatrix}=\begin{bmatrix}\mathbf{\Phi} & \mathbf{\Phi}_{D^{\xi}}\\ \mathbf{\Phi}_{D^{\mathbf{x}}} & \mathbf{\Phi}_{D^{\mathbf{x}}D^{\xi}}\end{bmatrix}^{-1}\cdot\begin{bmatrix}\mathbf{f}\\ \mathbf{Df}\end{bmatrix} \tag{5}$$

The problem of solvability of the system depends on the type of RBF used and it is not studied in detail in the paper. In some cases, the interpolant (1) should be augmented by a polynomial term to ensure the inversion of the system matrix. Some notes on this issue can be found in [1]. For problems analyzed in the paper the system (5) has had unique solutions.

2.1. Accuracy and conditioning of the problem

The most popular RBFs, listed in Table 1, contain shape parameter *c*. The shape parameter has a significant influence on accuracy. A larger value of this parameter should theoretically make the solution more accurate but leads to an ill-conditioned system, which may not be accurately solved. Therefore, the choice of the appropriate value of *c* is an important issue in using RBF based methods.

Table 1. Examples of radial basis functions

Name	RBF
Multiquadric	$(r^2+c^2)^{1/2}$, $c \geq 0$
Inverse multiquadric	$(r^2+c^2)^{-1/2}$, $c > 0$
Gaussian	e^{-r^2/c^2}, $c>0$

So far there is no general approach to this end and this value is assumed mostly on the basis of numerical experiments or researchers' experience [1]. Recently, in [8] an algorithm based on a heuristic kind has been proposed, which relates accuracy to condition number of the system of equations and number of significant digits assumed for the computation. It enables to automate the choice of the value of shape parameter. The algorithm searches for the largest value of *c*, which makes the exponent of the condition number of the interpolation matrix close to the number of significant digits but does not exceed this number. In the case of RBF, it ensures acceptable accuracy and stable solution of Eq. (4). The main condition, which the algorithm is based on, is as follows:

$$\log 10\, \kappa(\overline{\mathbf{\Phi}}) \in [r_l, r_u] \Rightarrow c^* \tag{6}$$

where $\kappa(\overline{\mathbf{\Phi}})$ denotes the condition number of the system matrix from Eq. (4) and r_l and r_u are lower and upper bound of a range associated with the number of significant digits. Usually r_u is 16, when one operates double precision and r_l is a little less. Note that $\kappa(\overline{\mathbf{\Phi}})$ depends on the value of *c*. Defining a loop, where the value of *c* is increased or decreased to fulfil Eq. (6) one can determine the quasi optimal value of shape parameter c^*.

3. Numerical experiments

To validate the method, several numerical experiments have been carried out. Below there are examples of two-variable test functions used in these experiments:

$$f_1(x_1, x_2) = \sin(4x_1) \cdot \cos(5x_2) \tag{7}$$

$$f_2(x_1,x_2)=\frac{3}{4}e^{-1/4\left((9x_1-2)^2+(9x_2-2)^2\right)}+\frac{3}{4}e^{-1/49(9x_1+1)^2-1/10(9x_2+1)^2} \tag{8}$$

$$+\frac{3}{4}e^{-1/4\left((9x_1-7)^2+(9x_2-3)^2\right)}-\frac{1}{5}e^{-(9x_1-4)^2-(9x_2-7)^2}$$

To obtain data points, functions (7)–(8) have been discretized with the use of scattered node distributions presented in fig.1

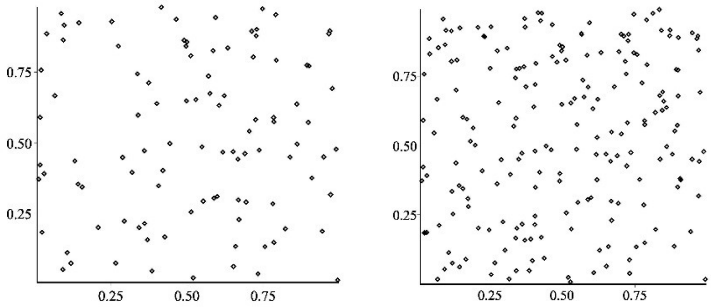

Fig. 1. Scattered node distribution for numerical experiments: N = 100 (left), N=200 (right)

At N^D chosen grid points some derivatives of the test functions have been assumed as given data. Accuracy of the approach has been determined by a kind of L_2 error norm in the following form:

$$\delta=\sqrt{\sum_{i=1}^{NN}(u_i-f_i)^2}\Big/\sqrt{\sum_{i=1}^{NN}(f_i)^2} \tag{9}$$

where u_i and f_i denote values of the interpolation function and the test one respectively, evaluated at NN regularly distributed points. The obtained results are presented in Tabs. 2 and 3. For comparison, similar results, obtained using classical RBF interpolation (without derivatives) are included in the tables.

Table 2. Results obtained with multiquadrics RBF

		Hermite approach			classical approach		
		c^*	$\delta(f_1)$	$\delta(f_2)$	c^*	$\delta(f_1)$	$\delta(f_2)$
N = 100	N^D = 18	0.60	1.064e-3	3.306e-2	0.70	1.107e-3	5.524e-2
	N^D = 36	0.50	1.748e-3	1.328e-2			
N = 200	N^D = 18	0.40	8.943e-4	4.346e-4	0.45	9.337e-4	1.413e-3
	N^D = 36	0.35	9.225e-4	7.095e-4			

Comparing the results of Hermite interpolation with those obtained using classical approach, one can notice that the introduction of information about derivatives in most cases leads to better accuracy of the approximation. It should be taken into account that more information (function and derivative values) increase the dimension of the system matrix from Eq. (4) making this matrix more ill-conditioned. Therefore, the value of the shape parameter has to be smaller to guarantee a stable solution and, finally, the accuracy may not be improved.

Table 3. Results obtained with invers multiquadrics RBF

		Hermite approach			classical approach		
		c^*	$\delta(f_1)$	$\delta(f_2)$	c^*	$\delta(f_1)$	$\delta(f_2)$
$N = 100$	$N^D = 18$	0.70	1.040e-3	4.561e-2	0.85	8.022e-4	1.074e-1
	$N^D = 36$	0.65	1.301e-3	4.140e-2			
$N = 200$	$N^D = 18$	0.45	1.443e-3	5.950e-4	0.55	9.002e-4	3.928e-3
	$N^D = 36$	0.45	9.174e-4	7.536e-4			

4. Conclusion

In the paper, the Hermite type interpolation of a function given at scattered nodes has been shown. To this end, an interpolant built with RBFs has been applied. Treating these functions as functions of two vector variables (interpolation point and center), one can obtain symmetric system matrix, which facilitates its assembling and accelerates the solution process. In the paper, special attention is paid to determining appropriate value of the shape parameter included in RBFs. This parameter is determined as a result of a trade-off between accuracy and conditioning of the system of equations following form interpolation conditions. It ensures a stable solution of the problem.

References

[1] Fasshauer G.E., *Meshfree Approximation Methods with Matlab*, World Scientific Publishing, Singapore 2007.

[2] Belytschko T., Krongauz Y., Organ D., Flrming M., Krysl P., *Meshless methods: an overview and recent developments*, Computer Methods in Applied Mechanics and Engineering, Vol. 139, 1996, 3–47.

[3] Liu G.R., *Meshlees Methods – Moving beyond the Finite Element Method*, CRC Press, Boca Raton, Florida 2003.

[4] Buhmann M.D., *Multivariete interpolation using radial basis functions*, Ph.D. Dissertation, University of Cambridge, 1989.

[5] Schaback R., *Creating surfaces from scattered data using radial basis functions*, [in:] M. Dehlan, T. Lyche, L. Schumaker (Eds): *Mathematical Methods for Curves and Surfaces*, Vanderbilt University Press, Nashville 1995, 477–496.
[6] Wu Z., *Hermite–Birkhoff Interpolation of Scattered Data by Radial Basis Functions*, Approximation Theory and its Applications, Vol. 8, 1992, 1–10.
[7] Krowiak A., *Hermite type radial basis function-based differential quadrature method for higher order equations*, Applied Mathematical Modelling, Vol. 40, 2016, 2421–2430.
[8] Krowiak A., *On choosing a value of shape parameter in Radial Basis Function collocation methods*, Numerical Methods for Partial Differential Equations, submitted for publication.

TECHNICAL TRANSACTIONS 8/2017
CZASOPISMO TECHNICZNE 8/2017
MECHANICS
DOI: 10.4467/2353737XCT.17.143.6894

Michał Maniowski
Slawomir Para(s.para@sbg.at)
Institute of Automobiles and IC Engines, Faculty of Mechanical Engineering, Cracow University of Technology

Comparison of computing efficiency of different hydraulic vehicle damper models

Porównanie efektywności obliczeniowych różnych modeli amortyzatorów samochodowych hydraulicznych

Abstract

This paper deals with comparisons of computing efficiency of 20 damper models with functional and hybrid approaches, which can be used to solve typical problems in vehicle dynamics. Efficiency is evaluated based on model accuracy and computing time. The computed results of different damper models are compared to measurements of an actual car damper. Its damping characteristics were measured on a hydraulic damper test rig with three different excitations.

Keywords: vehicle dynamics, modelling, hydraulic damper, shock absorber

Streszczenie

W artykule porównano efektywność dwudziestu modeli amortyzatorów, funkcjonalnych i hybrydowych, które można stosować przy rozwiązywaniu podstawowych problemów dynamiki pojazdów. Efektywność jest oceniana przez dokładność odwzorowania i czas obliczeń. Odpowiedzi kolejnych modeli amortyzatora porównywano z wynikami badań rzeczywistego amortyzatora samochodowego na stanowisku ze wzbudnikiem.

Słowa kluczowe: dynamika pojazdu, modelowanie, amortyzator hydrauliczny

1. Introduction

Dampers used in vehicle suspensions can be regarded as mechanical-hydraulic systems, which generate resistance forces (F) in dependency on kinematic excitation (x), outside/ambience temperature (T_z) and inside temperature (T_w). This resistance force (F) can consist of several ingredients [1]. The damping force is a force generated by a damper as a function of damper velocity ($v = dx/dt$).

Formulating a damper model can be regarded with the same difficulty as setting up a tire model. The response of a damper is dynamic and extremely non-linear with regard to the amplitude and frequency of excitation [2]. High impact of the damping medium temperature leads to a diversification of damping characteristics within each next damping cycle [10]. The valves inside a damper can be described as three dimensional, serial and parallelly arranged hydraulic obstacles with constant as well as variable areas. Physical and chemical properties of the damping medium (e.g. viscosity, density, compressibility, vapor pressure, heat extension) depend on the proportions of the liquid phase (oil), gaseous phase (nitrogen) and intermediate phase (emulsion, foam) [4].

The aim of this paper is to compare the efficiency of several vehicle damper models, which can be used to solve basic problems of vehicle dynamics. The efficiency is evaluated by calculation of accuracy and computing time. This article describes numerical examples which show comparisons of computed responses of 20 different models and the measured damping behavior obtained at a test rig [3]. The damping characteristics of real vehicle dampers were measured on a hydraulic damper test rig with three different excitations, here with a sine signal of low frequency (W1), high frequency signal (W2) and a sine on sine signal (W3).

The results of this paper can be useful for all those who are working on measuring and modeling dampers and vehicle dynamics.

2. Numerical examples

The numerical examples are based on characteristics of an actual vehicle damper [8]. By making use of a test bench with an electro-hydraulic excitation ram, damping force characteristics were gathered. Three different excitations profiles (W1, W2, W3) were considered in this paper.

Within the MATLAB environment, 20 different damper models were formulated. The simulation results (damping forces as function of damper velocity) are compared to appropriate measurement data for the same excitation.

Because of the work constraints, only three different model outputs (Fig. 1–3) are presented as graphical examples.

All the 20 models are described briefly below, including their advantages and drawbacks. Model deviations are calculated as RMS errors of the computed and measured damping forces and summed up in Fig. 4.

M1) Model M1 (functional approach) is described by one dimensional linear interpolation (algebraic relation) between damping force and damper velocity ($F=f(v)$) with 12 nodes on the measurement data. **Model advantages.** M1 model is simple in implementation. Its prediction deviations (Fig. 4) are at average level (ca 100 N) for all the excitations and its simulation time is quite short (ca 0.2 s). **Model drawbacks**. M1 model is not continuous and does not consider a dynamic response, because of limited use in vehicle dynamics.

M2) Model M2 is based on model M1. Instead of a linear interpolation, a "spline" interpolation with 12 nodes is used. **Model advantages.** Deviations are at a similar level (100 N), compared to M1. **Model drawbacks**. In addition to the disadvantages of M1, the simulation time of M2 is very high (up to 1 s).

M3) Model M3 describes a damping force similar to model M1. Instead of using 12 nodes, this model is set up with two linear sections (Fig. 1), which should describe the damping force. **Model advantages.** This model is very fast (simulation time < 0.1 s) **Model drawbacks**. Model M3 insufficiently describes the damping force. The mean deviation at all excitations is about 370 N.

M4) Model M4 is based on model M3. Instead of using only two linear sections, here four linear sections are used (Fig. 1). **Model advantages.** This model is very fast (simulation time < 0.1 s) and easy to implement. Deviations of the damping force are at an average level (110 N). **Model drawbacks.** As the models described before, M4 does not consider any dynamic response.

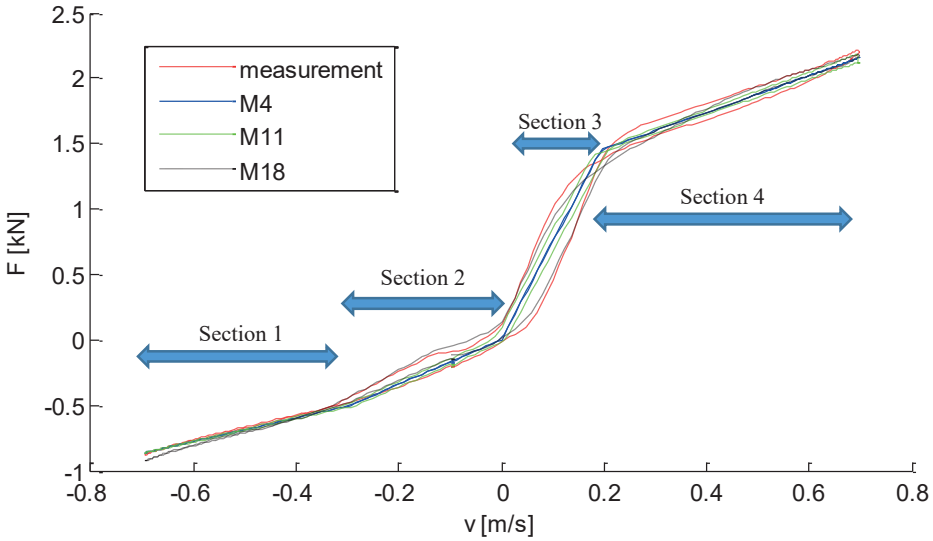

Fig. 1. Damping force vs velocity for W1 excitation. Comparison of M4, M11, M18 models with measured data

M5) Model M5 is an adaption of model M4. In addition, the valve opening behaviour in the rebound phase is considered. **Model advantages.** This model is still very fast (simulation time < 0.1 s) and easy to implement. Compared to model M4 it is slower. Damping force deviations are at an average level (100 N). **Model drawbacks.** Although some dynamic effect is considered, deviation does not enhance significantly.

M6) Model M6 consists of 4 sections (Fig. 1), where section 1 and section 4 are described with a linear function and the remaining sections are described with a 3rd order function. **Model advantages.** The simulation time remains low (< 0.1 s) and deviations of the damping force are similar to model M4 (110 N). **Model drawbacks.** A description of the damping force with functions of higher order does not enhance the model accuracy.

M7) Model M7 is a derivate of model M4. It is described by two dimensions ($F=f(v,x)$), by damper velocity and damper deflection. In this model, the so-called gas forces are taken into account. **Model advantages.** This model has a short simulation time (< 0.1 s). **Model drawbacks.** Damping force deviations remain at an average level (100 N)

M8) Model M8 has again a two dimensional approach (based on M4). Compared to M7, this model is based on damper velocity and damper acceleration ($F=f(v,a)$). **Model advantages.** This model is still fast (simulation time < 0.1 s) and its deviation is at an average level (100 N). **Model drawbacks.** The complexity of additional dimensions does not lead to better correlations between measurement and model results.

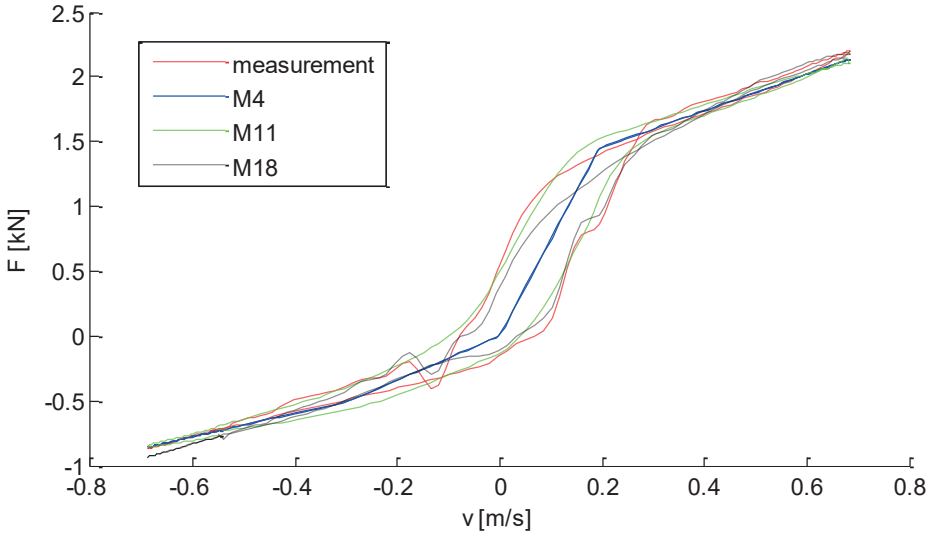

Fig. 2. Damping force vs velocity for W2 excitation. Comparison of M4, M11, M18 models with measured data

M9) Model M9 is built up as a rheological, 1st order inertial system [13]. Its parameters are constant. It is combined with model M4. **Model advantages.** Due to a physical description, the damper's dynamic behaviour is considered, which lowers the average value of deviations (90 N). **Model drawbacks.** Simulation times rises up even to more than one second.

M10) Model M10 is built up analogically to model M9, but with parameters which are dependent on the damping force. **Model advantages.** The damping force deviation is at an average level (90 N). **Model drawbacks.** Simulation times are unacceptably high with more than one second.

M11) Model M11 is a rheological, 1st order system with parameters which are dependent on the damping force, but combined with model M5, which takes into account the valve opening behaviour. **Model advantages.** The damping force deviation is at an average level (90 N). **Model drawbacks.** Simulation times (up to one second) are not feasible for vehicle dynamics simulations.

M12) Model M12 makes use of a neural network of FFB type (2 layers, 10 neurons). It is trained (alg. L-M) on excitations W1 with the damping force as a function of damping velocity ($F=f(v)$). **Model advantages.** Simulation time is very short (< 0.5 s) and the damping force deviation is in the average range of (110 N). **Model drawbacks.** To obtain suitable accordance between measurement data and simulation results, optimal parameters for training have to be determined. Also, the training procedure takes a while.

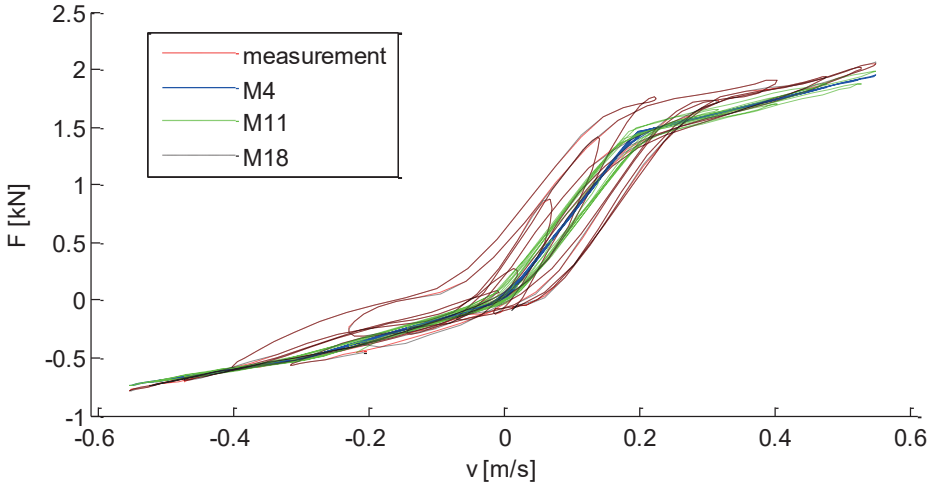

Fig. 3. Damping force vs velocity for W3 excitation. Comparison of M4, M11, M18 models with measured data

M13) Model M13 has the same parameters for the neural network as M12. M13 is trained on excitation W3 with the damping force learn input as a function of velocity and movement ($F=f(v,x)$). **Model advantages.** The results of this model have the best accordance to the damping force at excitation W3 compared to all the aforementioned models. Simulation time is still short (< 0.5 s). **Model drawbacks.** See M12.

M14) Model M14 has the same parameters for the neural network as M12. M14 is trained on excitation W2 with the damping force learn input as a function of velocity and movement ($F=f(v,x)$). **Model advantages.** The results of this model have the best accordance to the damping force at excitation W2 compared to all the aforementioned models. Simulation time is still short (< 0.5 s). **Model drawbacks.** Simulation results at excitation W1 and W3 unfit completely.

M15) Model M15 has the same parameters for the neural network as M12. M15 is trained on excitation W1 with the damping force learn input as a function of velocity and movement ($F=f(v,x)$). **Model advantages.** The results of this model have the best accordance to the damping force at excitation W1 compared to all the aforementioned models. Simulation time is still short (< 0.5 s). **Model drawbacks.** Simulation results at excitation W2 and W3 have a high deviation (200 N).

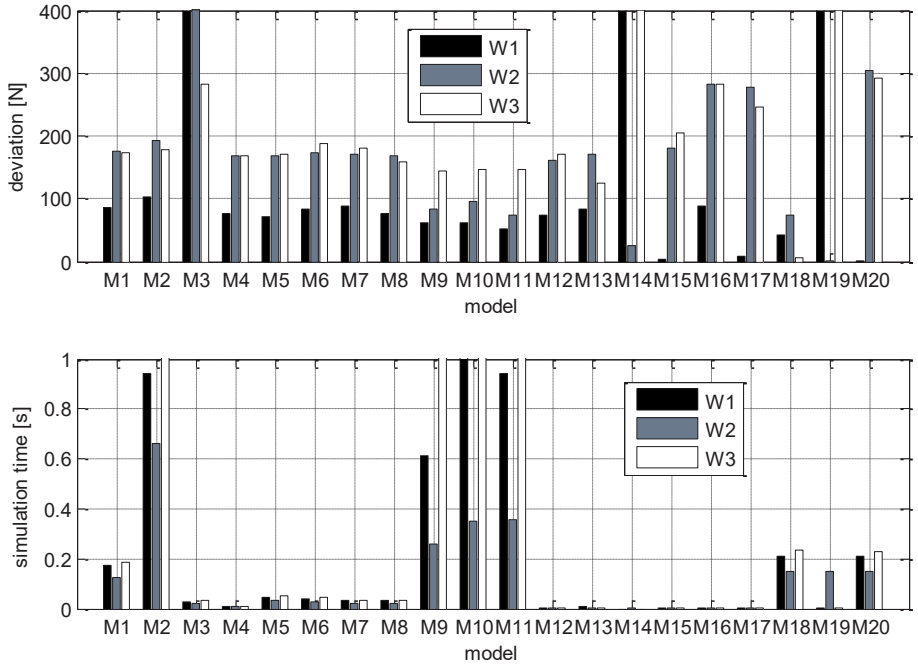

Fig. 4. Overview of deviations and calculation times of the considered damper models for W1, W2 and W3 excitations

M16) Model M16 has the same parameters for the neural network as M12. M15 is trained on excitation W1 with the damping force learn input as a function of velocity, movement and acceleration (F=f(v,x,a)). **Model advantages.** Simulation time is still short (< 0.5 s). **Model drawbacks.** An additional dimension for NN training does not lead to an improvement. Compared to M12, M16 has lower accuracy. For excitation W2 and W3, high deviation (280 N).

M17) Model M17 is a hybrid, by combining model M4 and M13. **Model advantages.** Simulation time is still short (< 0.5 s). **Model drawbacks.** The effort of joining the two models does not lead to the expected enhancement of simulation accuracy. Deviation of simulation results at W2 and W3 are high (250 N).

M18) Model M18 makes use of neural networks of the NARX structure [9]. The model was learned with 17 layers at excitation W3 with the damping force learn input as a function of velocity and damper movement ($F=f(v,x)$). **Model advantages.** The accuracy of the simulated damping force at excitation W3 is the best overall (5 N deviation). At the remaining excitations, deviation is less than 80 N, which is a very good accordance. **Model drawbacks.** Simulation time rises up to 0.2 s.

M19) Model M19 has the same parameters for the neural network as M18. M19 is trained on excitation W2. **Model advantages.** The accuracy of the simulated damping force at excitation W2 is the best overall (1 N deviation). **Model drawbacks.** At the remaining excitations, deviation is too high (> 400 N). Simulation time is high (0.2 s).

M20) Model M20 has the same parameters for the neural network as M18. M20 is trained on excitation W1. **Model advantages.** The accuracy of the simulated damping force at excitation W1 is the best overall (2 N deviation). At the remaining excitations, deviation is too high (300 N). **Model drawbacks.** Simulation time is high (0.2 s).

3. Conclusions

Dampers, as parts of the suspension, have a huge impact on active safety, travelling comfort and the durability of vehicles. Numerical modelling of dampers is still an up-to-date and complex problem. Real damping characteristics highly depend on the time-based excitation, given by e.g. hysteresis loops or other phenomena which are usually omitted in simpler models, but have a major impact on vehicles drivability [12].

The choice of the adequate damper model type should depend on the following aspects: aim of analysis, simulation time, effort for the modelling process and simplicity of model parameter estimation. Applying the appropriate damper model will lead to reducing the time of choosing optimal damping forces for particular use [6], prediction of the influence of damper defects on safety [7] or ride comfort.

In this paper, three different damper model simulation outputs are visualized. M4 is the quickest functional model with average deviation. M11, a rheological model, with best fit but long simulation time. M18 with best fit to all excitations, due to the use of a neutral network. Bar plots with simulation times and model deviations are compiled to the present summary of all 20 models.

As further work, an implantation of the aforementioned damper models in a quarter vehicle model is considered. This enables a dynamic study of damper settings influence on driver vibrations.

References

[1] Caffarty S., Tomlinson G. R., *Characterization of automotive dampers using higher order frequency response functions*, Proc. IMechE, Vol. 211, PartD: J. Automobile Engineering, 1997, 181–203.

[2] Duym S., *Simulation Tools, Modelling and Identification, for an Automotive Shock Absorber in the Context of Vehicle Dynamics*, VSD, Vol. 33, 2000, 261–285.

[3] Dzierżek S., Knapczyk M., Maniowski M., *Extending passive dampers functionality for specific ride and handling requirements*, Czasopismo Techniczne z. 6–M, Wydawnictwo Politechniki Krakowskiej, 2008, 39–47.

[4] Guzzomi F., et al., *Investigation of Damper Valve Dynamics Using Parametric Numerical Methods*, Australian Fluid Mechanics Conference, Crown Plaza, Australia, 2007, 1123–1130.

[5] Liberati M., et al., *Grey–box Modelling of a Motorcycle Shock absorber*, 43rd IEEE Conference on Decision and Control, Atlantis–Bahamas, 2004, 755–760.

[6] Lion A., Loose S., *Thermomechanically Coupled Model for Automotive Shock absorbers: Theory, Experiments and Vehicle Simulations on Test Tracks*, Vehicle System Dynamics, Vol. 37, no. 4, 2002, 241–261.

[7] Lozia Z., Zdanowicz P., *Wykorzystanie różnych formalizmów opisu tarcia suchego w modelu ćwiartki samochodu stosowanym do symulacji testu diagn. stanu amortyzatorów*, Teka Kom. Motoryzacji, PAN, z. 33–34, Kraków, 2008, 215–222.

[8] Maniowski M., *Porównanie efektywności modeli amortyzatorów hydraulicznych*, VIII Międzynarodowa Konf. Naukowo–Techn., Problemy Bezpieczeństwa Pojazdów, Kielce–Cedzyna, 2012.

[9] Patel A., Dunne J. F., *NARX Neural Network Modelling of Hydraulic Suspension Dampers for Steady–state and Variable Temperature Operation*, Vehicle System Dynamics, Vol. 40, no. 5, 2003, 285–328.

[10] Ramos J.C., et al., *Development of a thermal model for automotive twin–tube shock absorbers*, Applied Thermal Engineering, Vol. 25, 2005, 1836–1853.

[11] Schiehlen W., Hu B., *Spectral simulation and shock absorber identification*, Int. Journal of Non–Linear Mechanics, 38, 2003, 161–171.

[12] Van Kasteel R., et al., *A new shock absorber model for use in vehicle dynamics studies*, Vehicle System Dynamics, Vol. 43, no 9, 2005, 913–631.

[13] Zach C., et al., *On the performance of rheological shock absorber models in full vehicle simulation*, Vehicle System Dynamics, Vol.45, 2007, 981–999.